Generative Modeling: An Approach to High Level Shape Design for Computer Graphics and CAD

Thesis by

John M. Snyder

In Partial Fulfillment of the Requirements

for the Degree of

Doctor of Philosophy

California Institute of Technology

Pasadena, California USA

1991

(Defended May 22, 1991)

Abstract

Generative modeling is an approach to computer-assisted geometric modeling. The goal of the approach is to allow convenient and high-level specification of shapes, and provide tools for rendering and analysis of the specified shapes. Shapes include curves, surfaces, and solids in 3D space, as well as higher-dimensional entities such as surfaces deforming in time, and solids with a spatially varying mass density.

Shape specification in the approach involves combining low-dimensional entities, especially 2D curves, into higher-dimensional shapes. This combination is specified through a powerful shape description language which builds multidimensional parametric functions. The language is based on a set of primitive operators on parametric functions which include arithmetic operators, vector and matrix operators, integration and differentiation, constraint solution and global optimization. Although each primitive operator is fairly simple, high-level shapes and shape building operators can be defined using recursive combination of the primitive operators.

The approach encourages the modeler to build parameterized families of shapes rather than single instances. Shapes can be parameterized by scalar parameters (e.g., time or joint angle) or higher-dimensional parameters (e.g., a curve controlling how the scale of a cross section varies as it is translated). Such parameterized shapes allow easy modification of the design, since the modeler can interact with parameters that relate to high-level properties of the shape. In contrast, many geometric modeling systems use a much lower-level specification, such as through sets of many 3D control points.

Tools for rendering and analysis of generative models are developed using the concept of interval analysis. Each primitive operator on parametric functions has an inclusion function method, which produces an interval bound on the range of the function, given an interval bound on its domain. With these inclusion functions, robust algorithms exist for computing solutions to nonlinear systems of constraints and global minimization problems, when these problems are expressed in the modeling language. These algorithms, in turn, are developed into robust approximation techniques to compute intersections, CSG operations, and offset operations.

Acknowledgments

My adviser, Jim Kajiya, first presented me with the idea of generative models at the end of 1987. It was an intriguing approach that encompassed many of the shape representation schemes I had often pondered, and even implemented. Jim and I began work on a SIGGRAPH paper, setting out to test the effectiveness of the idea by modeling some complicated shapes. Although our SIGGRAPH paper was rejected, we learned many things in that initial flurry of activity, not the least of which was that there much more research that could be done. I decided to investigate generative modeling further as my Ph.D. project.

Jim gave me wide latitude in this work, but he has closely watched my progress, He has given me good global advice about the right way to implement the interface. He has helped me in the theoretical basis of this work as well. I can recall many discussions with Jim about such things as how the language should be designed, how to connect boundary intersections in implicit curve approximation, and how to prove some of the interval analysis results of Chapter 5. I also thank Jim for his enthusiasm for the project, even when it took unexpected turns.

Jim's other graphics graduate student, Tim Kay, has been my friend and helpmate throughout my long graduate career. Tim and I have worked together on computer animation projects, SIGGRAPH papers, and hardware installation and maintenance. Tim has always given me good advice about this project and many others, which I have always listened to and sometimes even followed. I also owe Tim thanks for his help to make the hidden line eliminated figures in this thesis.

I would also like to thank my software guinea pigs, those who have used some version of my modeling program: Jed Lengyel, Devendra Kalra, Paula Sweeney, Cavi Arya, and David Laidlaw. Nothing so brings a software designer down to earth as users. Jed Lengyel deserves special thanks for many thoughtful suggestions during the formative phase of this project. I look forward to showing Jed the more mature version of the incipient program he used so extensively.

I owe thanks to Al Barr and his graphics group for the use of his workstations to do much of the typesetting work of this thesis. Thanks also go to my examining committee: Jim Kajiya, Al Barr, Jim Blinn, Steve Taylor, and Joel Burdick, for their time to read my thesis, and for their helpful suggestions. Special thanks go to Jim Blinn for finding a long list of typographical errors not one of which was also found by the Caltech proofreader. Jim Blinn and Clark Brooks have pointed out many imprecise or confusing sections, which I hope I have corrected.

Finally, my greatest thanks is reserved for my wife, Julia, and my parents. My wife has borne a great deal, especially in the hectic last months of writing. I only hope that I respond similarly when the time comes for her to finish her thesis. My parents too have always been supportive. Unintentionally (I believe), they have provided perhaps the most urgent reason for the completion of this work in the form of nonrefundable plane tickets.

Contents

List of Figures

Chapter 1

Introduction

The computer is emerging as a powerful tool in the design and analysis of 3D shape, an important concern in fields such as computer aided design and manufacture (CAD/CAM), computer graphics, art, animation, mathematics, computer simulation, computer vision, and robotics. As the computational speed of computers continues to increase, so does their potential to model shapes with greater interactivity and sophistication. Recognizing this potential, researchers in both academia and industry have devoted much attention in the last twenty years to the area of geometric modeling, the study of the representation and analysis of shape.

Perhaps the greatest strides in geometric modeling have been made in the use of computers to make fast, high quality images of geometric models. At the same time, many techniques have been developed to allow human designers to specify and manipulate geometric models inside the computer. Yet, entering 3D shape into the computer remains a difficult task. In this chapter, a set of criteria are presented for evaluating shape representations. Methods of shape representation used in the past are examined in light of these criteria. Problems in these past representations are discussed, and a new approach, called generative modeling, is proposed as a solution.

1.1 Criteria for Evaluation of a Shape Representation

In this discussion, it is important to distinguish between a *user representation* of shape, a representation manipulated by a human designer which serves as an interface between man and computer, and a *machine representation*, manipulated solely by the computer. The criteria for evaluation of a shape representation which follow are intended to apply to user representations. The overall efficiency of shape design and analysis is directly related to the quality of the user representation. The machine representation affects design efficiency only insofar as it affects the speed and robustness of shape manipulations. For example, if the machine representation is only an approximation to the user representation, then conversion from user to machine representation introduces approximation errors.

Three criteria may be used to evaluate the quality of a shape representation:

1. Ease of specification — how easy is it for a designer to enter shapes into the computer?
2. Renderability — how quickly and realistically can images of the the shapes be generated?
3. Analyzability — what analytical operations are allowed on shapes? How fast and robust are these operations?

Ease of Specification

The first criterion, ease of specification, assesses how efficiently designers can enter and change their designs. The ease of specification thus relates to the cost of design. Moreover, the shape specification guides the designer and structures his thinking, making some types of shapes easy to reason about and specify, some more difficult, and some entirely out of the domain of consideration. It is possible then that some potentially better designs are excluded by the nature of the shape specification.

Ease of specification may be further broken down into the following categories:

- Naturalness — does the representation correspond to the way designers think about the shape?
- Compactness — how small is the information required to specify the shape?
- Completeness — how large is the class of shapes that can be represented?
- Controllability — can the designer predict what shape will result from a given input?
- Editability — can the designer modify shapes easily?

- Validity — is it impossible for designers to specify invalid shapes?
- Accuracy — is the representation only an approximation of the designer's intention? If so, how faithful is the approximation?
- Closure — if shapes are specified by composing operators on lower level shapes, is the result of the operations always a valid shape which can be used as input in further operations?

These categories are adapted from [REQU80], with some modifications to shift the emphasis from machine representation to user. For example, [REQU80] also includes as a criterion the concept of *uniqueness*; that is, whether a given shape has a single representation. It seems unlikely that the designer should be too concerned with uniqueness, and in fact, would probably prefer that a rich set of representations exist from which he can pick the most convenient. Uniqueness, however, may be an important consideration for a machine representation, which may need to test two representations for equality, at considerable computational cost.

Renderability

The second criterion, renderability, measures the quality of visual feedback given the designer. This visual feedback is the single greatest verification of the design. Ideally, rendering should be fast and provide a good idea of the shape. In practice, a rendering method is a compromise between computational speed and quality of visualization. Different shape representations admit different forms of rendering, which lie on a spectrum of speed/quality tradeoffs.

Current technology for shape rendering comes in a variety of forms. Wireframe (line drawing) and depth buffered, solid shaded images are common and useful forms of visual feedback. These forms of rendering are fast enough on many of today's engineering workstations to allow real time or near real time rendering of quite complex shapes. More photorealistic forms of rendering, such as ray tracing and radiosity, are currently too slow for interactive feedback, but provide additional cues such as shadows, transparency, and more sophisticated lighting models which may aid in visualizing the shape. It is anticipated that these higher quality, slower rendering techniques will soon become fast enough for interactive use.

Analyzability

The last criterion, analyzability, evaluates how suitable the shape representation is for analyzing and simulating collections of shapes. Shape operations that are important in this context include

- compute physical quantities about the shape — moments of inertia, center of mass, surface area, volume
- compute geometric queries about the shape or shapes — proximity with other shapes and collision detection, finding curves of intersection between surfaces, determining whether a given surface is a valid solid boundary
- compute feasible/optimal parameters for parameterized shapes — find a parameter for a parameterized family of shapes that solves some set of constraints and/or optimizes some objective function

In assessing the analyzability of a shape representation, it is important to consider the generality of operations that are allowed, the accuracy of these operations, and their computational speed. Often, there is a natural relationship between a shape representation and its analytical properties [TIMM80, LEE82a]. For example, the volume of a solid specified as an extrusion of a 2D closed curve is simply the product of the area enclosed by the curve and the height of the extrusion. On the other hand, the natural forms of analysis admitted by a shape representation are not the only ones that need be used. A representation can be converted to one more amenable to analysis. Of course, the conversion required may involve substantial computational cost and/or introduce approximation error.

1.2 Previous Work in Shape Representation

Not surprisingly, the major emphasis in shape representation research has been on curves, surfaces, and solids. Since the beginnings of the field of computer graphics, curve and surface representation research has largely focused on piecewise parametric polynomials, especially cubic polynomials such as the Coons patch [COON67], Bezier curves and surfaces [BEZI74], and B-spline curves and surfaces [RIES73, GORD74]. Algebraic curves and surfaces, (i.e., shapes specified as a solution to a polynomial equation) are another widely used form [BLIN82, HANR83, SEDE85, SEDE89]. New shape representations are also being studied, including deformations, and more general implicit and parametric shapes.

For many applications, such as for computer aided manufacture, shapes must be modeled as solids. The area of *solid modeling* is concerned with the design and analysis of 3D solids. Solid model representations being developed involve two main representational themes, boundary representations and CSG. *Boundary representation* or b-rep models represent solids by their surface, curve, and point boundaries. *Constructive solid geometry* or *CSG* models represent objects as a composition of Boolean set operations on points contained within the solids [REQU77c, REQU78]. These two techniques are not mutually exclusive. The Alpha_1 modeler developed at the University of Utah allows CSG operations on b-rep shapes [COHE83].

The following sections analyze current shape representation schemes according to the criteria established in Section 1.1.

1.2.1 Polyhedra

Polyhedra are solids bounded by a set of polygons. Because they are defined by the polygons that form their surface, polyhedra are a simple boundary representation. Polyhedra were investigated as a computer shape modeling representation by Baumgart [BAUM72, BAUM74] in a system for computer vision research called GEOMED. In the work, he introduced the idea of *Euler operations*, which transform objects by adding or removing faces, edges, or vertices. Baumgart's work has formed the basis for many systems that allow users to interactively create and edit polyhedral shapes.

Research into polyhedral representations remains active. Chiyakura and Kimura [CHIY83] combined polyhedra with polynomial parametric patches to round corners of solids and represent curved faces. Several researchers have investigated computation of Boolean set operations on polyhedra: Turner [TURN84], Requicha and Voelcker [REQU85], Putnam and Subrahmanyam [PUTN86], Laidlaw, Trumbore, and Hughes [LAID86], and Naylor, Amanatides, and Thibault [NAYL90]. Segal [SEGA90] has studied error control and validity maintenance for toleranced polyhedral shapes.

Polyhedral representations are clearly natural in representing a useful class of objects — objects that are bounded by planar facets. They are not appropriate as a user representation for general, curved solids but can be used as an approximate machine representation. Such an approximation has many drawbacks which will be discussed later. Perhaps the greatest advantage of polyhedral representations is their renderability. Polygons are easy to render, especially with graphics hardware available today. The analyzability of polyhedra may also be attractive. Lien and Kajiya [LIEN84] have presented algorithms for the direct computation of integral properties for polyhedra.

1.2.2 Piecewise Parametric Polynomial Shapes

Piecewise parametric polynomials are the main shape representation of computer graphics and CAD/CAM. The research literature contains numerous specializations, extensions, surveys, and applications of the piecewise polynomial form ([DEBO72, DEBO78, COHE80, TILL83, KOCH84, BOHM84, BARN85, BART87, BARS88]). Parametric polynomial shapes are typically specified through a series of control points, which the curve or surface interpolates. The resulting shapes tend to be easy to control and edit for free form specification and allow designers control over simple aspects of the shape, such as its continuity.

A very general form, called NURBS, for nonuniform, rational, b-splines, is being used in many new geometric modeling systems. The advantage of NURBS over traditional (nonrational) representations is their ability to represent simple quadrics like spheres, cones, and cylinders exactly.

Piecewise parametric polynomials are a complete representation. Given enough patches to interpolate the desired shape, any shape, however complicated, can be specified to any degree of accuracy. Despite its generality, specifying a multitude of control points over a shape is often an undesirable method of modeling. Specification tends to be uncompact. It is hard to edit a collection of many, unstructured control points. Shapes can not be parameterized with parameters meaningful to designers.

The rendering of piecewise parametric polynomial surface has received much attention. Conversion of parametric polynomials into polygonal meshes can be done by very efficient algorithms. New hardware is also being developed to directly rasterize these shapes [SHAN87, SHAN89]. Rendering using ray tracing is an ongoing area of research

[KAJI82, SEDE84].

Analyzability of parametric polynomials is quite good. Global properties, such as volume and moments of inertia of solids bounded by nonrational polynomial patches, can be computed analytically. Proximity and intersection testing involves solving polynomial equations. Such polynomial solution becomes numerically intractable as the degree of the polynomial grows.

1.2.3 Algebraic Shapes

An algebraic shape is a shape formed by the zeroes of a polynomial equation, typically of low degree. For example, algebraic cubic curves (the solution of a third-degree polynomial in two variables), and quadric surfaces (the solution of a second-degree polynomial in three variables) have been used many times in geometric modeling.

Algebraic shapes have been used in some very early modeling/rendering systems [WEIS66, WOON71]. These systems used quadric surfaces as the basic modeling tool, and were therefore not general in the types of specifiable shapes. Sederberg [SEDE85] has proposed the idea of piecewise algebraic shapes. Like the parametric polynomials shapes discussed previously, these shapes form a complete representation, but a very low-level one.

Several algorithms exist for direct, scan line rasterization of quadric surfaces [WEIS66, WOON71, SARR83]. Algebraic shapes may also be rendered by ray tracing. Quadric surfaces are especially simple, since ray/surface intersections can be computed by solving a quadratic equation. Ray intersection for more general algebraic shapes is investigated in [HANR83, HANR89]. Both direct rasterization and ray tracing fail to take advantage of fast graphics hardware geared towards the rendering of polygons, making piecewise parametric shapes more attractive for real time rendering.

The analyzability of algebraic shapes is attractive for several reasons. Point classification (determining whether a point is inside or outside the shape) can be done with a simple polynomial evaluation. Intersections between algebraic shapes also require solution of polynomials of lower-degree than with parametric polynomials. Computation of the intersections between quadric surfaces, for example, is described in [SARR83] and [MILL87]. Both characteristics of algebraic shapes are useful in solid modeling systems. Quadric surfaces and polyhedra have also been combined in a geometric modeling system [CROC87].

1.2.4 Sweeps

A *sweep* represents a shape by moving an object (called a *generator*) along a trajectory through space. The simplest sweep is an *extrusion* which translates a 2D curve along a linear path normal to the plane of the curve. Surfaces of revolution are also sweeps of 2D curves around an axis. Sweeps need not use only 2D curves; for example, sweeps of surfaces or solids are useful operations. Sweeps whose generator can change size, orientation, or shape are called *general sweeps.* General sweeps that use 2D curve generators are *generalized cylinders* [BINF71].

Several researchers have studied sweeps ([GOLD83, CARL82b, DONA85, WANG86, COQU87]). Barr's *spherical product* ([BARR81]), is an example of a sweep that uses a constant 2D curve generator with translation and scaling. Carlson [CARL82b] introduced the idea of varying the sweep generator. Wang and Wang [WANG86] explored sweeps of surfaces for use in manipulating numerically controlled milling machine cutter paths.

Sweeps have been used in solid modeling systems for many years (e.g., GMSolid, ROMULUS). Lossing and Eshleman [LOSS74] developed a system using sweeps of constant 2D curves. Alpha_1, a modeling system developed at the University of Utah, has a much more sophisticated sweeping facility [COHE83].

One of the advantages of sweeps is their naturalness, compactness, and controllability in representing a large class of man-made objects. For example, objects which are surfaces of revolution or extrusions are best represented as sweeps. Sweeps are not complete however. Verification of the validity of sweeps also causes problems. For example, it is easy to generate degenerate closed sweeps which do not enclose a solid area by translating a generator curve in the plane of the curve.

Direct rendering of general sweeps is difficult. Rendering using ray tracing has been studied [KAJI83, VANW84a, VANW84b, BRON85] for various limited forms of sweeps. Kajiya [KAJI83] studied ray tracing of extrusions. van Wijk studied ray tracing of conical sweeps which translate and scale a 2D cubic spline curve ([VANW84a]), and ray tracing of tubes formed by sweeping a sphere ([VANW84b]). Bronsvoort and Klok [BRON85] give an algorithm for ray tracing curves swept along arbitrary 3D trajectories.

Rendering may also be achieved through conversion of the sweep to another form such as a polygonal mesh. Since sweeps are naturally converted to general parametric functions, this method is fast and easy as will be discussed in Section 1.2.6.

Analyzability of sweeps is good. Calculation of volume integrals over the region enclosed by a sweep can often be simplified using Gauss's theorem from vector calculus. Under certain conditions, integrals can further be simplified into products of line integrals over appropriate sweep curves. As in the case of renderability, the discussion of analyzability of general parametric functions in Section 1.2.6 applies.

1.2.5 Deformations

Deformations are operations that transform simple shapes to more complex by deforming the space in which the simple shape is embedded. For example, given a sphere in $\mathbf{R}^3$, a more complicated shape can be designed by deforming the sphere via a function $D : \mathbf{R}^3 \rightarrow \mathbf{R}^3$. Each point on the sphere is transformed through the function D, yielding a deformed sphere. The concept of deformations has received little attention in geometric modeling. Barr [BARR84] has examined a set of primitive deformations (bending, tapering, and twisting) that are useful in modeling, as well as differentially specified deformations. This work demonstrated the usefulness of deformations as a geometric modeling tool, but left open many problems of how to represent and specify a general set of deformation primitives.

Several researchers have also examined 3D deformations that are represented using cubic polynomials specified with 3D control points [SEDE86a]. Such deformations tend to become unwieldy for complicated shapes since many control points must be specified, but may be useful for free-form sculpting of shape.

Rendering and analysis of shapes formed with deformations varies with the types of primitive shapes that are deformed and the types of allowable deformations. A deformation of a parametric surface, for example, yields another parametric surface and so can be treated in the same way (see Section 1.2.6). Deformations of implicit surfaces can also be treated as implicit surfaces, if the deformation is invertible.

1.2.6 Parametric Shapes

It is reasonable to expect that parametric shapes based on a more general representation than piecewise polynomials could provide a more compact and powerful basis for modeling than piecewise polynomials, while still retaining their generality. However, parametric surfaces more general than piecewise polynomials have not received much attention in the fields of computer graphics and computer aided geometric modeling. Specific types of nonpolynomial parametric shapes have been used, such as Barr's superquadric surface [BARR81].

Parametric shapes are amenable to fast rendering with polygon-based graphics hardware. The shapes are sampled by evaluated the parametric function over a series of points in parameter space to form polygons. Rendering using ray tracing is more difficult, but has been studied by several researchers [TOTH85, JOY86, BARR86].

The analyzability of parametric shapes is mixed. Computation of physical properties of parametric shapes is often simple, especially when the parametric domain is suitably restricted (e.g., to a rectangle for parametric surfaces). Calculation of the proximity or intersection between general parametric shapes has been a difficult problem (although it has been solved for some particular examples, such as Bezier curves), which has been traditionally solved with ad hoc and non-robust numerical methods.

1.2.7 Implicit Shapes

Implicit shapes of more generality than the algebraic shapes discussed previously have been used to a limited extent in geometric modeling. The TIPS solid modeler [OKIN73] represented solids as Boolean operations on implicitly represented half-spaces. Blobby models, models formed by the isosurfaces of decaying fields of point sources, are another example of implicit shapes [BLIN82, NISH83, WYVI86]. While not more general than algebraic shapes, they are a useful representation for modeling smooth surfaces surrounding a collection of points.

Rendering of implicit shapes is most easily accomplished using ray intersection algorithms. For this type of rendering, implicit shapes are computationally superior to parametric shapes, since the required numerical iteration takes place over a lower-dimensional space. Kalra and Barr [KALR89] have presented a robust algorithm for intersecting rays with general implicit surfaces. Alternatively, implicit shapes can be polygonalized and rendered using polygon-based graphics hardware. Polygonalization of implicit shapes is a difficult problem; a heuristic approach is described in [BLOO88].

Analyzability of implicit shapes is mixed. Geometric queries such as point classification (i.e., is the point inside or outside the shape) are simple for implicitly described shapes.

On the other hand, sampling of points over an implicit shape is difficult, often requiring elaborate, non-robust, and slow numerical algorithms.

1.3 Areas for Improvement in Shape Representation

The current techniques for shape representation are lacking in several fundamental ways: in the generality of synthetic techniques they admit, in their ability to combine the various representational approaches, in their ability to handle more than three dimensions, in their ability to parameterize shape models, and in their control of approximation error.

Generality of Synthetic Techniques

Synthetic techniques for shape representation establish a set of primitive shapes, and a set of primitive operations. Complicated shapes are then built from simpler by composition of the primitive operations. CSG, the most common example of a synthetic technique, is an extremely useful and natural means of specifying complicated shapes. Yet, in existing implementations, its usefulness is hampered by restrictions on the set of allowable primitives. Sets of primitives which current CSG implementations support include polyhedra, sets of specific primitives such as blocks, spheres, and cylinders, general quadric surfaces, and b-reps bounded by NURBS. Each of these sets of primitives is useful but hardly complete.

Designers also face a lack of synthetic operations other than CSG. Researchers are currently studying operations such as filleting, blending, and offsetting. Blending, for example, allows two solids to be joined such that the interface between the two is smooth rather than sharp as in CSG. These newer synthetic operations show promise as a higher-level specification tool but are much more difficult to manipulate and analyze.

Combinations of Techniques

It is probable that each of the various methods of shape representation have some realm of applicability. One representation may not be the best for every shape a designer wishes to specify. Yet there have been only limited attempts to combine the various representations into a single system. Especially significant is the inability of modelers to handle both parametric and implicit shape representations because of the difficulty of conversion.

Multidimensionality

Current geometric modeling work has mostly avoided multidimensional representation schemes and concentrated on modeling rigid surfaces and solids in three dimensions. Modeling of important systems such as shapes that deform in time, or shapes that contain nonhomogeneous distributions of mass, temperature, and stress, are mostly beyond the capabilities of current technology. Systems that do include some multidimensional modeling do so in a post-processing simulation phase that separates specification of the "extra" dimensions from the 3D geometric information, and makes more difficult the feedback of information from simulation phase to design phase.

Parameterizability

Related to the lack of multidimensionality of shape representations is the lack of parameterizability. Many solid modeling programs supply predefined generic primitives that let the designer vary a few simple parameters to create instances of the shape. For example, families of gear or bracket shapes are commonly parameterized. Unfortunately, current shape representations do not allow designers to create parameterized shapes themselves. For example, a designer might like to design a shape where positions of drill holes can vary according to their position on another part, or design a connecting part that can bend around another part whose size is presently unknown. Once a shape is parameterized, it then becomes useful to allow the designer to specify constraints for the parameters, or functions that the parameters should optimize. Results of such parameter selection should then be allowable input to the continuing design process. Such parameterizability is currently beyond the state of the art.

Control of Error

Control of approximation error is a problem area for shape design systems. This is especially true for non-exact systems in which the machine representation of shape is only an approximation for the user representation. For example, a polyhedral approximation to a curved solid will give incorrect results for geometric queries such as intersection. These errors are typically difficult to control. As a result, approximation error may be limited in an ad hoc manner (e.g., increase the number of polygons in a polyhedral approximation until the result "looks" right). Even if the errors can be controllably limited, an unacceptably high computational cost may be required.

Approximation error becomes an even greater problem when approximate intermediate results are fed back to the design. For example, consider approximating a general parametric surface by a piecewise polynomial parametric surface. The surface is deformed, a solid is subtracted from it using Boolean set operations, and the result is deformed again. It is then tested for intersection with another surface. At each stage, the original approximation error is magnified so that the last intersection test may yield incorrect results.

1.4 Overview of the Generative Modeling Approach

Specification

The generative modeling approach developed in this thesis is an extension of the sweep method of representing shape. Objects are built using 2D curves which control cross sections, deformation schedules, and other aspects of the shape. The curves are combined to produce shapes using a powerful language for building multidimensional parametric functions. The language is based on a set of recursive operators from vector calculus and differential geometry. The set of shapes expressible in this language is more general than in other shape representation systems and is a superset of the parametric polynomials, deformations, and sweeps discussed previously.

Investigation of modeling using the generative modeling approach shows it to be a natural, compact, controllable, and editable shape representation for a large class of shapes. For example, an airplane wing is naturally viewed as an airfoil cross section which is translated from the root to the tip of the wing. At the same time its thickness is modified, it is twisted, swept back, and translated vertically according to other curves. Many other types of objects are naturally described in this way: propellers, turbine blades, even bananas. Those that are not may have parts that are describable in this way. The use of Boolean operations, deformations, and other synthetic techniques can then complete the specification.

The generative modeling approach allows the construction of parameterized objects, called *meta-shapes*. A meta-shape takes scalar quantities, curves, or other parameters as inputs and produces an output shape, called an *instance.* For example, an extrusion can be viewed as a meta-shape whose inputs are a 2D curve to be extruded and the height of the extrusion. Once a meta-shape exists, it provides a highly controllable and editable method of designing instances, often simply by modifying 2D curves.

Renderability

Although direct rendering of shapes in the approach is difficult, interactive rendering speed is achieved through conversion to a more suitable form such as a polygonal mesh. This conversion can be done quickly, with only ad hoc error control, or more slowly with direct control over approximation error. Slower, higher quality rendering is also possible with ray tracing.

Analyzability

The representation admits a diverse set of operations, including many unavailable in other modeling systems. These operations can be used to compute physical quantities like arclength, surface area, and volume of objects. They can be used to compute the proximity of objects to a specified tolerance, to approximate curves of intersection of surfaces to a specified tolerance, and to choose parameters for parameterized objects that solve a given system of constraints and/or optimize a given function. To compute these operations, shapes are not approximated by a less general form such as a collection of polygons or polynomial patches. Instead, operations are done directly on the shapes as specified so that errors can be controlled, even when intermediate results of operations are fed back to produce more complicated shapes.

The technique of interval analysis allows operations to be done directly on shapes represented as multidimensional parametric functions. At the same time, it gives control over approximation and numerical error.

1.4.1 Previous Work Related to Generative Modeling

Much of the work in geometric modeling forms the basis of generative modeling. In particular, the idea of sweeps (Section 1.2.4) forms the conceptual basis of the generative modeling shape representation. Little research, however, has focused on the following questions:

- how can sweeps be specified by the modeler in a general and powerful way?
- what tools are appropriate to allow swept shapes to be rendered and simulated?

This thesis research has been an attempt to expand the power of the sweeping technique, and provide robust tools for rendering and analysis of swept shapes.

The idea of geometric modeling with constraints is not new. Researchers have studied several modeling systems that employ automatic, numerical constraint solvers. Sutherland's Sketchpad system [SUTH63] solved linear constraints involving line segments and arcs of circles, a technique still employed in many of today's interactive CAD systems. Nelson's JUNO system [NELS85] solves more complicated constraints using Newton-Raphson iteration, still in two dimensions. Borning's THINGLAB [BORN81] supports solution of 3D constraints. While the use of constraints in geometric modeling is frequently convenient, it is only one possible design style. A procedural approach, in which the shape is directly transformed via an explicit formula is also a useful design style. The generative modeling approach combines both design styles by making constraint solution a primitive operator, which can be combined procedurally with other operators. A numerical solution method is also presented that is more robust than local iteration methods which typically require a good starting point to converge.

Rossignac [ROSS88] has advocated the idea of using a high-level representation for shape. Conventional CAD systems interpret the modeler's specification to produce a list of low-level operations on the model. The original specification is then discarded or stored independently of the resulting model. He proposes a CAD system which captures the high-level intent of the designer using an interpreted language. A 2D prototype system, called MAMOUR, is described which implements these ideas. The generative modeling approach extends this work to three-dimensional (and higher-dimensional) shapes.

This work also borrows from the work of researchers in sampling and approximating general parametric surfaces. Von Herzen [VONH89] investigates the approximation of general parametric surfaces using Lipschitz bounds, a special case of an interval method. In this work, a single Lipschitz constant was specified for the entire parametric shape. The generative modeling approach extends this work by generalizing the kind of inclusion functions used, and providing for automatic generation of the inclusion function. The bounds thus obtained are much tighter and are automatically computed from the shape representation.

Although it has received scant attention, the use of interval methods in computer graphics and geometric modeling is not new, Mudur and Koparkar [MUDU84] presented an algorithm for rasterizing parametric surfaces using interval arithmetic. They also suggest the utility of such methods for other operations in geometric modeling. Toth [TOTH85] has demonstrated the usefulness of interval based methods for the direct ray tracing of general parametric surfaces. Most recently, interval methods have been used for error bounding in computing topological properties of toleranced polyhedra [SEGA90].

1.4.2 New Work in this Thesis

The following new work is presented in this thesis:

- An approach to geometric modeling is described which is new in several respects:
  - It handles multidimensional and parameterized objects, and objects of different dimensionality simultaneously.
  - It encourages the combination of low-dimensional shapes, especially 2D curves, into higher-dimensional objects.
  - It is based on a shape description language of greater generality than used in previous work. In particular, it makes available operators such as integration, differentiation, constraint solution, and global minimization as modeling primitives.
  - It advocates a separation of the design process into the design of meta-shapes and instances.
  - It controls errors through a consistent use of interval based methods.
  - It is extensible and modular. The representation is based on a set of primitive operators on parametric functions, each having a few methods.
- A set of examples is presented illustrating how a modeler constructs shape using the generative modeling approach. Many of these examples involve modeling paradigms not described elsewhere.

- A new application of interval based algorithms to geometric modeling is described, to solve problems such as:
  - proximity computation, point enclosure, and ray intersection
  - computing curve and surface offsets without self-intersection
- A set of new algorithms for operating on parametric shapes is described, including
  - approximating implicitly defined curves to user-defined tolerances
  - approximating implicitly defined surfaces to user-defined tolerances
  - approximating parametric surfaces according to user-defined sampling criteria
  - approximating the results of CSG operations on solids bounded by parametric surfaces
- A prototype system, called GENMOD, is described which includes an interpreter for the shape representation language, and a set of interactive tools for shape visualization and analysis.

Chapter 2

Shape Representation

In Chapter 1, a set of shape representations was examined and a new approach, called generative modeling, was summarized. This chapter defines generative models and discusses their utility in shape modeling. It examines how generative models may be represented in a way that is easy to specify, render, and analyze. Specifically, it answers the following questions:

- Why represent generative models as parametric functions specified by recursive operators?
- What set of recursive operators should be used?
- What computations should be performed on generative models? How should these computations be performed?

Finally, this chapter looks at the history of generative modeling representations that have been implemented as part of this research.

2.1 Generative Models: A Domain of Shapes

A general modeling system could represent any physically meaningful shape (mechanical parts, faces, trees, clouds), so that it could be specified, rendered, and analyzed easily. This is impossible for current technology. Even if we restrict ourselves to man-made, mechanical parts, the representation problem is still very difficult. Modeling systems "solve" this problem by restricting the shapes they deal with to a narrow domain. Polyhedra, parametric polynomials, and Boolean operations on simple solids are the most common shape domains. The goal of this thesis work is to extend the domain of shapes in modeling systems through the use of generative models.

A *generative model* is a shape generated by the continuous transformation of a shape called the generator. Typically, a generative model is formed by transformation of a lower-dimensional generator. As an example, consider a curve $\gamma(u) : \mathbf{R}^1 \to \mathbf{R}^3$, and a parameterized transformation, $\delta(p, v) : \mathbf{R}^3 \times \mathbf{R} \to \mathbf{R}^3$, that acts on points in $p \in \mathbf{R}^3$ given a parameter v. A generative surface, $S(u, v)$, may be formed consisting of all the points generated by the transformation δ acting on the curve γ, i.e.,

$$S(u,v) = \delta(\gamma(u), v)$$

More specifically, a cylinder is an example of a generative model. The generator, a circle in the xy plane, is translated along the z axis. The set of points generated as the circle is translated yield a cylinder. Mathematically, the generator and transformation for a cylinder are

$$\begin{aligned}
\gamma(u) &= \begin{pmatrix} \cos(2\pi u) \\ \sin(2\pi u) \\ 0 \end{pmatrix} \\
\delta(p,v) &= \begin{pmatrix} p_1 \\ p_2 \\ p_3 + v \end{pmatrix} \\
S(u,v) &= \begin{pmatrix} \cos(2\pi u) \\ \sin(2\pi u) \\ v \end{pmatrix}
\end{aligned}$$

Generative models are a general form of sweeps. Sweeps in the CAD and computer graphics literature are limited to the movement of the generator along a trajectory through space, accompanied by simple (usually linear) transformations of the generator. Generators are typically curves in 2D or 3D space. A generative model allows arbitrary transformations of generators. Generators and transformations may be embedded in space of any dimension. They may be functions of any number of parameters. This research has focused on generative models that are continuous and piecewise smooth.

2.1.1 Why Generative Models?

Generative models are natural for specifying many man-made shapes. Manufacturing processes are often conveniently expressed as transformations on generators. For example, the shape of an extruded solid can be represented by a transformation of a planar area. A milled shape can be represented by Boolean subtraction of a generative model from a block (or appropriate initial shape of the work piece). The generative model appropriate in this case is formed by a transformation of the cutter tool shape that simulates its movement through space as it removes material from the work piece.

The usefulness of the generative modeling approach is not limited to the mimicking of manufacturing processes. Totally synthetic generators and transformations can be used. Generative modeling can be seen as a device for human modelers to conceptualize shape. Very complicated shapes can be built with a series of transformations that act on simpler generator shapes. Chapter 3 will discuss many examples of generative models not directly tied to simulation of manufacturing processes.

Generative models are easy to control and edit, since they encourage building high-dimensional shapes from low-dimensional components. For example, it is easier for a designer to specify a few 2D curves controlling the cross section, trajectory, and scaling of a shape than to specify hundreds or thousands of 3D points on the shape.

Generative models are not limited to rigid 3D shapes. They can represent shapes deforming in time, shapes that are functions of manufacturing variables, or shapes composed of nonuniform materials. Such shapes can be represented using generators and transformations that are functions of desired parameters (e.g., parameterized by time), or that are embedded in a space of dimension greater than three (e.g., a 4D space (x, y, z, d) where d is the component representing density). Generative models allow meta-shapes through parameterized generators and transformations. Chapter 3 presents many examples of meta-shapes.

Renderability of generative models is good through approximation by polygons or patches (renderability will be treated in Chapter 4). Analyzability is good for computing integral properties. This thesis presents some further algorithms for analysis using interval methods, as will be discussed in Chapter 5.

2.2 Specifying Generative Models

To make the idea of generative models useful, we need a method of specifying generators and the transformations that act on them. In doing this, we must necessarily restrict the domain of all mathematically conceivable generators and transformations to a set that can be specified in a computer-implementable system. Choosing a method of specification involves a trade-off between power of expression and speed of computation.

This thesis proposes specifying generative models through recursive operators that build parametric functions. By *recursive* operators, we mean simply that the operators can be applied to their results from a previous application (e.g., the unary operator `op` can be reapplied to its result on an argument `arg`, as in `op(op(arg))`). The following sections motivate and discuss this specification scheme.

2.2.1 Parametric Functions and the Closure Property

As we have seen from the cylinder example, a generative model can be expressed as a parametric function. If a generator is represented as a parametric function, a generative model that transforms this generator is also a parametric function. To see this, let a generator be represented by the parametric function

$$F(x) : \mathbf{R}^l \rightarrow \mathbf{R}^m$$

A continuous set of transformations can be represented as a parameterized transformation

$$T(p; q) : \mathbf{R}^m \times \mathbf{R}^k \rightarrow \mathbf{R}^n$$

where the p argument is a point to be transformed, and the q argument is additional parameters that define a continuous set of transformations. The generative model is the parametric function[1]

$$T(F(x); q) : \mathbf{R}^{l+k} \rightarrow \mathbf{R}^n$$

.

The ability to use a generative model as a generator in another generative model will be called the *closure property* of the generative modeling representation. The use of parametric generators and transformations yields closure because transformation of a generator can be expressed as a simple composition of parametric functions, resulting in another parametric function. In fact, the use of parametric generators and transformations blurs the distinction between generator and transformation. Both are parametric functions; the domain of a generator must be completely specified, while the domain of a transformation is partly specified and partly determined as the image of a generator.

Parametric functions that are evaluated on *rectilinear domains*, domains that are composed of cartesian products of intervals of $\mathbf{R}$, are especially convenient for rendering and computation of global properties. The simple form of the domain makes sampling and integration easy in a computer implementation. As will be shown in Section 2.2.1.2, restriction of the domain of parametric functions to rectilinear subsets of $\mathbf{R}^n$ does not result in a practical loss of generality. Any "reasonable" domain can be expressed as a union of images of parametric functions evaluated over rectilinear domains.

Parametric functions are not the only basis for representing generative models one could choose. Generators and transformations can also be determined by implicit functions. An implicit function describes a shape as the set of points that solve a system of equations rather than as the set of points that are the image of a mapping. We first consider implicitly defined generators. Given a transformation,

$$T(p; q) : \mathbf{R}^n \times \mathbf{R}^k \rightarrow \mathbf{R}^n,$$

and a function that determines an implicit generator,

$$F(x) : \mathbf{R}^n \rightarrow \mathbf{R}^m,$$

[1]More precisely, the generative model is the set of points in the image of $T(F(x); q)$ over a domain $U \subset \mathbf{R}^{l+k}$.

a generative model can be expressed as the set

$$\left\{ T(x;q) \mid F(x) = 0,\ q \in \mathbf{R}^k \right\}.$$

Such a generative model representation is partly parametric and partly implicit; that is, a generative model is represented as a parametric function part of whose domain is specified implicitly.

The set of transformations can also be determined implicitly. Under certain conditions, a function

$$T(p;q) : \mathbf{R}^n \times \mathbf{R}^k \rightarrow \mathbf{R}^k$$

can be seen as a transformation of p by determining a q for each p that solves $T(p;q) = 0$. Such a formulation has problems in that T may determine more than one or no q for a given p.

Although an implicit representation is valuable in many circumstances, rendering of general implicit shapes is a costly computation. Interactive rendering methods currently available require computation of the boundary of a shape, which must be approximated as a mesh of polygons or polynomial patches. Finding points on an implicitly represented shape requires numerical solution of systems of equations. In contrast, a parametric representation can often be rendered by repeated evaluation of simple analytic formulae.

2.2.1.1 Terminology

A parametric function, F, is a function from $\mathbf{R}^n$ (*parameter space*) to $\mathbf{R}^m$ (*object space*) :

$$\begin{aligned} F &: \mathbf{R}^n \rightarrow \mathbf{R}^m \\ X &= (x_1, x_2, \ldots, x_n) \\ F(X) &= (F_1(X), F_2(X), \ldots, F_m(X)) \end{aligned}$$

The variables $x_1, x_2, \ldots, x_n$ are called the *parametric variables* or *parametric coordinates.* The number of parametric coordinates on which F depends, n, is called the *input dimension* of the parametric function. The number of components in the result of F, m, is called the *output dimension* of the parametric function. The parameter space used for evaluation is a

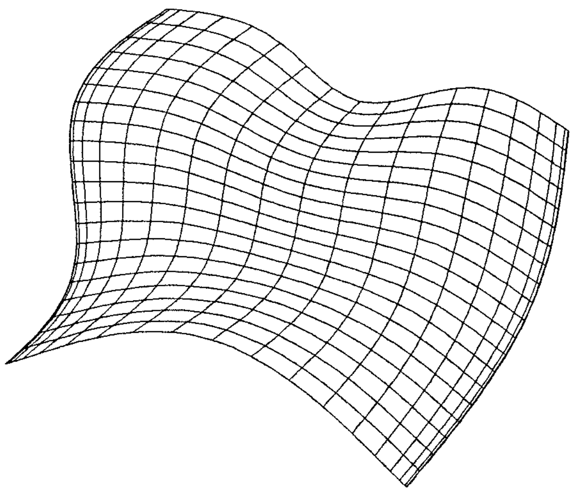

Figure 2.1: Rectilinear parametric function with $\mathbf{R}^2$ topology – A parametric function representing a warped sheet is defined over the rectilinear domain $[0,1] \times [0,1] \subset \mathbf{R}^2$. Its parameterization is one-to-one and hence is topologically identical to $\mathbf{R}^2$. The parameter lines over the surface are not periodic, and no singularities or "poles" exist.

rectilinear region of $\mathbf{R}^n$:

$$X = [a_1, b_1] \times [a_2, b_2] \times \ldots \times [a_n, b_n]$$

The image of F over X defines the shape of interest.

2.2.1.2 Non-Cartesian Topology Using Parametric Functions

Many useful shapes have topologies other than that of a rectilinear subset of $\mathbf{R}^n$, such as the surfaces shown in Figures 2.2 through 2.4. As a basis for comparison, Figure 2.1 illustrates a surface whose topology is identical to rectangular subset of $\mathbf{R}^2$. These shapes can be still be represented by parametric functions evaluated on rectilinear domains, by using non-injective (not one-to-one) parameterizations. For example, a surface with spherical topology can be obtained with a parameterization that maps into a point at the limits of one parameter and is periodic in the other parameter. Similarly, a surface with cylindrical topology can be obtained by letting the parameterization be periodic in one parameter, while a surface with toroidal topology can be obtained by letting the parameterization be periodic in both parameters.

Very complicated topologies with many holes and handles can be represented using con-

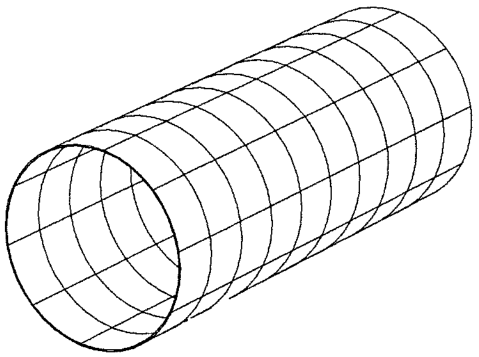

Figure 2.2: Rectilinear parametric surface with cylindrical topology – A parametric function representing a cylinder can be defined over the rectilinear domain $[0,1] \times [0,1] \subset \mathbf{R}^2$ using the parametric function

$$S(u,v) = \begin{pmatrix} \cos(2\pi u) \\ \sin(2\pi u) \\ lv \end{pmatrix}$$

The l parameter controls the length of the cylinder. This parametric function is periodic in the u parameter; that is, for a given v, $S(0,v) = S(1,v)$.

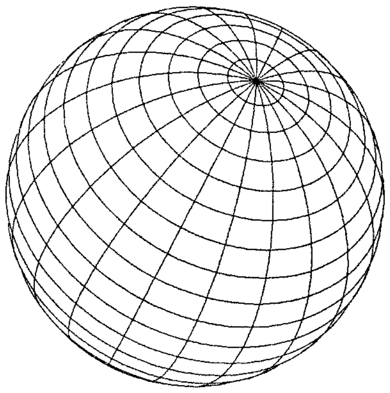

Figure 2.3: Rectilinear parametric surface with spherical topology – A parametric function representing a sphere can be defined over the rectilinear domain $[0,1] \times [0,1] \subset \mathbf{R}^2$ using the parametric function

$$S(u,v) = \begin{pmatrix} \cos(2\pi u)\sin(\pi v) \\ \sin(2\pi u)\sin(\pi v) \\ -\cos(\pi v) \end{pmatrix}$$

This parametric function is periodic in the u parameter; that is, for a given v, $S(0,v) = S(1,v)$. The function has singularities at $v = 0$ and $v = 1$; that is, $S(u,0)$ and $S(u,1)$ are constants with respect to u.

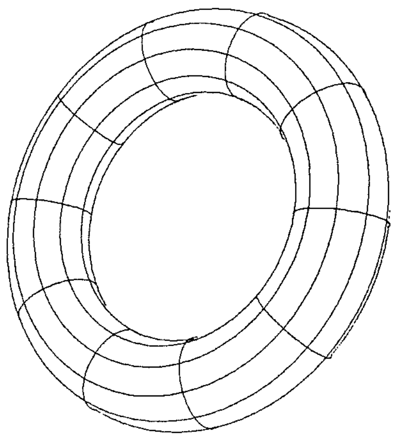

Figure 2.4: Rectilinear parametric surface with toroidal topology – A parametric function representing a torus can be defined over the rectilinear domain $[0,1] \times [0,1] \subset \mathbf{R}^2$ using the parametric function

$$S(u,v) = \begin{pmatrix} \cos(2\pi u)(R + r\cos(2\pi v)) \\ \sin(2\pi u)(R + r\cos(2\pi v)) \\ R + r\sin(2\pi v) \end{pmatrix}$$

The parameter R controls the size of the torus hole, while the parameter r controls the thickness of the torus. This parametric function is periodic in the both the u and v parameters; that is, for a given v, $S(0,v) = S(1,v)$, and for a given u, $S(u,0) = S(u,1)$.

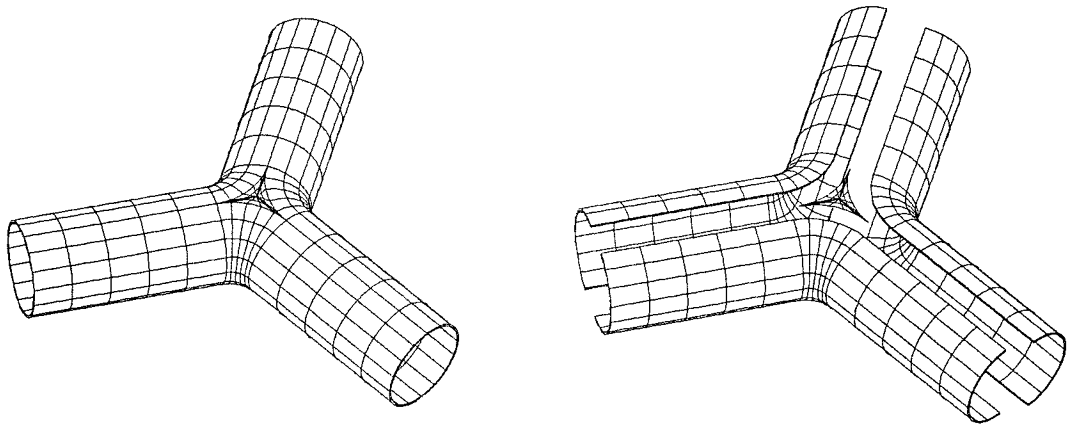

Figure 2.5: A three way branching tube surface can be defined using connected sets of parametric surfaces, each defined over a rectilinear domain. In this example, 5 separate parametric surfaces are meshed together.

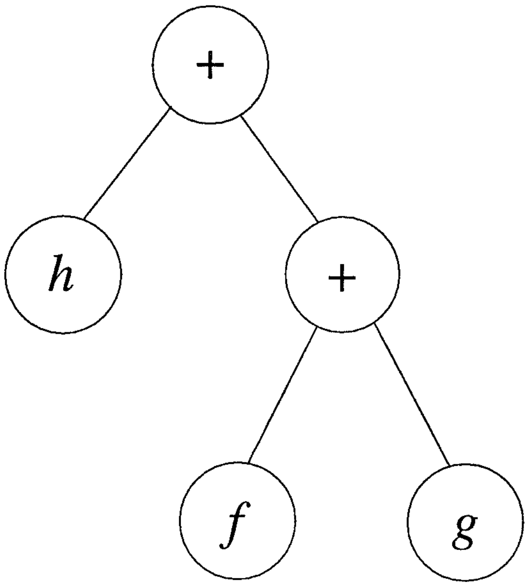

Figure 2.6: A parametric function $(f + g) + h$ is represented as a tree. Addition nodes have two subtrees. The f, g, and h nodes are parametric functions (e.g., constants or parametric coordinates).

nected sets of generative models. For example, Figure 2.5 shows a three way branching tube surface. This surface can not be defined by a continuous mapping from a single rectilinear domain. Instead, it is constructed from five separate, continuous parametric surfaces each defined over a rectilinear domain. Data structures for connected sets of parametric functions that keep track of adjacency information are described in [THOM85].

2.2.2 Using Recursive Operators To Specify Parametric Functions

One way of specifying parametric functions is by selecting a set of recursive operators. A recursive operator is a function that takes a number of parametric functions as input and produces a parametric function as output. For example, addition is a recursive operator that acts on two parametric functions f and g, and produces a new parametric function, $f + g$. The addition operator is recursive in that we can continue to use it on its own results or on the results of other operators, in order to build more complicated parametric functions (e.g., $(f + g) + h$).

A parametric function represented as the composition of recursive operators can be viewed as a tree (see Figure 2.6). Each node of the tree is a recursive operator. Each subtree is a lower level parametric function used as an argument to its parent operator. The terminal nodes of the tree are parametric coordinates or constants.

Of course, it is not enough to represent parametric functions; we must also be able to compute properties about the parametric functions so that the shapes they represent can be rendered and analyzed. Such computations can be implemented by defining a *method* for each operator. The method computes some property of a parametric function given the results of corresponding methods on the subtree parametric functions. Consider evaluation of a parametric function at a point in parameter space. For the addition operator, this can be implemented by evaluating the subtree parametric functions (by calling their respective evaluation methods), and adding the two intermediate results. By writing appropriate methods for each operator, we can compute properties of a parametric function formed by arbitrary composition of these operators.[2]

The use of recursive operators is natural for human beings, and is omnipresent in the language of mathematics and computer science. The use of recursive operators also allows a modular, easily extensible implementation. Extension of the implementation is accomplished by adding new primitive operators, for which a few simple methods should be created. Section 2.2.2.3 will discuss the specific methods required.

2.2.2.1 Characteristics of a Set of Operators

The set of operators used to specify parametric functions should have several characteristics. The set should form a complete basis for all desired generators and transformations using as few different operators as possible. The set should be closed; that is, each operator should accept as an argument the result of any other.[3] The set should be based on the mathematical language of vector calculus and differential geometry, the language developed

[2]This is not to say that every conceivable property of parametric functions is computable in a completely modular fashion. For example, symbolic integration of a parametric function can not be computed simply by integrating the subtree parametric functions and processing the result. Specifically, given two arbitrary parametric functions f and g, we can not compute $\int f/g$ given only $\int f$ and $\int g$. Fortunately, many useful properties about parametric functions can often be computed using recursive evaluation of methods, including evaluation at a point in parameter space, symbolic differentiation, and inclusion functions.

[3]Of course, operators may constrain the output dimension of their arguments. For example, an operator may accept only a scalar function as an argument and prohibit the use of functions of higher output dimension. In special circumstances, it may be desirable to constrain other properties of operator arguments. For example, the inversion operator expects its argument to be a monotonic scalar function. In this context, closure of the set of operators implies that an operator not arbitrarily prohibit any "reasonable" arguments, given the nature of the operator.

by mathematicians experienced in representing and analyzing geometric shape.

Why Aren't Rational Polynomials Enough? Some geometric modeling systems specify parametric functions using rational parametric polynomials. The set of operators in such modeling systems is reduced to polynomial addition, subtraction, multiplication, and division. Such a set of operators is attractive because it limits the complexity of computations required for analysis. Polynomials are very simple to evaluate and integrate (integration is especially easy for nonrational polynomials). Unfortunately, rational polynomials are a limited basis for modeling shapes.

Rational polynomials are not closed under many simple operations. For example, representing the distance between points on two polynomial curves requires a square root operator. Similarly, rotation of curves or surfaces by an exact angle requires operators, such as trigonometric functions, that can't be expressed as rational polynomials. Even a simple arc that is parameterized by polar angle is not expressible as a rational polynomial. Most of the higher-level operations presented in this thesis, such as reparameterizing parametric curves by arclength and computation of intersections between curves and surfaces are also not expressible using rational parametric polynomials.

Modeling systems may solve these problems by approximation. That is, a rational parametric polynomial is computed that is close to the desired shape. This solution has two problems:

1. It implies the existence of a higher-level specification allowing operations that can't be expressed as rational polynomials. Thus, the rational polynomials are reduced to a machine representation. The problem of identifying what types of operations are useful as a user representation remains. This is the central issue addressed by this thesis.

2. Even as a machine representation, rational parametric polynomials suffer problems. Systems using parametric polynomials control errors in a way that leads to numerical instability. Accuracy is achieved either by increasing the number of segments into which polynomial curves and surfaces are divided, or by increasing the degree of the approximating polynomial. As approximate results are fed back to the modeling system, error control quickly becomes intractable. On the other hand, when error

control is done for higher-level operators, more appropriate algorithms can be used and better decisions concerning speed/accuracy tradeoffs can be made.

2.2.2.2 Specific Operators

In this section, we examine specific operators that form a basis for specifying a quite flexible variety of shapes. Many of the operators described here were found to be useful after experimentation in building example shapes. Techniques that seemed convenient in specifying examples were analyzed to extract a small, functionally independent set of operators.

It is not envisioned that the operators described here comprise a set fully adequate for any modeling task. Instead, operators that seem general purpose or immediately useful are described. This set of operators will be used in Chapter 3 to show the capability of the generative modeling approach for combining such low-level operators into complex and useful modeling tools.

2.2.2.2.1 Constants and Parametric Coordinates Parametric coordinates and constants are terminal operators (operators that have no parametric function arguments) that specify the most basic parametric functions. The constant operator represents a parametric function with a real, constant value, such as $f = 2.5$. The parametric coordinate operator represents a particular parametric coordinate, such as $f = x_2$.

2.2.2.2.2 Arithmetic Operators Arithmetic operators are addition, subtraction, multiplication, division, and negation of parametric functions. They are useful for such geometric operations as scaling and interpolation, and in many other more complicated operations. For example, a cross section curve can be multiplied by a constant to yield a scaled cross section. It can also be scaled by a parametric function that relates the amount of the scale to the inputs of the parametric function. Such a scaling parametric function can be used in a sweep surface where the scale of a cross section curve is allowed to vary as a function of a sweep parameter.

2.2.2.2.3 Elementary Operators Elementary operators include square root, trigonometric functions, exponentiation, exponential, logarithm, etc. The square root operator, for example, is useful for computing distance between points in space. The sine and cosine operators are useful in building parametric circles and arcs.

2.2.2.2.4 Vector and Matrix Operators Vector operators include projection, cartesian product, vector length, dot product, and cross product. Projection and cartesian product allow extraction and rearrangement of coordinates of parametric functions. For example, given two 2D curves, an extrusion can be defined by appending the second coordinate of the second curve to the first curve. That is, given two curves $\gamma(u)$ and $\delta(v)$, we define a surface, $S(u, v)$ as

$$S(u,v) = \begin{pmatrix} \gamma_1(u) \\ \gamma_2(u) \\ \delta_2(v) \end{pmatrix}$$

This extrusion definition uses projection to extract desired coordinates of the two curves, and cartesian product to assemble the result into a 3D surface. Vector length, dot product, and cross product find many applications in defining geometric constraints on parameters of meta-shapes.

Vector operator analogs of the arithmetic operators are also useful for geometric modeling. These operators include addition and subtraction of vectors, and multiplication and division of vectors by scalars.

Matrix operators include multiplication and addition of matrices, matrix determinant, and inverse. Matrix multiplication is especially useful in defining quasi-linear transformations, which are used extensively in simple sweeps (see Section 3.1.1.4).

2.2.2.2.5 Differentiation and Integration The differentiation operator returns the partial derivative of a parametric function with respect to one of its parametric coordinates. This is useful, for example, in finding tangent or normal vectors on curves and surfaces. Tangent vectors are useful in defining sweeps where cross sections are moved along a plane curve or space curve, while remaining perpendicular to it. Normal vectors are necessary in computing offsets (see Section 3.1.2.2.1) and generating normals for shading.

The integration operator integrates a parametric function with respect to one of its parametric coordinates, given two parametric functions representing the upper and lower limits of integration. For example, the function

$$\int_{b(u)}^{a(u,v)} s(v,\tau)d\tau$$

can be formed by the integration operator applied to three parametric functions, where $s(v,\tau)$ is the integrand, $a(u,v)$ the upper limit of integration, and $b(u)$ the lower limit of integration.[4] Integration can be used to compute arclength of curves, surface area of surfaces, and volumes and moments of inertia of solids.

2.2.2.2.6 Indexing and Branching Operators A useful operation in geometric modeling is concatenation, the piecewise linking together of two shapes. For example, consider two curves, $\gamma_1(u)$ and $\gamma_2(u)$, that are both parameterized by $u \in [0,1]$. It is often useful to define a new curve, $\gamma(u)$, that first follows γ_1 and then continues with γ_2. Mathematically, γ may be defined as

$$\gamma(u) = \begin{cases} \gamma_1(2u) & u \in [0,\ 0.5] \\ \gamma_2(2u-1) & u \in (0.5,\ 1] \end{cases}$$

Note that γ is continuous if

$$\gamma_1(1) = \gamma_2(0)$$

The concatenation of surfaces or functions with many parameters can be defined similarly, where the concatenation is done with respect to one of the coordinates. A further generalization is concatenation of more than two shapes. For example, the concatenation of the set of n curves $\gamma_1(u), \gamma_2(u), \ldots, \gamma_n(u)$ may be defined as

$$\gamma(u) = \begin{cases} \gamma_1(nu) & u \in [0, 1/n] \\ \gamma_2(nu-1) & u \in (1/n, 2/n] \\ \vdots & \\ \gamma_n(nu-(n-1)) & u \in ((n-1)/n, 1] \end{cases}$$

[4]Of course, the integration operator is not limited to parametric function arguments of this form. The example only demonstrates that one is not limited to functions of a single parameter for the integrand or limits of integration. Furthermore, the functions representing the integrand and limits of integration may share input parameters.

This kind of concatenation is *uniform* concatenation, because each concatenated segment is defined in an interval of equal length $(1/n)$ in parameter space. It is commonly used in defining piecewise cubic curves such as B-splines.

Uniform concatenation can be implemented using a indexing operator, which takes as input an array of parametric functions and an index function that controls which function is to be evaluated. Given the same $\gamma_i(u)$ curves used in the previous example, and an index function q, the index operator is defined as

$$\text{index}(q, \gamma_1(u), \ldots, \gamma_n(u)) = \gamma_{\lfloor q \rfloor}(u)$$

In addition to the indexing operator, it is also useful to have an evaluation operator to define a uniform concatenation. The evaluation operator allows a parametric function to be evaluated so that arbitrary parametric functions are substituted for some of its parametric coordinates. For example, this is necessary for taking one of the parametric curves $\gamma_i(u)$, originally defined for $u \in [0,1]$, and evaluating it instead on $nu - (i-1)$.

The index operator is a special case of a *branching operator*, an operator that allows different parametric functions to be evaluated depending on some conditions. An if-then-else operator is another example of a branching operator useful in shape modeling. Given c, a condition parametric function that evaluates to 0 (false) or 1 (true), and two parametric functions to be evaluated, f_1 and f_2, the if-then-else operator can be defined as

$$\text{if-then-else}(c, f_1, f_2) = \begin{cases} f_1 & \text{if } c = 1 \\ f_2 & \text{otherwise} \end{cases}$$

The if-then-else operator can be generalized to a multiway branch operator, which takes as input a sequence of conditional functions and evaluation functions. The result of the operator is the result of the first evaluation function whose corresponding conditional is true. This multiway branch operator can be used to define a *nonuniform* concatenation of parametric functions where each concatenated segment need not be defined on an equal interval in the concatenated parameter. Branching operators are also useful for implementing useful operators, such as the minimum and maximum of a pair of functions, for defining deformations that act only on certain parts of space, and for detecting error conditions (e.g., taking the square root of a negative number, or normalizing a zero length vector).

2.2.2.2.7 Relational and Logical Operators In order to support the definition of useful conditional expressions for the branching operators, it is useful to have the standard mathematical relational operators such as equality, inequality, greater than, etc. It is also useful to have logical operators (such as "and", "or", and "not") to allow construction of more complicated conditional expressions.

2.2.2.2.8 Curve and Table Operators Curve and table operators allow shapes to be specified from data produced outside the system.

The curve operator specifies continuous curves such as piecewise cubic splines, or sequences of lines and arcs. It is useful in combination with an interactive tool called a *curve editor*, which allows free-form creation of the curves.

The table operator is used to specify an interpolation of a multidimensional data set. For example, a simulation program may produce data defined over a discrete collection of points on a surface or solid. The table operator interpolates this data to yield a continuous parametric function, which can be used in definitions of more complex parametric functions. Additionally, the table operator can be used to approximate parametric functions whose evaluation is computationally expensive.

2.2.2.2.9 Inversion of Monotonic Functions The inversion of monotonic functions is a useful construct for shape definition. For example, one operation that requires such an inversion is the reparameterization of a curve by arclength. This is often a useful operation in computer animation where some object is to move along a given trajectory at a constant speed. To specify the object's trajectory, a curve may be used that has the right geometric shape, but yields a nonconstant speed. In particular, a piecewise cubic spline curve can easily be edited by a human designer to give a desired shape, but can not easily be modified to control the speed resulting from its use as a trajectory.

Let $\gamma(t)$ be a continuous curve specifying the object's trajectory, starting at $t = 0$ and ending at $t = 1$. The arclength along γ, $\gamma_{\mathrm{arc}}(t)$ is given by

$$\gamma_{\mathrm{arc}}(t) = \int_{t_0}^{t} \|\gamma'(\tau)\| d\tau$$

The integration and differentiation operators mentioned previously serve to define γ_{arc}. The reparameterization of γ by arclength, γ_{new}, is then given by

$$\gamma_{\mathrm{new}}(s) = \gamma\left(\gamma_{\mathrm{arc}}^{-1}\left(s\, \gamma_{\mathrm{arc}}(1)\right)\right)$$

The s parameter of γ_{new} actually represents normalized arclength, in that s varies between 0 and 1 to traverse the original curve γ, and equal distances in s represent equal distances in arclength on the curve. This reparameterization involves the inversion of the monotonic arclength function, γ_{arc}.

Many other useful operations can also be formulated in terms of the inversion of monotonic functions. Most often, these operations involve reparameterizing curves and surfaces so that parameters are matched by arclength, polar angle, or output coordinate to some other curve or surface. For example, it is useful to reparameterize a given curve so that its x coordinate matches that of another curve.

Consider two curves that represent how two different parameters are to be varied in some sweep surface. In both curves, the first coordinate is the same sweep parameter, and the second coordinate is the value of the corresponding parameter to be swept. Let $\gamma(u)$ and $\delta(v)$ be two plane curves defined on $u, v \in [0,1]$. Since the first coordinate of both curves is the sweep parameter, we assume that the first coordinate of both curves is a monotonic function of its input parameter and has an identical range.

Of course these curves may be defined so that their second coordinate is a function of the first, i.e.,

$$\begin{aligned} \gamma(u) &= \begin{pmatrix} u \\ y_\gamma(u) \end{pmatrix} \\ \delta(v) &= \begin{pmatrix} v \\ y_\delta(v) \end{pmatrix} \end{aligned}$$

In this case, the two curves are already tied together because $\gamma_1(w) = \delta_1(w)$. However, it may be easier for a human designer to specify the two curves as parametric functions in both the first and second coordinate, i.e.,

$$\begin{aligned} \gamma(u) &= \begin{pmatrix} x_\gamma(u) \\ y_\gamma(u) \end{pmatrix} \\ \delta(v) &= \begin{pmatrix} x_\delta(v) \\ y_\delta(v) \end{pmatrix} \end{aligned}$$

This kind of curve provides more flexibility in defining the desired relationship between sweep parameter and corresponding swept quantity. In this case, we no longer have that $\gamma_1(w) = \delta_1(w)$. One of the curves must be "tied" to the other: reparameterized so that its first coordinate is matched to the other curve. Tying the curve δ to γ can be accomplished using the inversion operator on the first coordinate of δ:

$$\delta_{\text{new}}(u) = \delta\left(\delta_1^{-1}\left(\gamma_1(u)\right)\right)$$

2.2.2.2.10 Constraint Solution Operator The constraint solution operator takes a parametric function representing a system of constraints, and produces a solution to the constrained system or an indication that no solution exists. Two forms of solution are useful: finding any point that solves the system, or finding all points that solve it, assuming there is a finite set of solutions. The operator also requires a parametric function specifying a rectilinear domain in which to solve the constraints.

For example, the constraint solution operator can be used to find the intersections between two planar curves. Let $\gamma^1(s)$ and $\gamma^2(t)$ be two curves in $\mathbf{R}^2$. These curves could be represented using the curve operator of Section 2.2.2.2.8, or using any of the other operators. The appropriate constraint is then

$$\gamma^1(s) = \gamma^2(t)$$

which can be represented using the equality relational operator. The constraint solution operator applied to this constraint produces a constant function representing points (s, t) where the two curves intersect.

Constraint solution has application to problems involving intersection, collision detection, and finding appropriate parameters for parameterized shapes. A robust algorithm for evaluating this operator will be presented in Chapter 5. Note that constraint solution can be used to define inversion of monotonic functions, making the inversion operator of Section 2.2.2.2.9 unnecessary. The 1D inversion operator has been retained because it can be computed using fast algorithms, such as Brent's method [PRES86], not available to an operator as general as multidimensional constraint solution.

2.2.2.2.11 Minimization with Constraints Operator The minimization operator takes two parametric functions representing a system of constraints and an objective function, and produces a point that globally minimizes the objective function, subject to the constraints. The operator also requires a parametric function specifying a rectilinear domain in which to perform the minimization. The minimization operator has many applications to geometric modeling, including

- finding intersections of rays with surfaces, useful in ray tracing
- finding the point on a shape closest to given point
- finding the minimum distance between shapes
- finding whether a point is inside or outside a region defined with parametric boundaries, called point-set classification

For example, consider a parametric surface $S(u, v)$ whose image over a 2D rectangle $D = [u_0, u_1] \times [v_0, v_1]$ forms the boundary of a compact, 3D region. Assume further that this surface has a consistent normal vector, $N(u, v)$, (i.e., N always points outside the interior of the bounded region). The point-set classification problem involves determining whether a point $p \in \mathbf{R}^3$ is inside or outside the region. Let $d(u, v)$ be the distance between a point on S and p

$$d(u, v) = ||S(u, v) - p||$$

Let $(u^{\min}, v^{\min})$ be a point in D that minimizes d, and let

$$\begin{aligned} S^{\min} &= S(u^{\min}, v^{\min}) \\ N^{\min} &= N(u^{\min}, v^{\min}) \end{aligned}$$

Note that $N^{\min}$ is either parallel or anti-parallel to the direction $S^{\min}-p$. We can therefore determine whether p is inside or outside the region bounded by S by

$$\begin{array}{ll} N^{\min}\cdot(S^{\min}-p)>0 & p \text{ is inside } S \\ N^{\min}\cdot(S^{\min}-p)<0 & p \text{ is outside } S \end{array}$$

Thus, unconstrained global minimization can be used to solve point-set classification problems for parametrically bounded regions.

A robust algorithm for evaluating parametric functions that use the minimization operator will be presented in Chapter 5.

2.2.2.3 Operator Methods

An operator method is a function defined for each recursive operator. It allows computation of a property of parametric functions formed using the operator, such as the value of the parametric function at a point in parameter space. The set of methods defined for each operator should be small, permitting convenient addition of new operators. At the same time, the set of methods should compute all the properties of parametric functions required for rendering and analysis. A prototype generative modeling system developed as part of this research has focused on three operator methods: evaluation of the parametric function at a point in parameter space, symbolic differentiation of the parametric function, and evaluation of an inclusion function for the parametric function. These methods will be discussed in more detail in the following sections.

2.2.2.3.1 Locally Recursive Operator Methods In the following discussion, a distinction is made between methods that can be defined in a completely modular fashion and methods that can not be so defined. An operator P that takes n parametric functions as inputs defines a parametric function $p = P(f_1,\ldots,f_n)$. A method on parametric functions is called *locally recursive for P* if its result on p is completely determined by the set of its results on each of the n parametric functions $f_1,\ldots,f_n$. Thus, a method to evaluate a parametric function at a point in parameter space is locally recursive for the addition operator because $f+g$ can be evaluated by evaluating f, evaluating g, and adding the result. A method to symbolically integrate a parametric function is not locally recursive for the division operator, because $\int f/g$ can not be computed given only $\int f$ and $\int g$. Generally, a locally recursive method can be simply implemented and efficiently computed.

2.2.2.3.2 Evaluation at a Point The generative modeling approach proposed in this thesis represents a shape as the image of a parametric function. Such a shape may be approximated by evaluating the parametric function over a series of points in parameter space, and computing a new shape that interpolates the resulting points. The approximate shape is typically a collection of simple, linked pieces, called a *tessellation*. For example, a surface is commonly approximated as a connected set of polygons. Approximate shapes can be used to transfer shape information to software that has no access to the generative representation, such as rendering and simulation modules.

A method to evaluate a parametric function at a point in parameter space is locally recursive for most of the operators discussed previously. Two operators are exceptions: the integration operator and the inversion operator.[5] In a prototype implementation, evaluation of the integration operator is computed numerically using Romberg integration [PRES86, pages 123–125]. As is typical in numerical integration algorithms, Romberg integration requires the integrand parametric function to be evaluated over many points in its domain. The results of repeated evaluations are added to produce an approximate integral. Evaluation of the inversion operator can be computed using a numerical, 1D root finder, such as Brent's method [PRES86, pages 267-269]. As in the case of integration, the parametric function representing the function to be inverted must be evaluated over many points, as the interval bracketing the inverse converges.

Two forms of the evaluation method have proved useful: evaluation at a single, specified point in parameter space and evaluation over a multidimensional, rectilinear lattice of points in parameter space. Evaluation of a parametric function over a rectilinear lattice gives information about how the function behaves over a whole domain, and is useful in "quick and dirty" rendering schemes. Although evaluation over a rectilinear lattice can be implemented by repeated evaluation at specified points, much greater computational speed can be achieved with a special method, as we will see in Chapter 4.

[5]Other operators are also exceptions including the derivative operator, and the constraint solution and global optimization operators. These operators will be discussed further in the next sections.

It has also proved useful to define the evaluation methods so that they return an error condition as well as a numerical result. The error condition signifies whether the parametric function has been evaluated at an invalid point in its domain (e.g., f/g where g evaluates to 0, or $\sqrt{h}$ where $h < 0$). Error checking during evaluation can be used to warn a designer that an interactively specified shape contains errors. It can also be explicitly included in a shape representation through the use of an error operator. The error operator returns the error condition result of evaluating a parametric function. It can be used, for example, as a conditional in a branching operator (e.g., if error($\sqrt{h}$) then $-\sqrt{-h}$ else $\sqrt{h}$).

2.2.2.3.3 Differentiation The differentiation method is used to implement the derivative operator introduced in Section 2.2.2.2.5. The differentiation method computes a parametric function that is the partial derivative of a given parametric function with respect to one of the parametric coordinates. The partial derivative is computed symbolically; that is, the partial derivative result is represented using the same set of recursive operators used to represent the parametric function whose derivative is being computed. For example, the partial derivative with respect to x_1 of the parametric function $x_1 + \sqrt{x_1 x_2}$ yields the parametric function $1 + x_2/(2\sqrt{x_1 x_2})$, which is represented with the addition, multiplication, division, square root, constant, and parametric coordinate operators.

Although the differentiation method is not locally recursive for most operators discussed previously, it is still relatively easy to compute. For example, the partial derivative of the parametric function $h = \cos(f)$ depends not only on the partial derivative of f, but also on f itself, since

$$\frac{\partial h}{\partial x_i} = -\sin(f)\frac{\partial f}{\partial x_i}$$

The differentiation method is therefore not locally recursive for the cosine operator, but may be computed simply if a sine operator exists. Similar situations arise for many of the other operators. Fortunately, it is a simple matter to extend a set of operators such that the set is closed with respect to the differentiation method, meaning that any partial derivative may be represented in terms of available operators.[6]

[6]For example, this implies that if the cosine operator is included in the set of primitive operators, then the sine operator must be included as well. Some operators, such as the global optimization operator, do not have easily expressible partial derivatives. For these operators, the partial derivative must be computed numerically.

In many respects, a symbolic integration method is similar to the the differentiation method discussed here, and could be used to implement the integration operator. The use of symbolic integration can result in much faster evaluation of parametric functions defined with the integration operator. In a prototype implementation, we have chosen not to implement symbolic integration. Parametric functions that use the integration operator are evaluated using a numerical method, rather than by evaluating a new parametric function that is produced by symbolic integration.

Symbolic integration was avoided for two reasons. First, the set of operators discussed in Section 2.2.2.2 can not be closed with respect to the symbolic integration method by adding a finite number of new operators. Second, symbolic integration requires complex and costly algorithms. A better implementation of the generative modeling approach may use existing mathematical symbolic manipulation tools, such as Mathematica. Such a system could compute symbolic integrals when they are representable, reverting to numerical procedures when the symbolic manipulation fails to produce a result.

2.2.2.3.4 Evaluation of an Inclusion Function An inclusion function computes a rectilinear bound for the range of a parametric function, given a rectilinear domain. It is used to evaluate parametric functions defined with the global optimization and constraint solution operators. Chapter 5 will explain how evaluation of these operators may be computed using inclusion functions.

Although an inclusion function computes a global property of a parametric function, it can often be computed using locally recursive methods. As we will see in Section 5.1.2.3, an inclusion function method for the multiplication operator can be computed by simple processing on the intervals resulting from evaluating inclusion functions on the parametric functions being multiplied.

Computing solutions to nonlinear systems of equations and nonlinear, constrained optimization problems is a very difficult problem for systems of arbitrary functions. The approach advocated here restricts the set of allowable functions to those formed by recursive composition of operators for which an inclusion function can be computed. It is quite surprising, but nonetheless true, that such a difficult problem can be solved for this special case, given only a set of methods to evaluate inclusion functions.

2.2.2.3.5 Other Operator Methods The modeling system can be extended by adding a new method to each primitive operator. If the method is locally recursive, then its addition requires little implementation effort. Methods that are not locally recursive require more knowledge of the subtree parametric functions than simply the results of their methods.

An example of a useful operator method is a method that determines whether a parametric function is continuous or differentiable to a specified order over a given rectilinear domain. Many times, algorithms for rendering and analysis require that the functions accepted as input be differentiable (see Section 5.1.3.4.2). The differentiability operator can therefore be used to select whether an algorithm that assumes differentiability is appropriate, or if a more robust (and probably slower) algorithm must be used instead.

The differentiability/continuity method is locally recursive for most of the operators discussed previously, but there are exceptions. For example, the differentiability/continuity method for the division operator can not simply check that the two parametric functions being divided are differentiable. It must also check whether the denominator can evaluate to 0 in the given domain. This is easily accomplished using an inclusion function method.

Other operator methods, whose implementation is still a research issue, include one-to-oneness over a rectilinear domain for functions $f : \mathbf{R}^n \rightarrow \mathbf{R}^n$. A similar method is *degree*, defined as

$$d(f, D, p) = \text{cardinality}\,\{x \in D \mid f(x) = p\}$$

where $D \subseteq \mathbf{R}^n$.

2.3 Development of the Generative Modeling Representation

The representation of generative models proposed in this chapter is not the first representation we imagined or implemented. The representation is the final result of many implementation iterations. These implementation iterations have followed a natural progression starting with systems allowing relatively little interactivity and power of expression and progressing to much more powerful and interactive systems. This section traces the history of generative modeling representations implemented as part of this research.

It is hoped that this discussion will show that the generative modeling approach advocated here is mature, arrived at after rejection of simpler and more obvious possibilities. This historical treatment also identifies for future implementors considerations that are important in a modeling system.

2.3.1 System 1 – Nonrecursive Transformations and Generators

The first generative modeling system we implemented used a predefined, nonrecursive set of transformations. A transformation accepted one or more curves as input, and performed a simple sweep, producing a surface as output. The input curves were used both to specify generators and to specify parameters for parameterized transformations.

For example, the set of transformations included a profile product transformation acting on two planar curves. One planar curve specified a generator, which was translated and scaled according to the second planar curve. Mathematically, the profile product transformation was an operator on two planar curves, $\gamma(u)$ and $\delta(v)$, that produced a surface given by

$$\text{profile\_product}(\gamma, \delta)(u, v) = \begin{pmatrix} \gamma_1(u)\delta_1(v) \\ \gamma_2(u)\delta_1(v) \\ \delta_2(v) \end{pmatrix}$$

Another example of a transformation was the interpolate-and-sweep transformation. It accepted as input two planar cross section curves, a scalar curve specifying how to interpolate between these cross sections, and three more scalar curves specifying scaling (in x and y), and translation (in z) of the cross section. This transformation was defined as an operator on two planar curves, $\gamma(u)$ and $\delta(u)$, and four scalar curves, $\alpha(v)$, $x(v)$, $y(v)$, and $z(v)$, that produced a surface given by

$$\text{sweep}(\gamma, \delta, \alpha, x, y, z)(u, v) = \begin{pmatrix} x(v)(\gamma_1(u)\alpha(v) + \delta_1(u)(1 - \alpha(v))) \\ y(v)(\gamma_2(u)\alpha(v) + \delta_2(u)(1 - \alpha(v))) \\ z(v) \end{pmatrix}$$

Curve inputs to the transformations were selected from a set of parameterized families including constants, lines, arcs, and sinusoids. For example, a family of arcs was parameterized in terms of the arc origin, radius, and two angular limits. Piecewise cubic curves created with a curve editor program could also be used as transformation inputs. A representation of a piecewise cubic curve was transferred from the curve editor program to the modeling program through a file interface.

This early modeling system allowed testing of the generative modeling approach with a minimum of implementation effort, but was essentially unsatisfactory. The representation was limited to surfaces, and the set of transformations and curves were too limited. For example, one could not create a sweep surface where the cross section was translated, rotated, and then translated again. Nor could a curve be formed using useful operations such as the concatenation of several primitive curves. Finally, the modeling process was not sufficiently interactive. One could not see a shape change as the curves used in its specification were edited. Instead, significant time and user interaction were required to write to disk the modified curve files and reread them in the modeling program.

2.3.2 System 2 – Limited Recursive Transformations

We next implemented a generative modeling system whose transformations were expressed using recursive composition of simple, primitive transformations. A shape in this system was represented using an modeling entity called a *u-curve*, mathematically representable as a parametric surface, $S(u, v) : \mathbf{R}^2 \rightarrow \mathbf{R}^3$ A u-curve was recursively defined as a primitive curve, or a transformation of a u-curve specified through a set of parameterized transformations. This recursive definition allowed an arbitrary series of transformations on a primitive curve.

For example, one transformation in this second system translated a u-curve along a coordinate axis. In particular, the translate-in-z transformation was defined as an operator on a u-curve, $T(u, v)$, and a scalar curve, $z(v)$, that produced the transformed u-curve

$$\text{translate-in-}z(T, z)(u, v) = \begin{pmatrix} T_1(u, v) \\ T_2(u, v) \\ T_3(u, v) + z(v) \end{pmatrix}$$

As another example, the set of transformations included interpolation, defined as an operator on two u-curves, $S(u, v)$ and $T(u, v)$, and a scalar curve $\alpha(v)$, that produced the

u-curve

$$\text{interpolate}(S, T, \alpha)(u, v) = \begin{pmatrix} S_1(u)\alpha(v) + T_1(u)(1 - \alpha(v)) \\ S_2(u)\alpha(v) + T_3(u)(1 - \alpha(v)) \\ S_3(u)\alpha(v) + T_3(u)(1 - \alpha(v)) \end{pmatrix}$$

Parameterized transformations included many other types, including

- scaling of any coordinate of a u-curve
- rotation of the u-curve about any axis
- moving a u-curve perpendicular to a trajectory specified by a planar curve or a space curve
- simultaneous translation and scaling of a u-curve, specified by a planar profile curve
- simultaneous translation and scaling of a single coordinate of a u-curve, specified by two "rail" curves
- warping a u-curve by addition of a quadratic function of any of its coordinates to any other coordinate

In each case, transformation inputs were of two types: u-curves and primitive curves. One or more u-curves specified the generator of the transformation, while primitive curves specified other parameters of the transformation (e.g., the scale factor for the scale transformation, or the amount of rotation for the rotate transformation).

This second modeling system represented shape much more flexibly than the first. Composition of any number of transformations, in any order, was allowed. The new system could represent all the transformations in the first system, as well as an infinite variety of new ones. Nevertheless, the second system was lacking in several respects. As in the previous implementation, only 3D surfaces were represented.

Furthermore, the representation of curves in the system was not general enough. Curves were still specified as an instance of a parameterized family or with a curve editor, and could not be modified or operated upon. Curves could not be built using operations that computed distances or derivatives, found intersections between curves, or evaluated a u-curve over a curve in its parameter space. Transformations that could be applied to a u-curve could not be applied to other transformation inputs. For example, the scalar curve parameter of the translate-in-z transformation had to be a primitive curve rather than the interpolation of a pair of scalar curves, or some other transformation of a simpler scalar curve.

One enhancement to the curve specification part of the modeling program was implemented: a reparameterization operator. This operator reparameterized a planar curve based on arclength, x or y component, or polar angle, to produce a new planar curve. It was used to match curves that were used as transformation inputs in the same shape. Although crudely implemented, this operator gave rise to the idea that curves (or more generally, parameterized transformation inputs) should be recursively defined in the same way that transformations were.

While using this second system, we realized that it would be useful to allow users to define their own transformations by packaging a series of primitive transformations into a transformation "subroutine". As an example, the interpolate-and-sweep transformation discussed in Section 2.3.1 could be defined by an interpolation transformation, followed by scale-in-x, scale-in-y, and translate-in-z transformations. We suspected that many shapes could be defined using similar transformation sequences. Therefore, modeling time would be reduced if the modeler could select from a library of such transformation subroutines rather than duplicating the results of the subroutine for each new shape. The next implementation iteration addressed this issue as well as the lack of generality of the curve representation.

2.3.3 System 3 – Fully Recursive Transformations and Generators

The third system represented generative models with fully recursive transformations and generators, as this chapter proposes. Soon after the second system was completed, we realized that an improved modeling system should allow a rich set of operations, such as arithmetic operations, vector and matrix operations, differentiation, and integration. This set of operators should be used to specify both transformation subroutines and the inputs to these transformation subroutines. Transformations should apply equally well to shapes of any input dimension, including curves, surfaces, or solids. Thus, the u-curve of the previous system evolved into a multidimensional parametric function, while the set of primitive transformations on u-curves evolved into a set of primitive operators on parametric functions.

In order to implement a modeling system based on this approach, we added some new features to an existing modeling program. The modeling program accepted a simple command line language to specify surface geometry, associate shading characteristics with the surfaces, position surfaces in the scene, and specify lighting and camera positioning for the scene. We added several new commands to this modeling program to allow specification of curves and surfaces using the new recursive generative modeling approach.

The `surface` command caused the parametric function specified as an argument to be sampled, approximated with a polygonal mesh, and added to the rest of the scene. The specification of a parametric function in this command was aptly described by one user as "lisp without the parentheses". For example, the command

```
surface  output begin  cos mult u twopi  sin mult u twopi   v  end
```

created a cylinder. The `output begin ...  end` operator specified a cartesian product of all the arguments between the `begin` and `end` (three arguments in this case). The `cos` and `sin` operators specified cosine and sine, respectively, of the following argument. The `mult` operator specified multiplication of the next two arguments. Finally, the `u` and `v` operators specified parametric coordinates, and the `twopi` operator specified the constant 2π. These three operators had no arguments. The surface specified in this example is therefore mathematically represented as

$$\begin{pmatrix} \cos(2\pi u) \\ \sin(2\pi u) \\ v \end{pmatrix}$$

This third modeling system also included a facility for defining transformation subroutines. The `define_operator` command was used to define such subroutines by creating higher-level operators that combined the primitive operators. For example, the command

```
define_operator interp 3  a in1 in2  \
    add  in1   mult sub in2 in1 a
```

defined an interpolation operator, called `interp`, which took three arguments, and used the primitive addition, multiplication, and subtraction operators. The operator specified can be mathematically represented as an operator on three parametric functions a, i_1, and i_2

that yields the parametric function

$$\text{interp}(a, i_1, i_2) = i_1 + (i_2 - i_1)a$$

Once defined, an operator could be used in the same way as the primitive operators already present in the system (i.e., in later definitions of surfaces and operators).

We do not hesitate to admit that the language described here was extremely inelegant and hard to use. Most of the syntactic inelegance was caused by grafting the parametric function parsing on top of the crude lexical analysis provided by the original modeling program's interpreter. Still, we were satisfied that the representational approach of this third system was the right one, even if its syntax was inadequate. In addition, the operator definition facility, primitive though it was, proved to be very useful. An extensive library of user-defined operators was developed that defined many kinds of sweeps, and general purpose mathematical operators that interpolated parametric functions, found normal vectors to surfaces, and reparameterized curves. Operators in this library were used repeatedly, saving the modeler the work of reinventing and reimplementing the operator.

Two aspects of this third system seemed particularly in need of improvement. First, the operator definition facility was too limited. It had no access to information about the parametric functions supplied as its arguments. Thus, user-defined operators could not perform error checking to test, for example, that an argument had an appropriate output dimension. Further, the operator definition could not accept arguments such as integers, floating point numbers, strings, or higher-level data structures; only parametric functions were allowed. Finally, operator definitions could not make use of programming language constructs such as loops or conditionals. Only recursive composition of primitive or previously defined operators could be used in the definition of a new operator.

Second, the connection between the generative modeling part and the rest of the modeling program was too restrictive. One could not define and render sets of generative models using programming constructs (e.g., a chain of links could not be specified using an iterative construct like a FORTRAN do statement). Information that could be computed about a generative model, such as its integral properties, could not easily be made available to the rest of the system.

2.3.4 System 4 – Using A General Purpose Language

It became clear that the problems with the third system could be solved if the user interacted with the modeling program through an interpreted, general purpose, programming language. The modeling program would make available to the user, through interpreted function calls, predefined libraries including the generative modeling module, graphics library, curve editor, and multidimensional data visualization module. The user would then have all the modeling system's data structures and code accessible in a single environment, and processable using general programming constructs. In particular, user defined parametric operators could be implemented as interpreted functions, solving the problems mentioned in Section 2.3.3.

This approach was used in the final implementation iteration, a system called GENMOD. Details of GENMOD's user interface can be found in Appendix A. Implementation of GENMOD was guided by the following principles:

- the modeling language should be derived from an already existing basis language. Users who already know the basis language would be spared some of the work required to learn the system. In addition, the programming constructs in the language would be "tried and true" constructs of an existing programming language.
- the modeling language should be interpreted. Users should be able to test and modify ideas for shapes as quickly as possible.
- the modeling language should allow a substrate of non-interpreted code. We expected that full interpretation of even the lowest-level code of the system would be very slow. Therefore, the system should allow some code sequences to be run as compiled units.

GENMOD's use of an interpreted, general purpose language has tremendously simplified the process of extending the system. For example, with only a modest implementation effort, we were able to tie together the shape visualization tool and the curve editor, so that the user can see a shape change as the curves used in its specification are edited.

Chapter 3

Shape Specification Examples

This chapter presents examples of generative shapes. It is not meant to be a complete catalog of techniques for specifying objects. Instead it shows how the generative modeling approach leads a designer to think about shape, and the size of the domain of shapes that can be represented.

3.1 Generative Surfaces

A useful class of generative shapes are 3D surfaces formed by a 1-parameter transformation acting on a curve generator. The curve generator may be thought of as the "cross section" of the generative surface. This section first examines modeling with generative surfaces using simple linear transformations of the generator curve. Next, more complicated and powerful nonlinear transformations are discussed.

3.1.1 Linear Cross Section Transformations

Many shapes can be modeled as a generative surface formed by a quasi-linear transformation of a single cross section. Quasi-linear transformations refer to transformations like translation, rotation, and scaling in 3D space, but will be precisely defined in Section 3.1.1.4.

3.1.1.1 Profile Products

A profile product [BARR81] is perhaps the simplest nontrivial generative surface. It is formed by scaling and translating a 2D cross section according to a 2D profile. More precisely, a profile product surface, $S(u,v)$, is defined using a cross section curve, $\gamma(u) = (\gamma_1, \gamma_2)$, and a profile curve, $\delta(v) = (\delta_1, \delta_2)$, where

$$S(u,v) = \begin{pmatrix} \gamma_1(u)\delta_1(v) \\ \gamma_2(u)\delta_1(v) \\ \delta_2(v) \end{pmatrix}$$

A profile product may be defined in the GENMOD language as follows:

```
MAN m_profile(MAN cross,MAN profile)
{
    return @(cross[0]*profile[0],
             cross[1]*profile[0],
             profile[1]);
}
```

As described in Appendix A, the `MAN` type (for *manifold*) is the basic data structure in GENMOD, which represents a parametric function. The `@()` operator is the cartesian product operator, which, in this case, combines three scalar functions into a 3D point. The `[]` operator returns a single output coordinate of a parametric function. In keeping with C language convention (and unlike the mathematical notation used in the definition of $S(u,v)$ and elsewhere in this thesis), coordinate indexing is done starting with index 0 for the first coordinate, rather than index 1.

Many shapes are conveniently represented as profile products. Cups, vases, and doorknobs, for example, are surfaces of revolution — profile products with circular cross sections. Figure 3.1 shows an example of a profile product doorknob. Profile products need not be surfaces of revolution. Figure 3.2 shows how a profile product can represent a polyhedron, in this case, a patio tile. Figure 3.3 presents an example of a profile product surface for a lamp stand shape.

Although profile products can represent a variety of shapes, they are more limited than one might expect. If the cross section is not *star-shaped* (not single valued in polar coordinates), then the profile product surface may self-intersect.[1] This is because smaller scales of the cross section do not remain in its interior. A different technique must therefore be used to sweep non-star-shaped cross sections. Profile products also have the undesirable

[1]Problems also occur if the profile curve self-intersects, or crosses the y axis.

property that points on the cross section move outwards at a rate proportional to their original distance from the origin and along rays from the origin. A technique for sweeping cross sections so that each point on the cross section moves outwards at the same rate and in a direction normal to the cross section will be discussed in Section 3.1.2.2.1.

3.1.1.2 Wire Products

A wire product is formed by translating a 2D cross section curve along a 2D wire curve, so that the cross section remains perpendicular to the wire. Let $\gamma(u)$ be a cross section curve, and $\delta(v)$ be a wire curve. The normalized tangent vector, t of δ is given by

$$\begin{aligned} \tilde{t}(v) &= \frac{d\delta}{dv} \\ t(v) &= \frac{\tilde{t}}{\|\tilde{t}\|} \end{aligned}$$

A normal vector to the wire curve, n, may be defined by

$$n(v) = \begin{pmatrix} -t_2 \\ t_1 \end{pmatrix}$$

The wire product surface, $S(u, v)$ may then be defined by sweeping the cross section so that its x axis aligns with n, its y axis aligns with the z axis of the wire, and its origin moves onto the wire:

$$S(u, v) = \begin{pmatrix} n_1\gamma_1 + \delta_1 \\ n_2\gamma_1 + \delta_2 \\ \gamma_2 \end{pmatrix}$$

A wire product may be defined in the GENMOD language as follows:

```
MAN m_wire(MAN cross,MAN wire)
{
    MAN t = m_normalize(m_tangent(wire));
    MAN n = @(-t[1],t[0]);
    return @(n*cross[0] + wire, cross[1]);
}
```

Like profile products, wire products are a quite general meta-shape. Figure 3.4 shows an example of a wire product surface representing a tennis racket head frame. Wire products

```
MAN cross = m_circle(m_x(0)*2*pi);
MAN profile = m_crv("profile.crv",m_x(1));
MAN doorknob = m_profile(cross,profile);
```

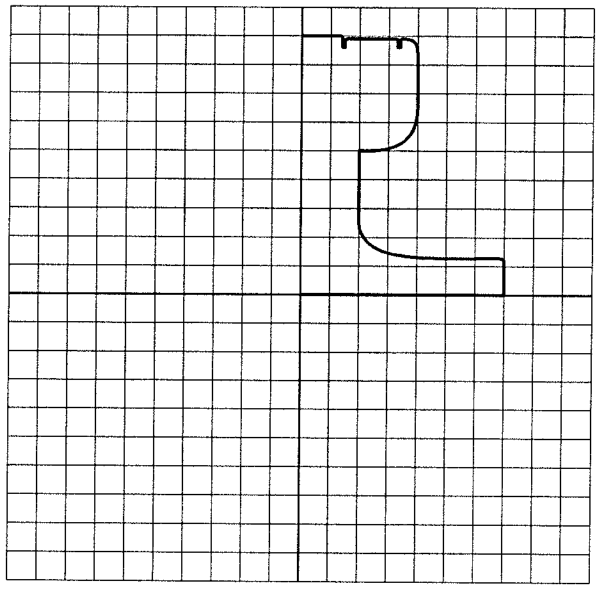

profile.crv

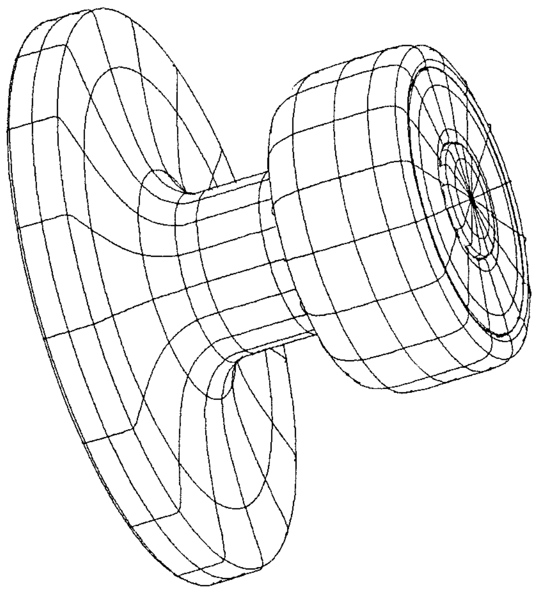

Figure 3.1: Doorknob example — A doorknob shape is represented by a profile surface. The cross section used is a circle; the doorknob is therefore a surface of revolution; The graph of the profile curve is plotted in a square whose extent is from -1 to 1 in x and y.

```
MAN cross = m_crv("cross.crv",m_x(0));
MAN profile = m_crv("profile.crv",m_x(1));
MAN block = m_profile(cross,profile);
```

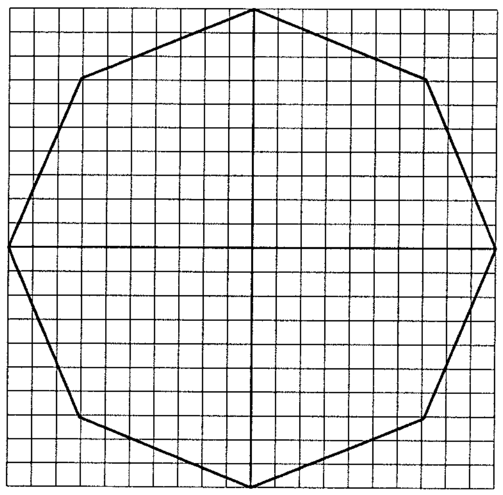
cross.crv

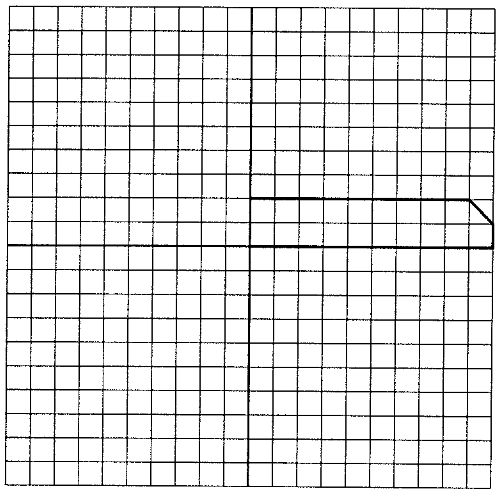
profile.crv

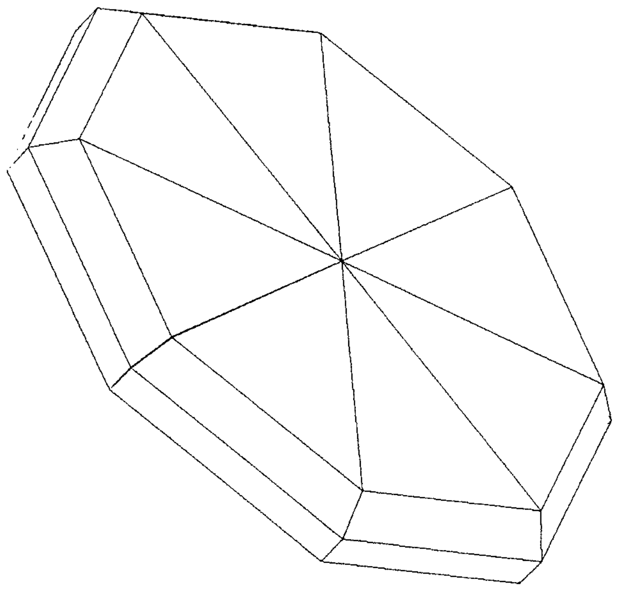

Figure 3.2: Patio tile example — A patio tile shape is represented by a profile surface. In this case, the two curves used in the profile product are composed of straight line segments. The resulting shape is therefore a polyhedron. The graphs of the two curves are both plotted in a square whose extent is from -1 to 1 in x and y.

```
MAN cross = m_crv("cross.crv",m_x(0));
MAN profile = m_crv("profile.crv",m_x(1));
MAN lampstand = m_profile(cross,profile);
```

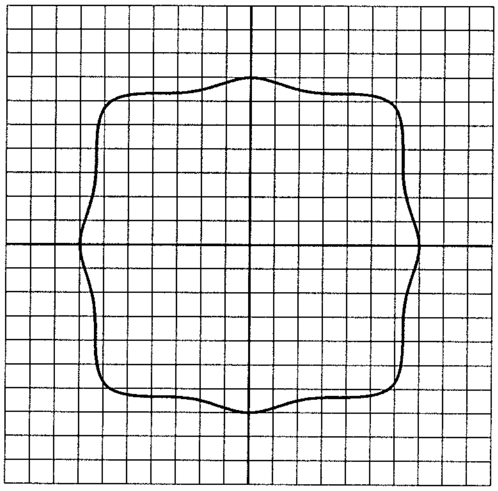

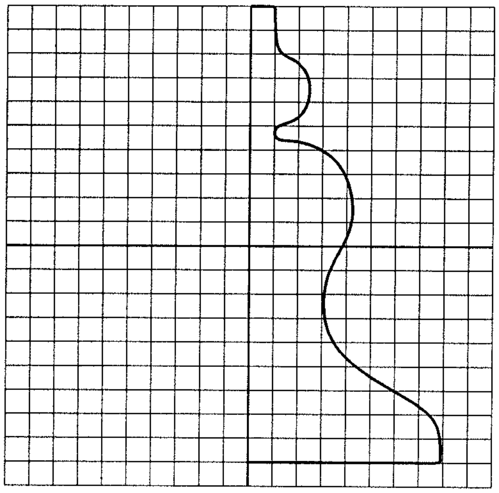

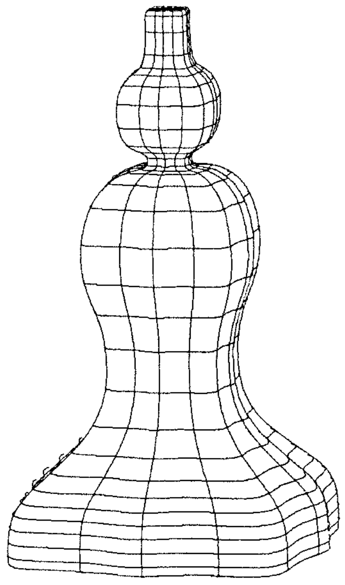

Figure 3.3: Lamp stand example — A lamp stand shape is represented by a profile surface. The GENMOD definition of a lamp stand is shown, followed by graphs of the two curves used in the definition, and a solid shaded image of the shape. The graphs of the two curves are both plotted in a square whose extent is from -1 to 1 in x and y.

self-intersect if the wire curve's radius of curvature is too small in relation to the cross section size.

3.1.1.3 Rail Products

A rail product is formed by sweeping a 2D cross section so that if falls between two 2D rail curves. Let $\gamma(u)$ be the cross section curve, and $\delta^1(v)$ and $\delta^2(v)$ be the two rail curves. The orientation vector, t, between the two rail curves is

$$t(v) = \begin{pmatrix} t_1 \\ t_2 \end{pmatrix} = \delta^2 - \delta^1$$

The rail product surface, $S(u,v)$ may then be defined by sweeping the cross section so that its x axis aligns with t (note that this involves a scale by the length of the orientation vector), its y axis aligns with the z axis of the rail, and its origin moves onto the mid point of the two rail curves, m, where

$$m = \frac{\delta^1 + \delta^2}{2}$$

We then have

$$S(u,v) = \begin{pmatrix} t_1\gamma_1/2 + m_1 \\ t_2\gamma_1/2 + m_2 \\ \gamma_2 \end{pmatrix}$$

A rail product may be defined in the GENMOD language as follows:

```
MAN m_rail(MAN cross,MAN rail1,MAN rail2)
{
    MAN t = rail2 - rail1;
    MAN m = 0.5*(rail1 + rail2);
    return @(0.5*t*cross[0] + m, cross[1]);
}
```

Figure 3.5 shows an example of a rail product surface representing a briefcase handle.

Note that the parameterizations, not just the shapes, of the two rail curves in a rail product are important. A particular cross section in a rail product surface is determined by a point on each of the two rail curves. Therefore the way points on the two rail curves are matched affects the shape of the resulting surface. Section 3.1.4.1 will discuss techniques for matching parameterizations.

```
MAN cross = m_crv("cross.crv",m_x(0));
MAN wire = m_crv("wire.crv",m_x(1));
MAN racket_frame = m_wire(cross,wire);
```

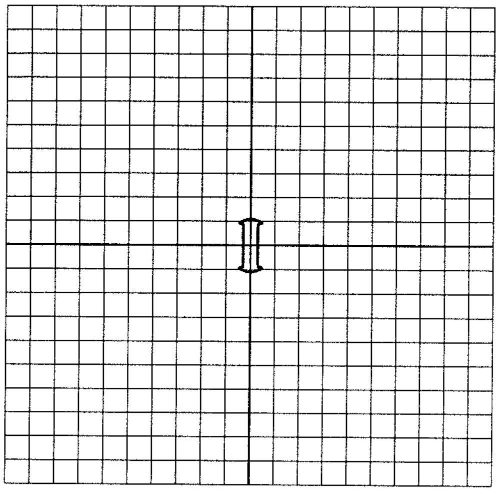

cross.crv

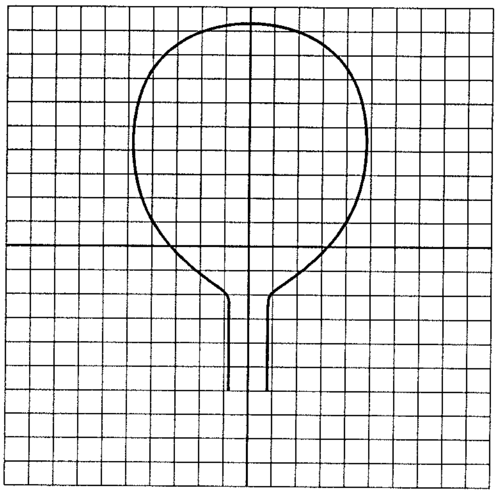

wire.crv

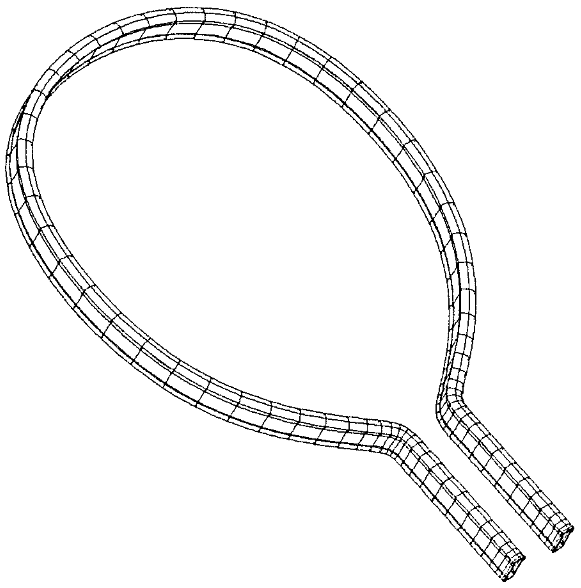

Figure 3.4: Tennis racket example — A tennis racket head frame is represented by a wire product surface. The graphs of the cross section and wire curves are both plotted in a square whose extent is from -1 to 1 in x and y. The cross section `cross.crv` has been scaled by a factor of three for display purposes.

```
MAN cross = m_crv("cross.crv",m_x(0));
MAN rail1 = m_crv("rail1.crv",m_x(1));
MAN rail2 = m_crv("rail2.crv",m_x(1));
MAN handle = m_rail(cross,rail1,rail2);
```

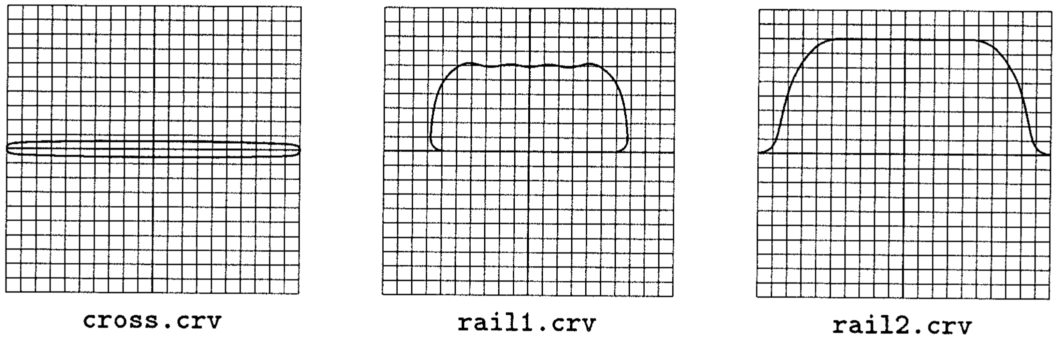

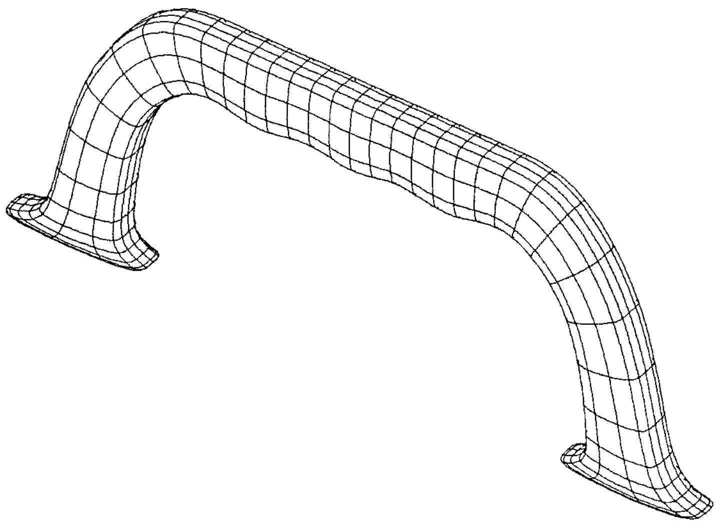

Figure 3.5: Briefcase handle example — A briefcase handle shape is represented by a rail product surface.

3.1.1.4 General Quasi-Linear Transformations

The ideas of the previous sections can be simply generalized with a quasi-linear transformation. Quasi-linear transformations can combine sweep techniques including scaling, translating, twisting, and skewing. They can be used to move a cross section along a given space curve while maintaining perpendicularity of cross section to space curve. They can be used to specify profile products, wire products, and rail products discussed previously,

A quasi-linear transformation shape uses a 2D or 3D curve generator and a transformation represented by a linear transformation and a translation. Let $\gamma(u)$ be a 3D curve. Let $M(v)$ be a linear transformation on 3D space, and let $T(v)$ be a 3D curve. A quasi-linear transformation surface, $S(u, v)$, is given by

$$S(u,v) = M(v)\gamma(u) + T(v)$$

Figure 3.6 presents an example of a quasi-linear transformation that represents a banana surface. Figure 3.7 presents an example of a quasi-linear transformation representing a turbine blade.

One method of representing quasi-linear transformations is to use 4 by 4 matrices. This is the same technique used in computer graphics, called *homogeneous transformations*, to represent 3D transformations including translation and perspective. In the case of a quasi-linear transformation, the 4x4 matrix is defined with M as the upper 3 by 3 part of the matrix, T as the fourth column of the matrix, and the fourth row the same as in the identity matrix. A 3D point is transformed by appending a fourth vector element equal to 1, post multiplying it as a column vector with the 4x4 transformation matrix, and eliminating the fourth coordinate, which is always equal to 1. Mathematically, the quasi-linear transformation is expressed as

$$\begin{pmatrix} S_1 \\ S_2 \\ S_3 \\ 1 \end{pmatrix} = \begin{pmatrix} & M & & T \\ 0 & 0 & 0 & 1 \end{pmatrix} \begin{pmatrix} \gamma_1 \\ \gamma_2 \\ \gamma_3 \\ 1 \end{pmatrix}$$

The advantage of this representation is that it allows quasi-linear transformations to be composed using the matrix multiply operator. Using this technique, we can define a quasi-linear transformation in the GENMOD language as follows:

```
MAN m_transform3d(MAN cross,MAN_MATRIX m)
{
    MAN_MATRIX transformed = m*m_matrix(@(cross,1),4,1);
    return @(transformed.m[0],
             transformed.m[1],
             transformed.m[2]);
}
```

Note that because the matrix transforms the cross section by premultiplying it, the transformations must occur in reverse order (i.e., transformations that affect the cross section first must appear last in the list of multiplied transformations).

3.1.2 Nonlinear Cross Section Transformations

Although a linear transformation of a cross section is quite useful as a modeling primitive, it is too inflexible to represent many common shapes. This section presents some sweep techniques that involve nonlinear transformations; that is, transformations that can not be expressed as a quasi-linear transformation of a single cross section.

3.1.2.1 Interpolating Cross Sections

Many times we want a cross section to change as it is swept in a generative surface. One of the simplest ways to specify this change is to specify two or more cross sections and interpolate between them [BINF71]. This interpolation can be straightforward linear interpolation or a higher order interpolation. For example, hermite interpolation, where tangent vectors as well as points are interpolated, is often useful in yielding a smooth interpolation between cross sections.

3.1.2.1.1 Linear Interpolation Let γ_1 and γ_2 be two points, and let α be a scalar between 0 and 1. A linear interpolation of these points, $\text{linear\_interp}(\alpha, \gamma_1, \gamma_2)$, is given by

$$\text{linear\_interp}(\alpha, \gamma_1, \gamma_2) = \gamma_1 + \alpha(\gamma_2 - \gamma_1)$$

```
MAN u = m_x(0);
MAN v = m_x(1);
MAN cross = m_crv("bancross.crv",u);
MAN scale = m_crv("banscale.crv",v)[1];
MAN banana = m_transform3d(@(cross,0),
    m_roty(m_interp(v,0.0,-0.4*pi)) *
    m_transz(m_interp(v,-1,1)) *
    m_scalex(scale) * m_scaley(scale)
);
```

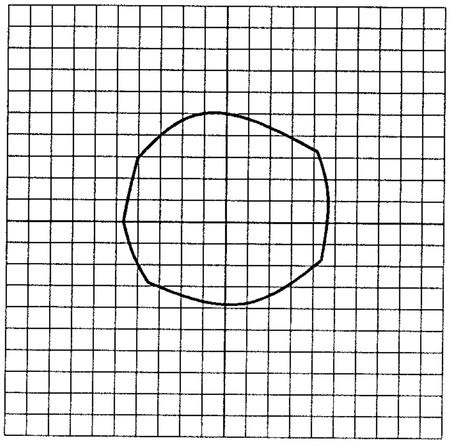

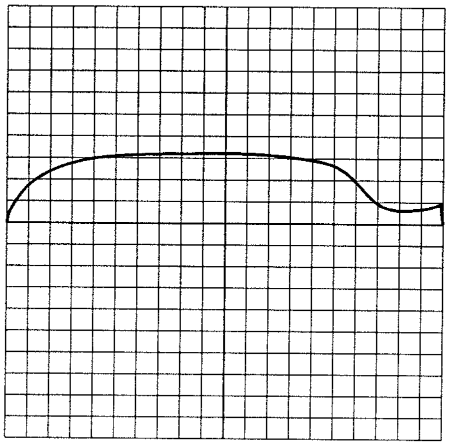

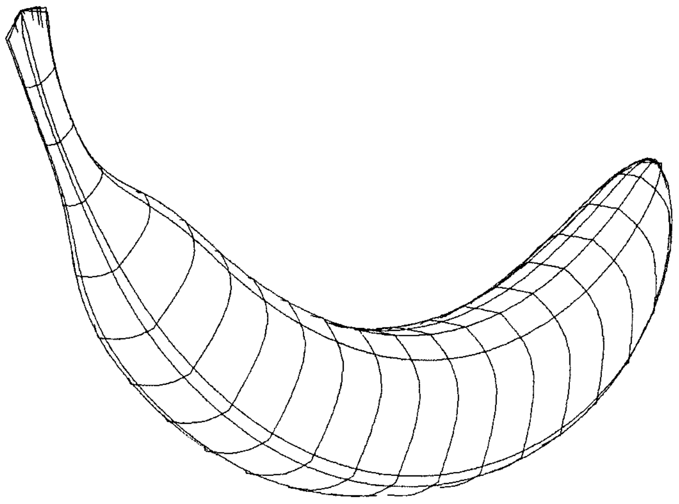

Figure 3.6: Banana example — A banana is represented by a quasi-linear transformation surface. The cross section is scaled, translated along z from -1 to 1, and rotated around the y axis. The graphs of the input curves are both plotted in a square whose extent is from -1 to 1 in x and y.

```
MAN u = m_x(0);
MAN v = m_x(1);
MAN cross = m_crv("bladecross.crv",u);
MAN blade = m_transform3d(@(cross,0),
    m_transz(m_interp(v,-1,1)) *
    m_transx(-0.5) *
    m_rotz(pi*m_crv("bladerot.crv",v)[1]) *
    m_transx(0.5) *
    m_scalex(m_crv("bladexscl.crv",v)[1]) *
    m_scaley(m_crv("bladeyscl.crv",v)[1]) *
);
```

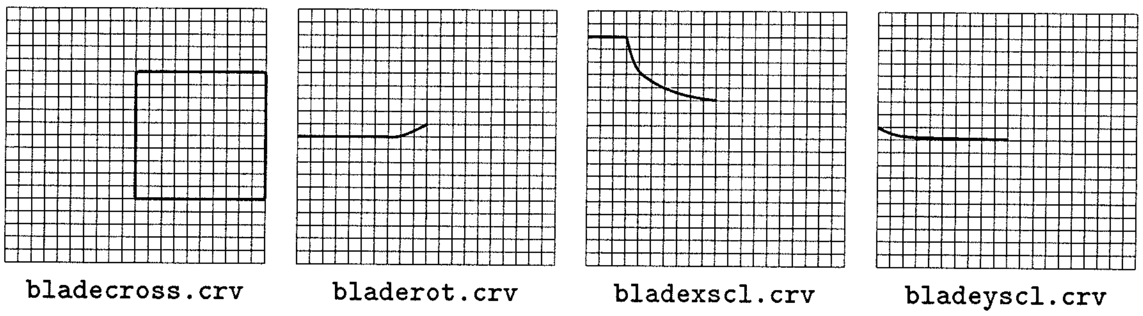

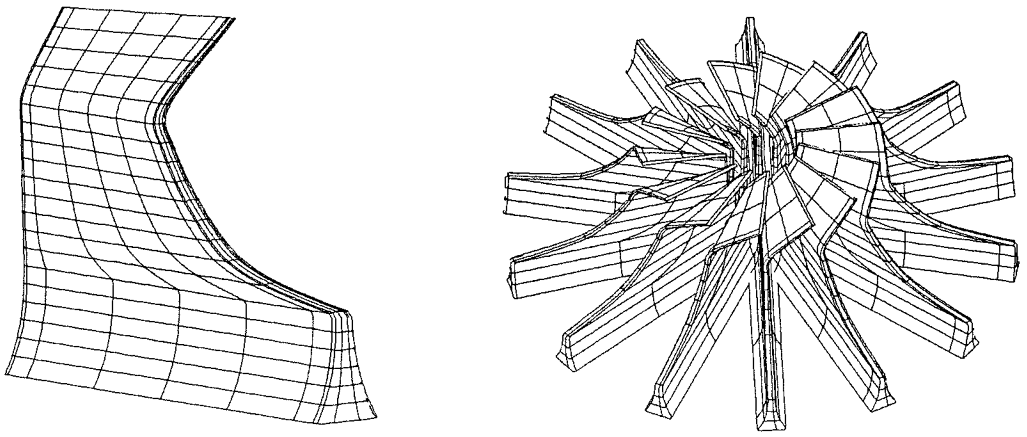

Figure 3.7: Turbine blade example — A turbine blade-like surface is represented by a quasi-linear transformation surface. The cross section is scaled separately in x and y, translated in x, rotated around z, translated back in x, and extruded along the z axis.

When α is 0, linear_interp is equal to γ_1. When α is 1, linear_interp is equal to γ_2. For α values between 0 and 1, linear_interp yields a point on the line segment joining γ_1 and γ_2.

The linear interpolation operator can be applied to curves as well as points. For example, we can define a linearly interpolated cross section using two curves and an interpolation scalar. Let $\gamma_1(u)$ and $\gamma_2(u)$ be the two cross section curves, and let $\alpha(v)$ be a scalar function that varies from 0 to 1. A linear interpolation of these cross sections, $R(u,v)$, is defined by

$$R(u,v) = \text{linear\_interp}(\alpha(v), \gamma_1(u), \gamma_2(u))$$

When $\alpha(v)$ is 0, R is equal to the first cross section. When $\alpha(v)$ is 1, R is equal to the second cross section. For $\alpha(v)$ values between 0 and 1, R is an interpolated cross section such that each point moves on a line joining the corresponding points of the two cross sections.

It is often convenient to use a curve to specify the interpolation function, α, thus relating the interpolation to other sweep parameters. For example, Figure 3.8 shows a gear with a round hole that is formed using linear interpolation. The cross section in this example is a linear interpolation between a gear-shaped curve and a circle. An interpolation curve is used to relate the extrusion of the cross section (in the z direction) to the amount of interpolation.

3.1.2.1.2 Hermite Interpolation Hermite interpolation is an interpolation in which the ending tangent vectors are specified as well as the ending positions. Let p^1 and p^2 be two points in $\mathbf{R}^n$, t^1 and t^2 be two vectors of the same dimension, and α be a scalar between from 0 to 1. The hermite interpolation, $H(\alpha) : \mathbf{R} \to \mathbf{R}^n$, of these points and vectors satisfies

$$\begin{aligned} H(0) &= p^1 \\ H(1) &= p^2 \\ \frac{dH}{d\alpha}(0) &= t^1 \\ \frac{dH}{d\alpha}(1) &= t^2 \end{aligned}$$

```
MAN u = m_x(0);
MAN v = m_x(1);
MAN cross1 = m_crv("cross.crv",u);
MAN cross2 = m_normalize(cross1)*0.25;
MAN interp = m_crv("interp.crv",v);
MAN gear = @(m_interp(interp[1],cross1,cross2),interp[0]);
```

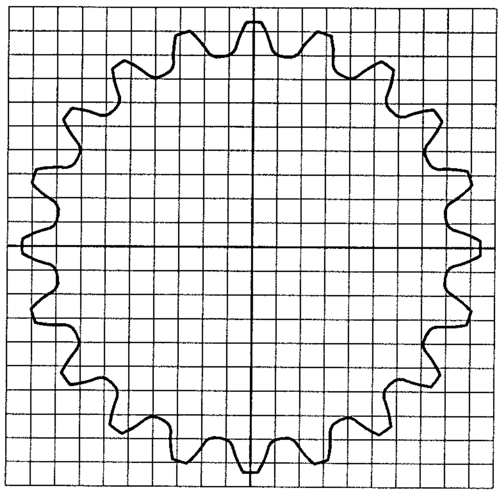

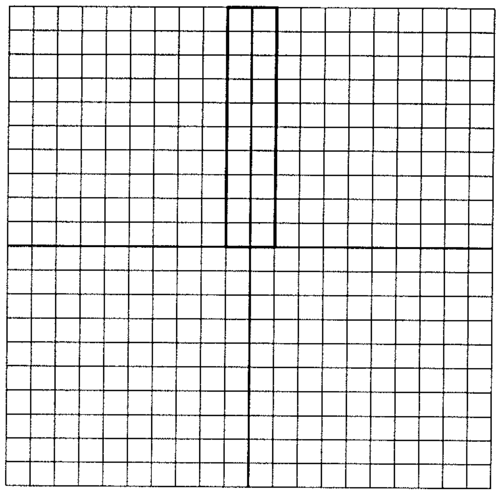

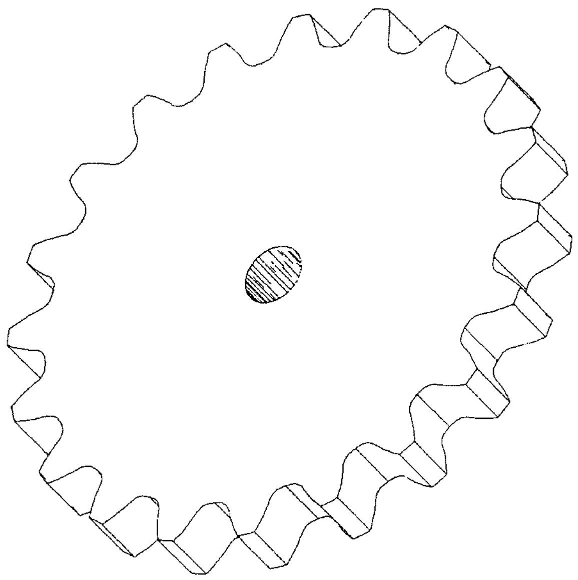

Figure 3.8: Gear example — A gear with a round hole is represented as a linear interpolation of a gear-shaped cross section and a circular cross section.

A cubic polynomial is the lowest degree polynomial for which these constraints can be satisfied. Letting $H(\alpha)$ be a cubic polynomial in α, we have

$$H(\alpha) = a\alpha^3 + b\alpha^2 + c\alpha^1 + d$$

where $a, b, c, d \in \mathbf{R}^n$. Solving for a, b, c, and d in the above constraints yields

$$\begin{aligned} a &= t^2 + t^1 + 2(p^1 - p^2) \\ b &= 3(p^2 - p^1) - 2t^1 - t^2 \\ c &= t^1 \\ d &= p^1 \end{aligned}$$

We can now define a hermite interpolation operator, $\mathrm{hermite\_interp}(\alpha, p^1, p^2, t^1, t^2)$, as

$$\mathrm{hermite\_interp}(\alpha, p^1, p^2, t^1, t^2) = a\alpha^3 + b\alpha^2 + c\alpha + d$$

where a, b, c and d are defined as before.

As in the case of linear interpolation, the hermite interpolation operator can be applied to curves as well as points. In other words, the arguments to hermite_interp can be functions of a parameter instead of constants. In this case, we can use hermite interpolation to define a surface that interpolates between two curves with specified tangents on these curves. This is useful in defining a fillet surface between two surfaces.

For example, Figure 3.9 shows a fillet between a cylinder and a sphere that was specified using hermite interpolation. The two curves being interpolated are the curves of intersection of a fillet cylinder with the sphere, S, and cylinder, C. Let these intersection curves be parameterized by $c_C(u)$ and $c_S(u)$ respectively. To maintain the fillet's smoothness, the direction of the fillet's normal vector must equal that of S and C where it intersects these surfaces. Let the unit normal vectors on S and C at each point on the curves of intersection be given by $n_C(u)$ and $n_S(u)$, and let $F(u, v)$ be the fillet surface. Constraining the fillet surface normal to have the same direction as the normals on the two intersection curves

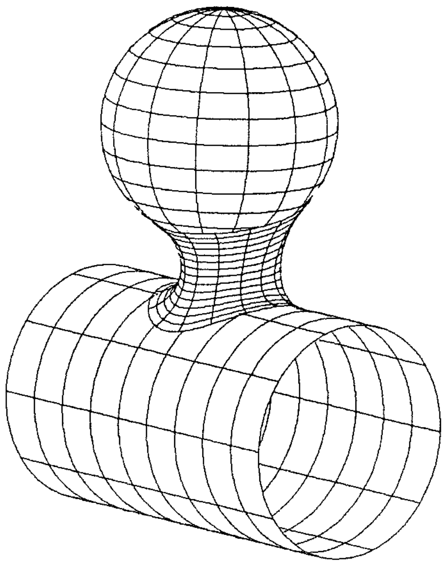

Figure 3.9: Sphere/cylinder fillet using hermite interpolation — A cylindrical fillet between a cylinder and sphere can be accomplished using hermite interpolation as described in Section 3.1.2.1.2. The GENMOD code for this example is given in Section B.1.

yields the following equations

$$\begin{aligned}
\frac{\partial F(u,v)}{\partial u}(u,0) \times \frac{\partial F(u,v)}{\partial v}(u,0) &= \lambda n_C(u) \\
\frac{\partial F(u,v)}{\partial u}(u,1) \times \frac{\partial F(u,v)}{\partial v}(u,1) &= \kappa n_S(u)
\end{aligned}$$

for arbitrary scalars λ and κ. For the hermite interpolation surface $F(u,v)$ defined as

$$F(u,v) = \text{hermite\_interp}(v, c_C(u), c_S(u), t_C(u), t_S(u))$$

the following hold

$$\begin{aligned}
\frac{\partial F(u,v)}{\partial u}(u,0) &= \frac{dc_C(u)}{du}(u) \\
\frac{\partial F(u,v)}{\partial u}(u,1) &= \frac{dc_S(u)}{du}(u) \\
\frac{\partial F(u,v)}{\partial v}(u,0) &= t_C(u) \\
\frac{\partial F(u,v)}{\partial v}(u,1) &= t_S(u)
\end{aligned}$$

Thus the constraints can be solved by setting the tangent vectors $t_C(u)$ and $t_S(u)$ to the following

$$\begin{aligned} t_C(u) &= \eta n_C(u) \times \frac{dc_C(u)}{du} \\ t_S(u) &= \nu n_S(u) \times \frac{dc_S(u)}{du} \end{aligned}$$

for arbitrary scalars η and ν. The choice of η and ν control how much the fillet bends inward near the intersection of the fillet with the cylinder and sphere, respectively. They may be thought of as indirect controls over the fillet "radius". It is even possible to specify η and ν as functions of u.

3.1.2.1.3 Matching Interpolated Cross Sections A significant problem involved in defining surfaces by interpolating cross sectional curves is that the cross sections can be mismatched. This problem is similar to *inbetweening* in computer animation, the automatic generation of many interpolatory points or curves between a small, specified (or *keyframed*) set (see, for example, [BART89]). Consider defining a conical segment by interpolating between two circles, one of radius 1 and the other of radius 2. Let the two circles be given by two parametric functions from $\mathbf{R}$ to $\mathbf{R}^2$, $c(u)$ and $d(u)$, respectively. Simply interpolating $c(u)$ and $d(u)$ as a function of v yields the surface

$$S(u,v) = \begin{pmatrix} c_1(u)(1-v) + d_1(u)v) \\ c_2(u)(1-v) + d_2(u)v \\ v \end{pmatrix}$$

$S(u,v)$ is not necessarily a cone along the z axis whose radius varies linearly from 1 to 2 as a function of z. For example, if the circles c and d are parameterized by polar angle, but c starts at $\theta = 0$, while d starts at $\theta = \pi$, then a cone with a singularity at $z = 1/3$ will result, since points on the circle c are matched to points on the opposite side of the circle d.

Typically, we would like to parameterize the cross section curves to be interpolated so that the projection of the first two parametric coordinates of S forms an invertible map from $(u,v) \in [0,1) \times [0,1]$ to the 2D region contained between the two curves.[2] While this

[2]Because the cross sections are closed, the map is necessarily not invertible everywhere because $S(0,v) =$

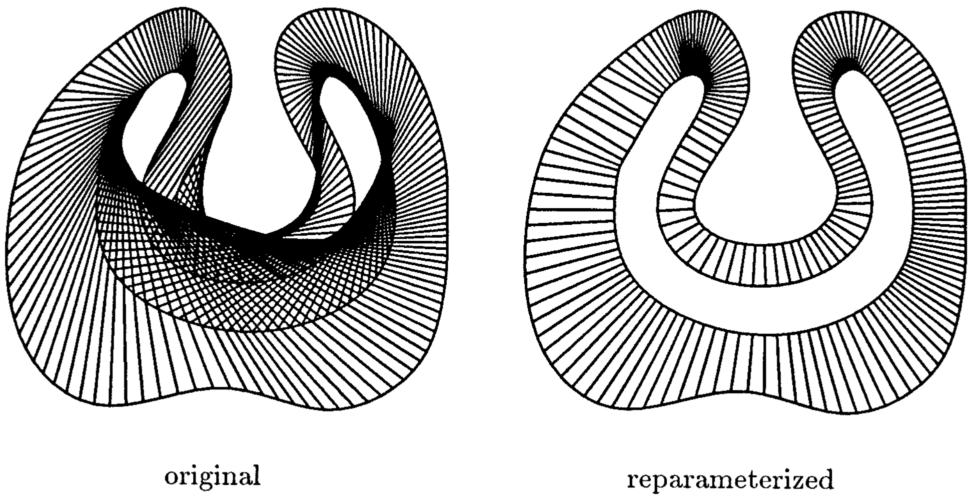

Figure 3.10: Reparameterizing cross sections based on minimum distance – Two closed cross sections are linearly interpolated. On the left, the curves are interpolated without reparameterization. On the right, the inner curve is reparameterized so that each point on it is matched to the nearest point on the outer curve. The linear segments show the matching of points on the two curves. Note that reparameterization is necessary to ensure that the interpolated cross section falls in the region between the two cross sections.

is a hard problem in general, it can be handled in several ways:

- by ad hoc control point matching
- by reparameterizing based on polar angle for star-shaped cross sections
- by reparameterizing based on minimum distance

The first technique gives the modeler the responsibility of specifying matched cross section curves. This is often very inconvenient. If the cross sections are star-shaped, then one can be reparameterized to match the polar angle of the other, using the inversion operator of Section 2.2.2.2.9. Alternatively, the first cross section can be reparameterized so that each point is matched to a point on the second cross section closest to it, using the global optimization operator, as shown in Figure 3.10. Although this technique does not work in every situation, it is useful if the two curves to be interpolated are similar.

$S(1, v)$ for all v. Thus, we restrict the u interval to $[0, 1)$ rather than $[0, 1]$.

3.1.2.2 Cross Section Offsetting

The offset to a smooth[3] planar curve is the curve formed by moving each point on the original curve a given distance along the curve normal. Alternatively, a curve offset may be viewed as the envelope of centers of circles of a given radius tangent to the curve. Two distinct offset curves may be defined for a given planar curve corresponding to the choice of normal vector (e.g., a non self-intersecting closed curve has an inside offset and an outside offset). Figure 3.11 illustrates offsets of planar curves.

Let $\gamma(u)$ be a 2D curve. Let $n(u)$ be the unit normal of γ:

$$\begin{aligned} \tilde{n}(u) &= \begin{pmatrix} -\frac{d\gamma_2}{du} \\ \frac{d\gamma_1}{du} \end{pmatrix} \\ n(u) &= \frac{\tilde{n}}{\|\tilde{n}\|} \end{aligned}$$

In this case, n points outward from a closed, non self-intersecting curve if the curve is traversed counterclockwise. The offset of radius r of γ, offset(γ, r), is an operator that takes as input a 2D curve γ, and a radius r, and yields a 2D curve. It is defined by

$$\text{offset}(\gamma, r) = \gamma + rn$$

The next two sections show examples of the use of curve offsetting in modeling.

3.1.2.2.1 Offset Products Offset products are similar to profile products presented in Section 3.1.1.1. In an offset product, a closed cross section curve is changed by offsetting rather than scaling about the origin as in a profile product.

An offset product surface, $S(u, v)$, is formed given a cross section curve, $\gamma(u)$, and a profile curve, $\delta(v)$. The profile curve relates the radius of offset, r, with the translation of the cross section in the z direction. Let n be the unit normal to the cross section curve γ.

[3] *Smooth* means that the a well defined, nonvanishing tangent vector exists at each point on the curve.

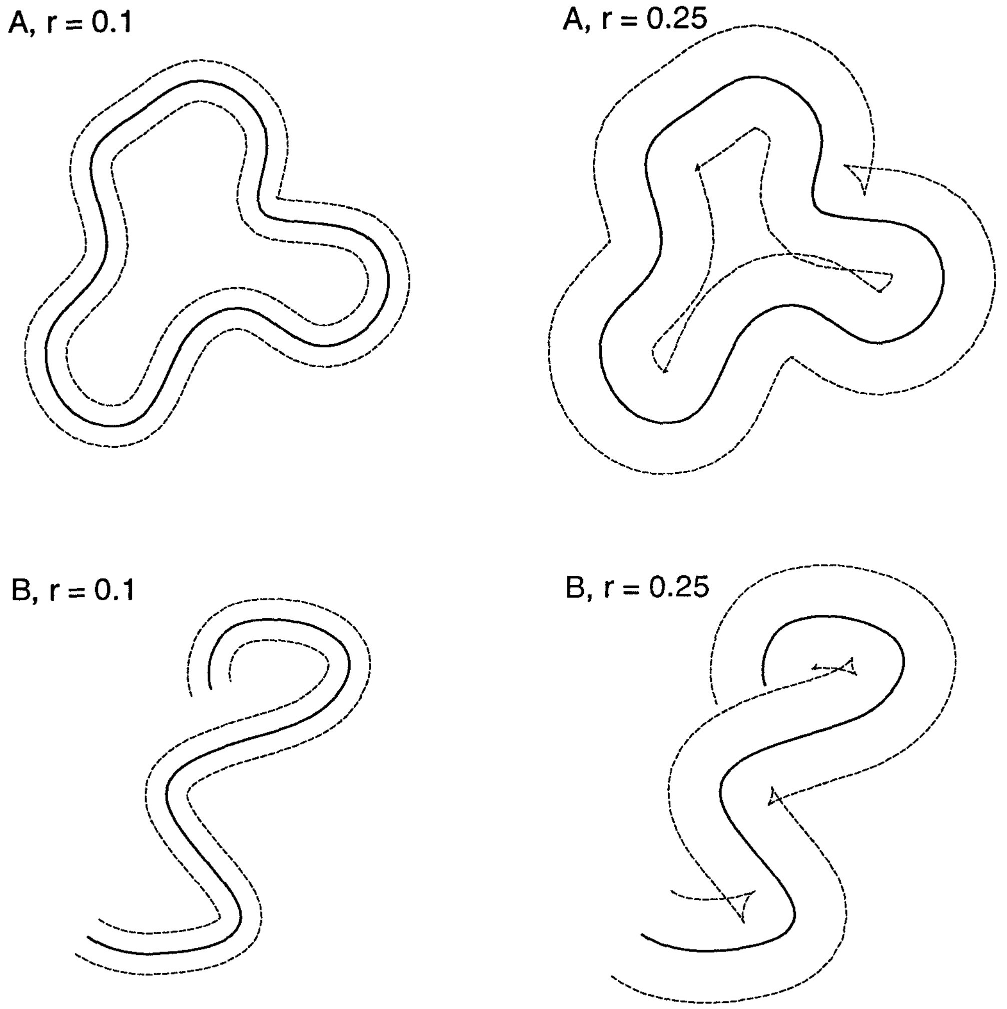

Figure 3.11: Planar curve offsets – Two smooth curves, A and B, are offset with offset radii equal to 0.1 and 0.25. Each curve has two offsets of a given radius, corresponding to the choice of normal vector. Curve A, for example, has an offset corresponding to the inward and outward pointing normals. Note that the offset curves self-intersect and cease to be smooth when the radius of the offset becomes larger than the radius of curvature of the curve, for positive radius of curvature.

$S(u,v)$ is defined by

$$S(u,v) = \begin{pmatrix} \gamma_1(u) + \delta_1(v)n_1(u) \\ \gamma_2(u) + \delta_1(v)n_2(u) \\ \delta_2(v) \end{pmatrix}$$

An offset product may be defined in the GENMOD language as follows:

```
MAN m_offset(MAN cross,MAN prof)
{
    MAN n = m_normalize(m_normal2d(cross));
    return @(cross[0] + prof[0]*n[0],
             cross[1] + prof[0]*n[1],
             prof[1]);
}
```

Offset products are convenient for defining extruded surfaces with rounded corners. Figure 3.12 shows an example of an offset surface that represents a thin plate with semicircular cuts and rounded corners.

3.1.2.2.2 Cross Section Formation Using Offsetting

Curve offsetting can also be used to define a cross section with a given thickness that surrounds a given non-closed curve, (see Figure 3.13). The resulting cross section is composed of four segments: two offsets of a given radius (using the curve normal of both senses), and two semicircular arcs around the endpoints of the curve. Under certain conditions,[4] the resulting curve is the boundary of the set of points whose distance from the curve does not exceed some constant. This constant is equal to the radius of the offset.

Figure 3.14 shows a spoon whose cross section was formed using this technique. In this case, the curve that was offset was a circular arc whose end points and radius are varied.

3.1.2.3 Cross Section Deformations

Deformations such as warps, bends, and tapers, are useful in defining shapes. They are particularly powerful when deformation parameters (such as the amount of bending) are allowed to vary as the cross section is swept. For example, consider a parabolic warping of

[4]The radius of the offset must not exceed the absolute value of the radius of curvature of the original curve.

```
MAN cross = m_crv("cross.crv",m_x(0));
MAN profile = m_crv("profile.crv",m_x(1));
MAN plate = m_offset(cross,profile);
```

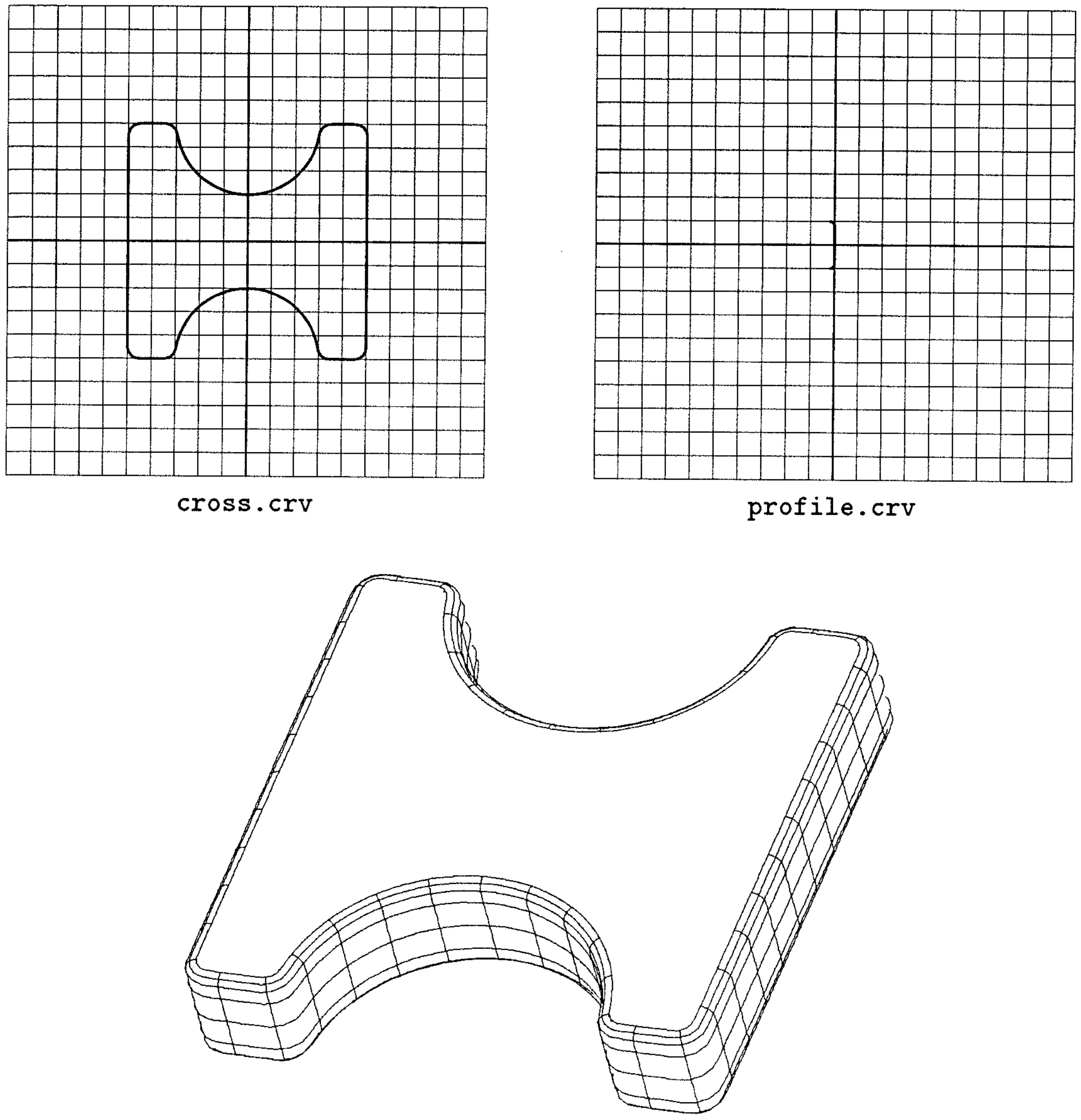

Figure 3.12: Offset product example – A thin plate with semicircular notches is formed using an offset product. The GENMOD definition is actually for the surface forming the sides of plate; the top and bottom are created by drawing two regions bounded by the cross section curve.

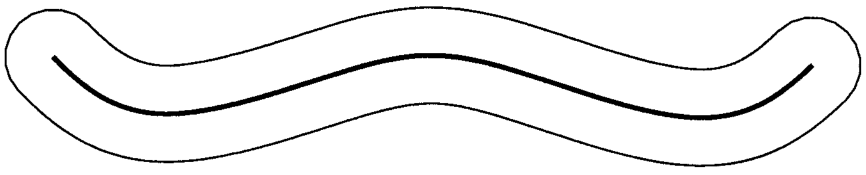

Figure 3.13: Defining a cross section using offsets and circular end caps — A closed cross section may be defined in terms of a non-closed curve by concatenating two offset curves and two circular end caps.

the z coordinate of a cross section as a function of the x coordinate. This deformation may be defined as

$$\mathrm{warp}(a,b)(\begin{pmatrix} x \\ y \\ z \end{pmatrix}) = \begin{pmatrix} x \\ y \\ z + ax^2 + b \end{pmatrix}$$

The amount of warping is controlled by the parameters a and b, which define a parabola. This warp deformation can be defined in the GENMOD language as follows:

```
MAN m_warp_z_by_x(MAN cross,MAN a,MAN b)
{
    return @(x,y,z + a*x@^2 + b);
}
```

Figure 3.15 illustrates the use of this warping deformation to define a key shape from a computer keyboard.

3.1.3 Boolean Operations on Planar Cross Sections

Constructive planar geometry (CPG) is the analog of constructive solid geometry for 2D areas. It is a modeling operation that uses Boolean set operations on closed planar areas to produce new planar areas. Figure 3.16 shows some examples of CPG operations.

CPG is simpler to reason about than CSG because the set operations take place in a lower-dimensional space, on lower-dimensional entities. It is also less costly to compute than

```
MAN u = m_x(0), v = m_x(1);
MAN shape = m_crv("shape.crv",v);
MAN bowl = m_crv("bowl.crv",v);
MAN bend = m_crv("bend.crv",v);
MAN thick = m_crv("thick.crv",v);
MAN p1 = @(-shape[1],0);
MAN p2 = @(shape[1],0);
MAN _arc = m_arc_2pt_height(p1,p2,bowl[1],u);
MAN arc = m_closed_offset(_arc,thick[1]);
MAN spoon = @(shape[0],arc[0],arc[1] + bend[1]);
```

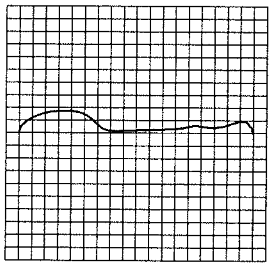
shape.crv

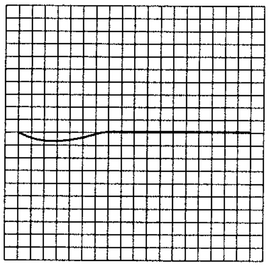
bowl.crv

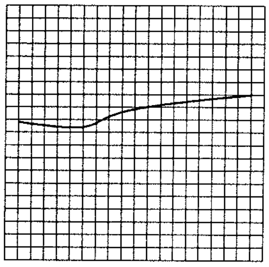
bend.crv

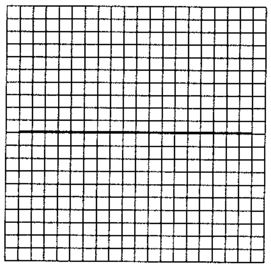
thick.crv

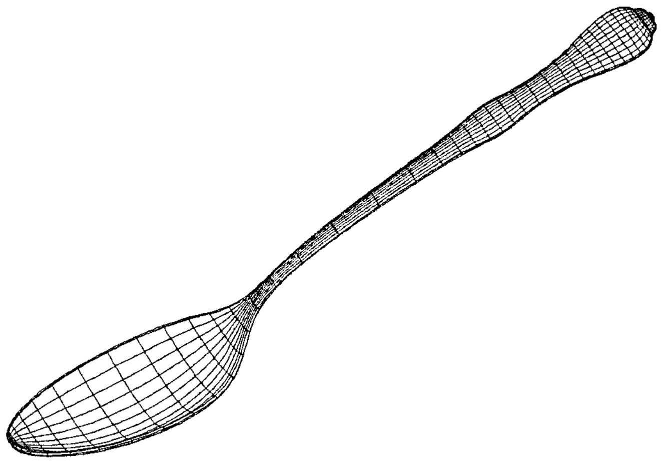

Figure 3.14: Spoon example – A spoon surface is formed using a cross section formed by the closed offset of an arc. A closed offset with circular end caps gives the spoon its thickness. The curve that is offset is deformed as it is extruded – its radius is increased to give the spoon its bowl, and its length is changed to shape the width of the spoon.

```
MAN u = m_x(0), v = m_x(1);
MAN cross = m_crv("cross.crv",u);
MAN yz_l = m_crv("yz_left.crv",v);
MAN yz_r = m_crv("yz_right.crv",v);
MAN xz = m_crv("xz.crv",v);

MAN cross_sides = (cross + @(MAN)(1,1)) * 0.5;
MAN yz_l = m_interp(v,yz_lb,yz_lt);
MAN yz_r = m_interp(v,yz_rb,yz_rt);
MAN x = m_interp(v,xb,xt);

MAN warp_scale = 0.2, warp_offset = -0.05;
MAN _sides = @(m_interp(cross_sides[0],-xz[0],xz[0]),
               m_interp(cross_sides[1],yz_l,yz_r));
MAN sides = m_warp_z_by_x(_sides,warp_scale*v,warp_offset*v);
```

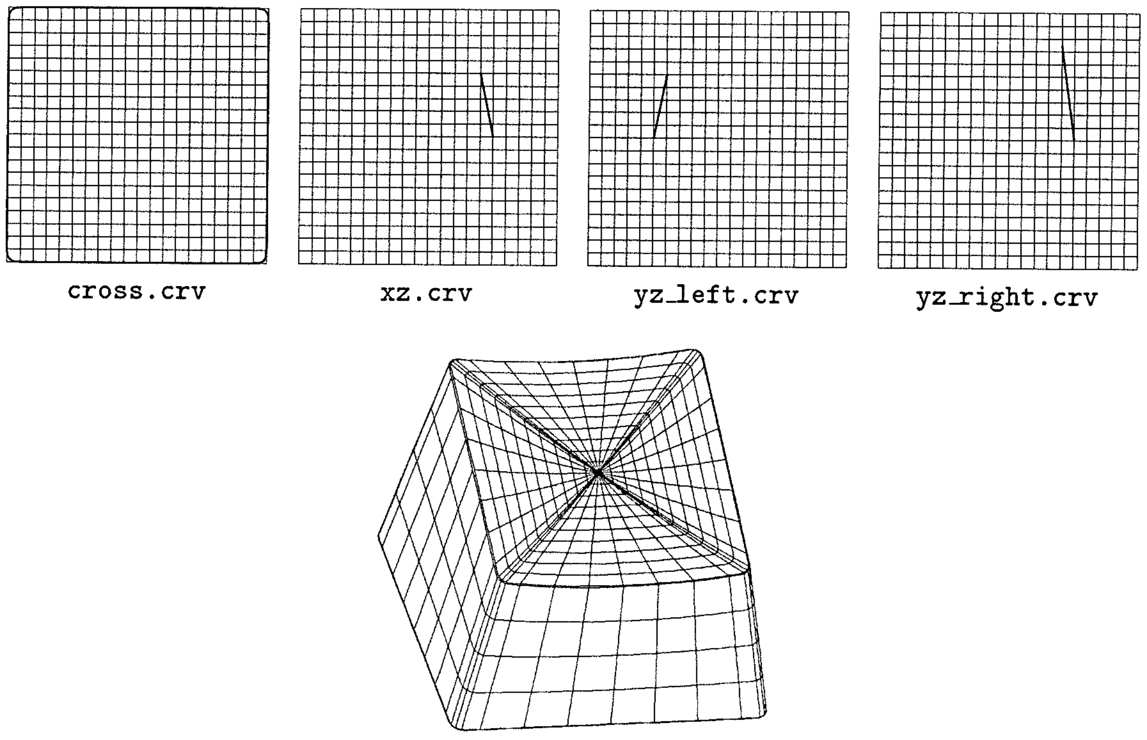

Figure 3.15: Key example — A key shape from a computer keyboard is represented by deforming a rounded square cross section. This cross section is transformed so that it lies between specified curves in the yz and xz planes. The cross section is also deformed using a parabolic warping deformation that causes the top of the key to curve as a function of x. The amount of this warping increases towards the top of the key: at the bottom there is no warping, and at the top there is maximum warping.

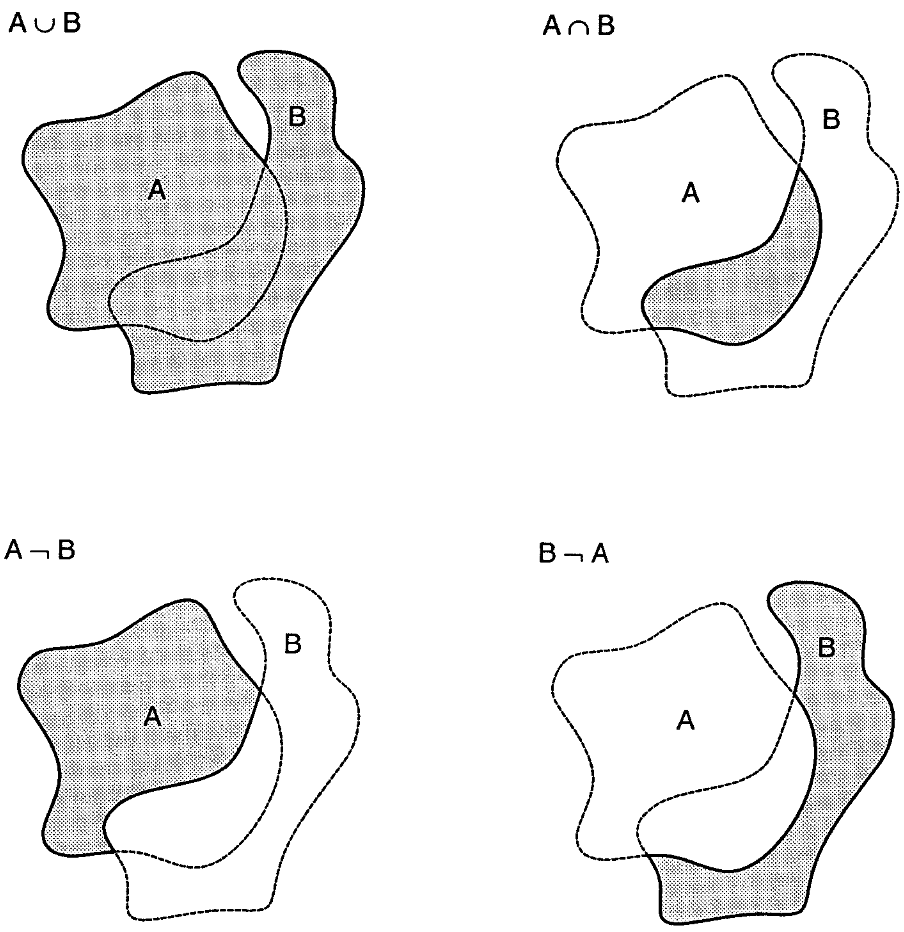

Figure 3.16: Constructive planar geometry – Two planar regions, A and B, are used in four binary CPG operations. The top left figure is the union of the two regions, the top right is the intersection, the bottom left is the subtraction of B from A, and the bottom right is the subtraction of A from B. The boundary curves of the regions are naturally separated into four segments: the boundary of A inside B, the boundary of A outside B, the boundary of B inside A, and the boundary of B outside A. The boundary of the result of each CPG operation is formed by the concatenation of two of these boundary segments. We can compute the boundary of the result of a CPG operation by computing the intersections of the boundaries of the regions, dividing the boundaries into segments at these intersections, and concatenating appropriate segments.

CSG operations. Yet CPG can be an extremely useful modeling paradigm. For example, many objects can be represented as surfaces where each cross section is a Boolean set subtraction of one closed area from another. The fact that the two planar areas may be swept according to different schedules before being subtracted makes the operation more powerful. Figure 3.17 shows two screwdriver blade tips specified using CPG. The Phillips blade, for example, is specified by sweeping a circle with a varying radius, from which is subtracted a notch of varying size.

CPG operations are handled most easily when the boundary of the resulting planar area is a single closed curve. (Note that this is not always the case: the union of two disjoint closed areas is an obvious exception). In this case, computing CPG operations may be accomplished by finding intersections between planar curves that bound the planar areas. These intersections separate the boundary curves into a number of segments. The boundary of the resulting planar area may then be found by concatenating an appropriate set of these segments.

Often, the intersections between boundary curves can be computed analytically. Consider regions whose boundary is represented as a piecewise series of line segments. Intersections between such regions can be computed by solving for intersections between line segments, which can be done analytically. When intersections can not be analytically computed, the constraint solution operator can be used.[5] The resulting segments can then be combined by concatenation as described in Section 2.2.2.2.6.

3.1.3.1 CPG with Filleting

The CPG operations described previously result in cross sections that are not smooth, even if the planar regions operated on have smooth boundaries. Smoothness is not maintained whenever a transition occurs between region boundaries; that is, at points of intersection between region boundaries. To maintain smoothness, we can add *fillets* to the boundary — small segments, such as circular arcs, that allow a smooth transition from one boundary to another. Figure 3.18 shows how this can be accomplished.

[5]The intersections of two planar curves, $\gamma_1(u_1)$ and $\gamma_2(u_2)$, are found by solving $\gamma_1(u_1) = \gamma_2(u_2)$. The constraint solution operator should be applied to this system of two equations (for equality of the first and second coordinates of the two curves) and two variables (u_1 and u_2).

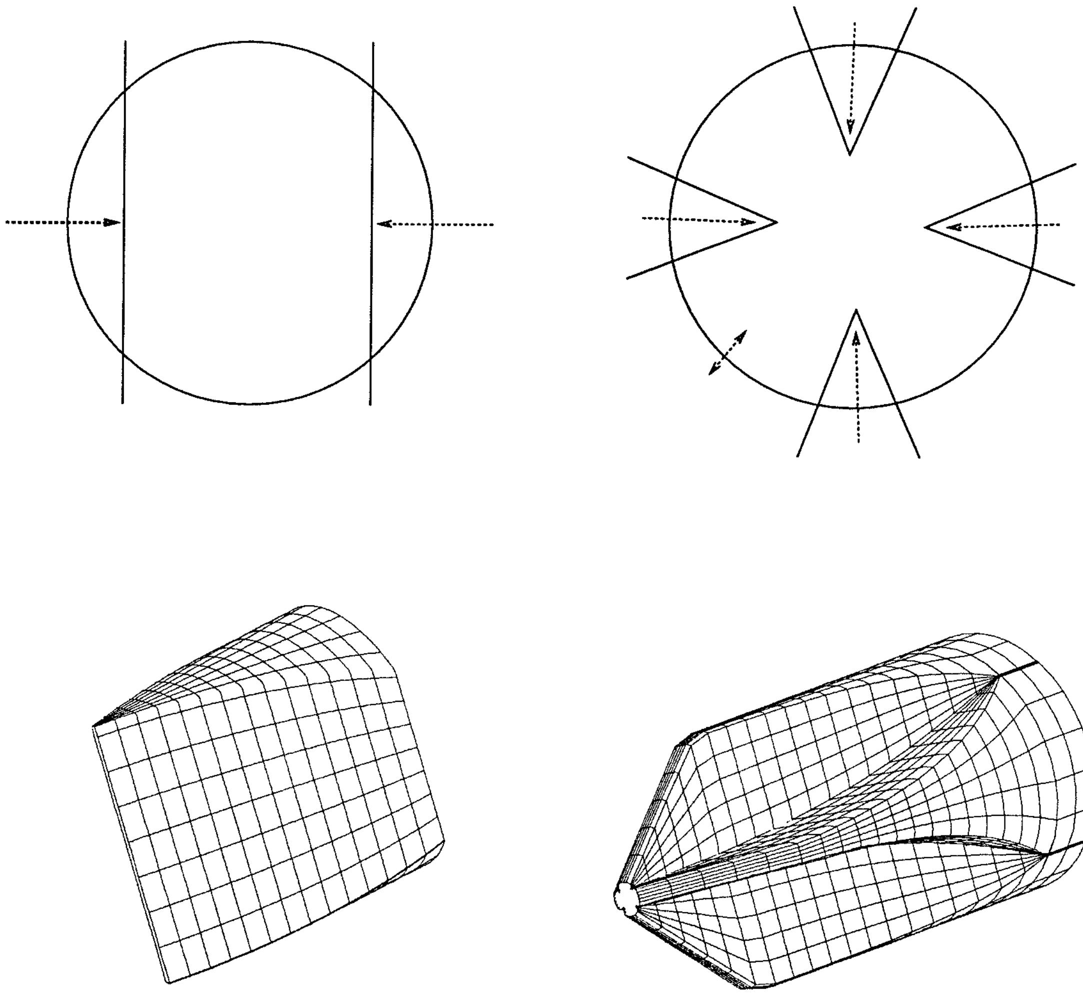

Figure 3.17: Screwdriver example – The tips of two screwdriver blades are constructed using CPG. The regular screwdriver on the left is generated using a cross section formed by subtracting two half-plane regions from a circle. The two half-planes are gradually moved toward each other as the cross section is translated to the tip of the screwdriver. The circle from which the half-planes are substrcted remains constant. The Phillips screwdriver on the right has a cross section formed by subtracting four wedge shaped regions from a circle. In this case, the wedge shaped regions are moved toward the circle's center as the cross section is translated to the tip of the screwdriver. The circle from which the wedges are subtracted is scaled down near the tip to yield a pointed blade. The GENMOD code for both examples is given in Section B.2.

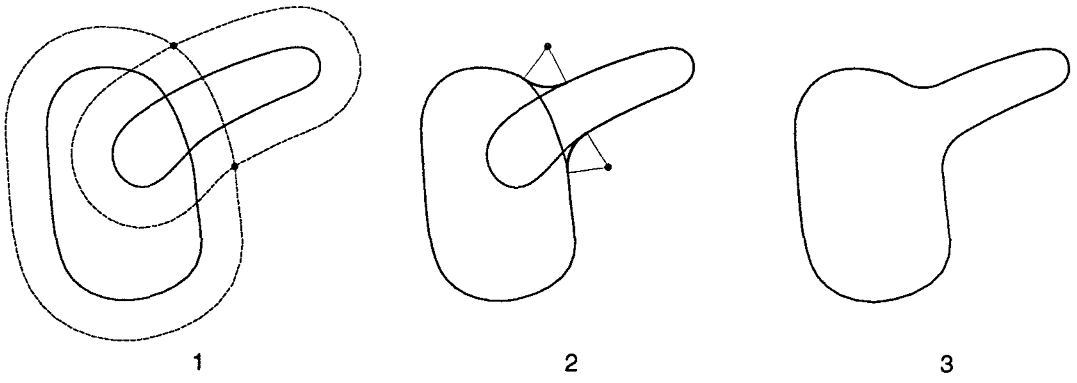

Figure 3.18: CPG with filleting — CPG operations can be done with filleting to produce smooth boundary curves. In this example, we wish to compute a smooth curve that bounds the union of two planar regions. To do this, we first compute the intersections of the offsets of the two curves (step 1). The radius of the offset controls how large a fillet will be used. Next, we compute circular arcs whose centers lie on the intersections of the offset curves (step 2). Each arc endpoint lies on a point on a boundary curve that corresponds to the intersection point on its offset curve. Finally, we concatenate the curve boundary segments and fillet arcs together to produce a filleted curve (step 3).

3.1.4 Parameterizing Cross Sections

Up to now, we have discussed surfaces formed by simple operations on a cross section, including quasi-linear transformations, interpolation, offsets, warps, and Boolean operations. The generative modeling operators allow a much greater range of operations than these. The idea of parameterized cross sections is a useful way of conceptualizing surface shape that takes advantage of the full power of the generative modeling approach.

The modeler designs a cross section curve, γ, given by

$$\gamma(u, x_1, x_2, \ldots, x_n) : \mathbf{R}^{n+1} \rightarrow \mathbf{R}^3$$

The curve γ is parameterized by u, and n additional parameters that affect its shape. A simple example is a circle, parameterized by radius

$$\gamma(u, r) = \begin{pmatrix} r\cos(u) \\ r\sin(u) \end{pmatrix}$$

Of course, the modeler is free to design quite arbitrary cross sections with many parameters, which can control the shape in convenient ways. A surface can than be formed using this parameterized cross section by letting the parameters $x_1, \ldots, x_n$ become functions of a single parameter, v, yielding the surface

$$S(u, v) = \gamma(u, f_1(v), \ldots, f_n(v))$$

Figure 3.19 illustrates an example of a shape formed in this way. In this case, a bottle is constructed using a cross section shaped like the top half of a square rotated 45 degrees. At three points on the cross section, the curve is rounded out. The curve is parameterized in terms of the radius of these rounds. Another curve is then used to relate this radius with other parameters of the cross section, including its scale, translation out of its plane, and warping out of its plane.

3.1.4.1 Matching Parameter Schedules

The most difficult part of representing surfaces using parameterized cross sections is choosing the functions f_i that relate cross sectional parameters to the single surface parameter v. As an example, consider a cross section parameterized by three variables: x_1, which controls the translation of the cross section in z, and x_2 and x_3, which control some specialized properties of the cross section (e.g., the radius of a circle). The surface is formed by simultaneously changing these variables as a function of v. Assuming the variables x_2 and x_3 have a functional relationship with x_1, one method of accomplishing this is to let x_1 vary linearly with v, and to specify x_2 and x_3 with two curves. One curve, $c_2(t)$, relates x_1 (on the x axis) with x_2 (on the y axis). The second curve, $c_3(t)$, relates x_1 (on the x axis) with x_3 (on the y axis). Of course, if c_2 or c_3 are not parameterized by their x coordinate, this requires an inversion operation to find the y value of c_2 or c_3 that corresponds to a given x value (i.e., value of x_1). Such an operation is called *matching* the x_2 and x_3 parameter

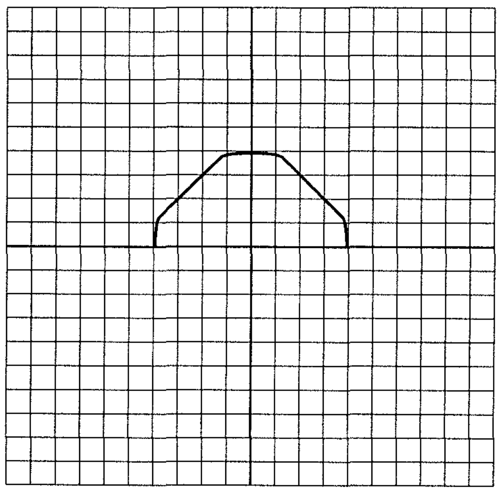

cross section instance

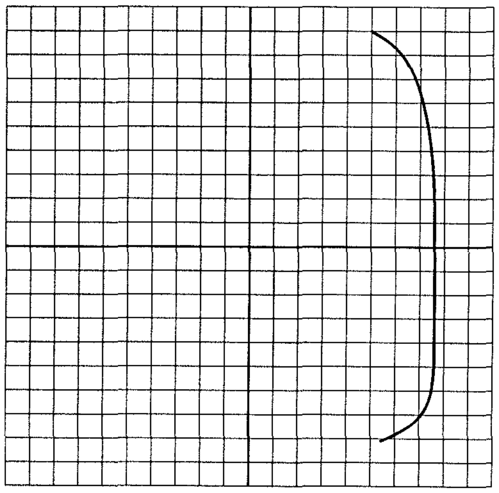

`face.crv`

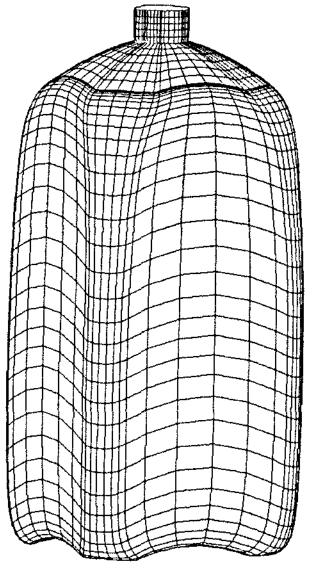

Figure 3.19: Bottle example — A bottle surface is represented by constructing a parameterized cross section. The cross section, for which one instance is illustrated, is parameterized in terms of several parameters. One parameter controls the radius of the circular segments at the left, top, and, right of the cross section. The second curve, `face.crv`, controls how this radius parameter is varied as the cross section is translated out of its plane. The result is one half of the bottle surface, which, when added to its mirror image about the xz plane, forms the whole bottle. The GENMOD code for the bottle example is given in Section B.3.

schedules, and can be achieved with the inversion operator discussed in Section 2.2.2.2.9.

Alternatively, the variables x_1 and x_2 can be related using an arbitrary two dimensional parametric curve, $d_1(t)$, so that we are not limited to a functional relationship between x_1 and x_2. A second curve, $d_2(t)$, can then be used to specify the functional relationship between x_3 and either x_1 or x_2. Again, the inversion operator can be used to match the x_3 schedule, d_3, to d_1.

3.2 Other Generative Shapes

The generative modeling approach allows many types of shapes other than surfaces to be specified. This is achieved by building parametric functions of different input and output dimensions. For example, a time dependent surface may be represented as the parametric function

$$S(u,v,t) : \mathbf{R}^3 \rightarrow \mathbf{R}^3$$

Another example is a vector field defined over a surface, represented as the parametric function

$$V(u,v) : \mathbf{R}^2 \rightarrow \mathbf{R}^6$$

In this case, the output of V is a 3D point and a 3D direction. This section examines some examples of specifying "multidimensional" generative shapes such as S and V.

3.2.1 Solids

A generative solid can be represented with a parametric function

$$S(u,v,w) : \mathbf{R}^3 \rightarrow \mathbf{R}^3$$

Essentially, the solid S is represented as a 3D deformation of a 3D "brick". Such a representation has two advantages. First, even if we require only the surface boundary of the solid for rendering or simulation, it is often convenient to model the entire solid at once, rather than separately modeling the 6 faces of the deformed brick. Second, we may need to parameterize the interior of the solid for simulation purposes. For example, a cubic lattice approximating the solid S may be required for finite element analysis. Furthermore, by parameterizing the solid S, we can easily associate with each point additional quantities such as a scalar representing temperature, or a direction representing a force.

Figure 3.20 illustrates an example of a generative solid.

3.2.2 Time Dependent Shapes

Time dependent shapes can be represented by including a time parameter in the parametric function representing the shape. For example, a time varying curve, $c(v,t)$, can be used to produce the wing motion of a creature included in a computer graphics animated sequence.

The curve c is a damped sinusoid, that has a time-varying phase, and that is truncated at a specific arclength, λ. Mathematically, c is given by

$$c(u,t) = \begin{pmatrix} u \\ \dfrac{\sin(2\pi(t - 0.1u))}{2u^2} \end{pmatrix}$$

The parametric range of the u parameter is from 0 to u_t, where u_t is determined by finding where the arclength of $c(u,t)$ is λ, i.e.,

$$u_t \ni \lambda = \int_0^{u_t} \|\frac{\partial c}{\partial u}\| du$$

Note that this formula can be computed using the integration (Section 2.2.2.2.5) and inversion (Section 2.2.2.2.9) operators. Figure 3.21 shows the time varying behavior of $c(u,t)$.

The time varying curve $c(u,t)$ can then be used to produce a time varying surface, representing the wing of the animated creature. In this case, $c(u,t)$ is used as the wire curve in the wire product of Section 3.1.1.2. The cross section of this wire product is an ellipse, one of whose axes is scaled and translated to produce the wing shape. The result is shown in Figure 3.22.

3.2.3 Vector Fields on Surfaces

In the previous section, shapes were produced with an extra input dimension representing time. The generative modeling approach can also represent shapes with "extra" output dimensions (i.e., more than three output dimensions). For example, a vector field defined over a surface can be represented with a parametric function of output dimension 6. This

```
MAN beam = m_wire(s,c);
```

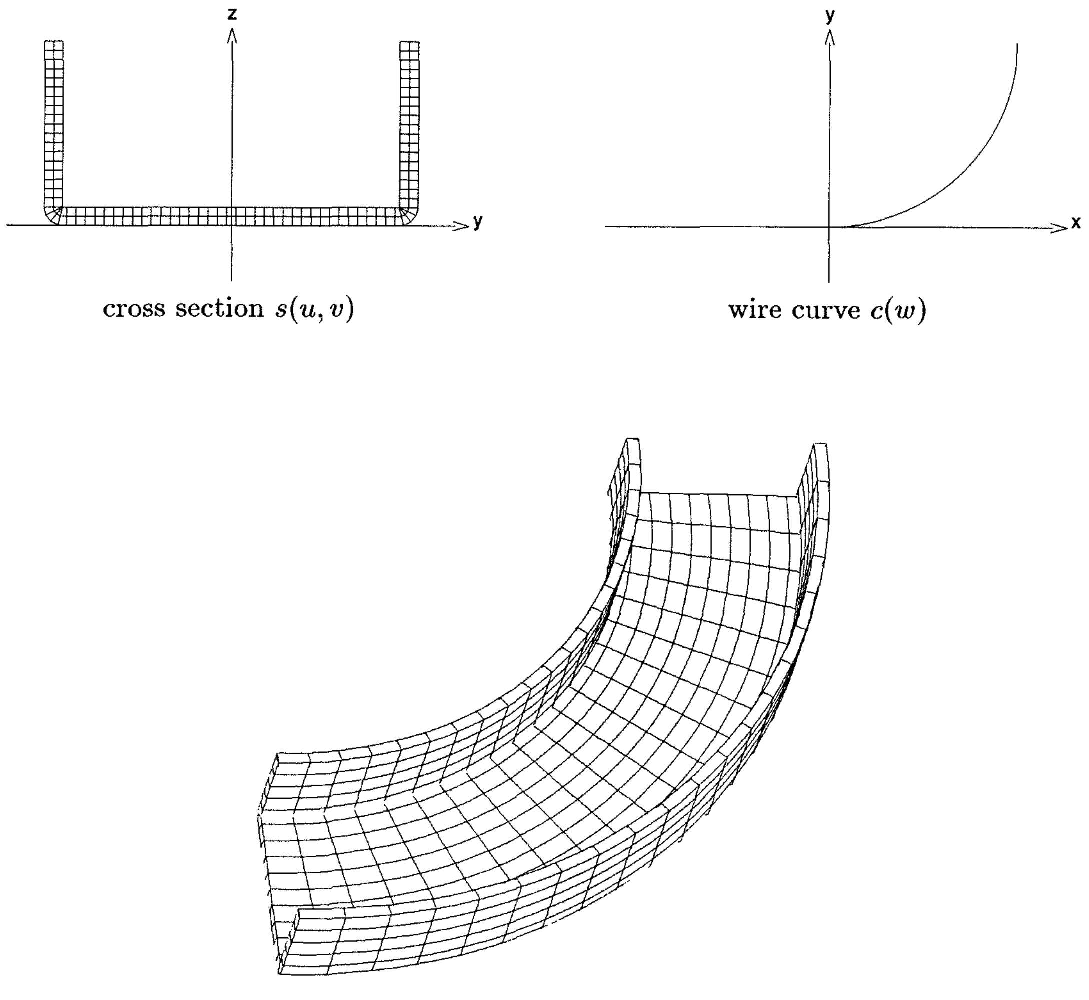

Figure 3.20: Circular beam example — A circular beam solid is modeled using the wire product of Section 3.1.1.2. In this case, a planar region rather than a boundary curve is used as the cross section. The region, $s(u, v)$, is swept along the two dimensional wire curve $c(w)$ to form a parametric solid with three input coordinates.

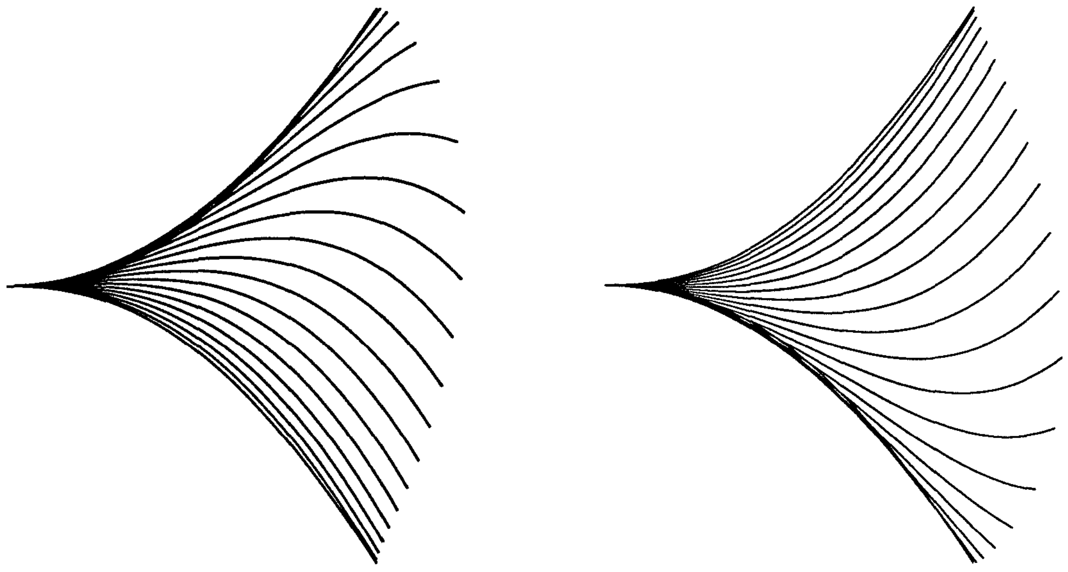

Figure 3.21: Time varying curve example — The left side shows the behavior of the curve $c(u, t)$ for $t \in [-0.1, 0.4]$ (the up stroke). The right side shows its behavior for $t \in [0.4, 0.9]$ (the down stroke).

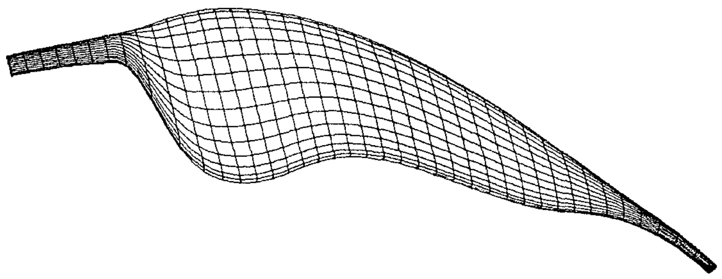

Figure 3.22: Time varying wing surface — A wing surface is constructed with a wire product using the curve $c(u, t)$ as the wire.

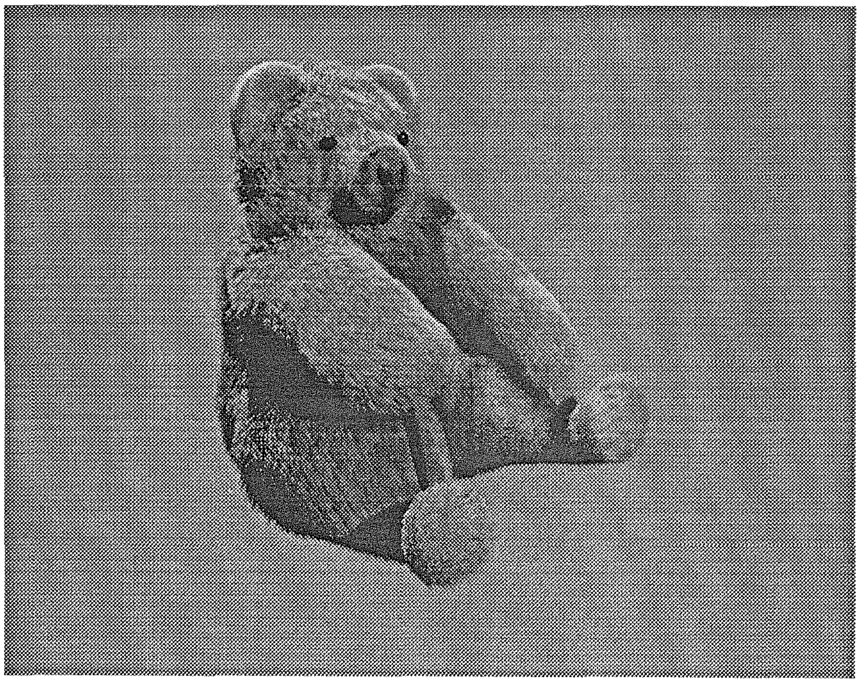

Figure 3.23: Modeling a furry bear as a vector field over a surface — The bear model was produced using an early version of the GENMOD program, which allowed interactive definition and rendering of vector fields defined over surfaces. The rendering technique is described in [KAJI89].

shape was useful in modeling a furry teddy bear [KAJI89], which was rendered using a new 3D texturing technique. The rendering method required not only the shape of the "scalp" of the bear, but also the behavior of the hairs on the bear's scalp. The hairs were modeled as straight segments whose orientation varied with respect to the scalp normal, simulating a combing of the hair. The hair was therefore modeled as a vector field over a surface representing the bear scalp. An image of bear model is shown in Figure 3.23.

Chapter 4

Shape Rendering

Rendering is the production of "images" of shapes, where images are synthetic pictures produced using computer graphics, or approximations of the shape suitable for postprocessing (e.g., manufacturing and simulation). The need for the latter form of rendering is obvious in a CAD/CAM system whose ultimate goal is the production of physical parts. It is less clear why pictures are necessary in a shape design system.

A picture of a designed shape provides information which is important for checking the design's validity. This information is presented in a way that is easy for a human being to assimilate. A picture can illustrate how close two objects are, where they are close, whether they intersect, and where the intersections occur. This information is more complete than a single bit telling the designer whether or not the shapes intersect.

Pictures allow the designer to be more "connected" with his design. That is, the designer can see that a selection of certain shape parameters yields a certain observable shape. As the parameters are varied, the shape's appearance changes correspondingly. Interactivity of the parameter selection/rendering cycle enhances this connectedness. In some cases, such as in designing a shape for a computer animation sequence, the parameter selection/rendering cycle is the preferred form of searching the parameter space. Once the shape looks right, there is no need to check it further. In other cases, the shape must be simulated as part of a larger assembly. It must fit together with other parts and have the right physical properties. Choosing the right shape and verifying its suitability in the larger assembly cannot be done solely with visual tools. Yet visual tools are extremely useful in debugging the choice of shape.

This chapter examines methods for visualizing shapes represented as generative models. Methods for sampling of generative models, a necessary component of almost all the rendering methods, is also presented. Lastly, this chapter describes how shapes are rendered in a generative modeling implementation that is geared toward fast, interactive feedback.

4.1 Methods of Shape Visualization

In this section, we look at methods for rendering shapes for visualization. In the following discussion, shapes are broken down into two categories: low-dimensional shapes and higher-dimensional shapes. Low-dimensional shapes are the familiar points, curves, surfaces, and solids in 3D space. They form the bulk of the shapes of interest in CAD systems and computer graphics. Higher-dimensional shapes are shapes that depend on parameters (like surfaces changing over time) or shapes that are embedded in space of dimension greater than 3.

4.1.1 Rendering Low-Dimensional Shapes

Many computer graphics techniques exist for rendering low-dimensional shapes including line drawing, z-buffering, ray tracing, radiosity methods, and volume rendering. Each of these rendering methods differs in several important respects

- in the sort of shapes that can be rendered.

  Line drawing techniques render curves; z-z-buffer and ray tracing techniques render surfaces; volume rendering techniques render scalar fields in 3D space. In addition, some rendering techniques are specialized for a particular modeling paradigm such as interval buffers for rendering of CSG objects.

- in the speed of rendering.

  Computer hardware has been developed to speed line drawing and z-buffer techniques. Ray tracing and radiosity methods are currently slow in comparison.

- in the realism/accuracy of rendering.

  Line drawing is an abstract rendering without much realism. Z-buffer techniques simulate shading but typically with very simple lighting models. Ray tracing and radiosity can simulate more sophisticated lighting models including shadows, reflections and refractions, and indirect lighting.

- in the special effects that can be achieved.
  Line drawings can be *depth cued* so that parts of lines further in depth are drawn in darker shades. Z-buffer algorithms can be modified to allow transparency of objects to show their internal structure. They can also be modified to allow variation of color across the object's surface (called *texture mapping*) to show how some parameter changes across the surface.

A geometric modeling system must choose, or allow the user to choose, a suitable rendering technique and any attendant special effects. This choice is determined by trading off rendering speed with the quality of shape visualization. For images produced during interactive shape design, we may be willing to sacrifice realism for real time rendering. For an image to be included in a document, a higher degree of realism is probably warranted at the expense of a higher computational cost.

4.1.1.1 How Important Is Realism?

A central question in geometric modeling is how realism in rendering is related to the quality of shape visualization. That is, does more realistic rendering result in better perception of properties of the shape being rendered. This question appears many times in different disguises, such as:

1. Are shadows useful for shape visualization? What about soft shadows?

2. How important is antialiasing?

3. Are fast line drawings better or worse than slow solid shaded drawings?

For some applications, such as production of a computer animation sequence for a television commercial, realism is clearly important. For CAD/CAM applications, the goal is to communicate to the designer whatever properties of the shape are of interest. These properties may or may not be related to visual properties of the shape. As a result, some researchers and developers in the CAD/CAM field question whether realism is a useful rendering goal. Even when realistic rendering is seen as useful, we must ask whether the degree of realism achieved with some rendering method is worth the computational cost.

It is probable that judicious use of realism enhances shape visualization. Human beings have a highly developed visual system geared to seeing shapes in the physical world. We use a host of visual cues to perceive shape – lighting, shading, shadow, perspective, and stereoscopic. The more realistic the rendering, the more we can relate the shape being rendered to shapes we have seen in real experience. Some of the bias against realistic rendering in the CAD/CAM community may be attributable to its slowness. If realistic rendering methods could be made real time, their use would become much more widespread. But real time ray tracing, for example, is already on the horizon. As general purpose computers get faster, and realistic rendering techniques are assisted with special purpose hardware, realism will become increasingly important.

Nevertheless, increased visual realism is not always desirable. Realism can mislead or be unnecessary. Assume that we wish to render an object so as to see the shapes of its internal cavities. Ray tracing the object as a solid piece of glass is likely to result in a confusing image because of refraction distortions. Most people are unused to seeing the world through oddly shaped pieces of glass. It is probably better to render the shape as a transparent, but not refractive, surface. Hard shadows (shadows from point light sources commonly seen in ray traced images) can also lead to confusion. They create sharp edges between shadowed and lighted regions on a surface, and obscure the geometrical shape of shadowed regions.[1]

Less realistic rendering can be more useful than realistic rendering in certain situations. Consider rendering a parametric surface using a line drawing technique. The surface is drawn by rendering a series of curves that follow parameter lines. This kind of rendering gives information not present in a solid shaded image. It may be important to see what the parameter lines look like on the surface, since the parameter lines reflect the way the surface was constructed. A line drawing also allows us to look through the surface to see parts of the shape that would be occluded if hidden surfaces were eliminated.

[1]Using soft shadows instead of hard shadows serves to alleviate many of these problems. Soft shadows are shadows that result from a light source that subtends a nonzero solid angle (in contrast to a point light source). The confusion that results from hard shadows probably results from our unfamiliarity with point light source lighting environments.

The generative modeling system developed as part of this thesis work has adhered to the following three principles that guide the choice of a rendering method:

1. Give the designer a choice of rendering methods. Users are not alike in their preferences; nor are the shape properties the designer wishes to see the same in every situation. Interactive control over the rendering method allows the designer to see different properties of the shape with the most appropriate method.

2. Use realistic rendering for checking overall, visual properties of shape. For example, when the designer is checking the shape of a 3D surface, or the spatial relationship of two surfaces, the more realistic the rendering, the better. On the other hand, if the designer is interested in some specific, nonvisual property of the shape, then realism is probably unnecessary. For example, to see the relationship of two scalar parameters, there is no more effective visualization than a simple, 2D plot of y vs. x.

3. Supply the designer with at least one real time rendering method. Because rendering is necessarily a projection of 3D space onto 2D, a single image of a shape is often insufficient for its understanding. Perhaps the most effective way to see shape is see it from a variety of angles, letting the user simulate turning the shape in his hands. It is therefore important to have at least one real time rendering option that allows the user to see the shape as it is moved around.

4.1.1.2 Curves

Most graphics hardware available today is designed to draw 3D vectors quickly. Graphics workstations now commonly achieve speeds of hundreds of thousands of vectors per second. Given this available hardware, the most attractive rendering method for curves is to convert them to a sequence of 2D or 3D vectors. Since curves in the generative modeling approach are represented as parametric functions, we require a method of approximating parametric functions as a sequence of vectors.

Let $\gamma(u)$ be a parametric curve where $u \in [0,1]$. Converting γ into a sequence of line segments involves sampling γ: choosing a sequence of n values for u, $u_1 = 0, u_2, \ldots, u_n = 1$,

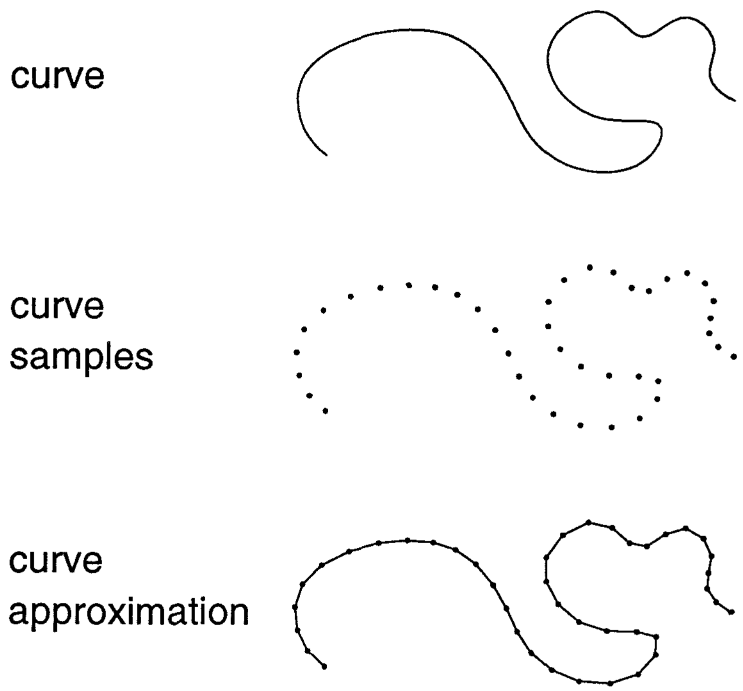

Figure 4.1: Approximating a parametric curve — A parametric curve is approximated by generating a sequence of points on the curve, and interpolating between these points. In this example, the curve is approximated by a series of line segments joining adjacent samples on the curve.

and evaluating γ at each, yielding a sequence of points

$$\gamma(u_1), \gamma(u_2), \ldots, \gamma(u_n)$$

Each pair of consecutive points determines a vector to be rendered with the graphics hardware (see Figure 4.1). The choice of the number of samples, n, and the sample locations, $u_1, u_2, \ldots, u_n$, trade off speed of curve rendering with the accuracy of the line segment approximation.

A curve approximation consisting of a series of line segments does not preserve smoothness of the original curve. To obtain a smooth approximation, a higher order interpolant, such as a quadratic or cubic curve, must be used. To compute such an approximation, derivatives of various orders can be sampled as well as points on the curve.

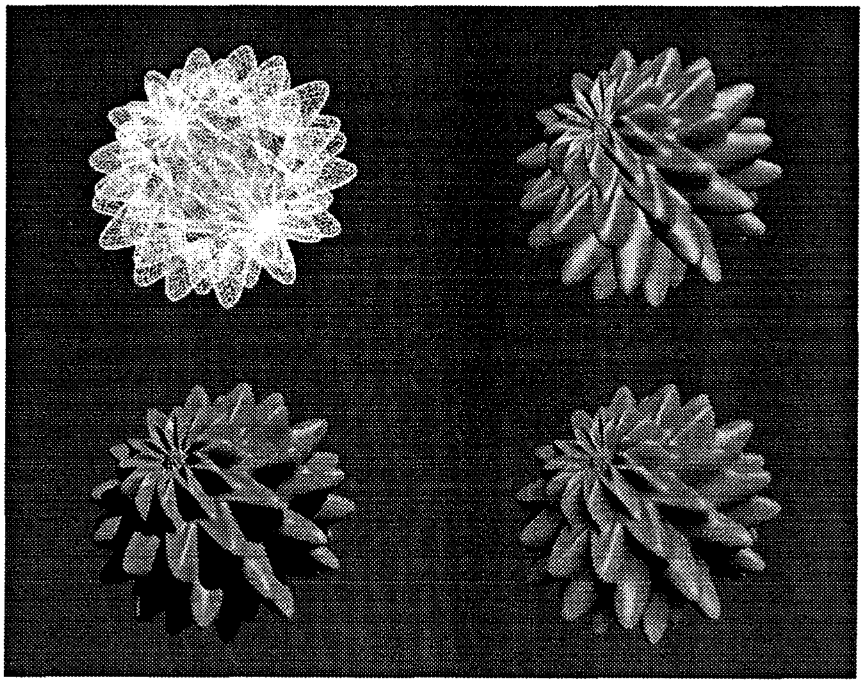

Figure 4.2: Rendering methods for surfaces — The figure compares the results of four rendering methods on a bumpy spherical shape. The rendering methods are (clockwise from upper left) line drawing, z-buffering, ray tracing with soft shadows, and ray tracing with hard shadows.

4.1.1.3 Surfaces

Surfaces in 3D space can be rendered using a variety of methods, including:

1. line drawing
2. z-buffering
3. ray tracing
4. radiosity methods

Figure 4.2 compares some of these rendering methods.

Line drawing of surfaces involves drawing curves on the surface, approximated by a series of line segments. Typically, the parameter lines of the surface are drawn, in which one of the parameters of the parametric surface varies while the other is held constant. Such line drawings give a reasonable idea of the surface's shape, especially if the user can rotate the surface interactively. The technique of hidden line elimination can also be used in order to eliminate parts of the curves that are occluded in a given view. This technique is much more costly than simple line drawing.

Z-buffering produces a solid shaded image of the surface. Rendering is accomplished by *tessellating* the surface into simple pieces, usually polygons. These polygons are scan converted (i.e., the pixels in the raster grid covered by the polygon's screen projection are visited), and a z value is computed at each pixel. This z value represents the depth of the surface from the screen, so that a surface with a smaller z value will occlude a surface with a larger z value. Graphics hardware is now available to do real-time z-buffering of quite complicated collections of surfaces.

Ray tracing produces a solid shaded image of a surface by simulating geometric optics. Light rays are traced backwards from the film plane or eye and into the collection of surfaces. Effects such as shadows, reflections and refractions can be realized. The fundamental operation in ray tracing is the intersection of a ray with a surface. This can be accomplished in two ways: we can directly compute such intersections [BARR86, JOY86, TOTH85], or tessellate the surface and compute intersections with the resulting collection of simple pieces [SNYD87]. The latter method, while approximate, is attractive because direct ray/surface intersections may be very costly to compute.

Both ray tracing methods are applicable to generative surfaces discussed in this thesis. Surface tessellation will be further discussed in Section 4.1.1.3.1. Intersecting a ray with a generative surface can be accomplished using the global optimization with constraints operator. A ray in $\mathbf{R}^3$ is defined as

$$a + bt$$

where $a, b \in \mathbf{R}^3$ and $t \in [0, \infty)$. The vector a is the ray origin, b is the ray direction, and t is the ray parameter. To intersect this ray with the parametric surface $S(u,v) : \mathbf{R}^2 \rightarrow \mathbf{R}^3$, we minimize t subject to the constraint system

$$a + bt = S(u,v)$$

Optimization is used because we require the first (minimum t) intersection of the ray with the parametric surface. An algorithm for solving such a system will be given in Chapter 5.

Radiosity methods attempt to balance light energy within an environment composed of surfaces. Surfaces are tessellated, and *form factors* are computed between each pair of tessellation elements. These form factors represent the proportion of energy emitted by one element that reaches the other. Assuming each surface is perfectly diffuse (scatters incident light energy in all directions equally), the energy balance can be accomplished by solving a large linear system. Radiosity methods can simulate diffuse inter-reflections between surfaces, an effect not realizable with standard ray tracing. Research is continuing to enhance radiosity methods with the ability to simulate non-diffuse surfaces. At the same time, ray tracing methods are being enhanced to handle inter-reflection of light between surfaces.

4.1.1.3.1 Surface Tessellation and Sampling The z-buffering, ray tracing, and radiosity rendering methods discussed previously all require surfaces to be tessellated – approximated by a set of connected pieces. Most often, surfaces are tessellated into a polygonal mesh. Other tessellation units can be used that allow more faithful approximation of the surface at the expense of slower rendering. For example, bicubic polynomial patches approximate a smooth surface better than a polygonal mesh, but are more difficult to z-buffer or ray trace directly.

Just as a curve is approximated by generating a sequence of points over the curve, a surface is tessellated by generating a network of points over the surface. An approximation to the surface results from interpolating this network of points using polygons, bicubic patches, or some other interpolation scheme. The simplest algorithm for generating a network of points over a parametric surface is called *uniform sampling.* It involves evaluating the surface over a rectangular, 2D lattice of points in parameter space.

Let $S(u, v)$ be a parametric surface where the domain of S is $[0, 1] \times [0, 1]$. To sample S uniformly, we choose the number of subdivisions in u and v (n_u and n_v), and evaluate S on $n_u n_v$ points given by

$$\begin{aligned} \begin{pmatrix} u_i \\ v_j \end{pmatrix} &= \begin{pmatrix} i/(n_u - 1) \\ j/(n_v - 1) \end{pmatrix} \\ i &= 0 \ldots n_u - 1 \\ j &= 0 \ldots n_v - 1 \end{aligned}$$

Given a uniform grid of points on S, a polygonal mesh can be constructed by generating a pair of triangles for each group of four adjacent points.

We can also tessellate S using *adaptive sampling.* In this case, samples of S can have an arbitrary distribution over its parameter space, rather than a uniform rectilinear distribution. Typically, samples are chosen so that the behavior of the surface inside a bounding box around each tessellation unit satisfies some criteria, such as the following:

1. size (e.g., volume, or maximum side length) of the bounding box does not exceed some threshold
2. area of the surface inside the box does not exceed some threshold
3. maximum variation of the surface's normal vector inside the bounding box does not exceed some threshold

Section 5.2.3 discusses an algorithm to sample parametric surfaces using general criteria such as the above.

Figure 4.3 compares uniform and adaptive sampling. Adaptive sampling allows samples to be chosen that guarantee certain properties about the resulting surface approximation. For example, using criteria 1 from the previous paragraph, an approximation can be generated that is no farther than a given distance from the original surface. Uniform sampling, in contrast, guarantees nothing about the quality of the approximation. The user merely chooses two integers controlling the fineness of sampling in the two parametric coordinates

On the other hand, adaptive sampling is usually much slower than uniform sampling. Computation is used both to check the adaptation criteria and to generate the tessellation mesh for the more complicated network of samples. In creating a polygonal mesh, for example, care must be exercised so that cracks do not form in the tessellation. Eliminating such cracks is trivial for uniform sampling, but much more complicated for adaptive sampling [VONH89]. In addition, Section 4.2.1.1 presents a speedup that increases the attractiveness of uniform sampling.

4.1.1.4 Solids

Solids in 3D space can be rendered by rendering the surfaces that form their boundaries. In this case, the discussion of the previous section is applicable. For example, solids represented

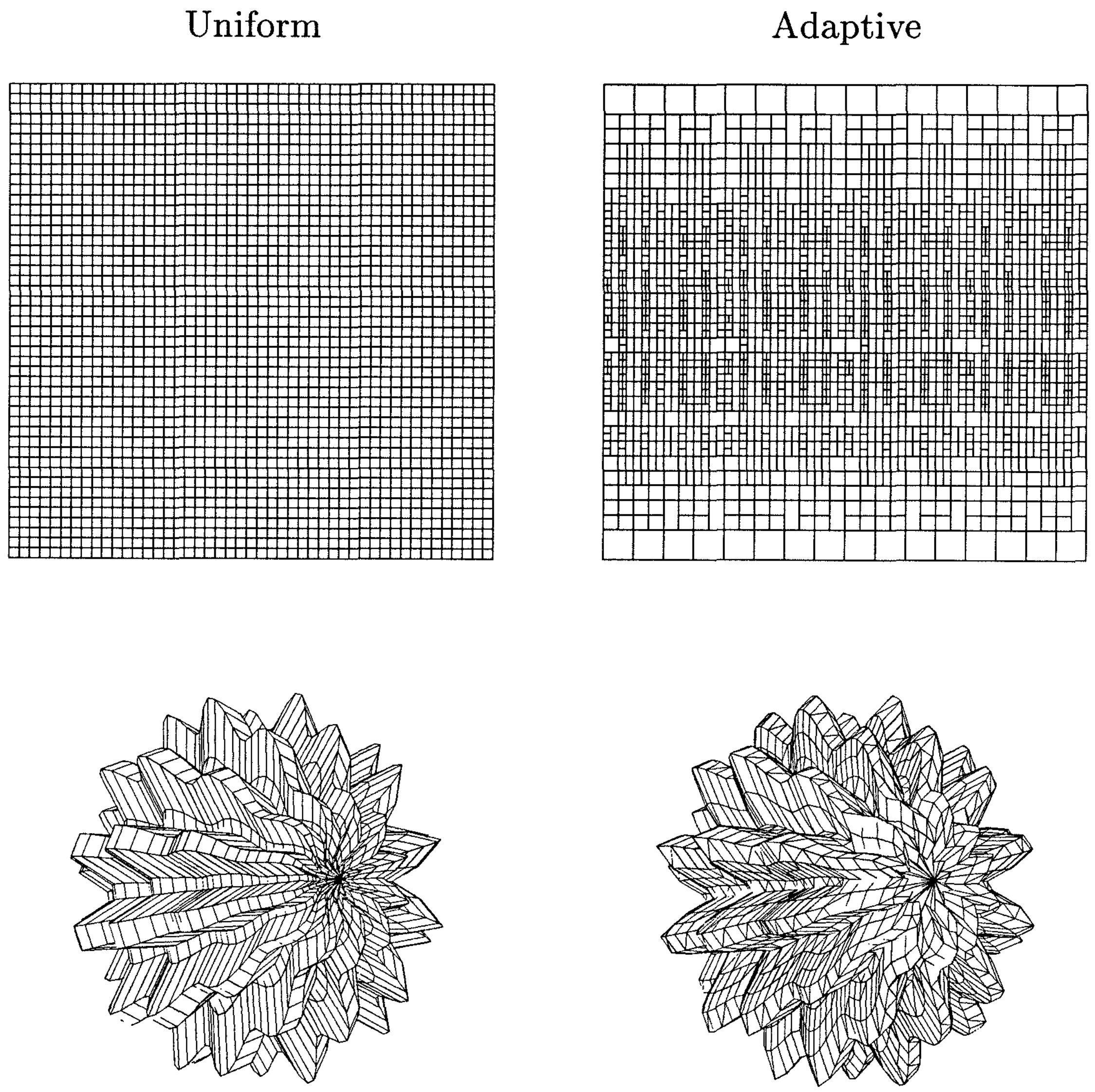

Figure 4.3: Uniform vs. adaptive sampling of a parametric surface — The left side of the figure illustrates uniform sampling of a parametric surface. In the top left, the parameter space of the surface is drawn. Samples are evaluated at each crossing of the parameter lines. The bottom left shows the resulting surface in $\mathbf{R}^3$, where each set of four adjacent points can is used to define a tessellation element. Rendered lines correspond to the sampled parameter lines. The right side of the figure illustrates the same surface, adaptively sampled. The number of tessellation units is approximately the same, but samples are distributed so as to limit the size of a bounding box around each tessellation unit. There are therefore fewer samples at the poles of the surface, and more near the equator.

using a b-rep can be rendered by rendering the collection of boundary surfaces. As another example, a solid can be represented using a generative model specified as a parametric function $S(u, v, w) : \mathbf{R}^3 \rightarrow \mathbf{R}^3$. The set of points in the solid is formed by the image of S over the rectilinear domain $[u_0, u_1] \times [v_0, v_1] \times [w_0, w_1]$. If S is differentiable and invertible, and the set of vectors $\{\frac{\partial S}{\partial u}, \frac{\partial S}{\partial v}, \frac{\partial S}{\partial w}\}$ is everywhere linearly independent, then S defines a solid whose boundaries are given by the transformation of the boundaries of the domain of S. The solid represented by S can therefore be rendered by rendering the 6 surfaces forming the boundary of S, i.e.,

$$\begin{aligned}
S_1(v, w) &= S(u_0, v, w) \\
S_2(v, w) &= S(u_1, v, w) \\
S_3(u, w) &= S(u, v_0, w) \\
S_4(u, w) &= S(u, v_1, w) \\
S_5(u, v) &= S(u, v, w_0) \\
S_6(u, v) &= S(u, v, w_1)
\end{aligned}$$

However, rendering of the boundary surfaces of a solid is not sufficient if the interior of the solid has structure that we wish to visualize. For example, a scalar representing temperature or mass density may be associated with each point of the solid. Such solids can be visualized with the technique of *volume rendering*, a relatively new area of computer graphics. Volume rendering techniques range from the simple summing of voxels projecting onto the same pixel, to complicated simulation using light scattering models. As in the case of surface and curve rendering, volume rendering requires sampling of the solid, which will be discussed in Section 4.2.

4.1.2 Rendering Higher-Dimensional Shapes

The generative modeling representational scheme allows the designer to build shapes of arbitrary input and output dimension. In this section, we consider the rendering of shapes that do not fit into the category of curves, surfaces, or solids in three dimensions.

4.1.2.1 High Input Dimension

Shapes of high input dimension include curves, surfaces, and solids that change as a function of time. For example the function

$$S(u, v, t) : \mathbf{R}^3 \rightarrow \mathbf{R}^3$$

can represent a generative surface that deforms in time. The time parameter t is called a *variable input parameter*, while the parameters u and v are called the *intrinsic input parameters.* We can also add more variable input parameters, to create a surface that is a function of several parameters. Such a surface is represented by the parametric function

$$T(u, v, x_1, \ldots, x_n) : \mathbf{R}^{n+2} \rightarrow \mathbf{R}^3$$

where the variable input parameters are $x_1, \ldots, x_n$. For rendering purposes, the variable input parameters are used to define a set of surfaces (or curves or solids) to be visualized.

There are two main techniques for the visualization of such continuous sets of shapes: superimposition and animation. Both techniques first sample the shape at various points in the variable input parameter space. We will term a single sample of the shape at a point in the variable input parameter space (e.g., the surface $S(u, v, t_0)$) an *instance* of the shape. Superimposition renders the shape by rendering the entire collection of instances in a single image. Animation renders a sequence of instances, one at a time. Superimposition thus allows simultaneous visualization of the whole set of shapes, but often creates cluttered images where instances can occlude one another.

Animation solves this problem, but requires real-time rendering of each instance. Alternatively, we can use a medium, such as a single frame tape recorder, that allows each image to be added to the animation after it is rendered. The entire animation can then be played back in real-time after it is recorded. In either case, user interaction is useful as a means of ordering the sequence of instances, especially if there is more than one variable input parameter. For example, the user can attach each of the variable input parameters to a 1D graphics input device, such as a dial. Changing a dial changes the value of the parameter to which it is attached.

4.1.2.2 High Output Dimension

An example of a shape of high output dimension is a vector field defined over a surface. Such a shape can be represented using the parametric function

$$S(u,v) : \mathbf{R}^2 \rightarrow (p,q) \in \mathbf{R}^6$$

where $p \in \mathbf{R}^3$ represents a 3D point, and $q \in \mathbf{R}^3$ represents a 3D direction. Another example of a shape of high output dimension is a quasi-linear transformation defined as a function of time:

$$R(t) : \mathbf{R} \rightarrow (M,T) \in \mathbf{R}^{12}$$

where $M \in \mathbf{R}^9$ represents a linear transformation of a 3D point, and $T \in \mathbf{R}^3$ represents a 3D translation. The resulting transformation of a point $p \in \mathbf{R}^3$ by R is given by

$$R(t;p) = M(t)p + T(t)$$

The output of S is therefore embedded in a 6D space, while the output of R is embedded in a 12D space.

We note that a color image is a 5D entity – two spatial dimensions and three color dimensions. How can entities such as S and R be visualized in this 5D image space? A natural way of visualizing S is to render both the surface $p(u,v)$, and a collection of line segments from the point p to the point $p+q$, as in Figure 4.4. R can be visualized by selecting a surface in $\mathbf{R}^3$, such as a sphere, and applying R to it. The surface can even be parameterized. For example, we can apply R to a sphere parameterized by three coordinates for its origin and one for its radius,

$$p(\theta,\phi,x,y,z,r) = \begin{pmatrix} x + r\cos(\theta)\cos(\phi) \\ y + r\sin(\theta)\cos(\phi) \\ z + r\sin(\phi) \end{pmatrix}$$

We can then visualize the resulting shape $R(t)(p(\theta,\phi,x,y,z,r))$, as a surface with five variable input parameters (t,x,y,z,r), using the ideas already discussed in Section 4.1.2.1.

In general, the method of visualization appropriate for a shape depends on the inter-

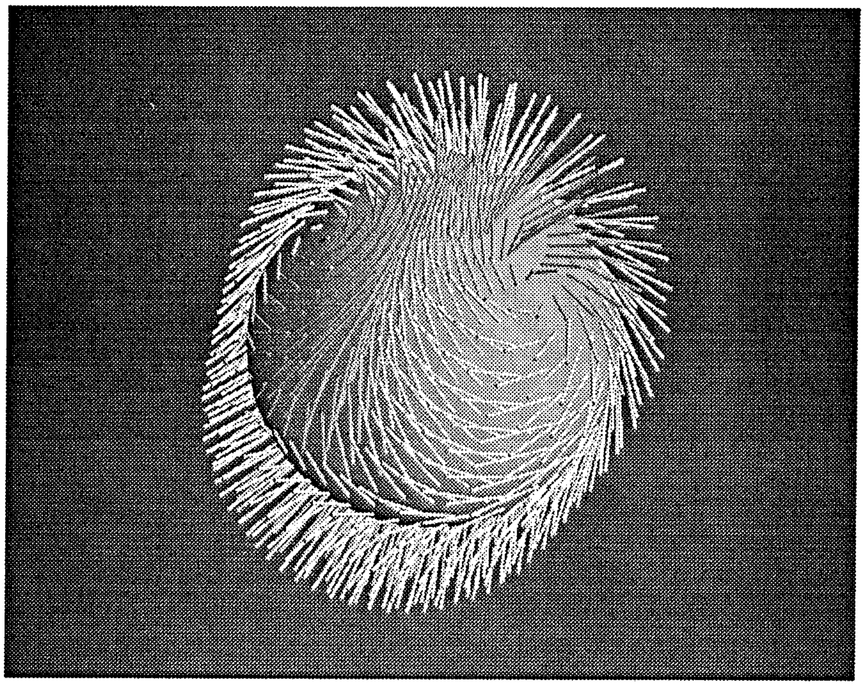

Figure 4.4: Visualization of a vector field defined over a surface – A parametric function of input dimension 2 and output dimension 6 can be visualized by rendering a surface, representing the vector field origin, and a set of line segments, representing the vector field direction.

pretation of the shape. We can not expect a single visualization method to be appropriate for two different shapes, even if their output dimension is the same. Nevertheless, several general techniques exist for visualizing shapes of high output dimension:

1. use of projection – the user can specify a transformation of the shape that projects it into a lower-dimensional embedding. This transformation can even be parameterized, allowing the user to change the projection using the techniques of Section 4.1.2.1.

2. use of color – the three color dimensions of the image can be used to convey information rather than to enhance the realism of the rendering. The technique of *texture mapping*, for example, allows the color of a surface or solid to vary as a function of the parametric coordinates.

3. use of graphics output devices – images of a shape can be augmented by the output of devices that stimulate nonvisual senses of the user. For example, force feedback

output devices allow the user to feel a varying force that can be attached to the outputs of a shape.

A modeling system should allow flexible use of all these techniques. The user should be allowed to specify different projection functions and methods of mapping shape outputs into color space. Faster and more capable graphics hardware is always being developed that can aid in shape visualization. Modeling systems should allow incorporation of new hardware in the system without too much effort. A specific implementation of these ideas will be discussed in Section 4.3.

4.2 Sampling Shapes

As we have seen, many methods of rendering shapes require approximation of the shape into units such as cubes, polygons, or line segments. Such approximation, in turn, requires *sampling* – computation of points over the shape. In the generative modeling approach, a shape is represented by a parametric function

$$S : \mathbf{R}^n \to \mathbf{R}^m$$

parameterized by the n variables $(x_1, \ldots, x_n)$. The shape is generated by the the image of S over a rectilinear domain

$$(x_1, \ldots, x_n) \in [a_1, b_1] \times \ldots \times [a_n, b_n]$$

This section discusses two methods for sampling such parametric functions: uniform sampling and adaptive sampling.

4.2.1 Uniform Sampling

Uniform sampling of a parametric function involves evaluating the function over a rectilinear lattice of domain points. For each parametric coordinate x_i, we pick a number of samples, N_i. The parametric function S is then evaluated over the $\prod_{i=1}^{n} N_i$ samples given by

$$\left(a_1 + \frac{i_1(b_1 - a_1)}{N_1 - 1}, \ldots, a_n + \frac{i_n(b_n - a_n)}{N_n - 1}\right)$$

Each of the indices i_j independently ranges from 0 to $N_j - 1$. This evaluation is done by calling the uniform evaluation method of S (see Section 2.2.2.3).

4.2.1.1 Uniform Sampling Speedup using Table Lookup

A substantial speedup of uniform parametric evaluation can be accomplished by constructing evaluation tables for subfunctions [FRAN81]. As discussed in Section 2.2.2, a subfunction is a subtree in the tree of recursive operators representing a parametric function, For example, let $f : \mathbf{R}^3 \rightarrow \mathbf{R}$ be the following function:

$$f(x_1, x_2, x_3) = (x_1 x_2 + x_2 x_3)\mathrm{e}^{x_2}$$

which we wish to uniformly sample using n_i samples for x_i. This can be done by evaluating f at each of the $n_1 n_2 n_3$ lattice points in parameter space. Alternatively, we can construct evaluation tables for the subfunctions $f_1(x_1, x_2) = x_1 x_2$, $f_2(x_2, x_3) = x_2 x_3$, and $f_3(x_2) = \mathrm{e}^{x_2}$, so that these subfunctions are not reevaluated at each lattice point. Here is a table of the number of operations required for the two methods of evaluating f:

function	$*$ ops	$+$ ops	e^x ops
evaluation point by point			
$f = (x_1 x_2 + x_2 x_3)\mathrm{e}^{x_2}$	$3 n_1 n_2 n_3$	$n_1 n_2 n_3$	$n_1 n_2 n_3$
evaluation using tables			
$f_1 = x_1 x_2$	$n_1 n_2$	0	0
$f_2 = x_2 x_3$	$n_2 n_3$	0	0
$f_3 = \mathrm{e}^{x_2}$	0	0	n_2
$f = (f_1 + f_2) * f_3$	$n_1 n_2 n_3$	$n_1 n_2 n_3$	0
total	$n_1 n_2 n_3 + n_1 n_2 + n_2 n_3$	$n_1 n_2 n_3$	n_2

The table shows that substantial computational savings result when the lower-dimensional subfunctions are evaluated and stored in tables. In general, **evaluation tables should be constructed for each subfunction that has an input dimension smaller than its**

parent. For example, the subfunction e^{x_2}, of input dimension 1, should be tabulated because its parent function f has input dimension 3. Such a subfunction should be tabulated at the lattice points of its particular input variables. For example, evaluations from the subfunction e^{x_2} are stored in a 1D table of size n_2, while evaluations from the subfunction x_1x_2 are stored in a 2D table of size $n_1 \times n_2$. The tabulated results can then be retrieved rather than computed when the parent parametric function is evaluated. This process can be applied recursively. That is, in evaluating the table of results for a subfunction, evaluation tables can be computed for any of its subfunctions whose input dimension is smaller than its parent.

Alternatively, some needless evaluation can be avoided without the use of tables (and the memory necessary for their storage) simply by saving the last computed value of a subfunction rather than recomputing it. For example, consider the problem of uniformly sampling the function

$$f(x_1, x_2) = g(x_1)h(x_2)$$

in order to construct a list of values of f, in which the x_2 variable varies most rapidly. We can evaluate g at some value of the 1D x_1 lattice, say at a_1. This result, $g(a_1)$, may then be multiplied by each value of h on the appropriate 1D lattice for the x_2 variable. Thus, $f(x_1, x_2)$ can be computed without evaluating g once for each point in the 2D lattice. However, without a table to store values for the evaluation of h over the x_2 lattice, these evaluations must be recomputed when they are multiplied with the value of g at the next x_1 lattice point, a_2. The table approach described here avoids these needless evaluations.

4.2.1.2 Uniform Sampling and Uncoupled Transformations

Uniform sampling evaluates a parametric function at equally spaced points in each of the parametric coordinates. This restriction can be loosened to some extent through the use of uncoupled transformations. An *uncoupled transformation* is a function $T : \mathbf{R}^n \rightarrow \mathbf{R}^n$ that transforms each input coordinate independently, i.e.,

$$T(x_1, \ldots, x_n) = (f_1(x_1), \ldots, f_n(x_n))$$

Uncoupled transformations can be applied to the domain of a parametric function S to independently adjust the sampling densities in each of the domain coordinates. Uniform sampling of the adjusted function still allows the table lookup optimization discussed in Section 4.2.1.1. We can evaluate the n functions f_i into 1D tables. Uniform evaluation of $S(T(x))$ then requires the same number of function evaluations as did the uniform evaluation of $S(x)$.

As an example of the usefulness of uncoupled transformations, consider a surface defined by sweeping a circle of radius r perpendicular to a space curve $s(v) : \mathbf{R} \rightarrow \mathbf{R}^3$. Let $n(v)$ and $b(v)$ be differentiable vectors along this curve that are mutually perpendicular and perpendicular to the tangent vector of s, given by

$$\frac{ds}{dv}(v)$$

The sweep surface $S(u, v) : \mathbf{R}^2 \rightarrow \mathbf{R}^3$ is then given by

$$S(u, v) = s(v) + r(n(v)\cos(u) + b(v)\sin(u))$$

Depending on its parameterization, a uniform sampling of the space curve $s(v)$ may not yield a good approximation with a reasonable number of samples. However, we can reparameterize $s(v)$ by arclength, or so that the sampling density increases in areas of high curvature. Let the function $t(v) : \mathbf{R} \rightarrow \mathbf{R}$ be such a reparameterization, yielding a new curve $\tilde{s}(v) = s(t(v))$. The sweep surface can incorporate this reparameterization of v using the uncoupled transformation:

$$\begin{aligned} T &: \mathbf{R}^2 \rightarrow \mathbf{R}^2 \\ &(u, v) \mapsto (u, t(v)) \end{aligned}$$

4.2.2 Adaptive Sampling

Adaptive sampling can be used to generate approximations that satisfy criteria [VONH87]. For example, we may wish to bound the maximum distance of the approximation from the original parametric shape. To accomplish this in a reasonable number of samples, it is probable that some areas of parameter space should be sampled more finely than others.

While uniform sampling could be used, it would probably require an inordinate number of samples since the sampling is constant and independently fixed for each input coordinate.

An algorithm for adaptively sampling parametric shapes according to user specified criteria will be presented in Section 5.2.3. This algorithm requires evaluation of the shape at an unstructured collection of points. Evaluation is done by calling the shape's point evaluation method (see Section 2.2.2.3).

4.2.2.1 Adaptive Sampling Speedup Using Cacheing

Adaptive sampling can be enhanced by cacheing the last computed value of a subfunction. Both the input point and the subfunction result are stored. If, in a future evaluation, the input point matches the cached point, then the cached function result may be used without reevaluation. Candidate subfunctions are those that have lower input dimension than their parent, or that are repeated (i.e., shared subexpressions). Cacheing can be used for inclusion function evaluation as well as point evaluation.

Consider the following three examples. First, let $f(x_1)$ be given by

$$f(x_1) = x_1 + \int_0^1 g(x_2)dx_2$$

In sampling f for various values of x_1, the constant subfunction $\int_0^1 g(x_2)dx_2$ can be cached. It is then evaluated only once, rather than reevaluated for each value of x_1. Second, let $f(x_1)$ be given by

$$f(x_1) = g(x_1)^{1/2} + g(x_1)$$

In this case, the subfunction $g(x_1)$ is repeated, so that cacheing saves an evaluation of g. Repeated subfunctions are common, especially when symbolic derivatives are used in defining the function f. Finally, consider the function $f(x_1)$ defined by

$$f(x_1) = \int_0^1 g(x_1, x_2)dx_2$$

If the integral is numerically computed, the function g must be evaluated at many values of x_2 while the value of x_1 stays fixed. For example, if $g(x_1, x_2) = h(x_1) + s(x_1, x_2)$, then the result of the subfunction $h(x_1)$ can be cached, saving many evaluations in calculating the value of the integrand.

A limited form of this cacheing enhancement is part of the GENMOD system. That is, the system does not actually find common subexpressions in a parametric formula, but relies on the designer to use the same subexpression rather than redefining it. For example, in the second example discussed above, cacheing will not increase speed unless the designer defines a parametric function (i.e., a MAN type) representing $g(x_1)$ and uses this result in two places, as in

```
MAN g = foo(m_x(1));
MAN f = m_sqrt(g) + g;
```

A more sophisticated system could take advantage of common subexpressions without requiring the user to point them out in this way. The speedup implied by the first and third examples is effective without user attention.

4.3 Interactive Shape Visualization in the GENMOD System

A prototype implementation of the ideas of this thesis, called GENMOD, was developed as part of this research. This section discusses how GENMOD performs visualization on shapes represented using the scheme of Chapter 2.

4.3.1 Visualization Methods

A *visualization method* takes a shape and produces a renderable object. Shapes in the GENMOD system are parametric functions represented as a tree of recursive operators. Visualization methods in GENMOD approximate such shapes, converting them into a form suitable for interactive manipulation using z-buffer graphics hardware.

GENMOD implements five visualization methods: points, curves, planar areas, surfaces, and transformations. A point is rendered as a dot in 2D or 3D space. A curve is rendered as a sequence of line segments. A planar region is rendered as a single polygon formed by the interior of an approximated curve. The curve must not self intersect, and must lie in a plane.[2] A surface is rendered as a collection of triangles. A transformation can be applied

[2]Planar regions are convenient for forming end caps of generalized tubes, where the tube cross-section is

to any of the other renderable objects, deforming them via a pseudo-linear transformation (i.e., R of Section 4.1.2.2).

Each of the visualization methods expects a shape of a given output dimension (e.g., a function $S(u,v)$ must have output dimension three to be used as input to the surface visualization method). Each visualization method also expects an input dimension at least as large as the intrinsic input dimension of the shape. For example, a function $C(t) : \mathbf{R} \rightarrow \mathbf{R}^3$ can be used in the curve visualization method, as can $D(t,s) : \mathbf{R}^2 \rightarrow \mathbf{R}^3$, since C and D have input dimension at least 1. On the other hand, a constant function is not appropriate for the curve method, nor is a function of a single coordinate appropriate for the surface method. The following table shows the number of intrinsic input parameters and output parameters of GENMOD's visualization methods:

name	**intrinsic dim.**	**output dim.**
point	0	2 or 3
curve	1	2 or 3
planar area	1	2 or 3
surface	2	3
transformation	0	12

Functions that have an input dimension greater than the visualization method's intrinsic dimension are still valid input to the visualization method. The extra input coordinates, termed variable input coordinates in Section 4.1.2.1, can be visualized by animating or superimposing. The visualization method therefore requires an argument specifying which of the variable input coordinates are to be superimposed. The rest of the variable input coordinates are attached to dials and animated. For example, consider a function $C(s, x_1, x_2)$ that is visualized using the curve method with s as the intrinsic parameter, x_2 as an animated parameter, and x_1 as a superimposed parameter. C will be rendered as a 1D family of curves that changes as the dial attached to x_2 is turned. If instead both x_1 and x_2 are chosen as superimposed parameters, then a 2D family of curves is rendered, leaving no animation parameters. Finally, both x_1 and x_2 can be chosen as animated parameters, in

bounded by an arbitrary planar curve. Surfaces can also be used for this purpose, but are less convenient, since they require a 2D parameterization of the region's interior, rather than a simple boundary curve.

which case a single curve is rendered, changing shape as either of two dials, representing x_1 and x_2, is turned.

GENMOD's visualization methods approximate shapes using uniform sampling. The number of samples to be evaluated in each parametric coordinate is specified as an argument to the visualization method. Sampling is precomputed for all the shape's input coordinates, including the variable input coordinates. This scheme has the advantage that real-time animation is possible, even when the shape is represented using complicated functions. The disadvantage is that large amounts of memory is used in storing the precomputed samples, especially when there are many input coordinates. Another disadvantage is that the modeler must choose the sampling densities before the shape is visualized. An alternative technique that addresses these problems is discussed in the next section.

Since visualization methods can be applied to arbitrary parametric functions (as long as they satisfy input and output dimension restrictions), the modeler can visualize shapes of high output dimension by applying a projection transformation to his shape to produce a shape with a smaller output dimension. The GENMOD language allows the modeler to build projection functions easily. The projection function can be parameterized, as in the example of Section 4.1.2.2.

4.3.2 Non-precomputed Visualization

Precomputing the shape samples and then dialing through them is useful but very restrictive. GENMOD provides a more dynamic alternative using a curve editor interface. This alternative calls the visualization method during the visualization process rather than as a preprocessing step. Parameters to be varied are attached to 2D points or curves. Changing a point or curve in the curve editor then causes a new shape to be approximated and rendered.

For example, consider a 1D family of curves $C(s,t) : \mathbf{R}^2 \rightarrow \mathbf{R}^3$. The visualization method of the previous section samples C over a 2D lattice, with a pre-specified number of samples in s and t. The non-precomputed visualization method attaches the variable input parameter t to, for example, the x coordinate of a point in the curve editor. Changing this point causes a new curve, $C(s,t_0)$, to be approximated, where t_0 is computed from the x coordinate. Of course, performance may be poor if approximation of C requires extensive computation.

4.3.3 Interactive Rendering

GENMOD provides a tool for interactively visualizing a collection of renderable objects, once they have been created with the visualization methods. The modeler uses a 3D track ball to interactively rotate the objects in three dimensions. Three 1D dial devices are used to translate the objects along each of the coordinate axes, and another dial to scale the objects. Dial devices can also be attached to animated input variables. Different shapes with the same animated input variable are simultaneously changed when the dial attached to that variable is turned. This allows parameterized assemblies of objects to be visualized.

The track ball and dial devices are used to position the whole collection of objects as a group, or to move an individual object with respect to the others. The tool also has modes to allow the user to change the lighting and camera characteristics. Finally, the user can interactively change the following rendering characteristics:

1. How the tessellation units are derived from the uniform lattice of samples – the user can reduce the number of polygons or line segments that are derived from the uniform sampling of the shape, to increase rendering speed. This is done simply by disregarding some of the samples.

2. Whether surfaces are solid shaded or drawn with lines – the user can switch between these rendering modes, using line drawing to improve rendering speed.

3. Whether line drawings are depth cued – depth cueing enhances interpretation of line drawings, at a slightly increased rendering cost.

Versions of GENMOD have been developed on a Silicon Graphics IRIS 4D-80GTB and an HP 9000/800 graphics workstation. Both machines allow real-time rendering of shapes containing on the order of thousands of polygons, using a z-buffer algorithm. This rendering speed has proved adequate for the design of simple shapes, such as the examples of Chapter 3. More advanced rendering methods, such as ray tracing, can not be interactively chosen, but are available by writing the shape approximation to a file, and running a ray tracing program as a separate task.

Chapter 5

Interval Methods for Shape Synthesis and Analysis

This first part of this chapter discusses two basic algorithms that use interval methods to compute solutions to systems of constraints and constrained global optimization problems. We will refer to such problems as *global problems* in the following text. The second part presents applications of the two algorithms to geometric modeling problems, such as the computation of CSG operations on generative models.

Many of the basic ideas of this chapter are not new, including the use of interval methods to solve global problems. The following elements of this chapter are original work:

- the proofs of the theorems: the second-order convergence of the mean value form, the convergence of Algorithms 5.1 and 5.2, and the Bao-Rokne theorem specifying conditions guaranteeing the existence of a unique zero of a system of equations, are new. However, we did not discover these theorems, and they are stated and proved elsewhere (except for the Bao-Rokne theorem, which we have seen stated, but not proved).
- the inclusion function developed in Section 5.1.2.6 is new.
- the idea of using linear optimization in interval Newton methods, and in testing the conditions of the Bao-Rokne theorem, is new (Section 5.1.3.4.1).
- the idea of global parameterizability, its relevance to approximation algorithms, and

Theorem 5.5 specifying sufficient conditions for it, are all new.

- the idea of the b-offset (Section 5.2.1.1) is new, as is the interval-based approach for computing it.
- the algorithms for approximating implicit curves (Algorithm 5.3), approximating implicit surfaces (Algorithm 5.5), and approximating the results of CSG-like operations on generative shapes (Algorithm 5.4), are all new.

5.1 Interval Analysis for Constraint Solution and Global Optimization

In Sections 2.2.2.2.10 and 2.2.2.2.11 we introduced the constraint solution and global optimization operators and enumerated some of their uses in a geometric modeling system. This section explains how these operators can be implemented using the theoretical tool of interval analysis.

Interval analysis is a new but promising branch of applied mathematics. A general treatment of interval analysis can be found in [MOOR66] and [MOOR79] by R.E. Moore, the "inventor" of interval analysis as a tool for error analysis on digital computers. More recently, interval analysis has been used in a variety of algorithms to compute solutions to global problems (see, for example, [RATS88]). The ideas presented in this section are not new but find new application in the area of geometric modeling.

The interval analysis approach to solving global problems can be summarized as follows:

1. Inclusion functions are constructed that bound the ranges of functions used in the constraining equations and inequalities or the objective function (function to be minimized).
2. These inclusion functions are used in a branch and bound algorithm. An initial region of parameter space is recursively subdivided into smaller regions. Inclusion functions are used to test whether a particular region can be a solution to the global problem. For example, to test whether a region X may include a solution to the equation $f(x) = 0$, an inclusion function for f is evaluated over the region X. If the resulting bound on f does not contain 0, then X may be rejected. Similarly, an inclusion

function bound on the objective function in a minimization problem can reject a region if the objective function is too large to contain a global minimum. Subdivision proceeds until all regions are either rejected or accepted as solution regions.

In addition, such subdivision methods can be augmented by local techniques (e.g., Newton and quasi-Newton methods for constraint problems, steepest descent and conjugate gradient methods for optimization problems). Incorporation of these techniques can often dramatically improve the solution algorithm's performance.

5.1.1 Why Interval Analysis?

The interval analysis approach has several advantages over other solution approaches to global problems. Interval analysis controls approximation errors that result from doing imprecise floating point computation on a digital computer. Control of error is accomplished by ensuring that inclusion functions are valid bounds, even though these bounds must be represented with the machine's discrete set of floating point numbers. Interval analysis is an exhaustive technique; that is, all regions of the problem's input space are examined for solutions. The interval analysis approach thus allows global minima to be found, not just a local minimum that may be close to the global minimum. Furthermore, all minima or all solutions to a constraint system can be found, rather than a single solution.[1]

Interval analysis algorithms have two main problems as well. First, interval bounds tend to become very large as the "complexity" of the bounded function grows. By complexity, we mean, roughly, the number of primitive operations required to evaluate the function. This problem results because, in order to control approximation error and reduce computation, bounds are computed that are larger than the ideal, theoretical bounds. The excess size is added to and magnified with each operation. Although an interval analysis approach will not lose areas that contain solutions, it may fail to converge to adequately small regions if there is too much excess in the inclusion function bound. In particular, interval analysis approaches are often unacceptable for iterated solution methods, such as for ODE solution, because intermediate results of the algorithm are incrementally updated, giving a very complex result as the computation progresses.

[1]Actually, the interval analysis algorithms presented here yield a superset of the solutions.

Second, interval analysis approaches, because they are exhaustive, tend to be slow, especially as the dimension of problem's input space grows. Even when enhanced with non-interval techniques, interval approaches are not applicable to problems with large numbers of variables. For example, we would not expect interval methods to be appropriate for solving problems for which statistical optimization methods are commonly employed.

For the generative modeling approach advocated in this thesis, we believe the benefits of interval methods far outweigh their disadvantages. Functions can be represented with simple, noniterated formula for which relatively tight inclusion functions can be computed. Also, the global problems that arise tend to be defined in terms of a small number of parameters (e.g., two to compute the intersection of two curves, four to compute intersection of two surfaces, or to compute CSG operation on two surfaces). For problems with such small numbers of variables, satisfactory performance has been achieved with interval methods in a prototype implementation. At the same time, interval methods have allowed robust control of error. They have allowed computation of all solutions to global problems, a property employed in many of the algorithms that follow.

5.1.2 Inclusion Functions

An inclusion function produces a bound for the range of a function, given a bound on its domain. These bounds take the form of a vector of real intervals; a more precise definition will follow in Section 5.1.2.1. The goal of an inclusion function is to bound a function as tightly as possible, using as little computation as possible. Tight bounds allow domain regions to be rejected earlier in the algorithms summarized in Section 5.1, saving further computation to subdivide the region and bound its subregions.

This section defines inclusion functions and describes some of their mathematical properties. Methods are presented for computing inclusion functions of functions represented as the recursive composition of operators like those introduced in Section 2.2.2.2.

5.1.2.1 Terminology and Definitions

An *interval*, $A = [a, b]$, is a subset of $\mathbf{R}$ defined as

$$[a, b] \equiv \{x \mid a \leq x \leq b,\ x, a, b \in \mathbf{R}\}$$

The numbers a and b are called the *bounds* of the interval; a is called the *lower bound* and b, the *upper bound.* The lower and upper bounds of an interval are written

$$\begin{aligned} \mathrm{lb}[a,b] &\equiv a \\ \mathrm{ub}[a,b] &\equiv b \end{aligned}$$

The symbol $\mathbf{I}$ denotes the set of all intervals. A *vector-valued interval of dimension n*, $A = (A_1, A_2, \ldots, A_n)^T$, is a subset of $\mathbf{R}^n$ defined as

$$A \equiv \{x \mid x_i \in A_i \text{ and } A_i \in \mathbf{I} \text{ for } i = 1, 2, \ldots, n\}$$

For example, a vector-valued interval of dimension 2 represents a rectangle in the plane, while a vector-valued interval of dimension 3 represents a "brick" in 3D space. An interval A_i that is a component of a vector-valued interval is called a *coordinate interval of A.* The symbol $\mathbf{I}^m$ denotes the set of all vector-valued intervals of dimension m.

The *width* of an interval, written $w([a,b])$, is defined by

$$w([a,b]) \equiv b - a$$

The *midpoint* of an interval, written $\mathrm{mid}([a,b])$, is defined by

$$\mathrm{mid}([a,b]) \equiv \frac{a+b}{2}$$

Similarly, the width and midpoint of a vector-valued interval, $A \in \mathbf{I}^n$, is defined as

$$\begin{aligned} w(A) &= \max_{i=1}^{n} w(A_i) \\ \mathrm{mid}(A) &= (\mathrm{mid}(A_1), \mathrm{mid}(A_2), \ldots, \mathrm{mid}(A_n))^T \end{aligned}$$

Hereafter, we will use the term interval to refer to both intervals and vector-valued intervals; the distinction will be clear from the context.

Given a subset D of $\mathbf{R}^m$, let $\mathbf{I}(D)$ be defined as the set of all intervals that are subsets of D:

$$\mathbf{I}(D) \equiv \{Y \mid Y \in \mathbf{I}^m \,\mathrm{and}\, Y \subseteq D\}$$

Let $f : D \to \mathbf{R}^n$ be a function and $Y \in \mathbf{I}(D)$. An *inclusion function* for f, written $\Box f$, is defined as

$$\Box f : \mathbf{I}(D) \to \mathbf{I}^n \text{ such that } x \in Y \Rightarrow f(x) \in \Box f(Y)$$

Thus, $\Box f$ is a vector-valued interval bound on the range of f over a vector-valued interval bound on its domain. An inclusion function $\Box f$ is called *isotone* if

$$Y \subseteq Z \Rightarrow \Box f(Y) \subseteq \Box f(Z)$$

An inclusion function $\Box f$ is called *convergent* if

$$w(X) \to 0 \;\Rightarrow\; w(\Box f(X)) \to 0$$

Note that f must be continuous for its inclusion function to be convergent.

The *ideal inclusion function* of a function f, written $\overset{\mathrm{id}}{\Box} f$, is an inclusion function for f that results in the "tightest" interval possible. That is, for any domain interval, the resulting range interval consists of a vector of real intervals for which no lower bound may be increased, or upper bound decreased, while the result remains a bound on the range of f. We note that the ideal inclusion function is always isotone. The quality of an inclusion function, $\Box f$, may be measured by its *excess width*, defined as the difference in width between the inclusion function and an ideal inclusion function for the same function:

$$w(\Box f(Y)) - w(\overset{\mathrm{id}}{\Box} f(Y)) \text{ for } Y \in \mathbf{I}(D)$$

An inclusion function, $\Box f$, is called *order* α if its excess width is of the order of its domain width, raised to the power α, i.e.,

$$w(\Box f(Y)) - w(\overset{\mathrm{id}}{\Box} f(Y)) = \mathcal{O}(w(Y)^{\alpha})$$

A high order means that the inclusion function rapidly becomes a tight bound as the width of the domain interval shrinks. [2]

A function f is called *Lipschitz*, if there exists an inclusion function for f and a real constant K such that

$$w(\Box f(Y)) \leq K w(Y) \quad \forall\, Y \in \mathbf{I}(D)$$

5.1.2.2 Inclusion Functions for Arithmetic Operations

To see how inclusion functions can be evaluated on a computer, let us first consider functions defined using arithmetic operations. Let g and h be functions from $\mathbf{R}^m$ to $\mathbf{R}$, and let $X \in \mathbf{I}^m$. Let inclusion functions for g and h be given and evaluated on the interval X

$$\begin{aligned} \Box g(X) &= [a, b] \\ \Box h(X) &= [c, d] \end{aligned}$$

Given these interval bounds on g and h, we can bound an arithmetic combination, $g \circ h$, where $\circ$ represents addition, subtraction, multiplication or division.

This bound may be computed by bounding the set $Q_\circ$, defined as

$$Q_\circ = \{x \circ y \mid x \in [a, b], y \in [c, d]\}$$

$Q_\circ$ can be bounded within an interval using the well-known technique of *interval arithmetic*, whose rules are given by

$$\begin{aligned} Q_+ &= [a, b] +_\Box [c, d] &&= [a + c, b + d] \\ Q_- &= [a, b] -_\Box [c, d] &&= [a - d, b - c] \\ Q_* &= [a, b] *_\Box [c, d] &&= [\min(ac, ad, bc, bd), \max(ac, ad, bc, bd)] \\ Q_/ &= [a, b] /_\Box [c, d] &&= \left[\min(\tfrac{a}{c}, \tfrac{a}{d}, \tfrac{b}{c}, \tfrac{b}{d}), \max(\tfrac{a}{c}, \tfrac{a}{d}, \tfrac{b}{c}, \tfrac{b}{d})\right] \\ & && \quad \text{provided } 0 \notin [c, d] \end{aligned}$$

[2]Contrary to what one might expect, an excess width of 0 does not imply that an inclusion function is identical to the ideal inclusion function. In order for an inclusion function to have excess width 0, it must only be identical to the ideal inclusion function in whatever coordinate interval has the maximum width. To restore our mathematical intuition, many other widths can be defined (analogous to vector norms in $\mathbf{R}^n$), such as the sum of the widths of the coordinate intervals, the square root of the sum of their squares, and so forth. Theorems like Theorem 5.1 are easily amended for such definitions of the width of a vector valued interval.

These rules lead to the following inclusion functions for $f \circ g$ over the interval X

$$\begin{aligned}
\Box(g+h)(X) &= \Box g \;+_{\Box}\; \Box f \\
\Box(g-h)(X) &= \Box g \;-_{\Box}\; \Box f \\
\Box(g*h)(X) &= \Box g \;*_{\Box}\; \Box f \\
\Box(g/h)(X) &= \Box g \;/_{\Box}\; \Box f
\end{aligned}$$

Therefore, we can evaluate an inclusion function for $f \circ g$, given inclusion functions for the functions f and g.

Unfortunately, the inclusion functions defined above are only "theoretically" valid; that is, they rely on an infinitely precise representation for real numbers and arithmetic operations. Of course, such infinite precision can not be achieved using the floating point hardware of a digital computer. To perform interval analysis on a computer, an interval $A = [a, b]$ must be approximated by a *machine interval* $A_M = [a_M, b_M]$ that contains A, and that is representable on the computer (i.e., a_M and b_M are members of the machine's set of floating point numbers). A computer implementation of an inclusion function must ensure that machine intervals are produced that contain the range of the function.

Specifically, to perform interval arithmetic on a computer, we must be careful computing the arithmetic operations on the interval bounds. We can not assume that an inclusion function for $g + h$ can be constructed by producing the interval $[a +_M c, b +_M d]$, where the $+_M$ operator denotes the hardware addition operator. Hardware addition yields rounding errors, so it is possible that

$$a +_M c > a + c$$

in which case the interval $[a +_M c, b +_M d]$ might not be a valid bound for $g + h$. This problem can be solved on machines that support round-to-$-\infty$ and round-to-$+\infty$ rounding modes, such as those that conform to the IEEE floating point standard [ANSI/IEEE Std 754-1985, IEEE Standard for Binary Floating-Point Arithmetic]. Hardware operations that are performed in round-to-$-\infty$ mode result in a lower bound for the result of the operation, rather than a result that is close to the theoretical result, but may be greater or less. Hardware operations performed in round-to-$+\infty$ mode result in an upper bound for the result. A valid inclusion function for an arithmetic operator can therefore be computed using the round-to-$-\infty$ mode for computation of interval lower bounds (e.g., the addition $a +_M c$ for the lower bound of $g + h$) and round-to-$+\infty$ mode for computation of interval upper bounds (e.g., the addition $b +_M d$ for the upper bound of $g + h$).

5.1.2.3 Natural Interval Extensions

In the previous section we showed how inclusion functions may be evaluated for functions defined using arithmetic operators. In summary, given inclusion functions $\Box g$ and $\Box h$, we can construct an inclusion function for any arithmetic combination, $g \circ h$. Symbolically, we have

$$\Box(g \circ h) = \Box g \circ_{\Box} \Box h$$

where $\circ_{\Box}$ is an operator that takes the results of two inclusion functions and produces a bound on their arithmetic combination. For example, the $+_{\Box}$ operator is defined by

$$[a, b] +_{\Box} [c, d] = [a + c, b + d]$$

It is clear that this technique can be recursively applied to yield an inclusion function for an arbitrary, nested combination of arithmetic operators on a set of functions with known inclusion functions. For example, an inclusion function for $f + (g + h)$ is given by

$$\Box(f + (g + h)) = \Box f +_{\Box} (\Box g +_{\Box} \Box h) \tag{5.1}$$

Furthermore, this notion can be extended to non-arithmetic operators. For each operator, $P(f_1, f_2, \ldots, f_n)$, that produces a function given n simpler functions, we define a method, $P_{\Box}$, that evaluates an inclusion function for P, depending only on the interval results of the inclusion functions $\Box f_i$.[3] Let each of the functions f_i be defined on a domain D and let $X \in \mathbf{I}(D)$. An inclusion function for $P(f_1, \ldots, f_n)$ is then given by

$$\Box P(f_1, f_2, \ldots, f_n)(X) = P_{\Box}(A_1, A_2, \ldots, A_n)$$

where $A_i = \Box f_i(X)$ for $i = 1, \ldots, n$. In a generalization of Equation 5.1, given a set of

[3] In fact, this method is a locally recursive method (see Section 2.2.2.3.1).

operators like P, $P_1, P_2, \ldots, P_N$, an inclusion function can be evaluated for any function formed by their recursive composition (e.g., $P_1(P_2(f_1, f_2), P_3(f_3))$). Inclusion functions that are constructed with this recursive approach are called *natural interval extensions.*

Construction of an operator's inclusion function method may not be difficult if the operator's monotonicity intervals are known. Such inclusion functions are often ideal (i.e., have an excess width of 0). For example, an inclusion function evaluation method can be defined for the cosine operator. This definition is based on the observation that the cosine function is monotonically increasing in the interval $[\pi 2n, \pi(2n+1)]$, and monotonically decreasing in the interval $[\pi(2n+1), \pi(2n+2)]$, for integer n. Let f be a function from $\mathbf{R}^m$ to $\mathbf{R}$, and let $X \in \mathbf{I}^m$. Let an inclusion functions for f be given and evaluated on the interval X, yielding an interval $[a, b]$. An inclusion function for $\cos(f)$ can be evaluated on X according to the following rules[4]

$$\Box\cos(f)(X) = \begin{cases} [-1, 1], & \text{if } 1 + \lceil \frac{a}{\pi} \rceil \leq \frac{b}{\pi} \\ [-1, \max(\cos(a), \cos(b))], & \text{if } \lceil \frac{a}{\pi} \rceil \leq \frac{b}{\pi} \text{ and } \lceil \frac{a}{\pi} \rceil \bmod 2 = 0 \\ [\min(\cos(a), \cos(b)), 1], & \text{if } \lceil \frac{a}{\pi} \rceil \leq \frac{b}{\pi} \text{ and } \lceil \frac{a}{\pi} \rceil \bmod 2 = 1 \\ \begin{array}{l}[\min(\cos(a), \cos(b)) \ , \\ \max(\cos(a), \cos(b))],\end{array} & \text{otherwise} \end{cases}$$

Similar inclusion functions can be constructed for operators such as sine, square root, exponential, and logarithm.

As another example, the "square" operator, which raises its argument to the second power, has an easily constructed inclusion function. In this case, if the function f is defined as before, we have

$$\Box f^2(X) = \begin{cases} [a^2, b^2], & \text{if } a \geq 0 \\ [b^2, a^2], & \text{if } b \leq 0 \\ [0, \max(a^2, b^2)], & \text{otherwise} \end{cases}$$

where $\Box f(X) = [a, b]$. Interestingly, an inclusion function for the square operator can also be defined using the multiply inclusion function, $*_\Box$ (i.e., $\Box f^2(X) = \Box f(X) *_\Box \Box f(X)$).

[4]As in the case of the arithmetic operators, care should be exercised in computing the interval result for the cosine inclusion function. The numerical cosine evaluations implied by $\min(\cos(a), \cos(b))$, for example, must be computed so that they are a lower bound for the theoretical result.

Such an inclusion function is not as tight as the one described above if the interval to be squared straddles 0. For example, given $a > 0$,

$$[-a, a] *_\square [-a, a] = [-a^2, a^2]$$

but

$$[-a, a]^2 = [0, a^2]$$

This is typical of the behavior of inclusion functions, in that looser bounds are achieved when functionally dependent entities are combined as independent intervals.

Inclusion functions for the vector and matrix operations discussed in Section 2.2.2.2 are also easy to construct. For example, consider the dot product operator, which takes two functions of output dimension n, f and g, and produces a function, $f \cdot g$, of output dimension one, defined by

$$f \cdot g = \sum_{i=1}^{n} f_i g_i$$

An inclusion function method for the dot product operator can be defined using the interval arithmetic already discussed. To compute $\square(f \cdot g)$, we compute

$$(\square f_1 *_\square \square g_1) +_\square (\square f_2 *_\square \square g_2) +_\square \ldots +_\square (\square f_n *_\square \square g_n)$$

Note that the interval $\square f_i$ or $\square g_i$ is trivially computed by extracting the i-th coordinate interval of the vector-valued interval produced by $\square f$ and $\square g$, respectively. Similarly, interval arithmetic can be used to define inclusion function methods for the matrix multiply, inverse and determinant operators, and for vector operators like addition, subtraction, length, scaling, and cross product.

5.1.2.4 Inclusion Functions for Relational and Logical Operators

Inclusion functions can also be defined for relational and logical operators. These definitions allow natural interval extensions for functions that employ relational and logical operations (e.g., functions used as constraints).

A relational operator produces a result in the set $\{0, 1\}$, 0 for "false" and 1 for 'true". The operators **equal to**, **not equal to**, **less than**, and **greater than or equal to** are all binary relational operators. Inclusion functions for these operators must bound the result of the operator. For example, an inclusion function for **less than** can be easily defined. Let f and g be functions from $\mathbf{R}^n$ to $\mathbf{R}$. Let $\Box f$ and $\Box g$ be inclusion functions for f and g respectively. Let $X \in \mathbf{I}^n$, and

$$\begin{aligned} \Box f(X) &= [a, b] \\ \Box g(X) &= [c, d] \end{aligned}$$

Then we have

$$\Box(f < g)(X) = \begin{cases} [0,0], & \text{if } d \le a \\ [1,1], & \text{if } b < c \\ [0,1], & \text{otherwise} \end{cases}$$

Similarly, an inclusion function for the equality operator is given by

$$\Box(f = g)(X) = \begin{cases} [0,0], & \text{if } d < a \text{ or } b < c \\ [1,1], & \text{if } a = b = c = d \\ [0,1], & \text{otherwise} \end{cases}$$

Three results of a relational operator's inclusion function can be expected:

- $[0, 0]$ – the relation is false over the entire domain interval
- $[1, 1]$ – the relation is true over the entire domain interval
- $[0, 1]$ – the relation may be true or false in the domain interval

Logical operators combine results of the relational operators in Boolean expressions. The operators **and**, **or**, and **not** are examples of logical operators. An inclusion function for a logical operator must be defined with respect to the ternary output of the relational inclusion functions. For example, if r_1 and r_2 are two relational functions from $\mathbf{R}^n$ to $\{0, 1\}$, and $\Box r_1$ and $\Box r_2$ are their corresponding inclusion functions, then an inclusion function for the logical **and** of the relations, $r_1 \wedge r_2$, is given by

$$\square(r_1 \wedge r_2) = \begin{cases} [0,0]\,, & \text{if } \square r_1 = [0,0] \text{ or } \square r_2 = [0,0] \\ [1,1]\,, & \text{if } \square r_1 = [1,1] \text{ and } \square r_2 = [1,1] \\ [0,1]\,, & \text{otherwise} \end{cases}$$

An inclusion function for the logical **or** of the relations, $r_1 \vee r_2$, is given by

$$\square(r_1 \vee r_2) = \begin{cases} [0,0]\,, & \text{if } \square r_1 = [0,0] \text{ and } \square r_2 = [0,0] \\ [1,1]\,, & \text{if } \square r_1 = [1,1] \text{ or } \square r_2 = [1,1] \\ [0,1]\,, & \text{otherwise} \end{cases}$$

An inclusion function for the logical **not** of a relation, $\neg r_1$, is given by

$$\square(\neg r_1) = \begin{cases} [0,0]\,, & \text{if } \square r_1 = [1,1] \\ [1,1]\,, & \text{if } \square r_1 = [0,0] \\ [0,1]\,, & \text{otherwise} \end{cases}$$

5.1.2.5 Mean Value and Taylor Forms

Given a differentiable function $f : \mathbf{R}^m \to \mathbf{R}^n$, with parameters $x_1, x_2, \ldots, x_m$, an inclusion function, called the *mean value form*, can be constructed for f as follows:

$$\square f(Y) = f(c) +_{\square} \square f'(Y)(Y -_{\square} c) \tag{5.2}$$

where $c \in Y$, $Y \in \mathbf{I}^m$ and $\square f'$ is an inclusion function for the Jacobian matrix of f, i.e.,

$$\square f'(Y) = \left[\square \frac{\partial f_i}{\partial x_j}(Y)\right]$$

That the above formula represents a valid inclusion function for f is an immediate consequence of Taylor's theorem. Note that the addition, subtraction and matrix-vector multiplication operations implied by this definition are computed using interval arithmetic.[5]

[5]It should also be noted that to implement this mean value form on a computer, the interval $\square f([c,c])$ should replace $f(c)$. This is because the computer can not *exactly* compute $f(c)$ and must instead bound the result.

The rest of the treatment of interval analysis in this thesis will drop using the $\Box$ subscripts for interval arithmetic operations; it should be clear by the context whether the standard operations or their interval analogs are warranted. We also note that this mean value form can be easily implemented in the generative modeling approach by using the natural interval extension for the Jacobian matrix, which may be symbolically computed using the partial derivative operator.

If f' is Lipschitz, then the mean value form is order 2. This result means that a mean value form can result in very tight bounds as the width of the domain interval shrinks. On the other hand, the quadratic convergence of the mean value form implies that a poor bound will result for large intervals, Y. In this case, it may be better to use the natural interval extension for f, which may be order 1, and switch to a mean value form when the domain regions become small enough.

Choosing $c = \text{mid}(Y)$ in Equation 5.2 simplifies the calculations. This is because the interval subtraction result $Y - \text{mid}(Y)$ leads to symmetric intervals of the form

$$([-y_1, y_1], \ldots, [-y_n, y_n])^T$$

The matrix-vector interval multiplication implied by Equation 5.2 then requires multiplication of intervals (from the Jacobian inclusion function, $\Box f'$) by symmetric intervals (from $Y - c$), which can be computed by

$$[-y, y] *_{\Box} [a, b] = [-\max(|a|, |b|)y, \max(|a|, |b|)y]$$

Hence, the mean value form can be computed by finding the maximum of the absolute values of the Jacobian interval bounds, and computing simple scales of the Jacobian intervals rather than the more costly computation implied by the interval multiplication rule in Section 5.1.2.2. On the other hand, choosing a specific c not necessarily equal to mid(Y) can lead to a tighter bound for f [BAUM87].

The idea of a mean value form can be generalized to produce inclusion functions that incorporate more terms of a function's Taylor expansion. For example, an inclusion function called a *Taylor form of order 2* is defined by

$$\Box f(Y) = f(c) + f'(c)(Y - c) + \frac{1}{2}(Y - c)^T \Box f''(Y)(Y - c)$$

where $\Box f''$ is an inclusion function for the Hessian operator of f. Taylor forms of order n are treated in detail in [RATS84] and [RATS88].

Under certain conditions, mean value forms can also be used as inclusion function for functions that are not differentiable, using the concept of a *generalized gradient.* For example, the scalar function $f(x) = |x|$ is not differentiable at $x = 0$. Nevertheless, an inclusion function exists for its generalized gradient $\Box f'(X)$, given by

$$\Box f'([a, b]) = \begin{cases} [1, 1] & \text{if } a > 0 \\ [-1, -1] & \text{if } b < 0 \\ [-1, 1] & \text{if } 0 \in [a, b] \end{cases}$$

A mean value form that uses this generalized gradient inclusion function is a valid inclusion function for f. A more complete definition and treatment of generalized gradients and their inclusion functions can be found in [RATS88].

5.1.2.5.1 Second Order Convergence of the Mean Value Form We now prove the second order convergence of the mean value form, starting with two lemmas.

Lemma 5.1 Let $A, B \subset \mathbf{I}$ with $0 \in B$. Then

$$w(A *_\Box B) \leq w(B)(\max(|\operatorname{lb} A|, |\operatorname{ub} A|) + w(A))$$

Proof. Let $A = [a, b]$ and $B = [c, d]$. Let P be the hypothesized upper bound on the width of the product, i.e.,

$$P = w(B)(\max(|\operatorname{lb} A|, |\operatorname{ub} A|) + w(A))$$

We have that $c \leq 0$ and $d \geq 0$ because $0 \in B$. There are three cases to consider: $a \geq 0$, $b \leq 0$, and $0 \in [a, b]$.

If $a \geq 0$, then $\max(|a|, |b|) = b$, and

$$[a, b] *_\square [c, d] = [bc, bd]$$

Hence,

$$w(A *_\square B) = bd - bc = b(d - c) = w(B)b \leq P$$

If $b \geq 0$, then $\max(|a|, |b|) = |a| = -a$, and

$$[a, b] *_\square [c, d] = [ad, ac]$$

Hence,

$$w(A *_\square B) = ac - ad = -a(d - c) = w(B)|a| \leq P$$

Finally, if $0 \in [a, b]$, we first assume $|d| \geq |c|$. But, for arbitrary intervals X, Y, and Z

$$X *_\square (Y \bigcup Z) = (X *_\square Y) \bigcup (X *_\square Z)$$

and hence

$$w(X *_\square (Y \bigcup Z)) \leq w(X *_\square Y) + w(X *_\square Z)$$

Thus, since $[c, d] = [c, -c] \bigcup [-c, d]$,

$$\begin{aligned} w(A *_\square B) &\leq w([a, b] *_\square [c, -c]) + w([a, b] *_\square [-c, d]) \\ &\leq |c| \max(|a|, |b|) + dw(A) \\ &\leq w(B) \max(|a|, |b|) + w(A) \max(|c|, |d|) \\ &\leq w(B)(\max(|a|, |b|) + w(A)) \end{aligned}$$

since $\max(|c|, |d|) \leq w(B)$ if $0 \in B$. The case where $|c| < |d|$ can be treated similarly. ∎

Lemma 5.2 Let f be a differentiable function, $f : \mathbf{R}^n \longrightarrow \mathbf{R}$, over an interval domain, $X \in \mathbf{I}^n$, with coordinates $x_1, \ldots, x_n$. Let inclusion functions for $\dfrac{\partial f}{\partial x_i}$ exist, $\square \dfrac{\partial f}{\partial x_i}$, and let

$Q_i = \square\dfrac{\partial f}{\partial x_i}(X)$. Then

$$w(\overset{\text{id}}{\square}\, f(X)) \geq \sum_{i=1}^{n} w(X_i)|q_i|$$

for some choice of $q_i \in Q_i$, $i = 1, \ldots, n$.

Proof. Form the points $\alpha, \beta \in X$, as follows:

$$\alpha_i = \begin{cases} \operatorname{lb} X_i & \text{if } \operatorname{lb} Q_i > 0 \\ \operatorname{ub} X_i & \text{if } \operatorname{ub} Q_i < 0 \\ \operatorname{lb} X_i & \text{if } 0 \in Q_i \end{cases}$$

$$\beta_i = \begin{cases} \operatorname{ub} X_i & \text{if } \operatorname{lb} Q_i > 0 \\ \operatorname{lb} X_i & \text{if } \operatorname{ub} Q_i < 0 \\ \operatorname{lb} X_i & \text{if } 0 \in Q_i \end{cases}$$

Note that $\operatorname{lb} Q_i > 0$ implies that f is an increasing function of the coordinate x_i throughout the region X. Similarly, $\operatorname{ub} Q_i < 0$ implies that f is a decreasing function of the coordinate x_i throughout X. Hence,

$$w(\overset{\text{id}}{\square}\, f(X)) \geq |f(\beta) - f(\alpha)| = f(\beta) - f(\alpha)$$

But, by the Mean Value Theorem, and since X is convex,

$$f(\beta) - f(\alpha) = \sum_{i=1}^{n} \frac{\partial f}{\partial x_i}(\xi)(\beta_i - \alpha_i) \text{ for some } \xi \in X$$

We now show that, for each i,

$$\frac{\partial f}{\partial x_i}(\xi)(\beta_i - \alpha_i) \geq w(X_i)|q_i| \text{ for some } q_i \in Q_i$$

If $\operatorname{lb} Q_i > 0$, then $\beta_i - \alpha_i = w(X_i)$ by our definition of α and β. Also, $\dfrac{\partial f}{\partial x_i}(\xi) > 0$ for all $\xi \in X$. If $q_i = \dfrac{\partial f}{\partial x_i}(\xi)$, then

$$\frac{\partial f}{\partial x_i}(\xi)(\beta_i - \alpha_i) = w(X_i)|q_i|$$

Similarly, if $\operatorname{ub} Q_i < 0$, then $\beta_i - \alpha_i = -w(X_i)$ and $\dfrac{\partial f}{\partial x_i}(\xi) < 0$ for all $\xi \in X$. If $q_i = \dfrac{\partial f}{\partial x_i}(\xi)$, then

$$\frac{\partial f}{\partial x_i}(\xi)(\beta_i - \alpha_i) = -w(X_i)q_i = w(X_i)|q_i|$$

Finally, if $0 \in Q_i$, then $\alpha_i - \beta_i = 0$, and letting $q_i = 0$,

$$\frac{\partial f}{\partial x_i}(\xi)(\beta_i - \alpha_i) = 0 = w(X_i)|q_i|$$

Therefore, since $w(X_i)|q_i| \geq 0$, we have

$$w(\overset{\text{id}}{\square}\, f(X)) \geq f(\beta) - f(\alpha) \geq \sum_{i=1}^{n} w(X_i)|q_i| \quad \blacksquare$$

Theorem 5.1 (Krawczyk-Nickel (1982)) Let $f : \mathbf{R}^n \to \mathbf{R}^m$ be differentiable in region X. Let $\square f$ be the mean value form for f, i.e.,

$$\square f(Y) = f(c) + \square f'(Y)(Y - c) \text{ for } c \in Y,\ Y \subset X$$

If f' is Lipschitz, i.e.,

$$w(\square f'(Y)) < Kw(Y) \qquad \text{for all } Y \in \mathbf{I}(X)$$

then the mean value form has convergence order 2.

Proof. Without loss of generality, we can assume that f is a scalar function (i.e., $m = 1$), since if each component of f, f_i, has convergence order 2, we have

$$w(\square f_i'(Y)(Y - c)) - w(\overset{\text{id}}{\square}\, f_i(Y)) \leq c_i w(Y)^2$$

Hence,

$$\begin{aligned} w(\square f'(Y)(Y-c)) - w(\overset{\text{id}}{\square}\, f(Y)) &= \max_{i=1,\ldots,n} w(\square f_i'(Y)(Y-c)) - \max_{i=1,\ldots,n} w(\overset{\text{id}}{\square}\, f_i(Y)) \\ &\leq \max_{i=1,\ldots,n} (w(\square f_i'(Y)(Y-c)) - w(\overset{\text{id}}{\square}\, f_i(Y))) \\ &\leq \max_{i=1,\ldots,n} c_i w(Y)^2 \end{aligned}$$

$$\leq \; Kw(Y)^2 \text{ where } K = \max_{i=1,\ldots,n} c_i$$

Thus let f be a scalar function parameterized by $x_1, \ldots, x_n$, and let $\Box\frac{\partial f}{\partial x_i}(Y) = Q_i$. Because $\Box f'$ is Lipschitz, $Q_i \leq c_i w(Y)$. Let the excess width of the mean value form on the interval Y be named χ, given by

$$\chi(Y) = w\Big(\sum_{i=1}^{n} \Box\frac{\partial f}{\partial x_i}(Y)(Y_i - c_i)\Big) - w(\Box^{\text{idl}} f(Y))$$

Note that since $c \in Y$, $0 \in Y_i - c_i$. By Lemma 5.1, we have

$$\chi(Y) \leq \sum_{i=1}^{n} w(Y_i)(\max(|\operatorname{lb} Q_i|, |\operatorname{ub} Q_i|) + w(Q_i)) - w(\Box^{\text{idl}} f(Y))$$

Minimizing the second term, by Lemma 5.2,

$$\chi(Y) \leq \sum_{i=1}^{n} w(Y_i)(\max(|\operatorname{lb} Q_i|, |\operatorname{ub} Q_i|) + w(Q_i)) - \sum_{i=1}^{n} w(Y_i)|q_i|$$

for some choice of $q_i \in Q_i$. Therefore,

$$\begin{aligned}
\chi(Y) \;&\leq\; \sum_{i=1}^{n} w(Y_i)w(Q_i) + \sum_{i=1}^{n} w(Y_i)(\max(|\operatorname{lb} Q_i|, |\operatorname{ub} Q_i|) - |q_i|) \\
&\leq\; \sum_{i=1}^{n} w(Y_i)c_i w(Y) + \sum_{i=1}^{n} w(Y_i)w(Q_i) \\
&\leq\; 2\sum_{i=1}^{n} w(Y_i)c_i w(Y) \\
&\leq\; 2n \max_{i=1,\ldots,n} c_i w(Y)w(Y) \\
&\leq\; Kw(Y)^2 \;\blacksquare
\end{aligned}$$

5.1.2.6 Inclusion Functions Based on Monotonicity

Given a differentiable function, $f : \mathrm{R}^n \rightarrow \mathrm{R}$, an inclusion function with very little excess width can be formed by noting where f is monotonic with respect to its input parameters, $x_1, x_2, \ldots, x_n$. Let Y be an interval in which to evaluate an inclusion function for f, given by

$$Y_i = \left[y_i^0, y_i^1\right]$$

Note that the behavior of f in the interval Y with respect to one of its input parameters x_i can be categorized in three ways:

$$\begin{aligned}
\mathrm{lb}\,\square\frac{\partial f}{\partial x_i}(Y) \geq 0 &\Rightarrow f \text{ is non-decreasing in the interval } Y \\
\mathrm{ub}\,\square\frac{\partial f}{\partial x_i}(Y) \leq 0 &\Rightarrow f \text{ is non-increasing in the interval } Y \\
0 \in \square\frac{\partial f}{\partial x_i}(Y) &\Rightarrow \text{nothing can be concluded about } f
\end{aligned}$$

If f is non-decreasing in an interval with respect to a parameter x_i, then the minimum value of f occurs at the minimum value of x_i in the interval. The maximum value of f occurs at the maximum value of x_i. Similarly, if f is non-increasing with respect to x_i, then its minimum value occurs at the maximum value of x_i and its maximum value occurs at the minimum value of x_i.

We can thus form two intervals from Y, Y^- and Y^+, as follows

$$Y_i^- = \begin{cases} [y_i^0, y_i^0]\,, & \text{if } \mathrm{lb}\,\square\frac{\partial f}{\partial x_i}(Y) \geq 0 \\ [y_i^1, y_i^1]\,, & \text{if } \mathrm{ub}\,\square\frac{\partial f}{\partial x_i}(Y) \leq 0 \\ [y_i^0, y_i^1]\,, & \text{otherwise} \end{cases}$$

$$Y_+^- = \begin{cases} [y_i^1, y_i^1]\,, & \text{if } \mathrm{lb}\,\square\frac{\partial f}{\partial x_i}(Y) \geq 0 \\ [y_i^0, y_i^0]\,, & \text{if } \mathrm{ub}\,\square\frac{\partial f}{\partial x_i}(Y) \leq 0 \\ [y_i^0, y_i^1]\,, & \text{otherwise} \end{cases}$$

Assume that an inclusion function exists for f, $\square f$. For example, the natural interval extension for f can be used. A tighter inclusion function for f is then given by

$$[\mathrm{lb}\,\square f(Y^-)\,, \mathrm{ub}\,\square f(Y^+)\,]$$

This inclusion function is ideal if f is monotonic with respect to all its input parameters. If f is not a scalar function, then this technique can be used separately on each component of f.

Because an inclusion function based on monotonicity and the mean value form both evaluate inclusion functions for the partial derivatives of the function being bounded, it is reasonable to combine the two techniques and share these evaluations. This is easily accomplished since if $\Box_1 f, \Box_2 f, \ldots, \Box_n f$ are all inclusion functions for f, then so is

$$\bigcap_{i=1}^{n} \Box_i f$$

Thus the intersection of the bounds produced by the mean value form and the monotonicity-based inclusion function is also a valid inclusion function.

5.1.3 Constraint Solution Algorithm

A system of constraints can be represented as a function, $F : \mathbf{R}^n \rightarrow \mathbf{R}$, that returns a 1 if the constraints are satisfied and a 0 if they are not. Such a function can incorporate both equality and inequality constraints. It can be represented with the relational and logical operators discussed in Section 2.2.2.2. As discussed in Section 5.1.2.4, an inclusion function for F, $\Box F$, over a region $X \subset \mathbf{I}^n$ can take on three possible values:

$$\begin{aligned}
\Box F(X) = [0,0] &\Rightarrow X \text{ is an infeasible region} \\
\Box F(X) = [0,1] &\Rightarrow X \text{ is an indeterminate region} \\
\Box F(X) = [1,1] &\Rightarrow X \text{ is a feasible region}
\end{aligned}$$

An *infeasible region* is a region in which no point solves the constraint system. A *feasible region* is a region in which every point solves the constraint system. An *indeterminate region* is a region in which the constraint system may or may not have solutions. We now present an algorithm to find solutions to this constraint system.

Algorithm 5.1 (Constraint Solution Algorithm) We are given a constraint inclusion function $\Box F$ and an initial region, X, in which to find solutions $F(x) = 1$.[6]

[6]The initial region X can be infinite if the technique of *infinite interval arithmetic* is used (see [RATS88]).

```
place $X$ on list $L$
while $L$ is nonempty
    remove next region $Y$ from $L$
    evaluate $\Box F$ on $Y$
    if $\Box F(Y) = [1,1]$ add $Y$ to solution
    else if $\Box F(Y) = [0,0]$ discard $Y$
    else if $w(Y) < \epsilon$ add $Y$ to solution
    else subdivide $Y$ into regions $Y_1$ and $Y_2$ and insert into $L$
endwhile
```

Algorithm 5.1 finds a superset of solutions to the constraint system. In particular, by the property of inclusion functions, if this algorithm finds no solutions, then the constraint system has no solutions, because a region Y is rejected only when $\Box F(Y)$ shows that it is infeasible. We now prove that the constraint solution algorithm converges to the actual solution set, if the inclusion functions used in the equality and inequality constraints are convergent.

We first assume that Algorithm 5.1 is allowed to iterate forever. That is, no indeterminate or feasible solutions are accepted and removed from the list. Let S be the set of solutions to the constraint problem, given an initial region X. Let the constraint system, $F(x)$, be given by the simultaneous satisfaction of

$$\begin{aligned} g_i(x) &= 0 \quad i = 1, \ldots, r \\ h_j(x) &\leq 0 \quad j = 1, \ldots, s \end{aligned}$$

We assume that regions are added to the list L so that all regions present at an given iteration are eventually subdivided or discarded. For example, this can be achieved simply by inserting newly subdivided regions at the end of the list, and obtaining the "next" region Y from the top of the list. We further assume that subdivision occurs so that all dimensions of a region are eventually subdivided (see Section 5.1.3.1). The combination of these two assumptions implies

$$w(U_n^i) \to 0 \text{ as } n \to \infty$$

where U_n^i denotes the i-th region on the list after iteration n. The set of intervals $\{U_n^i\}$ for any n are called the *candidate intervals* of the algorithm. Let U_n be the union of all the candidate intervals after n iterations, i.e.,

$$U_n = \bigcup_{i=1}^{s_n} U_n^i$$

where s_n denotes the number of intervals on the algorithm's list after n iterations.

Theorem 5.2 Let the inclusion functions for the constraint system be convergent, i.e.,

$$\begin{aligned} w(\Box g_i(Y)) &\to 0 \quad \text{as} \quad w(Y) \to 0 \\ w(\Box h_j(Y)) &\to 0 \quad \text{as} \quad w(Y) \to 0 \end{aligned}$$

for $Y \in \mathbf{I}(X)$. Then the set of solutions generated by Algorithm 5.1 converges to S, i.e.,

$$S = \bigcap_{n=1}^{\infty} U_n$$

Proof. Clearly, $S \subset \bigcap_{n=1}^{\infty} U_n$ because no solution is discarded by the algorithm. We show that $x \in U_n$ for all n implies $x \in S$.

Assume $x \notin S$. Then $g_k(x) \neq 0$ for some $k \in \{1, \ldots, r\}$ or $h_l(x) > 0$ for some $l \in \{1, \ldots, s\}$. Consider first that $g_k(x) = q \neq 0$. Because $w(\Box g_k(Y)) \to 0$ as $w(Y) \to 0$, there exists an interval $V_x \subset X$ containing x such that $0 \notin \Box g_k(V_x)$. Furthermore, for any subset $W \subseteq V_x$, $0 \notin \Box g_k(W)$. But because $w(U_n^i) \to 0$ as $n \to \infty$, there exists $U_p^{i_p} \subset V_x$ for some p. Hence, $0 \notin \Box g_k(U_p^{i_p})$, so a region containing x is eventually discarded. This violates the condition that $x \in U_n$ for all n. The proof for the case of violation of an inequality constraint, $h_l(x) \leq 0$, is similar. ∎

Unfortunately, a computer implementation of the constraint solution algorithm can not iterate forever; it must terminate at some iteration n and accept the remaining regions as solutions. In particular, the algorithm may accept some indeterminate regions, which may contain zero, one, or more solutions. For example, consider solving a system of equations, $G(x) = 0$, for a function $G : \mathbf{R}^n \to \mathbf{R}^n$. Assume that the system, $G(x) = 0, x \in D$, has a finite, nonempty set of solutions for $D \subset \mathbf{R}^n$. Any neighborhood of these solution points will also contain points, y, for which $G(y) \neq 0$. Hence an inclusion function for the system $G(x) = 0$ will always yield an indeterminate result in the neighborhood of a solution. The algorithm will accept such regions as solutions when their width becomes smaller than ϵ. Of course, the algorithm may also accept an indeterminate region that contains no solutions; there is no way for the algorithm to make this distinction.

The problem that the constraint solution algorithm may yield regions that do not contain solutions, or regions that contain more than one solution, is mitigated by several factors. First, it may be enough to distinguish between the case that the constraint problem possibly has solutions (to some tolerance), and the case that it has no solutions. For example, to compute interference detection between two parametric surfaces

$$S_1, S_2 : \mathbf{R}^2 \rightarrow \mathbf{R}^3$$

a constraint system of three equations in four variables can be solved of the form

$$S_1(u_1, v_1) = S_2(u_2, v_2)$$

If we instead solve the relaxed constraint problem,

$$\|S_1(u_1, v_1) - S_2(u_2, v_2)\| < \epsilon$$

the algorithm can hope to produce feasible solution regions, for which the constraints are satisfied for every point in the region.[7] Such relaxed constraint problems are called ϵ-collisions in [VONH89]. If any feasible regions are found, the surfaces interfere to within the tolerance. If all regions are eventually found to be infeasible, the surfaces do not interfere within the tolerance, and in fact come no closer than ϵ. It is also possible that only indeterminate regions are accepted as solutions. In this case, we may consider the two surfaces to interfere to the extent that our limited floating point precision is able to ascertain.

Second, we may know a priori that the system has a single solution. This is not uncommon if the constraint solution problem is the result of a geometric modeling operation, such

[7]Note that the solution to the unrelaxed system is typically a curve of intersection between the two parametric surfaces. Any neighborhood of a point on this curve will also contain points for which the two surfaces do not intersect and hence do not solve the system of equations. The relaxed problem, on the other hand, has solutions for which a neighborhood of small enough size is completely contained within the solution space.

as computing the intersection of two curves. In this case, the algorithm can be run until a set of contiguous solution regions is produced of small enough combined width. A point inside the set of regions can be used as an approximation to the solution contained within it. If the inclusion functions bounding the constraint equality and inequality functions are convergent, then such a solution approximation achieves any degree of accuracy as ϵ goes to 0. The technique of combining contiguous solution regions, called ***solution aggregation***, will be discussed further in Section 5.1.3.2.

Third, we may be able to compute information about solutions to the constraint system as the algorithm progresses. For example, in solving the 1D system, $f(x) = 0$ for differentiable scalar function f, if we have that $f(x_0) < 0$ and $f(x_1) > 0$ and $\Box f'([x_0, x_1]) > 0$, then f is strictly increasing in the interval $[x_0, x_1]$, and hence has exactly one zero in this interval. This result can be generalized: Section 5.1.3.4 presents a theorem specifying conditions computable with interval techniques under which a region contains exactly one zero of a system of equations.

Finally, we can relax the constraints of a constraint system and/or accept indeterminate results of the algorithm. In practice, although we can not guarantee the validity of such results, they are nevertheless useful. For example, if the constraint solution algorithm is used as part of a higher-level algorithm (e.g., an algorithm to approximate implicit curves, as will be presented in Section 5.2.2), then the global consistency of the result of the higher-level algorithm verifies to some extent the results of the constraint solution algorithm.

The next sections will discuss elements of the constraint solution algorithm in more detail.

5.1.3.1 Subdivision Methods

Subdivision in Algorithm 5.1 can proceed in two ways. First, each input space dimension can be cyclically subdivided at its midpoint. This is accomplished by storing the last subdivided dimension along with each region on the candidate solution list. Let n be the dimensionality of the input space, and let d be the last subdivided dimension of a region,

$X = ([a_1, b_1], [a_2, b_2], \ldots, [a_n, b_n])$. The next dimension to subdivide, d', is computed as

$$d' = \begin{cases} d+1 & \text{if } d < n \\ 1 & \text{if } d = n \end{cases}$$

The two child regions are then given by

$$\begin{aligned} Y_1 &= ([a_1, b_1], \ldots, [a_{(d'-1)}, b_{(d'-1)}], [a_{d'}, (a_{d'} + b_{d'})/2], [a_{(d'+1)}, b_{(d'+1)}], \ldots, [a_n, b_n]) \\ Y_2 &= ([a_1, b_1], \ldots, [a_{(d'-1)}, b_{(d'-1)}], [(a_{d'} + b_{d'})/2, b_{d'}], [a_{(d'+1)}, b_{(d'+1)}], \ldots, [a_n, b_n]) \end{aligned}$$

The subdivided dimension, d', is stored along with the regions Y_1 and Y_2. This kind of subdivision is general and simple to implement. It also produces sets of solution regions with special properties required by some of the geometric modeling algorithms that follow.

On the other hand, regions can be subdivided based on other criteria. By knowing properties of the constraint system whose solutions are sought, we can often deduce regions smaller than Y_1 and Y_2 where the constraints can be satisfied. For example, in the method of Hansen-Greenberg [RATS88] for finding zeroes of m nonlinear equations of m variables, gaps may be discovered in coordinate intervals of the region X where zeroes can not exist. Hence, we can produce regions Y_1 and Y_2 that do not contain these infeasible points. Section 5.1.3.4 discusses another method for reducing the size of candidate intervals, known as an interval Newton method.

5.1.3.2 Solution Aggregation

Many times, we expect the solution set of a system of constraints to be a finite number of points. The constraint solution algorithm will typically return a collection of connected regions for each of the solution points, as shown in Figure 5.1. Using an argument similar to Theorem 5.2, if a finite set of solutions exist, then Algorithm 5.1 will eventually produce candidate regions that can be organized into a collection of sets of connected regions, each set containing a single solution and disjoint from all other such sets. The technique of solution aggregation presumes that such an appropriate iteration level has been achieved, so that an approximate solution is given by a point inside each set, to any degree of accuracy as the iteration level is increased. The number of solutions to the constraint system is assumed

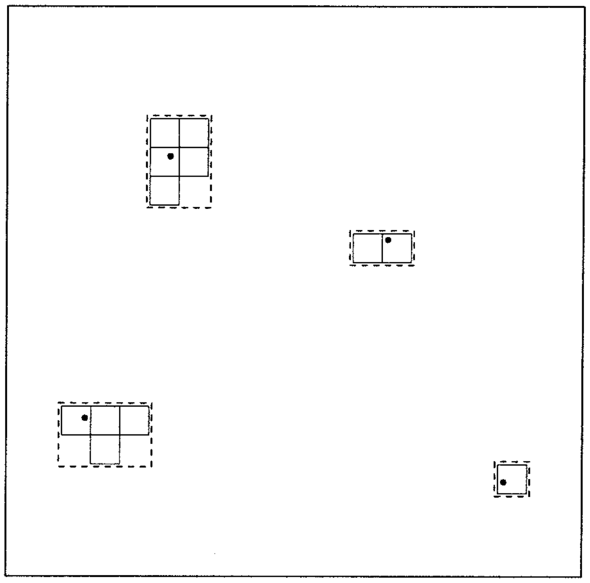

Figure 5.1: Solution aggregation – The solution regions returned by Algorithm 5.1 for an example problem with an input dimension of 2 are given by the collection of nondashed squares. The actual solutions are marked by dots. In this example, an adequate level of subdivision has been achieved so that sets of contiguous regions encompass each of the four solutions, and each contiguous region may be bounded in an interval (dashed boxes) that is disjoint from other such regions.

to be the number of disjoint sets produced. This technique may be used heuristically, or in combination with the condition for existence of a unique zero presented in Section 5.1.3.4.2.

We now define a simple algorithm for solution aggregation. Given $A, B \in \mathbf{I}^n$, we define the *merge* operator, $A \vee B$, as

$$(A \vee B)_i \equiv [\min(\operatorname{lb} A_i, \operatorname{lb} B_i), \max(\operatorname{ub} A_i, \operatorname{ub} B_i)]$$

Let S be a list of intervals, and X be an interval. We first define a function `add`(X, S) to add X onto the list S (with aggregation). We can then define a solution aggregation function, `aggregate`(Q), that takes a list of intervals, Q, and produces a new list of intervals, where all connected intervals are merged. The precise definitions of `add` and `aggregate` are shown in Figure 5.2.

```
add($X, S$)

for each interval $Y$ in $S$
    if $Y \bigcap X \neq \emptyset$ then
        $X = X \vee Y$
        delete $Y$ from $S$
    endif
endfor
insert $X$ into $S$
return $S$
```

```
aggregate($Q$)

initialize aggregate list $S$ to empty
for each interval $X$ in $Q$
    $S = $ add($X, S$)
endfor
return $S$
```

Figure 5.2: Algorithms for solution aggregation – The function `add` adds a region X to the list of regions S, merging if necessary. The function `aggregate` then uses `add` to aggregate the regions of a list Q.

5.1.3.3 Termination and Acceptance Criteria for Constraint Solution

A constraint system can be "solved" in four ways:

1. find a superset of solutions
2. determine whether a solution exists
3. find one solution
4. find all solutions

Slight modifications to Algorithm 5.1 regarding when the algorithm is halted and when indeterminate regions are accepted as solutions can make it applicable to each of these specific subproblems. The following discussion analyzes the application of Algorithm 5.1 to these subproblems, making the distinction between *heuristic* approaches, in which the results are not guaranteed to be correct, and *robust* approaches, in which the results are guaranteed correct.

An unmodified Algorithm 5.1 can be used to robustly find a superset of solutions to the constraint system. Computing bounds on the solution set is often useful in higher-level algorithms. As the ϵ parameter of Algorithm 5.1 is decreased, the bound on the solution set becomes tighter, at the expense of greater computation. The solution superset can also be visualized to obtain a rough idea of the nature of the solutions, even if the solutions form a multidimensional manifold rather than a finite set of points. This is useful, for example, in testing whether the constraint system models a desired geometric operation.

In using Algorithm 5.1 to determine whether the constraint system has solutions, two situations lead to a robust answer. If the algorithm terminates with an empty list of solutions, then the algorithm should terminate with the answer "no". If at any point the algorithm finds a feasible region, then the algorithm can immediately terminate with the answer "yes". If the algorithm can find only indeterminate regions, then nothing can be concluded with certainty. A heuristic solution to this problem is to return "yes" anyway. In practice, a region that has been subdivided to a very small size (e.g., around the precision of a double precision number) and is still indeterminate probably contains a solution to the constraint system. This heuristic approach can be made more robust through the use of acceptance criteria for indeterminate regions. For example, in solving the system $f(x) = 0$, it is reasonable that a region, Y, before being accepted as a solution, should satisfy

$$w(\Box f(Y)) < \delta$$

for some small δ. When such indeterminate acceptance criteria are used, the algorithm should report an error when none of the indeterminate regions satisfy the acceptance criteria. A robust solution to the problem can be achieved by robustly testing indeterminate regions for the existence of solutions, using the test of Section 5.1.3.4.2.

Finding a single solution to a constraint system is useful if we expect a single point solution, or want only a single point as a representative solution. As in the previous case, Algorithm 5.1 provides a robust solution to this subproblem in two situations. The algorithm may concluded that the entire starting region is infeasible, or find a feasible region. In the latter case, any point in the feasible region can be chosen as a representative solution and the algorithm can be halted. If indeterminate regions are found of width less than the tolerance ϵ, they can be accepted directly, or accepted depending on some further criteria. Both schemes are heuristic. A more robust approach involves analyzing the convergence of the solution superset as the algorithm iterates. Consider the sequence of summed widths,

w_n, of candidate solutions on the list L

$$w_n = \sum_{i=1}^{s_n} w(U_n^i)$$

where U_n^i represents the i-th interval on the list L after iteration n, and s_n is the number of such intervals. Iteration can be terminated when w_n becomes sufficiently small. A completely robust solution to this subproblem can be achieved using a robust test for the existence and uniqueness of a solution (see Section 5.1.3.4.2).

Finally, Algorithm 5.1 can be applied to the problem of finding all solutions to a constraint system, when a finite set of solutions is expected. In this case, if the algorithm terminates with an empty solution list, there are no solutions. If a feasible region is found, an infinite number of solutions exist. If only indeterminate regions are found, then a useful heuristic approach is to use solution aggregation to obtain a set of disjoint regions and pick a point inside each region as a solution. This approach can be made more robust in the following ways:

- ensure each aggregated region is sufficiently small
- check convergence of the widths of each aggregated region
- use further acceptance criteria for each aggregated region

If the number of solutions is known beforehand, then the algorithm can be terminated with an error condition if the machine precision is reached in subdivision with a number of aggregated regions unequal to the number of solutions. Of course, we note that although this approach almost always works correctly, it is still heuristic, since, for example, one region may contain no solutions while another contains two. A robust approach to the subproblem of obtaining all solutions to the constraint system is to use a robust test for solution existence in each aggregated region. In this case, reaching the machine precision limit during subdivision without being able to verify solution existence should result in an error termination.

5.1.3.4 Interval Newton Methods

Interval Newton methods are robust methods for finding zeroes of a system of n equations of n variables. They are the interval analogs of multidimensional Newton iteration for the simultaneous solution of nonlinear equations.

Consider the problem of finding all zeroes of a function $f : \mathbf{R}^n \rightarrow \mathbf{R}^n$ over an interval $X \in \mathbf{I}^n$. Let the coordinates of f be given by $x_1, x_2, \ldots, x_n$. By the Mean Value Theorem, given a $c \in X$, for each $x \in X$, there exist n points, $\xi_1, \xi_2, \ldots, \xi_n$ such that

$$f(x) = f(c) + J(\xi_1, \ldots, \xi_n)(x - c)$$

where the matrix J is given by

$$J_{ij} = \frac{\partial f_i}{\partial x_j}(\xi_i)$$

and where each ξ_i is a point on the line between x and c. Because X is an interval, and $x, c \in X$, each ξ_i is a member of X. Let $\square f'$ be an inclusion function for Jacobian matrix of f, i.e.,

$$\square f' = \left\{ J \mid J_{ij} \in \square \frac{\partial f_i}{\partial x_j} \right\}$$

If x is a zero of f, we have

$$\exists J \in \square f'(X) \ni f(x) = 0 = f(c) + J(x - c)$$

Therefore, if Q is the set of solutions

$$Q = \{x \mid \exists J \in \square f'(X) \ni f(c) + J(x - c) = 0\}$$

then Q contains all zeroes of f in X.

This leads to the following iterative algorithm for finding the zeroes of f, called an interval Newton method. The initial interval X_0 is set to X. The next interval X_{n+1} is computed from interval X_n as follows.

```
choose $c$ in $X_n$
find an interval $Z$ that bounds the set of solutions

    $\{x \mid \exists J \in \Box f'(X_n) \ni 0 = f(c) + J(x-c)\}$

if $Z$ is empty, no zeroes of $f$ exist in $X$
otherwise set $X_{n+1} = Z \bigcap X_n$
```

By the argument of the previous paragraph, no zero is ever lost by this iterative procedure. Remarkably, if at any stage of the iteration, $Z \subseteq X_n$, then f has a unique zero in X_n, a result we will prove in Section 5.1.3.4.2.

Interval Newton methods are typically combined with an exhaustive subdivision algorithm such as Algorithm 5.1. That is, when an interval Newton iteration is effective at reducing the size of the set of possible zeroes, its use is continued. Otherwise, exhaustive subdivision is performed. Interval Newton methods are also effective in concert with local methods, such as standard Newton or quasi-Newton iteration. This is because the interval Newton procedure is most effective when the point c is as close as possible to a zero of f. The Hansen-Greenberg algorithm for finding zeroes of f [RATS88] uses exhaustive subdivision, interval Newton methods, and local Newton methods.

The crux of the interval Newton algorithm is to find an interval Z that bounds the solutions of the linear interval equation. If the interval determinant of the matrix $\Box f'(X)$ is not zero, then the interval analog of LU decomposition can be used to find solutions. If the interval determinant does contain zero, then the interval analog of Gauss-Sidel iteration can be effective. Neither of these methods results in a tight bound for the solution set, which can be computed using linear optimization.

5.1.3.4.1 Interval Newton Methods and Linear Optimization In the previous section, we showed that the interval Newton method requires computation of a bound on the set

$$\{x \mid \exists J \in \Box f'(X) \ni 0 = f(c) + J(x-c)\}$$

To compute this, let $y = x - c$, and let Z' be an interval bound on the set

$$\{y \mid \exists J \in \Box f'(X) \ni Jy = -f(c)\}$$

Then the interval Z, defined by

$$Z = Z' +_{\square} [c, c]$$

is an interval bound on the original set. Thus, computing the interval Newton bound Z can be accomplished by solving a linear interval equation of the form

$$Mx = b$$

where M is a given $n \times n$ interval matrix, and b is a given interval vector. We require a bound on the set of solutions of this equation for x, given any matrix in M, and vector in b, i.e., on the set

$$\{x \mid \exists \mathcal{M} \in M, \beta \in b \ni \mathcal{M}x = \beta\}$$

Naively, this problem is not amenable to linear optimization algorithms because variables in M and x are multiplied together. However, it is possible to transform the problem so that it is posed as a linear optimization problem. We represent x as the difference of two vectors, y and z where each component of y and z is nonnegative. Let the matrix M be given by the component intervals

$$M_{ij} = [c_{ij}, d_{ij}]$$

and let b be represented by the component intervals

$$b_i = [p_i, q_i]$$

Let $m_{ij} \in M_{ij}$. We then get n constraints of the form

$$m_{i1}y_1 - m_{i1}z_1 + \cdots + m_{in}y_n - m_{in}z_n \in [p_i, q_i] \tag{5.3}$$

where $y_j, z_j \geq 0$. If we let all the variables y_j and z_j be 0 except for one, say y_k, then we can find an interval in y_k that solves (5.3). This interval is called the y_k *interval intercept* of (5.3). The interval intercept can be computed using the technique of infinite interval division, whose rules are given by

$$[a,b]/_{\square}[c,d] = \begin{cases} [\min(a/c, a/d, b/c, b/d)\ , & \\ \quad \max(a/c, a/d, b/c, b/d)] & \text{if } 0 \notin [c,d] \\ [b/c, +\infty] & \text{if } b \leq 0 \text{ and } d = 0 \\ [-\infty, b/d] \bigcup [b/c, +\infty] & \text{if } b \leq 0,\ c < 0, \text{ and } d > 0 \\ [-\infty, b/d] & \text{if } b \leq 0 \text{ and } c = 0 \\ [-\infty, a/c] & \text{if } a \geq 0 \text{ and } d = 0 \\ [-\infty, a/c] \bigcup [a/d, +\infty] & \text{if } a > 0,\ c < 0, \text{ and } d > 0 \\ [a/d, +\infty] & \text{if } a \geq 0 \text{ and } c = 0 \\ [-\infty, +\infty] & \text{if } a < 0,\ b > 0 \text{ and } 0 \in [c,d] \\ [-\infty, +\infty] & \text{if } c = d = 0 \end{cases}$$

The appropriate y_k and z_k interval intercepts are therefore given by

$$\begin{aligned} y_k &\in [p_i, q_i] /_{\square} [c_{ik}, d_{ik}] \\ z_k &\in [-q_i, -p_i] /_{\square} [c_{ik}, d_{ik}] \end{aligned}$$

Solutions to (5.3) are limited to the set of hyperplanes whose intercepts with each of the $2n$ variables y_j and z_j lie in the appropriate interval intercept. Let the results of the interval division be given by

$$\begin{aligned} y_k &\in [e_k, f_k] \text{ or } [-\infty, f_k] \bigcup [e_k, +\infty] \\ z_k &\in [g_k, h_k] \text{ or } [-\infty, h_k] \bigcup [g_k, +\infty] \end{aligned}$$

If any of these results is a pair of semi-infinite intervals, then we consider each disjoint interval as a separate case, termed *splitting* the problem. Thus, assume $y_k \in [e_k, f_k]$ and $z_k \in [g_k, h_k]$ where each interval is finite, semi-infinite, or infinite, and where e_k, f_k, g_k and h_k are not equal to 0. The part of the set of hyperplanes with these interval intercepts that also satisfies $y_k, z_k \geq 0$ lies between two boundary hyperplanes in $\mathbf{R}^{2n}$. One hyperplane intersects each variable's axis at the lower bound of the interval intercept (e_k or g_k); the other intersects each variable's axis at the upper bound of the variable's intercept (f_k or

h_k).

We note that a hyperplane in $\mathbf{R}^m$ that intersects each coordinate axis x_i at the point $a_i \neq 0$, $i = 1, \ldots, m$ is given by the equation

$$x_1/a_1 + x_2/a_2 + \cdots + x_m/a_m = 1$$

The minimum and maximum boundary hyperplanes bounding the solution to (5.3) yield the following inequalities

$$y_1/e_1 + z_1/g_1 + \cdots + y_n/e_n + z_n/g_n \geq 1 \quad (5.4)$$

$$y_1/f_1 + z_1/h_1 + \cdots + y_n/f_n + z_n/h_n \leq 1 \quad (5.5)$$

If any of the e_i, f_i, g_i or h_i is infinite, the corresponding y_i or z_i variable is eliminated. If all the variables are eliminated in this way, the entire subproblem either has no solutions (first inequality) or is satisfied everywhere (second inequality).

For each subproblem (where a subproblem is one obtained by considering each half of a split interval intercept separately), we have a system of linear constraints where the constants e_i, f_i, g_i and h_i are given, and the y_j and z_j are variables. To find bounds on the solutions to this subproblem, we must solve $2n$ linear optimization problems to minimize and maximize the quantities

$$x_i = y_i - z_i$$

subject to the constraints (5.4) and (5.5).[8] If m of variable intercept are split, then 2^m subproblems must be solved, for each combination of split variable intercepts. Bounds on each of the subproblems are computed using linear optimization and then merged, using the technique of Section 5.1.3.2.

If the number of split variable intercepts is large, the computational requirements of bounding the linear interval equation's solutions becomes very large. This problem can be reduced by not splitting the interval intercepts when interval division yields a pair of semi-infinite intervals. Instead, the intercept can be replaced by the interval $[-\infty, +\infty]$, and the

[8]Note that a feasible point for the constraints need be computed once, and can be shared in each of the $2n$ linear optimization problems. If no feasible point exists, there is no solution to the subproblem.

problem solved as before. We then solve a single linear optimization problem rather than 2^m, but receive a looser bound. Alternatively, we may split only some of the semi-infinite intervals.

5.1.3.4.2 A Theorem Concerning the Existence of Zeroes An interesting and useful result can be proved that guarantees the existence of a unique zero in $f : \mathbf{R}^n \to \mathbf{R}^n$ in an interval domain X.

Lemma 5.3 Let $\Box M$ be an $n \times n$ interval matrix, i.e.,

$$\Box M = \{M \mid M_{ij} \in \Box M_{ij},\ \Box M_{ij} \in \mathbf{I},\ \ i,j \in \{1..n\}\}$$

If, for a vector b, the set of solutions

$$S = \{x \mid \exists M \in \Box M \ni Mx = b\}$$

is bounded and nonempty, then $\det M \neq 0$ for any $M \in \Box M$.

Proof. If a matrix $M \in \Box M$ exists such that $\det M = 0$, then the equation $Mx = b$ either has no solutions or an infinite, unbounded collection of solutions. Hence, because S is nonempty and bounded, there exists an A such that $\det A \neq 0$. Assume that another matrix B exists such that $\det B = 0$. We will prove that this yields a contradiction.

Consider changing the matrix A to the matrix B one matrix element at a time. Let C_i be a sequence of $n^2 + 1$ matrices defined by

$$\begin{aligned} C_0 &= (A_{11}, A_{12}, A_{13}, \ldots, A_{nn}) = A \\ C_1 &= (B_{11}, A_{12}, A_{13}, \ldots, A_{nn}) \\ C_2 &= (B_{11}, B_{12}, A_{13}, \ldots, A_{nn}) \\ &\vdots \\ C_{n^2} &= (B_{11}, B_{12}, B_{13}, \ldots, B_{nn}) = B \end{aligned}$$

Since A and B are members of $\Box M$, so is each C_i. Since $\det C_0 \neq 0$ and $\det C_{n^2} = 0$, there is some transition, C_i to C_{i+1}, such that $\det C_i \neq 0$ and $\det C_{i+1} = 0$. Hence, without loss of generality, let our matrices A and B be chosen so that $\det A \neq 0$, $\det B = 0$, and A and B differ in a single coordinate, i.e., $A_{pq} \neq B_{pq}$.

Let the matrix $C(t)$ be defined by

$$C(t) = A + (B - A)t$$

Note that $C(t) \in \square M$ for $t \in [0, 1]$. Let η be the solution to the equation $Ax = b$. Consider the solutions to the equation

$$C(t)x = b$$

Since A is nonsingular, this equation can be rewritten

$$\begin{aligned} A^{-1}C(t)x &= A^{-1}b \\ A^{-1}(A + (B - A)t)x &= \eta \\ (I + A^{-1}(B - A)t)x &= \eta \end{aligned}$$

where I represents the identity matrix.

Let $Q(t) = I + A^{-1}(B - A)t$. Note that $B - A$ is a matrix of all zero elements except for the pq component, with value $B_{pq} - A_{pq} = s \neq 0$. That is,

$$(B - A)_{ij} = \delta_{ip}\delta_{jq}s$$

Then,

$$\begin{aligned} Q_{ij}(t) &= \delta_{ij} + \sum_{k=1}^{n} A_{ik}^{-1}(B - A)_{kj}t \\ &= \delta_{ij} + \sum_{k=1}^{n} A_{ik}^{-1}\delta_{kp}\delta_{jq}st \\ &= \delta_{ij} + A_{ip}^{-1}\delta_{jq}st \end{aligned}$$

Hence $Q(t)$ is a matrix like the identity matrix except for its q-th column. Because of its simple structure, we can readily compute its determinant

$$\det Q(t) = 1 + A_{qp}^{-1}st$$

We now solve the equation $Qx = \eta$, or in component notation

$$\sum_{j=1}^{n} Q_{ij} x_j = \eta_i$$

Letting $i = q$ yields

$$x_q + A_{qp}^{-1} x_q st = \eta_q$$

which implies

$$x_q \det Q = \eta_q$$

Letting $i \neq q$ yields

$$x_i + A_{ip}^{-1} x_q st = \eta_i$$

which implies

$$x_i = \eta_i - A_{ip}^{-1} x_q st$$

Thus the equation $Qx = \eta$ can be solved if x_q exists.

There are two possibilities, $\eta_q = 0$ and $\eta_q \neq 0$. If $\eta_q = 0$, then $Q(1)x = \eta$ has an infinite, unbounded collection of solutions since $\det Q(1) = \det B = 0$. Therefore, any x_q solves the equation. If $\eta_q \neq 0$, then the solution diverges as $t \to 1$ since $\det Q(t) \to 0$ as $t \to 1$, and since $\det Q(t)$ is a continuous function of t. Hence, the solution set is unbounded. Therefore, there is no matrix $B \in \square M$ such that $\det B = 0$. ∎

Theorem 5.3 (Bao-Rokne (1987)) Let $f : \mathbf{R}^n \to \mathbf{R}^n$ be continuously differentiable in an interval domain X, and let $c \in X$. Let $\square J$ be the interval Jacobian matrix of f over X, i.e.,

$$\square J = \left\{ J \mid J_{ij} \in \square \frac{\partial f_i}{\partial x_j}(X) \right\}$$

Let Q be the solution set of the interval equation

$$f(c) + \square J(x - c) = 0$$

That is,

$$Q = \{x \mid \exists J \in \square J \ni f(c) + J(x - c) = 0\}$$

If $Q \neq \emptyset$ and $Q \subseteq X$, then f has a unique zero in X.

Proof. We will construct a matrix $J(x) \in \Box J$, a continuous function of x, such that

$$f(x) = f(c) + J(x)(x - c)$$

for any $x \in X$. By Lemma 5.3, for each $J \in \Box J$, we have that $\det J \neq 0$. Hence the inverse, J^{-1}, exists for each $J \in \Box J$. Thus the solution set Q may be written

$$Q = \left\{c - J^{-1} f(c) \mid J \in \Box J\right\}$$

Since $Q \subseteq X$, we have that $c - J^{-1} f(c) \in X$ for any $J \in \Box J$. Consider the function

$$S(x) = c - J^{-1}(x) f(c)$$

This is a continuous function of x since $J(x)$ is continuous. But since $S(x) \in X$ if $x \in X$, and since X is a convex set, $S(x)$ has a fixed point x^*. We have

$$\begin{aligned} x^* &= c - J^{-1}(x^*) f(c) \\ J(x^*)x^* &= J(x^*)c - f(c) \\ J(x^*)(x^* - c) + f(c) &= f(x^*) = 0 \end{aligned}$$

Therefore, f has a zero in X.

To see that this zero is unique, assume the contrary. Let x_1 and x_2 be zeroes of f such that $x_1 \neq x_2$. We have by the Mean Value Theorem,

$$0 = f_i(x_2) - f_i(x_1) = \nabla f_i(\xi_i) \cdot (x_2 - x_1)$$

for each component f_i of f. Combining these results for all components of f,

$$0 = f(x_2) - f(x_1) = J(x_2 - x_1) \text{ for some } J \in \Box J$$

But since $x_2 - x_1$ is not the zero vector, this implies that the matrix J is singular. But, $\det J \neq 0$ for any $J \in \Box J$. Hence, the zero is unique.

We now show how $J(x)$ may be defined. Let $x \in X$ be given. We define a sequence of points in X as follows

$$\begin{aligned}
y_0 &= (c_1, c_2, c_3, \ldots, c_n) = c \\
y_1 &= (x_1, c_2, c_3, \ldots, c_n) \\
y_2 &= (x_1, x_2, c_3, \ldots, c_n) \\
&\vdots \\
y_n &= (x_1, x_2, x_3, \ldots x_n) = x
\end{aligned}$$

Each of the points y_j are in X. By the Mean Value Theorem, there exists a point p_{ij} on the line from y_j to y_{j-1} such that, for each component function f_i of f

$$f_i(y_j) = f_i(y_{j-1}) + \frac{\partial f_i}{\partial x_j}(p_{ij})(x_j - c_j) \text{ for } j = 1, \ldots, n$$

Further, the required $\frac{\partial f_i}{\partial x_j}(p_{ij})$ is a continuous function of x since

$$\begin{aligned}
\frac{\partial f_i}{\partial x_j}(p_{ij}) &= \frac{f_i(y_j) - f_i(y_{j-1})}{x_j - c_j} \quad \text{if} \quad x_j \neq c_j \\
\frac{\partial f_i}{\partial x_j}(p_{ij}) &= \frac{\partial f_i}{\partial x_j}(y_j) \quad \text{if} \quad x_j = c_j
\end{aligned}$$

and because the f_i are continuously differentiable. But we have that

$$\begin{aligned}
f_i(x) &= f_i(y_n) - f_i(y_{n-1}) + \cdots + f_i(y_1) - f_i(c) + f_i(c) \\
&= \frac{\partial f_i}{\partial x_n}(p_{in})(x_n - c_n) + \cdots + \frac{\partial f_i}{\partial x_1}(p_{i1})(x_1 - c_1) + f_i(c)
\end{aligned}$$

where each $\frac{\partial f_i}{\partial x_j}(p_{ij}) \in \square \frac{\partial f_i}{\partial x_j}$. Combining these results for all the components of f,

$$\begin{aligned}
f(x) &= \sum_{j=1}^{n} \left[\frac{\partial f_i}{\partial x_j}(p_{ij}) \right] (x_j - c_j) + f(c) \\
&= J(x)(x - c) + f(c)
\end{aligned}$$

where $J(x)$ is a continuous function of x, and $J(x) \in \square J$. ∎

What happens if we have a bound for $f(c)$ (i.e., $\square f([c, c])$), rather than an exact value? This question is important because finite precision arithmetic does not allow exact computation of $f(c)$. Fortunately, a simple corollary to Theorem 5.3 exists that allows us to robustly compute conditions when exactly one zero exists to a system of equations, even when $f(c)$ can only be bounded.

Corollary 5.1 Let $f : \mathbf{R}^n \to \mathbf{R}^n$ be continuously differentiable in an interval domain X, and let $c \in X$. Let $\square J$ be the interval Jacobian matrix of f over X. Let Q be the solution set

$$Q = \{x \mid \exists J \in \square J, b \in \square f([c, c]) \ni b + J(x - c) = 0\}$$

If $Q \neq \emptyset$ and $Q \subseteq X$, then f has a unique zero in X.

Proof. The set Q is a larger set containing the old Q from Theorem 5.3. Hence the hypothesis of the corollary is actually more restrictive than that of the theorem, so the conclusion holds. ∎

5.1.3.5 A Constraint Evaluation Enhancement

Typically, the constraint function F in Algorithm 5.1 is composed of a logical combination of relational operators. For example, in the analysis of the algorithm, a constraint involving the logical **and** of $r + s$ relational subconstraints was used, of the form

$$\begin{aligned} g_i(x) &= 0 \quad i = 1, \ldots, r \\ h_j(x) &\leq 0 \quad j = 1, \ldots, s \end{aligned}$$

For a relational inclusion function, $\square r(X)$, (e.g., an inclusion function for the **equal to** operator), we have

$$Y \subset X \Rightarrow \overset{id}{\square} r(Y) \subset \overset{id}{\square} r(X) \subset \square r(X)$$

by the property of inclusion functions and ideal inclusion functions. In particular, this means that if the subconstraint is true (yields $[1, 1]$) in a region X, it is true for any interval subset of X. Similarly, if the subconstraint is false (yields $[0, 0]$) in a region X, it is false for any interval subset of X.

Algorithm 5.1 thus wastes computation whenever a subconstraint becomes exactly true or false (rather than indeterminate, i.e., yielding the interval $[0, 1]$) in some region Y that is not discarded or accepted. This is because the region Y will later be subdivided, and the same subconstraint evaluated over the child regions, with a result identical to the parent's.

It is therefore reasonable to associate with each candidate region an array of tags, one for each subconstraint, noting whether the subconstraint is true, false, or indeterminate in the candidate region. Whenever a region is subdivided, only those subconstraints that are indeterminate need be reevaluated; the rest are simply copied from the parent. The constraint function F is evaluated from this array of tags using the ternary logic introduced in Section 5.1.2.4.

5.1.4 Global Optimization with Constraints Algorithm

A global optimization with constraints problem involves finding the global minimum (or global minimizers) of a function $f : \mathbf{R}^n \to \mathbf{R}$, called the *objective function*, for all points that satisfy a constraint function $F : \mathbf{R}^n \to \{0, 1\}$. This constraint function is defined exactly as in Section 5.1.3. Algorithm 5.2 finds solutions to such problems.

Algorithm 5.2 (Optimization Algorithm) We are given a constraint inclusion function $\square F$, an inclusion function for the objective function, $\square f$, and an initial region, X. The variable u is a progressively refined least upper bound for the value of the objective function f evaluated at a feasible point. Regions are inserted into the priority queue L so that regions with a smaller lower bound on the objective function f have priority.

```
place $X$ on priority queue $L$
initialize upper bound $u$ to $+\infty$
while $L$ is nonempty
    get next region $Y$ from $L$
    if width($Y$) $< \epsilon$ add $Y$ to solution
    subdivide $Y$ into regions $Y_1$ and $Y_2$
    evaluate $\Box F$ on $Y_1$ and $Y_2$
    if $\Box F(Y_i) = [0, 0]$ discard $Y_i$
    evaluate $\Box f$ on $Y_1$ and $Y_2$
    if $\mathrm{lb}\,\Box f(Y_i) > u$ discard $Y_i$
    insert $Y_i$ into $L$ according to $\mathrm{lb}\,\Box f(Y_i)$
    if $Y_i$ contains an identified feasible point $q$
        $u = \min(u, f(q))$
    else if $Y_i$ contains an unidentified feasible point
        $u = \min(u, \mathrm{ub}\,\Box f(Y_i))$
    endif endwhile
```

Algorithm 5.2 uses a progressively refined least upper bound of the value of the objective function: the variable u. Regions encountered by the algorithm effect u in one of three ways:

1. If a feasible point q can be found in the region, then $f(q)$ can be used as an upper bound for f's global minimum. Thus, u may be updated by

$$u = \min(u, f(q))$$

   In particular, if Y is a feasible region then any point $q \in Y$ may be used.

2. If a feasible point is not explicitly identified, but it is known that one exists in the region Y, then $\mathrm{ub}\,\Box f(Y)$ is an upper bound for f's global minimum in the region Y. Therefore, the update

$$u = \min(u, \mathrm{ub}\,\Box f(Y))$$

   is appropriate. In particular, if Y is a feasible region, then every point in Y satisfies the constraints, so that u may be updated in this way.

3. If the region is indeterminate, and it can not be verified that the region contains at least one feasible point, then u can not be decreased.

Let the region U_n^i be the i-th region on the priority queue L after n while loop iterations of the algorithm. Let u_n be the value of u at iteration n, and let l_n be given by

$$l_n \equiv \mathrm{lb}\, \square f(U_n^1)$$

The interval U_n^1 is called the *leading candidate interval.* Let f^* be the minimum value of the objective function subject to the constraints. We note that if a region X contains feasible points for the constraint function F, then f^* exists. Given existence of a feasible point, an important property of Algorithm 5.2 is

$$l_n \leq f^* \leq u_n \quad \forall n$$

This property holds because no feasible regions that can possibly contain global minima to the constrained optimization problem are discarded by the algorithm. Because L is organized as a priority queue, the leading candidate interval has the smallest lower bound for f. Obviously, u_n is an upper bound for f^* by its construction. If the inclusion functions $\square F$ and $\square f$ are isotone, a further property of the algorithm is that the sequences $\{l_n\}$ and $\{u_n\}$ are monotonic in n.

Algorithm 5.2 is essentially identical to Algorithm 5.1, except that candidate regions are ordered with respect to the objective function. The algorithm also suffers the same problems that Algorithm 5.1 does. Specifically, an indeterminate region (i.e., a region Y for which $\square F(Y) = [0,1]$), may or may not include feasible points of the system of constraints. This implies that the algorithm may accept indeterminate regions as solutions that are, in fact, infeasible. Moreover, if the constraints are not satisfied exactly, (e.g., they are represented using equality constraints), then all candidate regions are indeterminate, so that u is never updated. In this case, the algorithm is unable to reject any of the candidate regions on the basis of the objective function bound and accepts all indeterminate regions as solutions.

A robust solution to this problem is to use an existence test such as the one presented in Section 5.1.3.4.2 to verify that a region contains at least one feasible point. A heuristic approach is to consider indeterminate regions of small enough width as if they contained a feasible point. These indeterminate regions may also be subjected to further acceptance tests that provide more confidence that the region contains a feasible point.

It should be noted that Algorithm 5.2 can be enhanced with a great many techniques, both local and global. Most of these techniques involve, first, finding a feasible point in a given interval so that a better upper bound can be found for the minimum function value, or, second, improving the upper bound by finding another feasible point with a smaller value of the objective function. [RATS88] discusses such enhancements in detail. Section 5.1.4.3 will discuss a further enhancement that rejects regions based on a monotonicity test.

5.1.4.1 Convergence of the Optimization Algorithm

We now turn to an analysis of the convergence of Algorithm 5.2. As in the analysis of Algorithm 5.1, we first assume that Algorithm 5.2 is allowed to iterate forever. That is, no solutions are accepted and removed from the list. To perform the theoretical analysis, we also modify Algorithm 5.2 slightly. Instead of using a priority queue for the list L, we use a LIFO, as in Algorithm 5.1. We assume that each dimension of each interval on the candidate list is eventually subdivided, so that the width of all candidate intervals goes to zero, i.e.,

$$w(U_n^i) \to 0 \text{ as } n \to \infty$$

This assumption does not hold if a priority queue is used, since some regions in the queue may never be subdivided, if they never rise to the top of the queue. In practice, Algorithm 5.2 does not iterate forever, and regions of small width are eventually removed from the queue, so that all regions are eventually considered. Therefore, use of a priority queue is reasonable for the actual implementation.

Let S be the set of solutions to the constraint system, $F(x)$, for $x \in X$, given by simultaneous satisfaction of

$$\begin{aligned} g_i(x) &= 0 \quad i = 1, \ldots, r \\ h_j(x) &\leq 0 \quad j = 1, \ldots, s \end{aligned}$$

We first prove a lemma.

Lemma 5.4 Let the inclusion functions for the constraint system be convergent, i.e.,

$$w(\Box g_i(Y)) \to 0 \quad \text{as} \quad w(Y) \to 0$$

$$w(\Box h_j(Y)) \to 0 \quad \text{as} \quad w(Y) \to 0$$

for $Y \in \mathbf{I}(X)$. The modified Algorithm 5.2 will reject any infeasible interval after a finite number of iterations.

Proof. Let Y be an infeasible interval. Clearly Y could be rejected by the algorithm because of objective function bounds checking, thus verifying the hypothesis. We assume it is not. Define $q(x)$ for $x \in X$ by

$$q(x) = \sum_{i=1}^{r} |g_i(x)| + \sum_{i=1}^{s} \max(0, h_i(x))$$

The function $q(x)$ is continuous because $g_i(x)$ and $h_j(x)$ are (since their inclusion functions are convergent). Since Y is an interval, q attains its minimum on Y, q^*. But because Y is infeasible, $q^* > 0$. Since $\Box g_i$ and $\Box h_j$ are convergent, and $w(U_n^i) \to 0$ as $n \to \infty$, the algorithm, after a finite number of iterations, is able to subdivide Y into a finite collection of regions V_k satisfying

$$\begin{aligned} w(\Box g_i(V_k)) &< \epsilon \qquad i \in [1, \ldots, r] \\ w(\Box h_j(V_k)) &< \epsilon \qquad j \in [1, \ldots, s] \end{aligned}$$

where

$$\epsilon = \frac{q^*}{2(r+s)}$$

Consider a specific element of this collection, V_k. Let $x \in V_k$. We have that $q(x) \geq q^*$. Hence, one of the following holds

$$\begin{aligned} |g_i(x)| &\geq \frac{q^*}{r+s} \quad \text{for some} \quad i \in [1, \ldots, r] \\ h_i(x) &\geq \frac{q^*}{r+s} \quad \text{for some} \quad i \in [1, \ldots, s] \end{aligned}$$

Therefore, one of the following holds

$$|\Box g_i(V_k)| \geq \frac{q^*}{r+s} - \frac{q^*}{2(r+s)} > 0 \quad \text{for some} \quad i \in [1, \ldots, r]$$

$$\text{lb}\,\Box h_i(V_k) \geq \frac{q^*}{r+s} - \frac{q^*}{2(r+s)} > 0 \quad \text{for some} \quad i \in [1, \ldots, s]$$

Therefore, V_k would be rejected by the algorithm's infeasibility test. ∎

Lemma 5.4 shows that if $\Box g_i$ and $\Box h_j$ are convergent, and no feasible points exist in X, (i.e., $S = \emptyset$), then a modified Algorithm 5.2 will eventually discard all candidate regions. Let f^* be the minimum value of f over the feasible region S. If $S \neq \emptyset$, then f^* exists. Let the region $\widetilde{U}_n$ be the region on the candidate list after iteration n that has the smallest $\text{lb}\,\Box f(U_n^i)$. Let l_n be this minimum lower bound, i.e.,

$$l_n \equiv \text{lb}\,\Box f(\widetilde{U}_n)$$

The following theorem proves the convergence of the algorithm in the case that S is nonempty.

Theorem 5.4 Let the inclusion functions for the constraint system and objective function be convergent, i.e.,

$$\begin{aligned} w(\Box f(Y)) &\to 0 \quad \text{as} \quad w(Y) \to 0 \\ w(\Box g_i(Y)) &\to 0 \quad \text{as} \quad w(Y) \to 0 \\ w(\Box h_j(Y)) &\to 0 \quad \text{as} \quad w(Y) \to 0 \end{aligned}$$

for all $Y \in \mathbf{I}(X)$. If $S \neq \emptyset$ then $l_n \to f^*$ as $n \to \infty$.

Proof. Clearly, if $S \neq \emptyset$, then $\{l_n\}$ is a well-defined infinite sequence. For any n, $l_n \leq f^*$. Let an arbitrary $\epsilon > 0$ be given. Assume that an interation level has been reached, given by m, such that

$$U \subseteq U_m^i \Rightarrow w(\Box f(U)) < \epsilon \qquad (5.6)$$

for all candidate intervals U_m^i. This is possible because $w(U_m^i) \to 0$ as $m \to \infty$, and because $\Box f$ is convergent.

Consider further the intervals in the collection $\{U_m^i\}$ that contain no feasible points. Since there are a finite number of them, by Lemma 5.4, they will be rejected after a finite number of further iterations of the algorithm. Not all will be rejected, since S is nonempty. Assume that this iteration level has been reached, given by n. We have, for any candidate interval of this iteration level, U_n^i,

$$U_n^i \subset U_m^j \text{ for some } j \tag{5.7}$$

since $n > m$. Let U_n^k be an interval having l_n as its lower bound for $\Box f$. We have that $f^* \in \Box f(U_n^k)$ because U_n^k contains at least one feasible point, and $l_n \leq f^*$. We also have that $w(\Box f(U_n^k)) < \epsilon$ by Equations (5.6) and (5.7). Therefore, $f^* \leq l_n + \epsilon$ or $l_n \rightarrow f^*$ as $n \rightarrow \infty$. ∎

5.1.4.2 Termination and Acceptance Criteria for Optimization

A constrained optimization problem can be "solved" in three ways:

1. find the minimum value of the objective function

2. find one feasible point that minimizes the objective function

3. find all feasible points that minimize the objective function

Slight modifications to Algorithm 5.2 regarding when the algorithm is halted and when indeterminate regions are accepted as solutions can make it applicable to each of these specific subproblems.

To find the minimum value of the objective function, f^*, Algorithm 5.2 should be terminated when a leading candidate interval, U_n^1, is encountered with $w(\Box f(U_n^1))$ sufficiently small, given that U_n^1 contains at least one feasible point.[9] In this case, the value $f(q)$ should be returned for some $q \in U_n^1$. This approach is justified because if U_n^1 contains a feasible point then

$$\text{lb}\,\Box f(U_n^1) \leq f^* \leq \text{ub}\,\Box f(U_n^1)$$

This approach assumes that we can verify the presence of a feasible point in an indeterminate region before the machine precision is reached in subdivision. Lack of this verification should

[9]If all candidate intervals are rejected, then no feasible points exist in the original region, so f^* does not exist.

result in some form of error termination. A heuristic approach is to accept indeterminate regions of small enough width (and, possibly, satisfying other criteria) as though they contained a feasible point.

Finding one or all minimizers of the objective function is a difficult problem that is currently not amenable to completely robust solution. Under certain conditions[10] Algorithm 5.2 converges, in a theoretical sense, to the set of global minimizers of the optimization problem. In practice however, we obtain a superset of the set of global minimizers after a finite number of iterations. Although techniques exist to verify whether a given interval in this superset contains a local minimizer of the optimization problem, we will not know, in general, if these local minimizers are also global minimizers.

If we know, *a priori*, that a single global minimizer exists, then the technique of solution aggregation (Section 5.1.3.2) can be used to collect candidate solutions into a single interval. We can then verify that the width of this interval tends to zero as the algorithm iterates. If we expect a finite set of global minimizers, then a reasonable heuristic approach is to aggregate solutions, and pick a point in each aggregated region as a global minimizer, Such an aggregated region should be small enough in width and satisfy other acceptance criteria that increases confidence that it contains a global minimizer.

5.1.4.3 Monotonicity Test

Consider the case that a candidate interval, Y, in Algorithm 5.2 is feasible, and the objective function, f, is monotonic with respect to any of the optimization problem's input variables $x_1, \ldots, x_n$. If Y is a subset of the interior of the problem's starting domain, X, then Y cannot contain a global minimum. On the other hand, if $Y \bigcap \partial X \neq \emptyset$[11], then Y can not be completely eliminated because points on $\partial X \bigcap Y$ may still be global minimizers. We can, however, replace Y with $Y' \bigcap \partial X$ where Y' is the interval Y with the monotonic coordinate interval replaced by a constant. Precisely, if $Y_i = [y_i^0, y_i^1]$, and f is monotonic in the interval

[10]A sufficient conditioni is the existence of a sequence of points in the interior of the feasible domain that converges to a global minimizer, see [RATS88].

[11]The notation ∂X denotes the boundary of the set X.

Y with respect to x_j, then Y' is given by

$$Y'_i = \begin{cases} [y_i^0, y_i^1], & \text{if } i \neq j \\ [y_i^0, y_i^0], & \text{if } i = j \text{ and } f \text{ is monotonically increasing in } Y \\ [y_i^1, y_i^1], & \text{if } i = j \text{ and } f \text{ is monotonically decreasing in } Y \end{cases}$$

This enhancement is called the *monotonicity test.* Note that the region Y must be feasible, (i.e., every point in Y satisfies the constraints), for the monotonicity test to be valid.

If f is a differentiable function, then f is monotonic with respect to any input variable x_i in a region Y if

$$0 \notin \Box\frac{\partial f}{\partial x_i}(Y)$$

We can therefore add the following test to Algorithm 5.2

```
if $F(Y) = [1,1]$ then
    if $0 \notin \Box\frac{\partial f}{\partial x_i}(Y)$ for some $i$ then
        if $Y \bigcap \partial X = \emptyset$ then reject $Y$
        else replace $Y$ with $Y' \bigcap \partial X$
    endif
endif
```

5.2 Applying Interval Methods to Geometric Modeling

The second half of this chapter discusses applications of the global problem algorithms (Algorithms 5.1 and 5.2) to the following problems:

- computing non-intersecting boundaries of offset curves and surfaces
- approximating implicitly defined curves
- approximating parametric shapes using arbitrary adaptive sampling criteria
- approximating trimmed surfaces and boundaries of CSG operations on solids bounded by generative surfaces
- approximating implicitly defined surfaces

5.2.1 Offset Operations

An *offset* of an object is an enlarged or reduced version of the object. In Section 3.1.2.2, the concept of a planar curve offset was introduced. This offset was defined as the locus of centers of circles of a given radius tangent to the curve. Such a definition suffers from the following problems

- The offset curve can self-intersect.
- Parameterization of the offset is easily accomplished only if the curve to be offset has a nonvanishing tangent vector.
- Points where the original curve is not differentiable create discontinuities in the resulting offset.

Requicha and Rossignac [ROSS86a] have defined a more robust offset operation, called an *s-offset* (for *solid offset*) that addresses these problems. They define the positive s-offset of radius r of an object S, written $S \uparrow r$, as the union of S and the set of points exterior to S within a distance r from the boundary of S. Mathematically,

$$S \uparrow r \equiv \{p \mid \|p - q\| \leq r \text{ for some } q \in S\}$$

Similarly, the negative s-offset of radius r of an object S, written $S \downarrow r$, subtracts from S all points within a distance r from its boundary. Mathematically, the negative s-offset can be defined as the complement of the positive offset of the complement of S, i.e.,

$$S \downarrow r \equiv \neg((\neg S) \uparrow r)$$

[ROSS86a] applies this definition to regular[12] solids in 3D space. S-offsets may also be applied to other objects, including objects of different dimension (e.g., 2D planar areas), and to non-regular objects (e.g., curves and surfaces in 3D space).

The s-offset operation is an extremely useful one in geometric modeling. [ROSS86a] cites many applications, such as design rule checking for VLSI, generation of NC milling tool paths, tolerance analysis for solid modeling, and collision detection and obstacle avoidance.

[12] A *regular* set is a set, S, for which $S = \overline{S^0}$, i.e., the closure of the interior of S equals S.

In addition, sequences of s-offset operations can be used as a blending operation. A positive followed by a negative s-offset results in an operation called *filleting*, which rounds concave corners and edges of an object. A negative followed by a positive s-offset results in an operation called *rounding*, which rounds convex corners and edges of an object.

Computing the boundary of an s-offset is an important operation. [ROSS86a] describes a technique that computes a superset of the s-offset boundary, given a boundary representation of the solid to be offset. This technique categorizes points on the boundary of the solid into three parts: faces, singular curves, and singular points. Faces are the smooth surfaces that form the boundary of the solid. Singular curves are space curves that form the non-smooth edge where faces are joined. Similarly, singular points are vertices that form the non-smooth corners where singular curves are joined. The resulting offset superset is formed by the union of the following:

1. normal offsets of the faces – each point on the face is transformed to a new point a distance r along the face normal. The resulting face is called a normal offset.

2. canal surfaces around singular curves – each point on the singular curve gives rise to a circle of radius r normal to the tangent vector to the singular curve. The resulting surface is called a canal surface.

3. spheres around singular points

We will term this offset superset the *singularity categorization offset.*

The next section discusses a more convenient and tighter representation for the boundary of an s-offset than the singularity categorization offset. Objects that may be offset are generative models (i.e., the image of a parametric function evaluated over a rectilinear domain). Such a class of primitive objects is more powerful than the set of simple solids: rectangular prisms, spheres, cylinders, cones, and tori, included in a prototype system in [ROSS86a]. The representation is convenient because it does not require a priori identification of singular points and curves on the parametric object. Approximation and bounding of the s-offset boundary is amenable to the interval analysis techniques previously discussed in this chapter.

5.2.1.1 The B-offset: A Tighter Representation for the S-Offset Boundary

Let S be a parametric object (e.g., curve, surface, etc),

$$S : D_S \to R_S, \quad D_S \in \mathbf{I}^m, \quad R_S \subset \mathbf{R}^n$$

with parameters $x = (x_1, x_2, \ldots, x_m) \in D_S$. Let $Y \in \mathbf{I}^n$ include all points at a distance r from R_S. We define the *b-offset* (for *boundary offset*) of S of radius r, written $S\partial r$, as the set of points

$$S\partial r \equiv \left\{ y \in Y \mid \min_{s \in R_S} \|y - s\| = r \right\}$$

i.e.,

$$S\partial r \equiv \left\{ y \in Y \mid \min_{x \in D_S} \|y - S(x)\| = r \right\}$$

Thus, the b-offset is described implicitly as a set of points solving a constraint problem whose constraint involves unconstrained minimization.[13]

We note that the b-offset of an object is a superset of the boundary of its positive s-offset, i.e.,

$$\partial(S \uparrow r) \subseteq S\partial r$$

Typically, the subset relation in the above can be replaced with set equality, although pathological cases, such as in Figure 5.3, do exist. Figure 5.4 compares the singularity categorization offset with the b-offset, for the case of a nonsmooth planar curve. It is easy to see that the b-offset produces a smaller superset of the boundary of the positive s-offset (in fact, it produces the exact boundary), and requires no identification of singularities on the curve.

5.2.1.2 A Constraint-Based Approach for Computing B-Offsets

Consider the use of the constraint solution algorithm (Algorithm 5.1) to find a superset of the b-offset of some parametric object. That is, we wish to compute a subset of Y

[13] *Unconstrained minimization* is minimization where the constraint function F in Algorithm 5.2 is a constant 1. Thus, every candidate interval is feasible, and the algorithm must only find the minimum value of the objective function over the entire starting region. Unconstrained minimization is appropriate here because the only constraint on x in the minimization is that $x \in D_S$ where $D_S \in \mathbf{I}^m$. This constraint is addressed simply by using D_S as the starting interval.

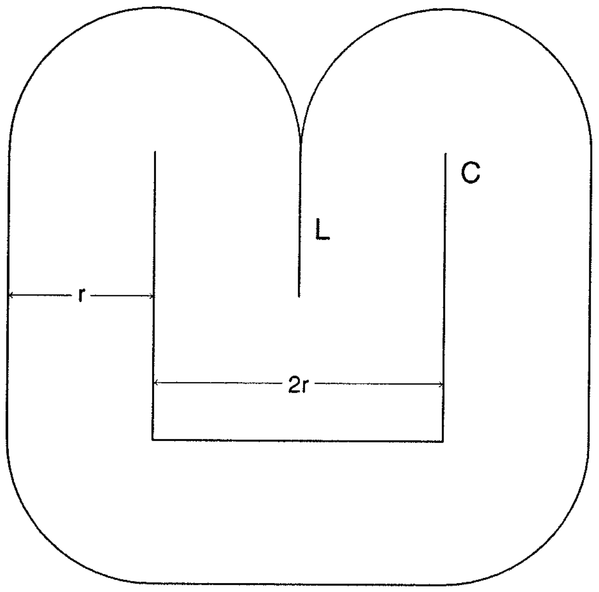

Figure 5.3: The b-offset is a superset of the s-offset boundary. C is a planar curve consisting of three line segments. The b-offset of radius r is shown surrounding it. This b-offset contains the segment L, which is not part of the boundary of the positive s-offset of C. A point on L is at a distance r from C, but is in the interior of the positive s-offset. A similar situation can arise when a surface is s-offset, yielding a surface (rather than a curve like L) in the b-offset that is not on the positive s-offset boundary. For example, if the curve C is extruded normal to the page, then the surface formed by the extrusion of the segment L is in the b-offset of the surface, but not on the s-offset boundary.

that bounds the b-offset. The constraint solution algorithm works by subdividing Y into smaller intervals, using an inclusion function to see whether the constraint is satisfied in each interval. In the case of a b-offset, the constraint is that the minimum distance of a point in the interval to the set R_S must be equal to r. Let $Z \in \mathbf{I}(Y)$ be an arbitrary interval processed by the constraint algorithm. To compute whether Z can satisfy the constraint, an unconstrained minimization subproblem can be solved, as shown in Figure 5.5. More precisely, let f be the function

$$f(x; z) = \|z - S(x)\|$$

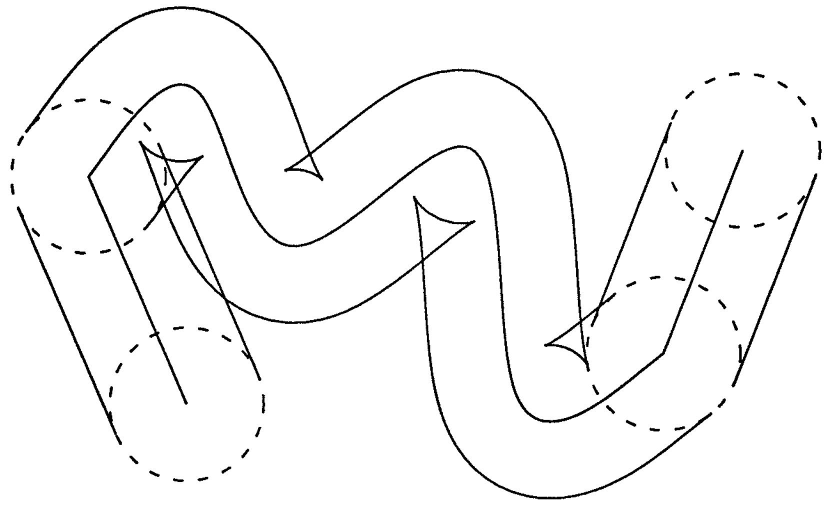

Singularity Categorization Offset

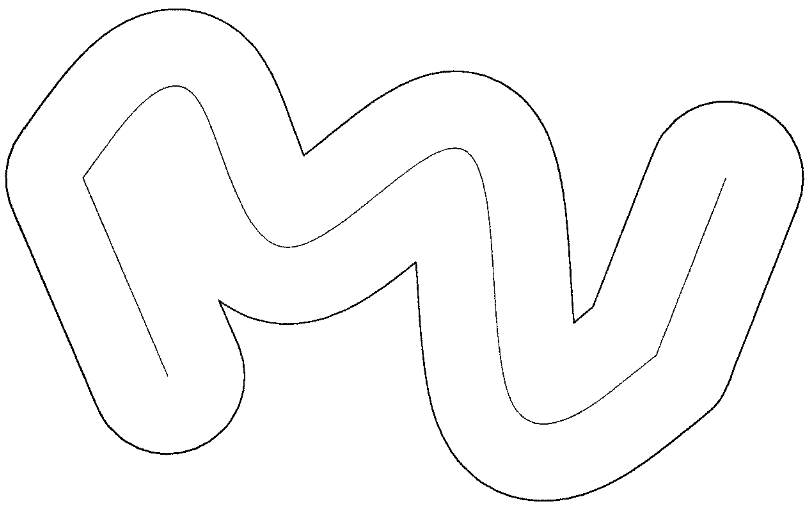

B-Offset

Figure 5.4: Singularity categorization offset and b-offset – The top figure shows a 2D planar curve and its singularity categorization offset boundary. The curve has a derivative discontinuity at two points, where two straight segment are joined to the middle bumpy curve. These two points and the two curve endpoints are the singular points, each of which contributes a circle to the offset superset. Note that the offset curves to the middle bumpy curve self-intersect and contain points that are not on the offset's boundary. The b-offset in the bottom figure, in contrast, gives the exact boundary of the offset.

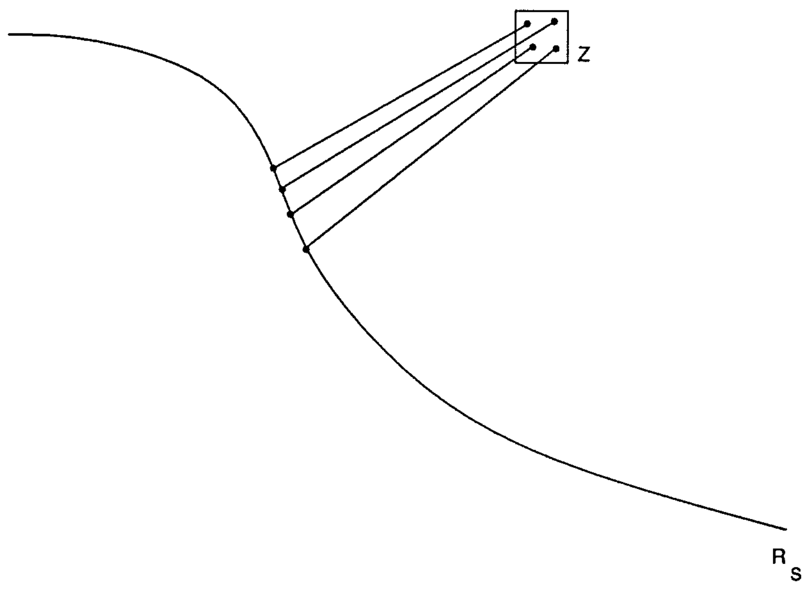

Figure 5.5: Example minimization problem in offset computation – In this case the object being offset is a planar curve (parametric range R_S). We require a bound on the minimum distance of a point in the interval Z to the set R_S. Four points in Z are selected as examples, connected by lines to their closest point in the set R_S. The required bound involves considering all such points in Z, finding their closest neighbor in R_S, and finding the maximum and minimum line lengths so obtained (i.e., $f^-(Z)$ and $f^+(Z)$). In this example, the interval Z is fairly large and close to the planar curve R_S. Therefore, the range of minimum distances that need to be bounded is fairly large.

where $z \in Z$ and $x \in D_S$. We require a bound on the minimum distance of a point in Z to the set R_S. That is, given an interval Z, we must find $f^-(Z)$ and $f^+(Z)$ given by

$$\begin{aligned} f^-(Z) &= \min_{z\in Z} \min_{x\in D_S} \|z - S(x)\| \\ f^+(Z) &= \max_{z\in Z} \min_{x\in D_S} \|z - S(x)\| \end{aligned}$$

Once this bound is obtained, it is tested in the constraint solution algorithm to see whether the minimum and maximum distance straddle r, i.e.,

$$f^-(Z) \le r \le f^+(Z)$$

The global optimization algorithm (Algorithm 5.2) can be used to obtain an interval containing $f^-(Z)$ and $f^+(Z)$. To do this, an inclusion function for f can be formed, $\Box f$.

Algorithm 5.2 then works with $\Box f(X, Z)$ as the objective function inclusion where Z stays fixed during the unconstrained minimization, while X is subdivided. At the start of the algorithm, $X_0 = D_S$. For any ϵ, the algorithm will produce a bound on $[f^-(Z)\ , f^+(Z)\ ]$, which becomes tighter as ϵ is decreased. Algorithm 5.2 is terminated at the first leading interval, $P \in \mathbf{I}(D_S)$, whose width is less than ϵ, since for any leading interval P we have

$$\mathrm{lb}\,\Box f(P, Z) \le f^-(Z) \le f^+(Z) \le \mathrm{ub}\,\Box f(p, Z) \le \mathrm{ub}\,\Box f(P, Z)$$

where p is any element of P. We note that a termination condition such as

$$\mathrm{ub}\,\Box f(P, Z) - \mathrm{lb}\,\Box f(P, Z) < \delta$$

is not appropriate in these circumstances since $f^+(Z) - f^-(Z) > 0$, in general.

Of course, it doesn't make sense to use a small ϵ in the minimization subproblems when Z is a big interval. The larger $w(Z)$, the larger one would expect $f^+(Z) - f^-(Z)$. In fact, we have

$$f^+(Z) - f^-(Z) \to 0 \text{ as } w(Z) \to 0$$

There is also some excess width in the inclusion function $\Box f$ with respect to the fixed interval Z, which remains no matter how small ϵ is chosen. This is because ϵ only affects subdivision of intervals in D_S, not in Z. This excess width is again related to the width of the interval Z. Because of these two factors, ϵ in the optimization algorithm should be related to the width of Z, so that ϵ shrinks as $w(Z)$ shrinks. Empirically, dramatic performance improvements result when ϵ is linearly related to $w(Z)$, rather than made a fixed, small constant for every minimization subproblem.

In summary, because the b-offset is defined in terms of the solution of a constraint involving minimization, it can be computed using the tools for solving global problems already discussed. An inclusion function is defined in terms of variables used in both the constraint problem and the minimization subproblem, i.e., the function $f(x; z) = \|z - S(x)\|$ where the z variable is manipulated in the "outer" constraint solution algorithm and the x variable is manipulated in the "inner" minimization algorithm. For each interval Z processed in the constraint solution algorithm, a new inclusion function $\Box f(X, Z)$ is defined.

The global optimization algorithm uses this inclusion function, looking for minima of $\Box f$ in terms of X, while Z stays fixed. Dramatic performance improvement results when the ϵ used in the minimization subproblems is related to the width of the interval Z.

This technique can also be used to find offsets of non-parametric objects (e.g., offsets of offsets to do blending operations). For example, $(S\partial r_1)\partial r_2$ can be computed by

$$\begin{aligned}(S\partial r_1)\partial r_2 &= \underset{z_2 \in Z_2}{\text{solve}} \left(\|z_2 - \underset{z_1 \in Z_1}{\text{solve}} \left(\min_{x \in D_S} \|z_1 - S(x)\| = r_1 \right) \| = r_2 \right) \\ &= \underset{z_2 \in Z_2, z_1 \in Z_1}{\text{solve}} \left(\|z_2 - z_1\| = r_2 \text{ and } \min_{x \in D_S} \|z_1 - S(x)\| = r_1 \right)\end{aligned}$$

where Z_1 and Z_2 are suitably chosen. The key to computing these operations is to use the global optimization algorithm to compute a bound on the minimum value of the objective function, some of whose variables remain fixed from the outer constraint problem.

Finally, we can use this technique not only to bound the b-offset in a convergent set of intervals, but also to approximate the b-offset, using techniques for approximating implicitly defined curves and surfaces. These techniques will be treated in following sections.

5.2.2 Approximating Implicit Curves

An implicit curve is the solution to a constraint system $F(x) = 1$, $x \in X \subset \mathbf{R}^n$, such that the solution forms a 1D manifold, except at a zero-dimensional collection of singularities.[14] Implicit curves are extremely useful in geometric modeling. They can represent, for example, the intersection of two parametric surfaces in $\mathbf{R}^3$, the b-offset of a planar curve (see Section 5.2.1.1), or the silhouette edges of a parametric surface in $\mathbf{R}^3$ with respect to a given view. Typically, the constraint system is represented as a system of $n-1$ equations in n parameters. However, it is often useful to define other constraint systems. For example, the union of two implicitly defined curves may be defined by

$$F_1(x) = 1 \text{ or } F_2(x) = 1$$

[14]A singularity is a point where the solution self-intersects or is isolated, i.e., for which a neighborhood exists containing no other solutions.

where $F_1(x) = 1$ and $F_2(x) = 1$ are constraint systems representing the curves to be unioned. Also, inequality constraints (e.g., **less than** and **not equal to**) are often useful in excluding unwanted parts of the implicit curve.

This section discusses an algorithm for approximating implicit curves that solve a constraint system represented using the recursive operators of Chapter 2. An implicit curve rarely has a global analytic parameterization, and must be approximated when points on the curve are required in geometric operations. For example, rendering a shape defined as a CSG operation on two solids bounded by generative surfaces may require approximation of the intersection curve between the two surfaces. Implicit curve approximation involves producing a sequence of points on the curve (possibly with curve tangent vectors or other information) and information about how these points are linked.

Many forms of interpolation exist with different characteristics of accuracy, speed of computation, appropriateness for different degrees of curve smoothness, etc. The simplest example of a continuous interpolation scheme is linear interpolation, where the implicit curve between each pair of solution points is approximated by a straight line in the parameter space of the constraint system. Higher order interpolation methods use additional information, such as the tangent vector of the implicit curve at each solution point, to obtain a smoother approximation. Interpolation can also take place in a space other than the constraint system's parameter space. For example, in approximating the curve of intersection between two parametric surfaces in $\mathbf{R}^3$, the approximation may be computed in $\mathbf{R}^3$, the output space of the parametric surfaces. Whatever the interpolation scheme, the same basic information is always required: a sequence of parameter space points that lie on the solution curve and a graph specifying how these solution points are linked (called the *local topology graph*).

Implicit curve approximation also involves a choice of an *approximation quality metric* – a measure of how well the approximation corresponds to the actual solution. Such a metric gives rise to acceptance criteria for the set of points used to approximate the curve: if the metric is satisfactory, the set of points is accepted, otherwise, more points must be computed. Perhaps the simplest example of an approximation quality metric is the maximum distance of the approximation from the solution curve. Many other metrics can be devised that are appropriate in special circumstances. For example, we may wish to approximate areas of high curvature on the implicit curve with more points, by weighting the solution-to-approximation distance metric with some function of the curvature.

The implicit curve approximation algorithm presented in the next section uses the constraint solution algorithm to find points on the implicit curve. It produces a sequence of points with linkage information to which different interpolation schemes can be applied. It also allows a diverse set of approximation quality metrics.

The robustness of this algorithm is superior to methods such as the one developed by Timmer [TIMM77, MORT85], and other such local methods [BAJA88]. Timmer's method separates implicit curve approximation into a hunting phase, where intersections of the implicit curve with a preselected grid are computed, and a tracing phase, where the curve inside each grid cell is traced to determine how to connect the intersections. The robustness of the algorithm proposed here is the result of two factors:

- computing points on the implicit curve is done with a global, robust technique (Algorithm 5.1) that guarantees a bound on the result. This method is superior to local methods, such as Newton iteration, which are not guaranteed to converge.
- finding disjoint components of the curve is done robustly, rather than in an ad hoc manner. Timmer's method fails to find a disjoint segment of the curve if it "falls within the cracks" of the sampling grid used in the hunting phase (i.e., it lies completely within one grid cell). The proposed algorithm uses a global parameterizability criterion that subdivides parameter space until no curve segment can be lost.

Furthermore, the algorithm described here can be applied to large array of implicit curve types, not just to systems of a single equation in two variables, or two equations in three variables.

5.2.2.1 An Implicit Curve Approximation Algorithm

The following are inputs to the approximation algorithm:

1. an interval $X \in \mathbf{I}^n$, called the *interval of consideration*, in which to approximate the implicit curve.
2. an inclusion function $\Box F(Y)$, $Y \in \mathbf{I}(X)$ for the constraint system defining the implicit curve.

3. an inclusion function $\square G(Y)$, $Y \in \mathbf{I}(X)$, called the approximation acceptance inclusion function. This inclusion function tells when an interval Y is small enough that the segment of the implicit curve it contains can be approximated by a single interpolation segment between a pair of solution points.[15] The approximation acceptance inclusion function thus encodes the approximation quality metric discussed previously.

Roughly, the algorithm works by subdividing the region X into subregions that contain the implicit curve, satisfy the approximation acceptance inclusion function, and allow simple computation of the local topology of the curve. Such a subregion is called a *proximate interval.* The algorithm makes the following assumptions:

1. The solution to the constraint system $F(x) = 1$ is a continuous, 1D manifold. This implies that the solution contains no self-intersections, isolated singularities, or solution regions of dimensionality greater than 1. It further implies that each disjoint curve segment of the solution is either closed or has endpoints at the boundary of the region X (i.e., a curve segment does not terminate in the interior of the interval of consideration).

2. The intersection of the solution curve with a proximate interval's boundaries is either empty or a finite collection of points (not a 1D manifold).

Under these assumptions, the local topology graph of the approximation becomes a simple linked list, where each solution point is linked to two neighbors, or possibly a single neighbor if the point is on the boundary of X. The output of the approximation algorithm is a list of "curves", where each curve is a linked list of points on a single, disjoint segment of the implicit curve, as shown in Figure 5.6. Relaxation of these assumptions will be treated in Section 5.2.2.4.

Algorithm 5.3 (Implicit Curve Approximation Algorithm)

1. **Subdivide X into a collection of proximate intervals bounding the implicit curve and satisfying the approximation acceptance inclusion function.** This

[15]This is not to say that Y contains only a single curve segment. Rather, Y is acceptable if *each* curve segment it contains can approximated by one interpolation segment between two solution points.

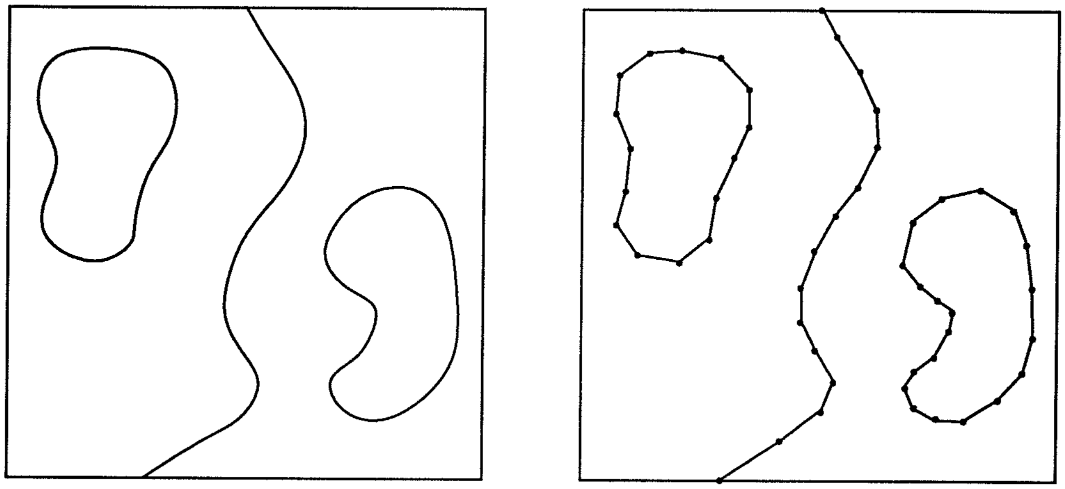

Figure 5.6: Implicit curve approximation – The figure on the left shows an implicit curve satisfying the algorithm's assumptions. This implicit curve is defined over a 2D parameter space and might be obtained by a constraint system such as $f(x, y) = 0$. The implicit curve consists of three segments: two closed segments, and one segment intersecting the boundary of the interval of consideration. The figure on the right shows an approximation of the implicit curve that might be computed by the approximation algorithm. In this case, the algorithm produces three linked lists of points on the implicit curve as output, one for each segment of the implicit curve. The linked list is shown by lines connecting the solution points.

can be accomplished using Algorithm 5.1 where a region Y is accepted if

$$F(Y) = [0, 1] \text{ and } G(Y) = [1, 1]$$

Note that $F(Y)$ will never yield the interval $[1, 1]$ since that would imply the solution manifold is n-dimensional, violating Assumption 1. Figure 5.7 shows an example of a collection of proximate intervals.

2. **Check each proximate interval for global parameterizability.** The implicit curve contained in a proximate interval Y is called *globally parameterizable in a parameter i* if there is at most one point in Y on the curve for any value of the i-th parameter. Figure 5.8 illustrates the concept of global parameterizability. The global parameterizability of the implicit curve (together with Assumption 1) implies that the curve has a simple local topology. In particular, we can find the points of intersection

of the implicit curve with each of Y's boundaries and sort these boundary intersections in increasing order of their i-th parameter. *The global parameterizability of the implicit curve means that only boundary intersections adjacent in this sorted list can possibly be connected by a segment of the implicit curve.* However, they may not be connected. A simple test verifies whether a pair of points is connected: we merely test whether the i-th hyperplane between these two points intersects the implicit curve. Figure 5.9 illustrates how global parameterizability is related to the connection of boundary intersections.

If the implicit curve is not globally parameterizable in Y for any parameter, then Y is recursively subdivided and tested again.

3. **Find the intersections of the implicit curve with the boundaries of each proximate interval, using Algorithm 5.1.** We assume (Assumption 2) that this intersection will be empty or a finite collection of points.

4. **Ensure that the boundary intersections are disjoint in the global parameterizability parameter.** The previous step produces bounds for the points of intersection of the implicit curve with each proximate interval's boundary. Let i be the global parameterizability parameter for a proximate interval Y, computed from Step 2. This step checks that Y's boundary/implicit curve intersections are non-overlapping in coordinate i, as shown in Figure 5.10. Disjointness in coordinate i implies that the boundary intersections can be unambiguously sorted in increasing order of coordinate i, necessary for connection testing in the next step.

   If Y's boundary intersections are not disjoint in parameter i, Y is recursively subdivided and retested.

5. **Compute the connection of boundary intersections in each proximate interval.** If an interval Y contains no boundary intersections it can be discarded. This is because the solution cannot be a closed curve entirely contained in Y, because of the global parameterizability condition. Nor can the solution be a curve segment that does not intersect Y's boundary, by Assumption 1. Hence, Y contains no part of the implicit curve.

If Y contains a single boundary intersection, then the solution is either tangent to a boundary of Y or passes through a corner or edge of Y. In either case, the solution does not intersect the interior of Y, so Y can be discarded.

If Y contains more than one boundary intersection, the boundary intersections are sorted in order of the global parameterizability parameter i. For each pair of boundary intersections adjacent in parameter i, Algorithm 5.1 is used to see if the solution curve intersects the i-th parameter hyperplane midway between the two boundary intersections. If so, the boundary intersections are connected in the local curve topology linked list.

6. **Find the set of disjoint curve segments comprising the implicit curve. Ensure a consistent ordering of points in each segment.** This is accomplished by processing the list of boundary intersection points, using the following algorithm

```
let $S$ be the set of boundary intersections
while $S$ is nonempty
        remove an intersection point $P$ from $S$
        find and remove all points $P'$ in $S$ that are
                (indirectly) connected to $P$
        associate $P$ and the set of $P'$ with a new curve
endwhile
```

We note that in accumulating the set of points on a particular curve using this algorithm, if a point P' is eventually found such that $P = P'$ then the curve is closed. Otherwise, the curve has two endpoints on the boundary of X by Assumption 1.

We now discuss the steps of the implicit curve approximation algorithm in more detail.

Step 1 of the algorithm combines the constraint inclusion with the approximation acceptance inclusion to create an initial collection of proximate intervals bounding the implicit curve. Consider approximating the intersection of two parametric surfaces, $S(u_1, v_1) : \mathbf{R}^2 \rightarrow \mathbf{R}^3$, and $T(u_2, v_2) : \mathbf{R}^2 \rightarrow \mathbf{R}^3$. An appropriate constraint function, $F(u_1, v_1, u_2, v_2)$, is given by a system of three equations in four parameters

$$\begin{aligned} S_1(u_1, v_1) &= T_1(u_2, v_2) \\ S_2(u_1, v_1) &= T_2(u_2, v_2) \\ S_3(u_1, v_1) &= T_3(u_2, v_2) \end{aligned}$$

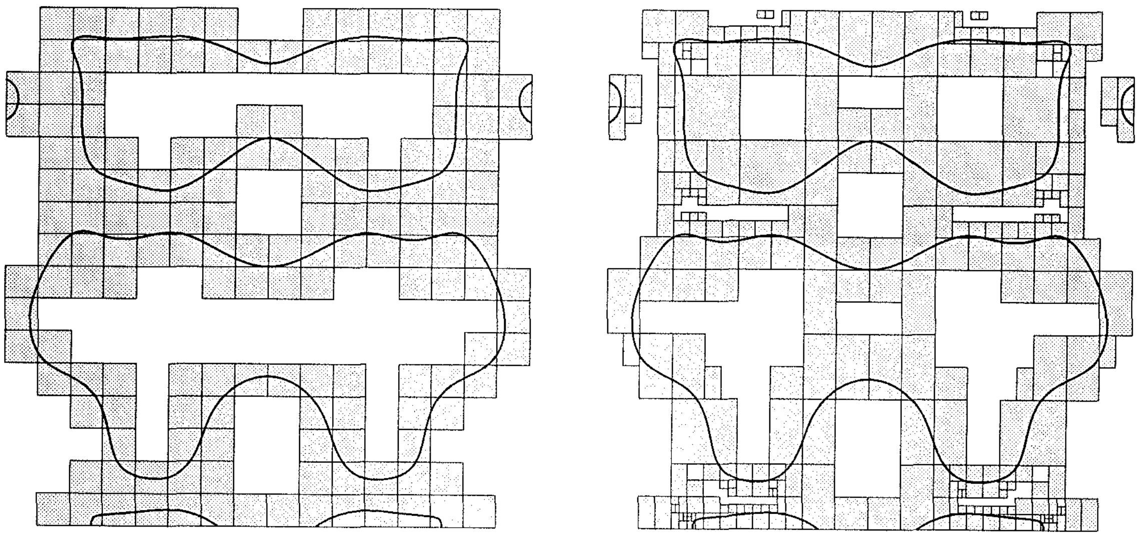

Figure 5.7: Collection of proximate intervals bounding an implicit curve – In these examples, the constraint system is given by the equation $f(x, y) = 0$ where

$$f(x,y) = x^2 + y^2 + \cos(2\pi x) + \sin(2\pi y) + \sin(2\pi x^2)\cos(2\pi y^2) - 1$$

The interval of consideration is $X = [-1.1, 1.1] \times [-1.1, 1.1]$. Let $Y \in \mathbf{I}(X)$ be one of the proximate intervals in the bounding collection. The approximation acceptance inclusion function for the left example is simply that the width of the parameter space interval should be less than a constant, i.e.,

$$w(Y) < 0.2$$

The approximation acceptance inclusion function for the right example is

$$\Box\frac{\partial f}{\partial x}(Y) \neq 0 \quad \text{or} \quad \Box\frac{\partial f}{\partial y}(Y) \neq 0$$

This test guarantees that the curve is globally parameterizable in either x or y, as we will see in Section 5.2.2.2.

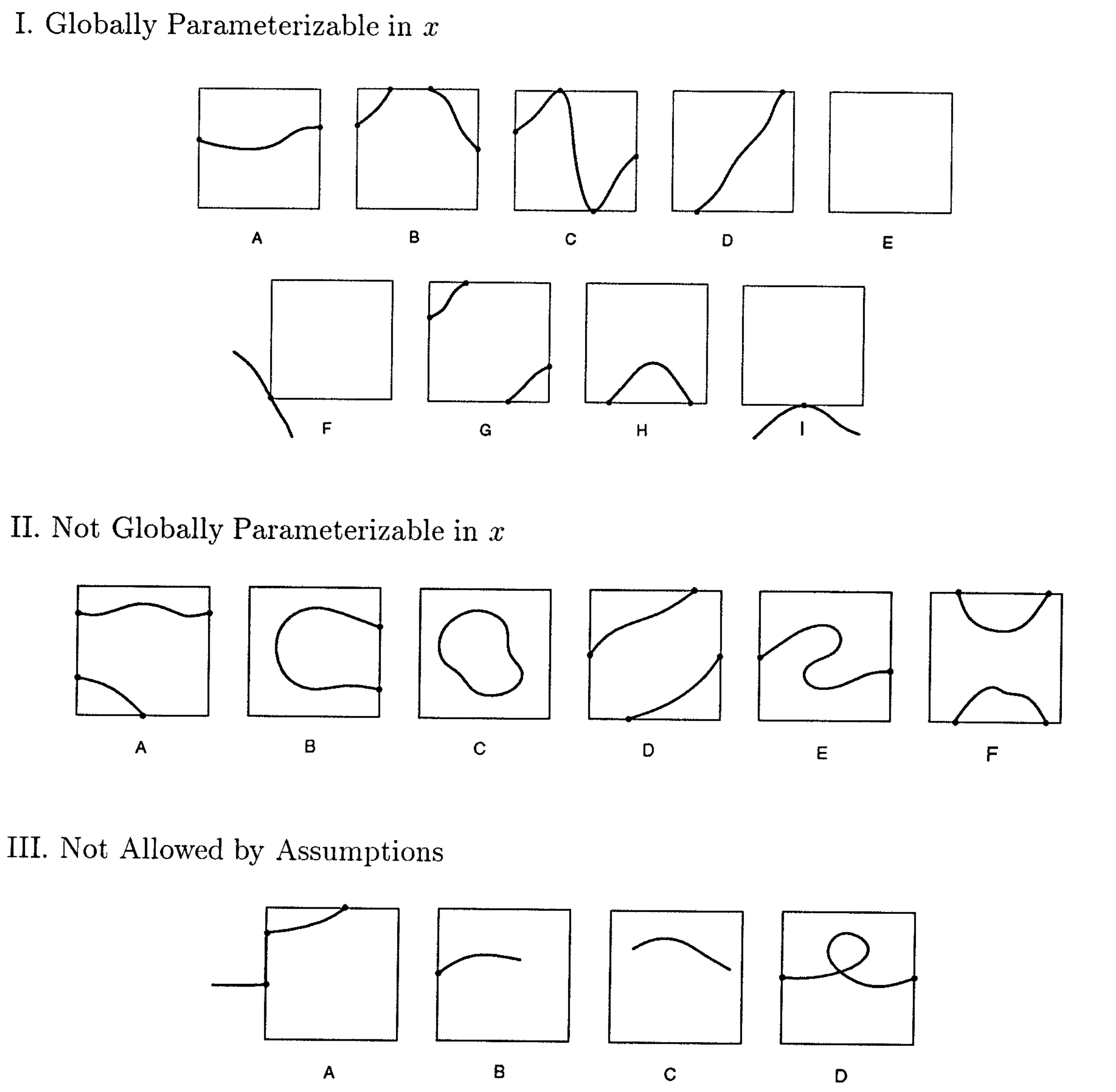
I. Globally Parameterizable in x
A
B
C
D
E
F
G
H
I
II. Not Globally Parameterizable in x
A
B
C
D
E
F
III. Not Allowed by Assumptions
A
B
C
D

Figure 5.8: Global parameterizability – The figure illustrates some of the possible behaviors of an implicit curve in an interval. In this case, the parameter space is 2D with the x parameter on the horizontal axis of the page. Case I shows intervals in which the implicit curve is globally parameterizable in x. This includes situations in which the interval contains a single segment (A,C,D,H), two segments (B,G), or no segments (E,F,I). Case II shows intervals in which the implicit curve is not globally parameterizable in x. In each case, there is a vertical line that intersects the solution in more than one point. Finally, Case III shows intervals in which the implicit curve exhibits behaviors not allowed by the assumptions of the algorithm. Example A shows an segment of the implicit curve contained entirely on the interval boundary. Examples B and C have curve endpoints that are not on the boundary of the interval of consideration. Example D self-intersects.

I. Boundary Intersections of an Implicit Curve

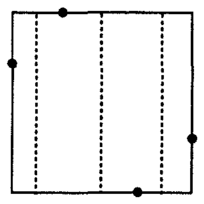

II. Eight Cases of Implicit Curve Behavior

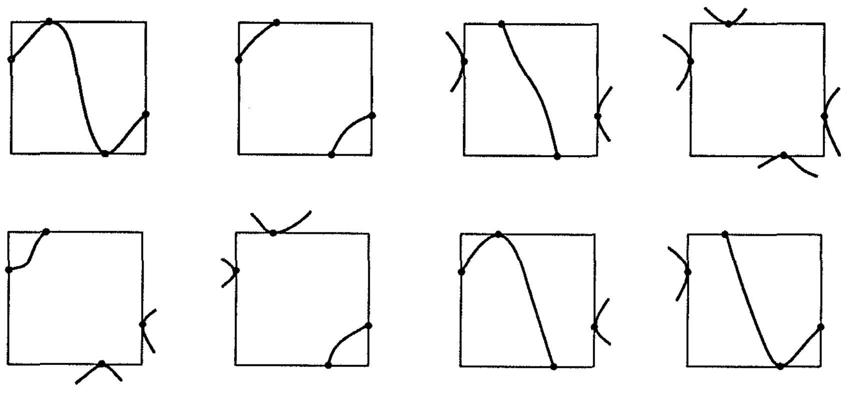

III. Not Allowed by Global Parameterizability

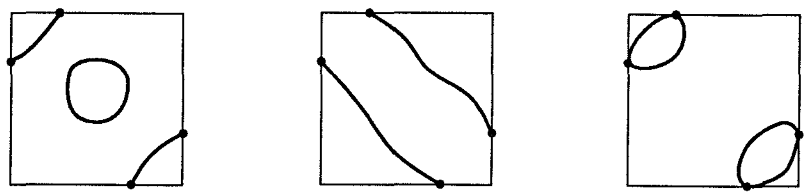

Figure 5.9: Global parameterizability and the linking of boundary intersections – In this figure, we assume an implicit curve defined in $\mathbf{R}^2$ is globally parameterizable in x in an interval. The implicit curve has four intersections with the interval's boundary, as shown in I. Because of global parameterizability and the curve approximation algorithm's assumptions, there are only eight possible ways the implicit curve can connect the boundary intersections, as shown in II. The possibilities shown in III are not globally parameterizable in x, and are therefore excluded. To disambiguate between these eight cases, we need only see if the implicit curve intersects the x hyperplane (dashed vertical line in I) between each pair of adjacent boundary intersections. If the implicit curve intersects the hyperplane, we connect the pair of points; otherwise, we do not.

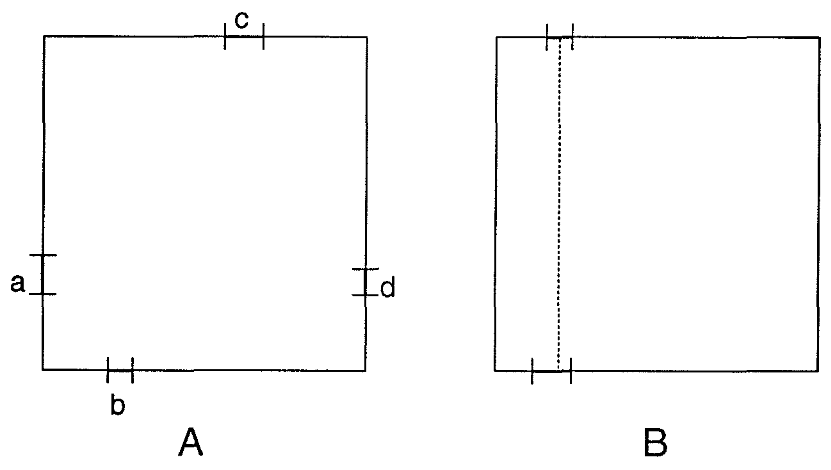

Figure 5.10: Boundary intersection sortability – Figure A illustrates a 2D interval containing four boundary intersections. Each boundary interval contains a single point of intersection of the implicit curve with the interval's boundary, as computed by the constraint solution algorithm. The boundary intersections are disjoint in the x parameter (horizontal axis). They can therefore be sorted in x, yielding the ordering a, b, c, d. In figure B, the two boundary intersections are not disjoint in x (the dashed line shows a common x coordinate). They are, however, disjoint in y.

Let a particular interval of step 1 be given by $Y = (U_1, V_1, U_2, V_2)$, where $U_1, V_1, U_2, V_2 \in \mathbf{I}$. A reasonable choice for the approximation acceptance inclusion function, $\Box G(Y)$ would be

$$w(\Box S(U_1, V_1) \bigcap \Box T(U_2, V_2)) < \delta$$

This implies that each segment of the approximate intersection curve (mapped into the output space of the parametric functions, $\mathbf{R}^3$) lies in a cube in $\mathbf{R}^3$ of width no larger than δ. In particular, this implies that the maximum distance of the approximation from the implicit curve is less than $\delta\sqrt{3}$. Of course, many other choices for $\Box G(Y)$ are possible.

Step 2 of the algorithm ensures that each proximate interval satisfy a global parameterizability criterion that allows simple computation of the local topology of the curve inside the interval. Intervals not satisfying this criterion are subdivided until each of their subregions do satisfy it. How can the algorithm know when the solution contained in a given interval is globally parameterizable? Section 5.2.2.2 presents a theorem identifying robust conditions for global parameterizability, computable with interval techniques already discussed. This

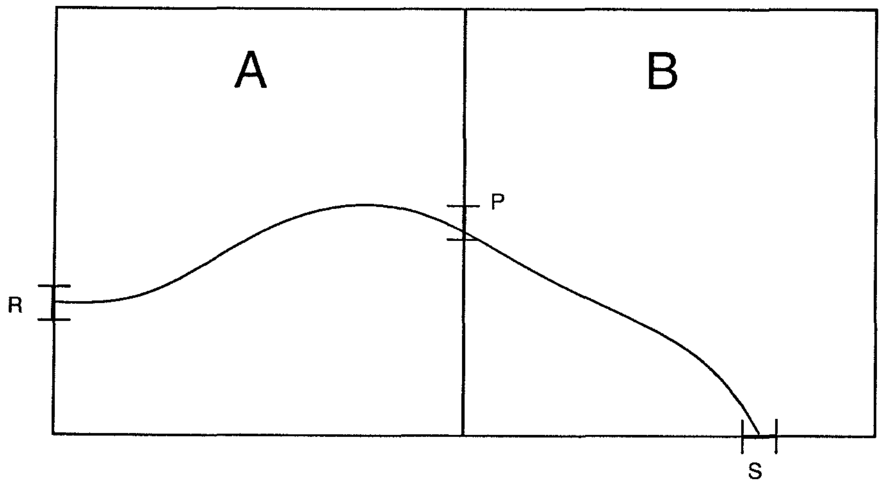

Figure 5.11: Boundary intersection sharing – Two contiguous intervals, A and B, share a boundary intersection interval, P. Each boundary intersection interval stores a pointer to two neighbors. After processing interval A, boundary intersection P is connected to R, so that P points to R. When interval B is processed, the boundary intersection P is searched for and reused. P is then connected to S, so that P points to both R and S, effectively attaching two curve segments together.

theorem pertains to the special case of a system of $n-1$ continuously differentiable equality constraints in n parameters. We have also developed a more general but heuristic test for global parameterizability, discussed in Section 5.2.2.3.

Step 3 of the algorithm computes the intersections of the implicit curve with the boundary of each proximate interval. Algorithm 5.1 is used with the original constraint inclusion, $\Box F(Y)$, and an initial region formed by one of the 2^n $(n-1)$-dimensional hyperplanes bounding the proximate interval. For each boundary hyperplane, Algorithm 5.1 searches for all the constraint system's solutions (see Section 5.1.3.3 for an explanation of the use of Algorithm 5.1 to find all solutions to a constraint system when the solutions form a finite set). Note that Algorithm 5.1 does not compute the precise solution points, but instead produces a set of intervals bounding them, called *boundary intersection intervals.*

Since neighboring proximate intervals share boundaries, boundary intersection intervals are shared between proximate intervals. When a proximate interval is processed, all neighboring intervals are first searched. Boundary intersection intervals in neighboring intervals that also lie on the interval's boundary are reused. This saves computation since Algo-

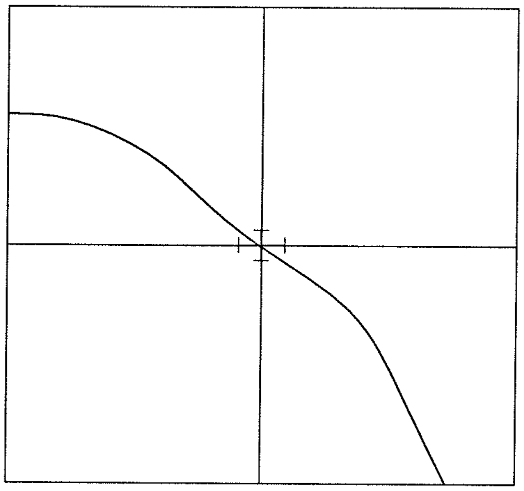

Figure 5.12: Corner boundary intersections – An implicit curve passes very close to the corner of four proximate intervals. In this case, two boundary hyperplanes in each of the four intervals will contain a boundary intersection interval. These boundary intersection intervals should be merged to reflect the fact that they contain only a single intersection point.

rithm 5.1 need not be invoked for boundary hyperplanes that have already been computed in a contiguous, previously visited interval (or a combination of such intervals). Sharing of boundary intersection intervals also allows the approximation linked list to be grown locally, as shown in Figure 5.11. Boundary intersection intervals on "corners" of the proximate interval (i.e., on the $(n-2)$-dimensional boundary of a boundary hyperplane) require special treatment. When the implicit curve intersects the proximate interval's boundary at or near such a corner, boundary intersection intervals may be computed for more than one boundary hyperplane, as shown in Figure 5.12. Such corner boundary intersections must be merged to eliminate multiple copies of the same boundary intersection. Merging involves computing the union of the intervals (see Section 5.1.3.1) and combining all neighbor pointers.

Steps 4 and 5 link boundary intersection intervals that are connected by the same segment of the implicit curve. Boundary intersection intervals are sorted in the global parameterizability parameter, and each pair of adjacent intersections is tested. The test uses Algorithm 5.1 to discover whether the implicit curve intersects a hyperplane midway between the pair of intersections. This application of the constraint algorithm need only ascertain whether a solution exists; the location of the intersection point is not required. On the other hand, the intersection point can be used to better approximate the implicit curve's behavior between the boundary intersections, at little extra computational cost.

Finally, Step 6 associates each of the boundary intersection intervals with a disjoint segment of the implicit curve. Step 6 also ensures a consistent ordering of intersections from beginning to end of each segment (e.g., the intersection's first pointer always points to the previous intersection on the curve, the second pointer always points to the next intersection). A point inside each of the boundary intersection intervals should be chosen to represent the actual point of intersection of the proximate interval's boundary with the implicit curve. This point can be chosen arbitrarily (e.g., midpoint of the interval) or computed using a local iterative technique such as Newton's method.

Figure 5.13 shows an example of the results of this algorithm for the problem of finding the silhouette curve of a surface with respect to a given orthographic view.

5.2.2.2 A Robust Test for Global Parameterizability

Consider an r-dimensional manifold defined as the solution to a system of $n-r$ equations in n parameters ($r = 0, 1, \ldots, n-1$):

$$\begin{aligned} f_1(x_1, x_2, \ldots, x_n) &= 0 \\ f_2(x_1, x_2, \ldots, x_n) &= 0 \\ &\vdots \\ f_{n-r}(x_1, x_2, \ldots, x_n) &= 0 \end{aligned}$$

Given a set of r parameter indices, $A = \{k_1, k_2, \ldots, k_r\}$, and an interval $X \ni \mathbf{I}^n$, we define a *subinterval* of X over A as a set depending on r parameters $(y_1, y_2, \ldots, y_r)$, $y_i \in X_{k_i}$, defined by

$$\text{subinterval}(y_1, y_2, \ldots, y_r; X) \equiv \left\{ x \in X \mid \begin{array}{ll} x_i = y_j & \text{if } i = k_j \in A \\ x_i \in X_i & \text{otherwise} \end{array} \right\}$$

Thus, a subinterval is an interval subset of X, r of whose coordinates are a specified constant, and the rest of whose coordinates are the same as in X.

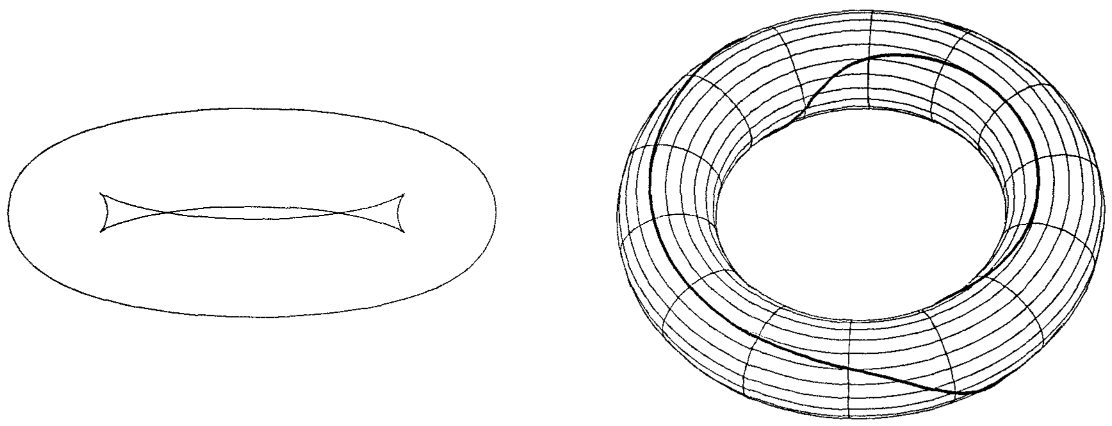

Figure 5.13: Silhouette curve approximation – The silhouette curve of a parametric surface with respect to a given orthographic view can be found with the implicit curve approximation algorithm. In this example, the surface is a torus, given by

$$S(u,v) = \begin{pmatrix} \cos(2\pi u)(r\cos(2\pi v) + R) \\ \sin(s\pi u)(r\cos(2\pi v) + R) \\ r\sin(2\pi v) \end{pmatrix}$$

where r and R represent the two torus radii. The silhouette is then given by the solution of a single constraint in the two variables u and v, that specifies that the dot product of the torus normal and the view direction, E, is 0, i.e.,

$$E \cdot (\frac{\partial S}{\partial u} \times \frac{\partial S}{\partial v}) = 0$$

The illustration shows the torus and its silhouette. Note that the silhouette consists of two disjoint closed segments. On the left, the torus is viewed with viewing direction E. On the right, it is viewed with another viewing direction.

The solution to a system of $n-r$ equations in n parameters is called *globally parameterizable* in the r parameters indexed by A over an interval X if there is at most one solution to the system in any subinterval of X over A. Put more simply, the system of equations is globally parameterizable if r parameters can be found such that there is at most one solution to the system for any particular value of the r parameters in the interval.

We define $\square J_{\{k_1,k_2,\ldots,k_r\}}(X)$, called the *interval Jacobian submatrix*, as an $(n-r)\times(n-r)$ interval matrix given by

$$\square J_{\{k_1,k_2,\ldots,k_r\}}(X) \equiv \left[\square \frac{\partial f_i}{\partial x_j}(X)\right]_{j\notin\{k_1,k_2,\ldots,k_r\}}$$

For an $n \times n$ interval matrix $\square M$, we write

$$\det \square M \neq 0$$

if there exists no matrix $M \in \square M$ such that $\det M = 0$. We now prove a theorem guaranteeing the global parameterizability of the solution in an interval X. This theorem, which might be called the Interval Implicit Function Theorem, is analogous to the Implicit Function Theorem from multidimensional calculus, except that it deals with the global parameterizability of the solution manifold rather than its local parameterizability.

Theorem 5.5 (Interval Implicit Function Theorem) Let the constraint functions $f_i(x)$, $i = 1, 2, \ldots, n-r$ be continuously differentiable. Let a region $X \in \mathbf{I}^n$ exist such that

$$\det \square J_{\{k_1,k_2,\ldots,k_r\}}(X) \neq 0$$

Then the solution to the system of equations $f_i(x) = 0$ is globally parameterizable in the r parameters indexed by $\{k_1, k_2, \ldots, k_r\}$ over X.

Proof. Assume the contrary. Then there exists two points $p, q \in X$ such that

1. $p \neq q$

2. p and q are in the same subinterval with respect to the index set $A = \{k_1, k_2, \ldots, k_r\}$

3. $f_i(p) = f_i(q) = 0$ for $i = 1, 2, \ldots, n-r$

But by the Mean Value Theorem, and since any coordinate of p and q indexed by the set A is equal, we have

$$f_i(p) - f_i(q) = \sum_{j \notin A} \frac{\partial f_i}{\partial x_j}(\xi_i)(p_j - q_j)$$

for $n - r$ points $\xi_i \in X$. But then

$$f_i(p) - f_i(q) = 0 = J(p - q)$$

where $J \in \Box J_A(X)$ and $p - q \neq 0$. Therefore J is singular. But this is impossible since $\det \Box J_A(X) \neq 0$. ∎

In the case of approximation of a 1D solution manifold, we have $r = 1$; i.e., we are solving a system of $n - 1$ equations in n variables. The theorem guarantees that if, in an interval X, we can find $n - 1$ parameters such that

$$\det \Box J_{\{k\}}(X) = \det \left[\Box \frac{\partial f_i}{\partial x_j} \right]_{j \neq k} \neq 0$$

then the solution manifold is globally parameterizable in X over the parameter x_k. This means that for any value of the parameter x_k in the interval X there is at most one solution to the system of equations in the x_k hyperplane of X.

We can verify that

$$\det \Box J_{\{k\}}(X) \neq 0$$

by forming an inclusion function for the determinant of any of the n interval Jacobian submatrices. The determinant inclusion function, $\det_\Box$, can be constructed using the interval arithmetic presented in Section 5.1.2.2. If, for any of the interval Jacobian submatrices, we have

$$0 \notin \det_\Box \Box J_{\{k\}}(X)$$

then the hypothesis of the theorem is satisfied.

5.2.2.3 A Heuristic Test for Global Parameterizability

This section discusses a heuristic test for global parameterizability in an interval Y. The test is useful because the implicit curve to be approximated may be represented with a constraint system that does not satisfy the hypothesis of Theorem 5.5 (i.e., not a system of $n-1$ equations in n parameters, equating continuously differentiable functions to 0). Also, we may wish to avoid computation at the expense of robustness. The heuristic test eliminates computation of interval Jacobian determinants, and often allows early acceptance of intervals (before they are subdivided because they do not satisfy the robust global parameterizability criterion). Early acceptance of intervals is significant because larger intervals require fewer implicit curve/boundary intersection computations.

In fact, the heuristic test discussed in this section is related to "connectability" of boundary intersections rather than to global parameterizability. That is, the test ensures that boundary intersections linked in Step 5 of the approximation algorithm are *connected* in Y: on the same segment of the implicit curve that is contained entirely in Y. This condition, which we will call *step 5 connectability*, is guaranteed by global parameterizability. Global parameterizability is, however, a much stronger condition, as Figure 5.14 shows. Unfortunately, the heuristic test is not robust in checking for this weaker condition of step 5 connectability. It assumes that the solution does not form a closed curve entirely contained in Y, termed the *nonperiodicity assumption* in the following text.

The test first finds all intersections of the solution curve with the boundaries of Y, yielding a set of intervals each containing a boundary intersection. This is the same computation that occurs in Step 3. The test checks that these intervals are disjoint in some parameter i, just as in Step 4. If the boundary intersection intervals are not disjoint in any parameter, the test fails, and Y must be subdivided. Otherwise, the boundary intersections can be unambiguously sorted in parameter i, The test then checks that the solution curve has only a single intersection with the i-th coordinate hyperplane of each of the boundary intersections, as shown in Figure 5.15. This check is called the *boundary univalence test.*

More precisely, let the intervals $X^1, X^2, \ldots, X^m \in \mathbf{I}^n$ be a sequence of intervals each bounding an intersection of the implicit curve and the boundary of $Y \in \mathbf{I}^n$. Let Y be given by

$$Y = [a_1, b_1] \times \ldots \times [a_n, b_n]$$

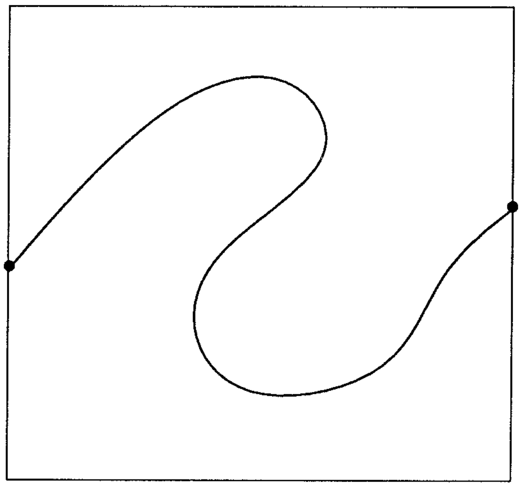

Figure 5.14: Step 5 connectability vs. global parameterizability – An implicit curve defined in a 2D parameter space has two intersections with the boundary of an interval. The implicit curve is not globally parameterizable in x or y, yet, it is step 5 connectable. Step 5 of the approximation algorithm will link the two boundary intersections after determining that an x or y hyperplane between the two boundary intersections intersects the implicit curve.

Assume that the boundary intersection sequence is sorted by parameter i, i.e.,

$$\mathrm{ub}\, X_i^k < \mathrm{lb}\, X_i^{k+1} \quad k = 1, 2, \ldots, m-1$$

where X_i^k represents the i-th coordinate interval of X^k. The i-th coordinate hyperplane of a boundary intersection X_k is an interval subset of X^k whose i-th coordinate is a constant:

$$\begin{array}{lll} X_j^k & & j \neq i \\ [x, x] & x \in X_i^k & j = i \end{array}$$

The boundary univalence test is based on the observation that if an i-th coordinate hyperplane of a boundary intersection interval X^k contains only a single intersection with the implicit curve, then no boundary intersections $X^p, p < k$ can be connected to boundary intersections $X^q, q > k$. If the boundary univalence test succeeds on each of the boundary intervals, X^k, then the implicit curve can only connect boundary intersections adjacent in parameter i, i.e., X^k and X^{k+1}. Assuming there are no closed segments of the implicit curve contained entirely within Y (nonperiodicity assumption), Step 5 of the approximation

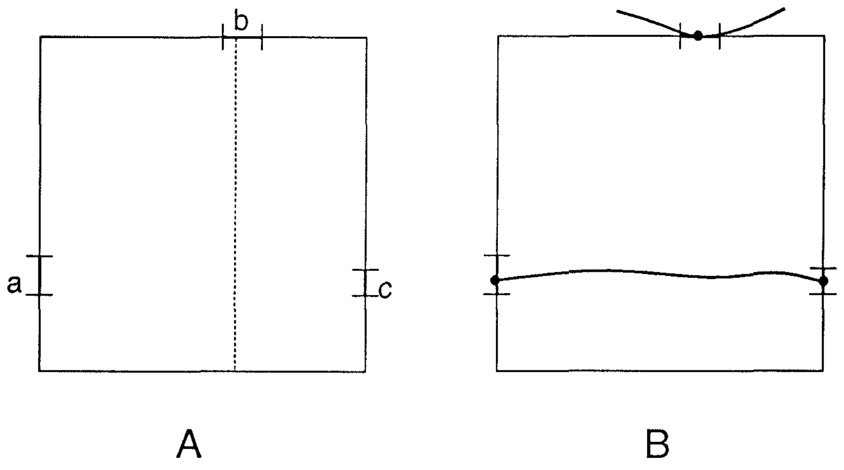

Figure 5.15: Boundary univalence test – In Figure A, three boundary intersections exist in a 2D interval. These intersections are disjoint in the x parameter, yielding the intersection ordering a, b, c. The boundary univalence test checks whether the implicit curve intersects the x hyperplane at intersection b, shown by the dashed line. If there is only a single intersection between the implicit curve and this hyperplane (i.e., the same intersection contained in b), then the implicit curve cannot connect the boundary intersections a and c. That is, the implicit curve can not have the behavior illustrated in Figure B, which would yield two implicit curve/hyperplane intersections. Thus, assuming there are no closed segments of the implicit curve contained entirely in the interval, the approximation algorithm will correctly connect the boundary intersections.

algorithm then correctly determines whether adjacent boundary intersections should be connected. Figure 5.16 illustrates why the nonperiodicity assumption is necessary.[16] If the boundary univalence test fails for any boundary intersection, the whole heuristic test fails, and Y must be subdivided.

The boundary univalence test need be performed only if there are more than two boundary intersections. Given the nonperiodicity assumption, if there are two boundary intersections, then either the implicit curve does not intersect the interior of Y, or it connects the two boundary intersections. These two possibilities are correctly distinguished by Step 5 of the approximation algorithm. In practice, the great majority of intervals Y contain no boundary intersections or a single pair. Thus, the heuristic test performs very little

[16]Fortunately, when the nonperiodicity assumption is violated, the approximation algorithm can easily detect when boundary intersections have been incorrectly connected. Incorrect connection, such as would occur in Figure 5.16, will lead to the linking of a boundary intersection that already has two distinct linked list neighbors.

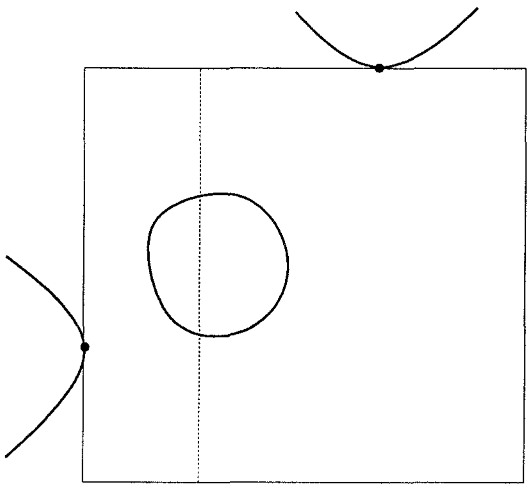

Figure 5.16: Necessity of the nonperiodicity assumption in the heuristic test – In this example, an implicit curve intersects the boundary of a region in $\mathbf{R}^2$ at two points. In fact, the implicit curve does not connect these two boundary points; instead, the curve is tangent to the boundary at these two points. Nevertheless, step 5 of the approximation algorithm will decide that the two points should be connected. This is because the x-coordinate hyperplane shown by the dashed line has a nonempty intersection with a closed segment of the implicit curve.

computation most of the time, compared with the robust test.

Furthermore, the boundary univalence test need be performed only on boundary intersections that do not lie on the i-th coordinate boundaries of Y. That is, if the first interval X^1 has $X_i^1 = [a_i, a_i]$, or the last interval X^m has $X_i^m = [b_i, b_i]$, then the boundary univalence test on these intervals is not required. This is because the univalence of such intervals is already guaranteed by the sortability condition.

One might reasonably ask why the boundary univalence test is required at all. Why not instead subdivide until each interval Y contains at most two boundary intersections with the implicit curve? The reason is that this scheme will lead to an inordinate amount of subdivision, in rarely occurring circumstances. Figure 5.17 illustrates one such pathological case.

5.2.2.4 Relaxing the Approximation Algorithm's Restrictions

Algorithm 5.3 assumes that the implicit curve to be approximated satisfies two assumptions. In this section, we examine these assumptions in more detail and show how the algorithm

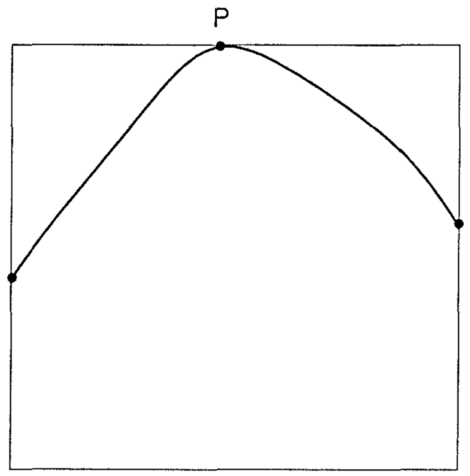

Figure 5.17: Pathological case for naive subdivision – The implicit curve has three intersections with the boundary of the interval. At the intersection labeled P, the implicit curve is exactly tangent to the interval's boundary. No matter how the interval is subdivided, any child interval containing P will also have three implicit curve/boundary intersections, unless the boundary interval containing P is split during subdivision in x. Depending on the size of the interval containing P, the original interval may have to be subdivided many times for this to happen.

can be enhanced to handle more general implicit curves.

5.2.2.4.1 Assumption 1a – No Self-Intersections or Isolated Singularities Algorithm 5.3 assumes that the implicit curve has no self-intersections or isolated singularities. One approach to handling curves that do contain such singularities is to distinguish proximate intervals in which the implicit curve is well-behaved from proximate intervals in which the implicit curve may have singularities. For example, for an implicit curve described by a system of $n-1$ continuously differentiable functions of n parameters equated to 0, the robust test for global parameterizability (i.e., the Interval Implicit Function Theorem of Section 5.2.2.2) guarantees that the implicit curve will not contain singularities. This is true because of the Implicit Function Theorem, whose conditions are sufficiently satisfied by those of the Interval Implicit Function Theorem. Since we expect the set of singularities to be zero-dimensional, it should be possible to subdivide the ill-behaved proximate intervals until their child intervals are either well-behaved or are small enough.

We can then process the well-behaved proximate intervals in the same way as before.

What should be done with the remaining (small) ill-behaved intervals? A reasonable course is to connect all their boundary intersections in a star-like graph. More precisely, the midpoint of the ill-behaved interval is connected to each of the interval's boundary intersections. Essentially, we assume that an ill-behaved interval represents a possibly multibranching self-intersection of the implicit curve, to some tolerance; this tolerance being the largest width of an ill-behaved proximate interval. Thus, such ill-behaved intervals create a local topology graph with more complexity than a simple linked list.

5.2.2.4.2 Assumption 1b – No Abrupt Endings We may also wish to handle implicit curves that violate the continuity part of Assumption 1; that is, curves that end abruptly in the interior of the region of consideration. An approach to relaxing this assumption is similar to the technique for relaxing the lack of singularities assumption of the previous section – proximate intervals in which the implicit curve may abruptly end are distinguished from intervals in which the curve satisfies Assumption 1. For example, an implicit curve may be described by the following constraint system:

$$\begin{aligned} f_i(x) &= 0 \quad i = 1, 2, \ldots, n-1 \\ g_j(x) &\geq 0 \quad j = 1, 2, \ldots, m \end{aligned}$$

where $x \in \mathbf{R}^n$, and f_i and g_j are continuous functions $f_i, g_j : \mathbf{R}^n \rightarrow \mathbf{R}$. Even if the equality constraints f_i determine a solution that is a continuous 1-manifold, this solution can still have abrupt endings in the interior of an interval whenever the inequality constraints reject parts of that solution curve. If for some proximate interval Y we have

$$0 \notin \Box g_j(Y) \text{ for any } j \in \{1, 2, \ldots, m\} \tag{5.8}$$

and again assuming the solution determined by the equality constraints is 1-manifold, then Y can contain no abrupt endings. We can therefore subdivide intervals until they satisfy the criterion in Equation 5.8, or are very small. Regions satisfying the criterion can be processed using Steps 2, 3, 4, and 5 of Algorithm 5.3.

The remaining small regions may contain abrupt endings. In general, the behavior of the implicit curve in these regions can not be easily analyzed because the inequality constraint may or may not cause breaks in the implicit curve that solves the system without the inequality constraint. It may be sufficient, however, to allow the curve's local topology to be uncertain within these small intervals. On the other hand, we may do better in many circumstances. For example, in the above constraint system, we can find solutions to the $n \times n$ system

$$\begin{aligned} f_i(x) = 0 \quad & i = 1, 2, \ldots, n-1 \\ g_j(x) = 0 \quad & j \in \{1, 2, \ldots, m\} \end{aligned}$$

using Algorithm 5.1. That is, we can find the points of intersection between the implicit curve satisfying the equality constraints and each of the m manifolds where $g_j(x) = 0$. Assuming the solution to the constraint system $f_i(x) = 0$ is globally parameterizable in the small region, the combined set of boundary intersections and solutions to the m $n \times n$ systems can be processed using Steps 4 and 5 of Algorithm 5.3.

5.2.2.4.3 Assumption 2 – No Segments along Proximate Interval Boundaries

Algorithm 5.3 assumes that the implicit curve has no segments that run along the boundary of a proximate interval. During Step 3, Algorithm 5.1 can detect violations of this assumption by detecting when the constraint system solutions fail to converge to a set of finite points. For example, we can check whether the number of candidate solution intervals continues to grow as the iteration proceeds.

If this checking determines that Assumption 2 is violated, then the parameter space of constraint system should be transformed. That is, given a constraint system $F(x) = 1$ and an invertible transformation $T(x) : \mathbf{R}^n \rightarrow \mathbf{R}^n$, then solving the system $F(T(x)) = 1$ transforms the implicit curve by T^{-1}. Thus, we can use Algorithm 5.3 on the transformed constraint system and transform each of the resulting points by T^{-1} to yield an approximation of the implicit curve that solves the original constraint system. T should be chosen so that the segment of the implicit curve no longer lies along the boundary of a proximate interval in the transformed parameter space. For example, a simple translation transformation,

$$T(x) = x + a$$

where a is chosen to translate the offending segment to the interior of the proximate interval, is sufficient.

5.2.3 Approximating Parametric Shapes Using Adaptive Criteria

In Section 5.2.2, an algorithm was presented to approximate implicit curves. The first part of this algorithm involved constructing a collection of intervals bounding the implicit curve and satisfying an approximation acceptance inclusion function. A similar technique can be applied to the problem of generating an approximation of a parametric shape that satisfies user specified criteria.

Let $F : \mathbf{R}^n \rightarrow \mathbf{R}^m$ be a parametric shape, and let $D \in \mathbf{I}^n$ be the domain of F. F can be approximated in three steps:

1. subdivide the domain D into a collection of subregions that satisfy some criteria.
2. choose a small number of points from each subregion (typically on the subregion's boundary), and evaluate F at each point.
3. construct an approximation of the shape in each subregion, using the samples from step 2. These approximations should fit together at the subregion boundaries.

The criteria of Step 1 are represented using an inclusion function $\Box G : \mathbf{I}(D) \rightarrow \mathbf{I}$. $\Box G$ takes a subregion X and produces the following results

$$\begin{array}{ll} [1,1] & \text{accept the region } X \\ [0,1] & \text{continue subdividing the region } X \end{array}$$

The interval $[0,0]$ is not returned because subregions are not rejected; they are subdivided until they are eventually accepted. An example of a useful subregion acceptance inclusion function is

$$\Box G(X) = w(\Box F(X)) < \delta$$

This inclusion function guarantees that each subregion is small enough that the output of the parametric function can be bounded in an interval of width at most δ.

5.2.3.1 Kd-trees

A convenient data structure for organizing the collection of subregions is a *kd-tree*, for *k-dimensional tree* (also called *bintrees* in [TAMM84]). A kd-tree represents a binary subdivision of multidimensional space, one dimension at a time. Each node stores a left and right subtree, and an index representing the subdivided dimension. Let $(left, right, d)$ represent a kd-tree node, where $left$ is the left subtree, $right$ is the right subtree, and d is the subdivided dimension. The special value NIL represents an empty kd-tree. For example, a leaf node is represented by the kd-tree (NIL,NIL,0), since both its child nodes are empty. Kd nodes can even have one child empty and another nonempty to represent spatial subdivisions that do not occupy all of the original space. Although such trees are not important in the current discussion, since we wish to sample the whole parameter space of F, they will be used in Section 5.2.4.

If we represent the collection of subregions in the approximation by a kd-tree, an algorithm for Step 1 may be defined using the following recursive function.

```
subdivide($X$,$\square G$,$d$)
    evaluate $Y = \square G(X)$
    if $Y = [1,1]$ then
        return (NIL,NIL,0)
    else
        subdivide $X$ in parametric dimension $d$ into $X_1$ and $X_2$
        let $d'$ be the next dimension to subdivide
        return (subdivide($X_1$,$\square G$,$d'$),subdivide($X_2$,$\square G$,$d'$),$d$)
    endif
```

Subdivision takes place along the midpoint of the parametric coordinate d. Step 1 is accomplished using the invocation subdivide$(D, \square G, 1)$.

Once an appropriate collection of subregions has been computed, a set of points must be chosen in each leaf of the kd-tree and the points must be interpolated in some manner. The next section discusses this process for the case when F is a parametric surface, and the approximating network is a polygonal mesh.

5.2.3.2 Approximating a Surface as a Triangular Mesh

Given a 2D kd-tree, a polygonal mesh approximating the surface can be generated. The parametric function is first evaluated at the corners of each kd-tree leaf, as shown in Figure 5.18. The corner samples are then used to construct a collection of triangles. Note that the evaluation of corner samples should be shared among leaves to avoid needless evaluation of the parametric function.

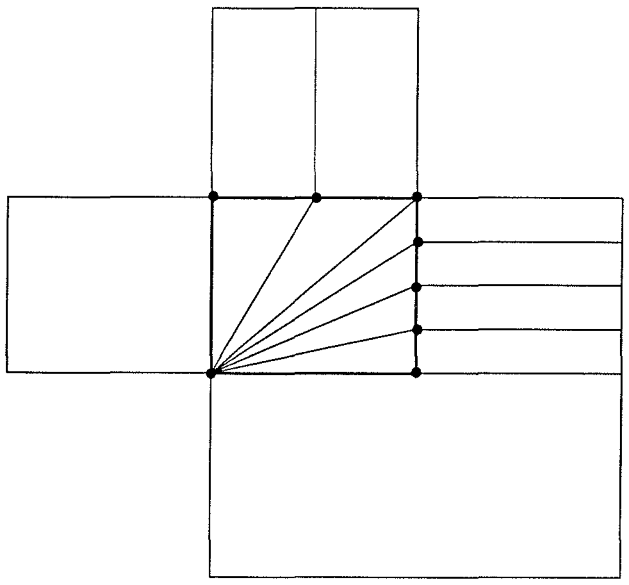

Figure 5.18: Approximating a surface as a polygonal mesh – The center rectangle is a kd-tree leaf, surrounded by its neighbors. The parametric function is evaluated at each point on the boundary of the leaf that is a corner of the leaf or of its neighbor. A collection of triangles is then generated so that each boundary point is a vertex of at least two triangles.

5.2.4 CSG-like Operations with Trimmed Surfaces

A *trimmed surface* is the image of a parametric surface over a domain specified with a collection of curves, called *trimming curves.* The trimming curves form the boundary of a region over which the trimmed surface is evaluated. Figure 5.19 shows an example of a trimmed parametric surface. Trimmed surfaces are a useful modeling tool. For example, by letting the trimming curve be the curve of intersection of one surface with another, simple CSG operations can be represented.

Let $S(u,v)$ and $T(s,t)$ be two non self-intersecting, continuous, closed, and bounded parametric surfaces in $\mathbf{R}^3$. Let the sets $S^\diamond$ and $T^\diamond$ be the regions in $\mathbf{R}^3$ bounded by S and T, respectively. A trimmed surface can be used to represent the part of S that lies outside $T^\diamond$. This is accomplished by computing the curve of intersection of S and T, in (u,v,s,t) space, and projecting it to the parameter space of S, (u,v). The projected intersection curve is then used as the trimming curve for a trimmed version of S. Similarly, another trimmed surface can be used to represent the part of T that lies inside $S^\diamond$. The union of the two resulting trimmed surfaces forms the boundary of the region $R = S^\diamond - T^\diamond$, where the $-$

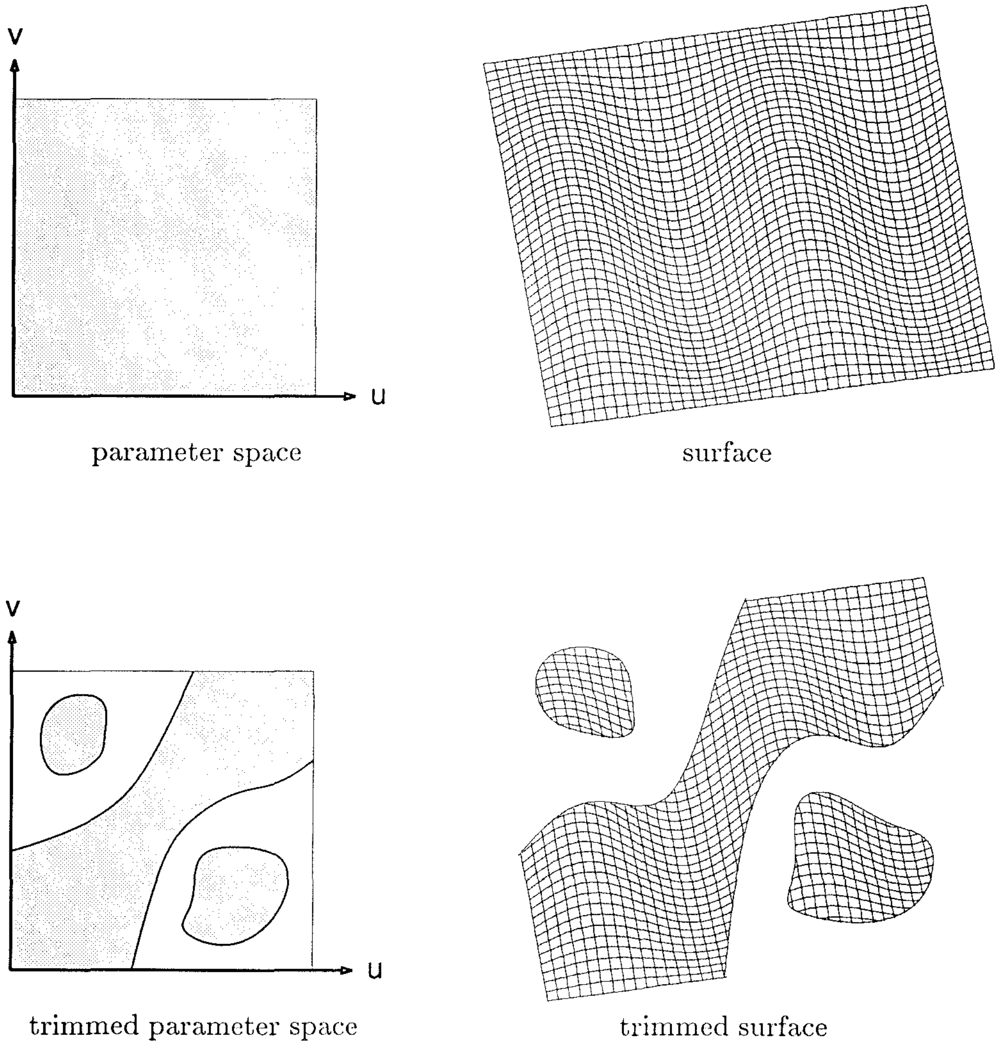

Figure 5.19: Trimmed parametric surface — The top of the figure shows a parametric surface $S(u, v)$ evaluated over a square region of (u, v) parameter space. The bottom shows a trimmed parametric surface. Four trimming curves have been used to define a new domain for S.

operator denotes set subtraction. Similar operations that compute Boolean set subtractions, unions, and intersections using trimmed surfaces will be termed *CSG-like operations.* CSG-like operations are distinguished from fully general CSG on parametric surfaces in that the results of a CSG-like operation can not be used as an input to another CSG-like operation. However, CSG-like operations are extremely useful, and can be developed into a more sophisticated technique to implement full CSG, as will be discussed in Section 5.2.5.

A difficult problem in geometric modeling has been to approximate the boundary of the result of CSG-like operations (such as R) so that the trimmed surfaces resulting from $S - T^{\diamond}$ mesh together without artifact with the trimmed surfaces resulting from $T - \neg(S^{\diamond})$[17]. In this section, an algorithm that solves this problem is presented. This algorithm uses the implicit curve approximation algorithm discussed in a previous section to compute the curve of intersection between the two parametric surfaces.

5.2.4.1 An Algorithm for Approximating CSG-like Operations

The ideas of Sections 5.2.3 and Section 5.2.2 can be combined to produce an algorithm that approximates the results of CSG-like operations. This algorithm ensures that the trimmed surfaces mesh together by guaranteeing that all samples on the curve of intersection between the two parametric surfaces are shared.

To continue the example of the previous section, let $S(u, v)$ and $T(s, t)$ be parametric surfaces. The following algorithm approximates the boundary of $S^{\diamond} \circ T^{\diamond}$ where $\circ$ represents a binary set operation such as union, intersection, or subtraction. The algorithm assumes that the curve of intersection between S and T satisfies the assumptions of Algorithm 5.3 (e.g., that the intersection curve does not self-intersect).

Algorithm 5.4 (CSG-like Operation Approximation Algorithm)

1. **Find the curve of intersection of S and T in (u, v, s, t) space.** Algorithm 5.3 is used to compute a set of linked points approximating the intersection curve. It also generates a kd-tree in (u, v, s, t) space whose terminal nodes are the proximate intervals bounding the intersection curve. Each terminal node stores the intersection points on or within its boundary.

[17]The $\neg$ operator denotes set complement.

2. **Project the (u, v, s, t) intersection kd-tree into (u, v) and (s, t) space.** The resulting 2D kd-trees will be referred to as *projected intersection kd-trees.*

3. **Join curve segments that intersect periodic parameter space boundaries.** For example, if a curve segment in (u, v) space does not end on the u, v parameter rectangle, it must have been artificially stopped by hitting a periodic s or t boundary. It should therefore be joined with another curve segment that continues from the opposite side of that boundary.

4. **Order the projected intersection curves based on $\circ$ so that the appropriate interior of the trimmed parameter space lies to the left of the trimming curves.** Initially, the curve segments are processed so that each closed curve segment is traversed in a counterclockwise manner (interior to the left), and the curve segments intersecting the parameter space rectangle are traversed to form closed regions with a counterclockwise traversal of any included parameter rectangle boundaries. A hierarchy of projected intersection curve segments is then constructed according to an inside/outside relationship. For example, the curve of intersection projected into (u, v) space may have two segments, A and B. Three possible relationships are possible: the two segments are disjoint, A is inside B, or B is inside A (intersection is not allowed by the assumption of the algorithm). The inside/outside relationship of two curve segments can be easily computed by performing two point-in-polygon tests (one point on A tested against segment B, and vice versa). Once this hierarchy is constructed, the ordering of each segment directly within another is switched, producing consistent counterclockwise traversal of the boundaries of a valid 2D region. Finally, a single bit of information remains unspecified since two valid regions can be constructed in this manner. That is, we can switch the ordering of every curve segment and create a new region that is the subtraction of the old region from the parameter space rectangle. This single bit of information can be determined by testing whether a single point in parameter space is in the desired set $S^{\diamond} \circ T^{\diamond}$, using the technique of point-set classification (see Section 2.2.2.2.11).

5. **Generate sampling kd-trees for S and T, using the algorithm of Section 5.2.2.** The sampling kd-trees represent an approximation of the entire surface S

or T, not considering the intersection. The two kd-trees will be referred to as *surface sampling kd-trees.*

6. **Merge the projected intersection kd-tree from Step 2 with the surface sampling kd-tree from Step 5 for each of S and T.** The merging operation produces a kd-tree whose terminal nodes are the union of the terminal nodes from the two kd-tree inputs, which will be referred to as a *merged kd-tree.* The merging must be done so that *no terminal kd node in the projected intersection kd-tree is further subdivided.* This is essential because subdivision of the projected intersection kd-tree will require additional sampling of the intersection curve to determine where it intersects the new subdivision boundary. It is then possible that intersection curve samples will be computed for S but not T (or vice versa) so that the intersection curve is no longer shared by the trimmed surfaces.

7. **Generate triangles for each trimmed surface.** This can be accomplished by applying the following neighbor-finding algorithm to each of the trimmed surfaces independently:

```
initialize the list $L$ with one node containing the intersection curve
while $L$ is nonempty
    pop node $X$ off the list $L$
    find all neighbors of $X$ that haven't been visited yet
    if $X$ has intersections
        generate triangles inside $X$
        label nodes sharing included boundaries as INSIDE
        label nodes sharing excluded boundaries as OUTSIDE
        leave nodes neighboring pierced boundaries unspecified
    else
        if $X$ is INSIDE generate triangles
        label all of $X$'s neighbors as same as $X$
    endif
    push unvisited $X$ neighbors onto list
    mark $X$ as visited
endwhile
```

Note that the generation of triangles inside a kd-node completely within the trimmed interior is done in the same manner as was discussed in Section 5.2.3.2.

We will now present an example of how Algorithm 5.4 works. Figure 5.20 shows two surfaces, $S(u, v)$ and $T(s, t)$, on which a CSG-like operation is to be performed. Specifically, the region bounded by T is to be subtracted from the region bounded by S, simulating a hole drilling operation. Figure 5.21 illustrates the steps of Algorithm 5.4 on the hole drilling example. Note that both the parametric surfaces are periodic in one parameter, $S(u, v)$ in u and $T(s, t)$ in s. During Step 3, one of the projected curve segments in (s, t) parameter space is artificially broken because its corresponding (u, v) projection hits the periodic u boundary. These two curve segments must be joined in order to complete the curve ordering of Step 4. The results of the CSG-like approximation are shown in Figure 5.22.

The key element of Algorithm 5.4 is the use of a kd-tree to encompass the intersection curve between two parametric surfaces. This kd-tree is projected into the parameter spaces of the two parametric surfaces in such a way that no extra subdivisions (and thus sample points on the curve) are produced. Prohibiting such subdivision thus guarantees that the approximated intersection curve intersects each of the terminal kd-nodes in **both** surfaces' parameter spaces in samples that have already been computed. The same approximated curve of intersection (with the same samples) thus forms the boundary where the two trimmed surfaces meet.

5.2.4.2 Kd-tree Algorithms for CSG-like Operations

Algorithm 5.4 requires two algorithms that operate on kd-trees: one to project a 4D kd-tree to a 2D kd-tree, and another that merges two kd-trees. This section describes the simple algorithms required for these tasks. We first define two primary algorithms that are used as tools in the kd-tree projection and merging.

These two algorithms, `insert_addonly` and `insert_nosubdivide`, both insert a kd node into a given kd-tree. The kd node to be inserted is described by its *kd-address*. The kd-address is an array of sequences of bits, one sequence for each dimension of the kd-tree. Each bit in the sequence represents whether the left or right side of the kd-tree must be traversed in the particular dimension in order to find the node, starting from the root of the kd-tree. For example, consider a 1D kd-tree representing a subdivision of the interval

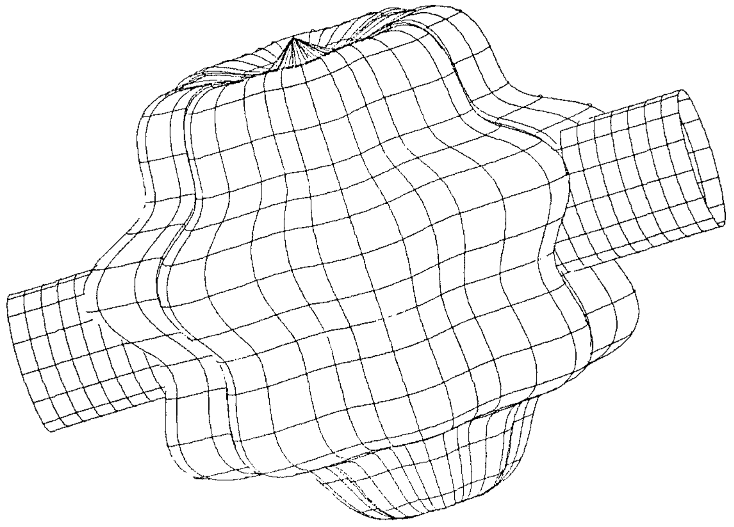

Figure 5.20: Hole drilling with trimmed surfaces (part 1) – A hole is to be drilled in the bumpy sphere shape by subtracting a cylinder from the shape. The bumpy sphere is a profile product of two curves, cross section $c(u)$ and profile $p(v)$ where

$$\begin{aligned} c(u) &= \begin{pmatrix} \cos(2\pi u) \\ \sin(2\pi u) \end{pmatrix} (1 + 0.1\sin(16\pi u)) \\ p(v) &= \begin{pmatrix} \cos(\pi(2v-1)/2 \\ \sin(\pi(2v-1)/2 \end{pmatrix} (1 + 0.1\sin(8\pi v)) \end{aligned}$$

The cylinder $T(s,t)$ is aligned with the x axis, extending from $x = -1.5$ to $x = 1.5$, with radius 0.3. The domain of u, v, s, and t is the interval $[0,1]$.

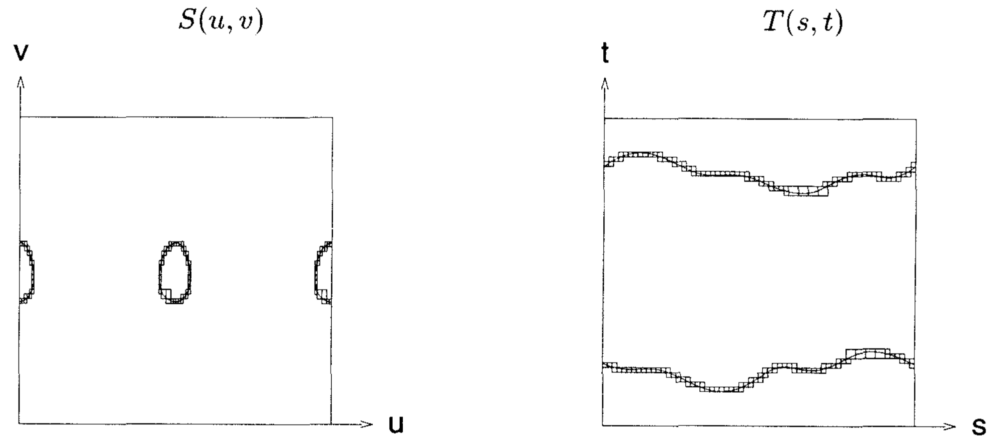

I. Projected Intersection Kd-Trees

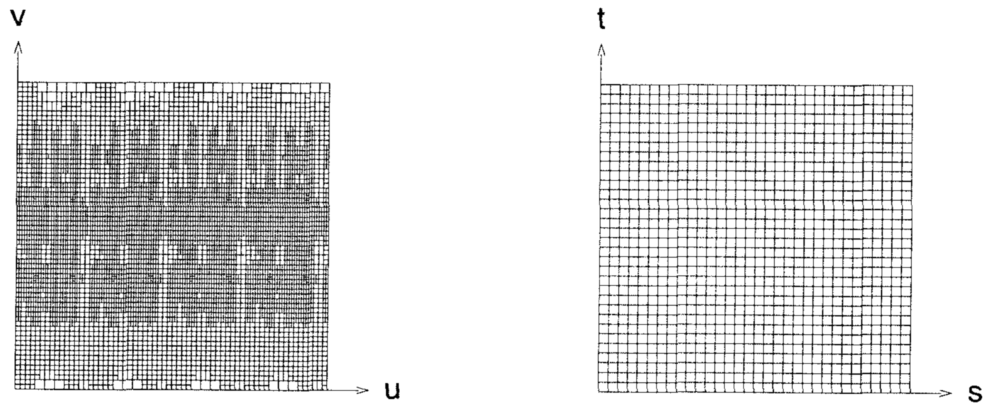

II. Surface Sampling Kd-Trees

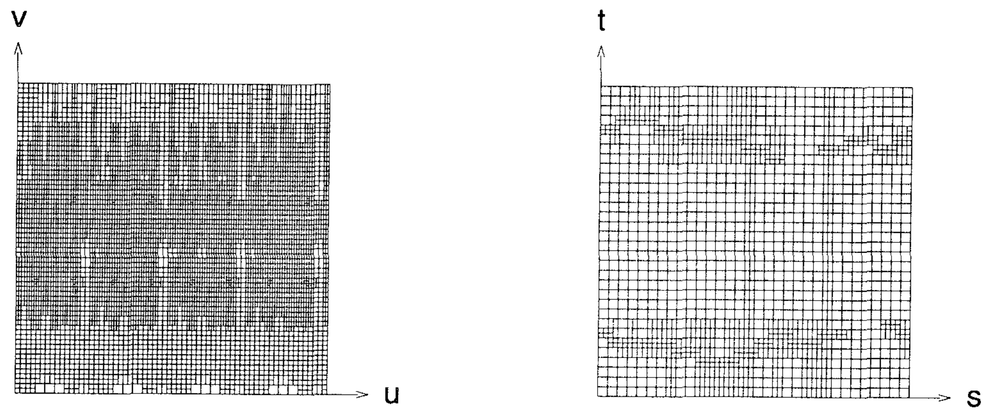

III. Merged Intersection/Surface Sampling Kd-Trees

Figure 5.21: Hole drilling with trimmed surfaces (part 2) – The results of Steps 2, 5, and 6 of Algorithm 5.4 are displayed. The (u,v) and (s,t) projection of the curve of intersection is also drawn with the projected intersection kd-trees.

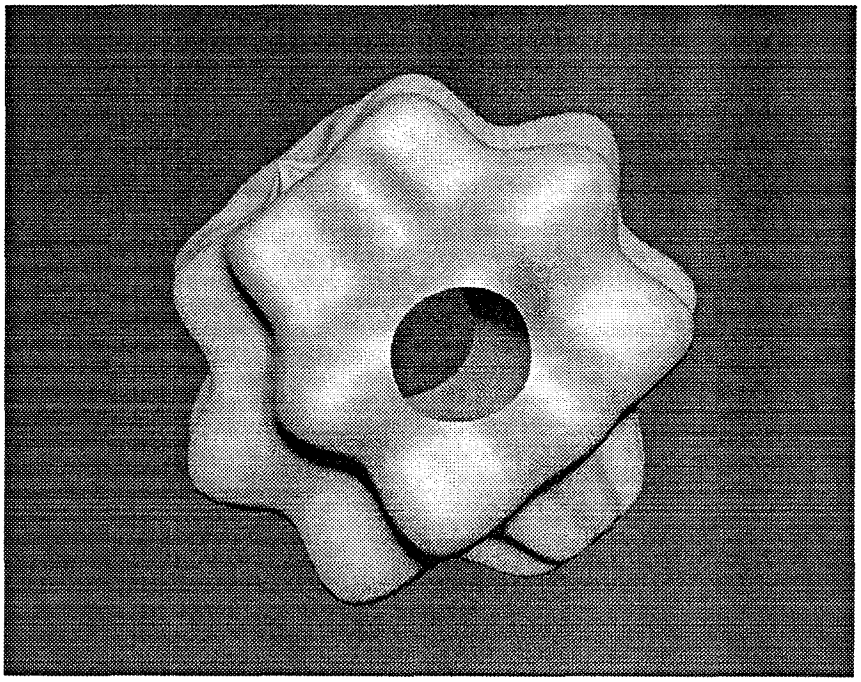

Figure 5.22: Hole drilling with trimmed surfaces (part 3) – The result of the hole drilling operation is illustrated. Note that the curve of intersection between the bumpy sphere and cylinder is approximated without visual artifacts.

[0, 1]. The following are examples of kd-address/interval correspondences:

$$\begin{array}{lcl} 00 & \rightarrow & [0, 0.25] \\ 01 & \rightarrow & [0.25, 0.5] \\ 10 & \rightarrow & [0.5, 0.75] \\ 11 & \rightarrow & [0.5, 1.0] \\ 0010 & \rightarrow & [0.125, 0.0.1875] \end{array}$$

Next consider a 2D kd-tree representing a subdivision of the interval $[0, 1] \times [0, 1]$. The following are examples of kd-address/interval correspondences:

$$\begin{array}{lcl} 00, 00 & \rightarrow & [0, 0.25] \times [0, 0.25] \\ 01, 10 & \rightarrow & [0.25, 0.5] \times [0.5, 0.75] \\ 0010, 1100 & \rightarrow & [0.125, 0.0.1875] \times [0.75, 0.8125] \end{array}$$

Here, the comma separates the bit address of the first dimension from the second.

The two primary algorithms differ only slightly. `insert_addonly` adds a node to a given kd-tree such that no node in the kd-tree is subdivided. `insert_nosubdivide` adds a node to a given kd-tree such that no node in the kd-tree is subdivided, and any nodes in the kd-tree that represent subdivisions of the node to be inserted are eliminated. Both algorithms take two parameters: a kd-tree, T, and the address of a kd node to insert, A. Figure 5.23 presents sketches of the two algorithms.

The insert primitives can be used to define two analogous merge algorithms: `merge_addonly` and `merge_nosubdivide`. `merge_addonly` takes two kd-trees as parameters, T_1 and T_2. Figure 5.24 illustrates the difference between these two algorithms. The algorithm for `merge_addonly` is given by

```
merge_addonly($T_1$,$T_2$)

for each leaf node $X$ of $T_2$
        find kd-address of $X$
        insert_addonly($T_1$,$X$)
endfor
```

The `merge_nosubdivide` algorithm is similar, except that it uses `insert_nosubdivide` in place of `insert_addonly`.

The `merge_addonly` algorithm is used to perform the merge operation between the projected intersection kd-tree and the surface sampling kd-tree. It is appropriate because it ensures that no node in the projected intersection kd-tree is subdivided. The `merge_nosubdivide` algorithm is used in a higher-level algorithm to project the 4D intersection kd-tree, using the algorithm `project` in Figure 5.25.

`project` takes as input a kd-tree (parameter N) and a set of indices representing the kd dimensions to project (parameter W), and returns a kd-tree whose leaf nodes are the appropriate projections of the leaf nodes of N. For example, to project the kd-tree, N, bounding the curve of intersection of surfaces $S(u, v)$ and $T(s, t)$ to (u, v) space, and assuming that the kd dimensions are mapped so that u is 1, v is 2, s is 3, and t is 4, the invocation `project`$(N, \{1, 2\})$ should be made.

```
insert_addonly($T$,$A$)

let $X$ be the node represented by address $A$

find furthest node $Y$ in $T$ that is ancestor to $X$
        by finding node whose address matches an initial
        substring of $A$ in each kd dimension

let $A'$ be the address of $X$ left over after deleting
        the initial matching

if $Y$ lacks the child that is ancestor to $X$
        lead_add($Y$,$A'$)
else if $Y$ is a leaf node
        leaf_add($Y$,$A'$)
else
        create left or right child of $Y$ if it doesn't exist
        insert_addonly($Y$.left,$A'$)
        insert_addonly($Y$.right,$A'$)
endif
```

```
insert_nosubdivide($T$,$A$)

let $X$ be the node represented by address $A$

find furthest node $Y$ in $T$ that is ancestor to $X$
        by finding node whose address matches an initial
        substring of $A$ in each kd dimension

let $A'$ be the address of $X$ left over after deleting
        the initial matching

if $Y$ lacks the child that is ancestor to $X$
        leaf_add($Y$,$A'$)
else if $Y$ is not a leaf node
        delete all of $Y$'s children
endif
```

Figure 5.23: Basic kd-tree algorithms – The function `insert_addonly` adds a node, representing by its address A, to a kd-tree T such that T is only affected by the addition of new kd-nodes; none of T's nodes are subdivided. The function `insert_nosubdivide` is similar, except that T's nodes are not subdivided and any of T's nodes that represent subdivisions of the node represented by kd-address A are eliminated (i.e., a subtree of T whose root is the furthest-from-root ancestor of A is replaced by a single terminal node). Insertion of a node into a leaf node of the kd-tree is accomplished using `leaf_add`.

merge_addonly

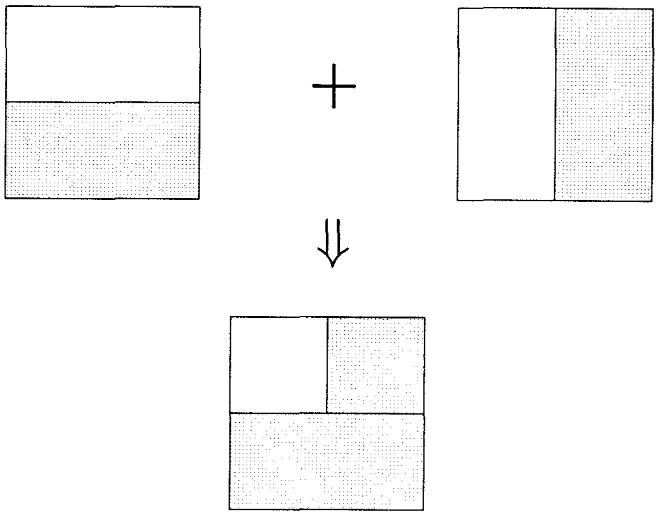

merge_nosubdivide

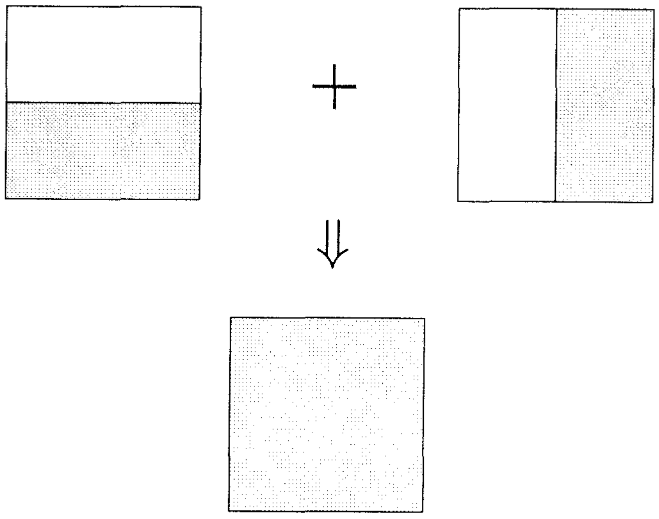

Figure 5.24: Kd-tree merging operations – The output of `merge_addonly` and `merge_nosubdivide` is compared for the case of the merging of a pair of 2D kd-trees, one containing the interval $[0,1] \times [0,0.5]$, and the other containing the interval $[0.5,1.0] \times [0,1]$. `merge_addonly` produces a kd-tree with two leaf nodes, so that the leaf node of the first kd-tree is not subdivided. `merge_nosubdivide` produces a kd-tree with a single leaf node, which is the ancestor to the leaf nodes of both input kd-trees. This is done because neither leaf node can be subdivided.

```
project($N$,$W$)

if $N$ is NIL return NIL
else if $N$ is leaf return (NIL,NIL,0)
else
    $L \leftarrow$ project($N$.left,$W$)
    $R \leftarrow$ project($N$.right,$W$)
    if $N$.d is in $W$
        return ($L$,$R$,$N$.d)
    else if $L \neq$ NIL and $R =$ NIL
        return $L$
    else if $L =$ NIL and $R \neq$ NIL
        return $R$
    else
        merge_nosubdivide($L$,$R$)
        delete $R$
        return $L$
    endif
endif
```

Figure 5.25: Kd-tree projection algorithm – The projection function, `project`, uses `merge_nosubdivide` to combine the kd-trees formed by projecting the left and right subtrees. This ensures that no extra subdivisions will occur that were not already present in the unprojected, 4D kd-tree.

5.2.5 Constructive Solid Geometry with Trimmed Surfaces

CSG-like operations can be used to implement full CSG on solid regions bounded by parametric surfaces. Full CSG operations differ from CSG-like operations in that the results of full CSG operations can be used in further CSG operations. That is, full CSG operates on parametric surfaces that may have been trimmed in previous operations. For example, consider the CSG operation $(A^\diamond - B^\diamond) - C^\diamond$, for three regions $A^\diamond$, $B^\diamond$, and $C^\diamond$, bounded by three parametric surfaces, A, B, and C. The CSG-like approximation algorithm described previously can compute an approximation of the boundary of $A^\diamond - B^\diamond$, yielding two trimmed surfaces (i.e., trimmed versions of the surfaces A and B). Algorithm 5.4 can not be applied to these trimmed surfaces to subtract C. A simple modification of the algorithm, however, suffices. Figure 5.26 shows how the CSG operation $(A^\diamond - B^\diamond) - C^\diamond$ can be computed, by computing Boolean operations on 2D parametric regions. Such 2D Boolean operations were called CPG operations in Section 3.1.3.

For each parametric surface in the Boolean expression, the modified algorithm stores the appropriate trimming curves, which are consistently ordered so that the interior of the trimming region lies to the left of the trimming curve. The trimming curves are bounded in a 2D kd-tree in the surface's parameter space. Let S^1 be a trimmed parametric surface resulting from a series of CSG operations, and let S be the corresponding untrimmed parametric surface. Let $T^\diamond$ be a closed region in $\mathbf{R}^3$ bounded by an untrimmed parametric surface T. A completely general CSG algorithm results from a description of how a CSG operation is performed on S^1 and T (e.g., $S^1 - T^\diamond$). A CSG operation like $(A^\diamond - B^\diamond) - C^\diamond$ can then be performed by a series of these operations. That is, the surface A is first trimmed by subtracting $B^\diamond$. The resulting trimmed version of A is then further trimmed by subtracting $C^\diamond$. Similar sequences of operations are performed on B and C, to yield the complete boundary of the nested subtraction.

The following algorithm outlines how to perform such a CSG operation on a trimmed surface, S^1, and untrimmed surface T, resulting in a trimmed surface S'. Although this algorithm has not actually been implemented in the GENMOD prototype system, all of the tools it uses have already been implemented and presented in this thesis.

1. Apply Algorithm 5.4 (Steps 1-4) to the untrimmed surfaces S and T, resulting in a trimmed surface S^2.

2. Compute the intersection points between the 2D trimming curves from S^1 and S^2. Note that the constraint solution algorithm can be used to robustly compute these points. The computed intersection points should be added to the trimming curves of S, and to all other parametric surfaces that share the intersection curve to which the points have been added.

3. Perform a CPG operation on the trimmed parameter spaces of S^1 and S^2, resulting in a new trimming region for S'. This operation discards parts of the trimming curves (and their bounding kd-trees) that are excluded by the Boolean operation. The kd-tree surrounding the trimming curves of S' must be constructed so that no nodes from either original kd-tree are subdivided. This is easily accomplished by choosing the closest containing ancestor node, rather than splitting.

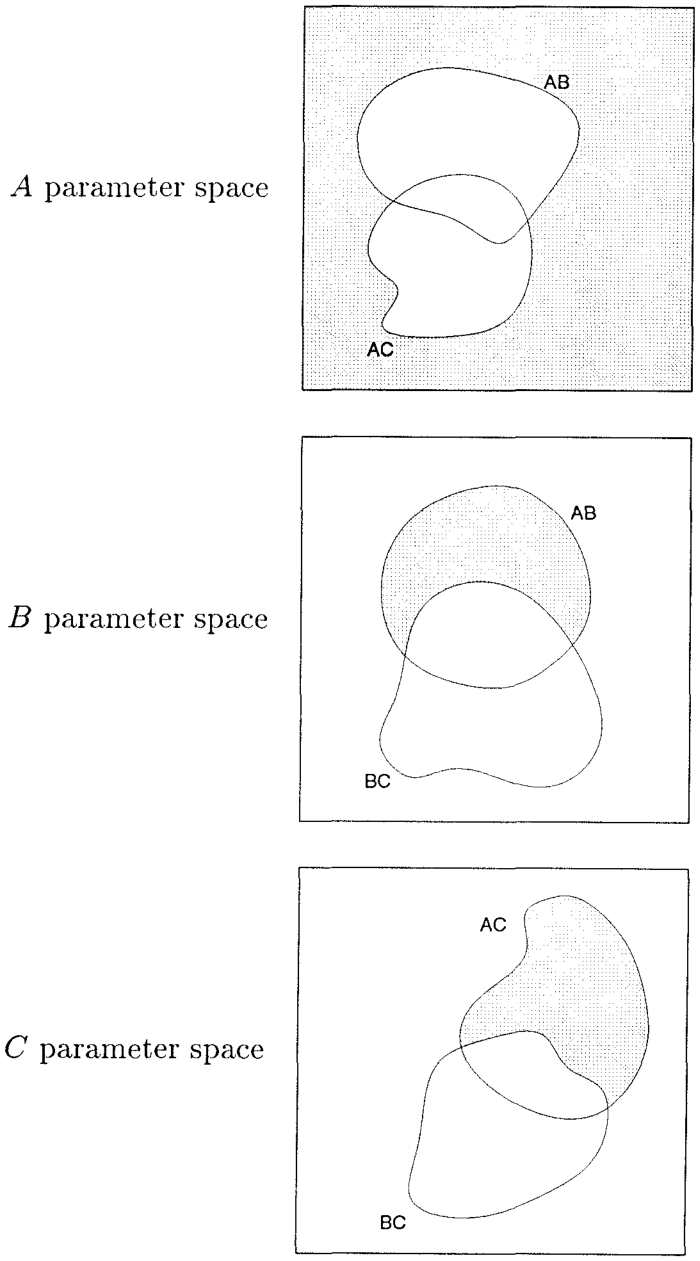

Figure 5.26: CSG operation on parametric surfaces – The boundary of the region $(A^\diamond - B^\diamond) - C^\diamond$ can be represented using trimmed parametric surfaces. The boundary surface is given by a combination of trimmed versions of the parametric surfaces, A, B, and C, bounding $A^\diamond$, $B^\diamond$, and $C^\diamond$, respectively. The intersection curves projected into the parameter space of each of the three surfaces are displayed. These intersection curves form a superset of the boundaries of the appropriate trimming regions, which are displayed in a darker shade. For example, the trimmed version of A must exclude the parts of A in either $B^\diamond$ or $C^\diamond$. This can be done by finding the parametric regions of A corresponding to $A - B^\diamond$ and $A - C^\diamond$ and computing their 2D intersection.

After a trimmed surface, such as S^1, has been processed with respect to all parametric surfaces in the CSG operation, Steps 5-7 of Algorithm 5.4 are computed. A surface sampling kd-tree is generated for S and merged with the final trimmed version of S^1. Triangles are then generated just as in Algorithm 5.4.

This approach processes all pairs of parametric surfaces. That is, to compute the approximation of a CSG operation involving n parametric surfaces, $\binom{n}{2}$ invocations of Algorithm 5.4 must take place, along with $(n-1)(n-2)$ CPG operations on trimmed regions. Typically, many of these operations can be eliminated by hierarchically organizing the collection of parametric surfaces, so that nonintersecting surface pairs are immediately recognized.

5.2.6 Approximating Implicit Surfaces

As a final application of interval analysis techniques to geometric modeling, we examine an algorithm to approximate implicit surfaces. For example, given a continuous function $f(x, y, z) : \mathbf{R}^3 \to \mathbf{R}$, the equation

$$f(x, y, z) = 0$$

describes an implicit surface. Similarly, any system of $n-2$ equations in n variables can be used to describe an implicit surface. The algorithm described in this section differs from others (such as [BLOO88]) in that the approximation is robust. That is, global information about the implicit surface's behavior is used to guarantee that no part of the surface is missed.

An algorithm very similar to Algorithm 5.3 for implicit curve approximation can be applied to implicit surface approximation. This algorithm restricts the kinds of surfaces it can approximate in a manner analogous to the restrictions of Algorithm 5.3. It requires that the surface not self-intersect, that it not stop abruptly in the interior of the interval of consideration[18], and that it intersect the edges of each proximate interval in a finite set of points.

In broad outline, this algorithm performs the same basic tasks as does Algorithm 5.3,

[18]More precisely, the implicit surface must be a 2D manifold in the interior of the region of consideration.

namely

1. compute proximate intervals bounding the implicit surface
2. test each proximate interval for global parameterizability
3. find edge points
4. connect edge points along faces
5. process completed network

In order to explain these tasks, several definitions are appropriate. The *face* of a proximate interval is the interval formed by holding one of the input variables at one endpoint, and letting the rest vary over their original intervals. Similarly, a *edge* of a proximate interval is the interval formed by holding two of the input variables at one endpoint, and letting the rest vary over their original intervals. A proximate interval in $\mathbf{R}^n$ thus has $2n$ faces and $4\begin{pmatrix} n \\ 2 \end{pmatrix}$ edges. A *proper face of a proximate interval* is a face that borders at most one neighbor, and that is a subset of the bordering neighbor's face. A neighbor refers to another, adjacent proximate interval in the bounding collection. A *face curve* is the intersection of the implicit surface with a proximate interval's face. An *edge point* is the intersection of the implicit surface with a proximate interval's edge.

Task 1 computes a collection of intervals bounding the implicit surface, and satisfying a user defined approximation acceptance inclusion function. This processing is exactly the same for curve or surface approximation. Task 2 tests each of the proximate intervals for global parameterizability. For surface approximation, and unlike curve approximation, two global parameterizability criteria must be satisfied:

1. the surface must be globally parameterizable in the proximate interval as a 2-manifold (see Section 5.2.2.2 for a definition of global parameterizability for 2-manifolds). This prevents cases where a closed surface exists entirely within a proximate interval.
2. each of the face curves must be globally parameterizable (as 1-manifolds). This allows robust connection of edge points.

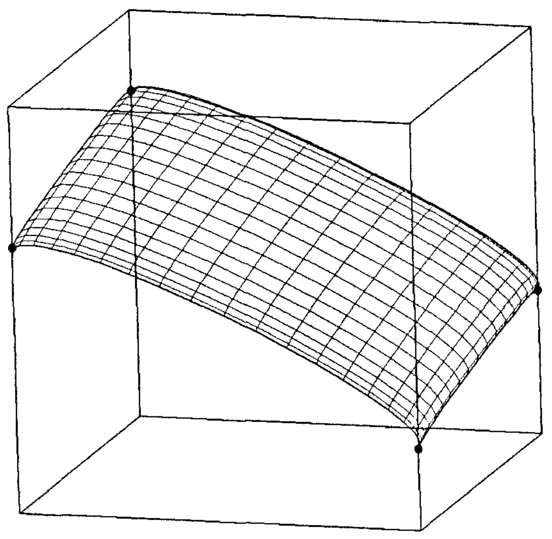

Figure 5.27: Behavior of an implicit surface in a proximate interval – The figure illustrates an implicit surface inside a proximate interval. The surface intersects the edges of the interval at four edge points, drawn with circles. The surface also intersects the faces of the proximate interval in four face curves. Each of the edge points is shared by two face curves. If neighboring proximate intervals are included, then edge points can be shared by up to four face curves.

Task 3 computes intersections of the implicit surface with each edge of each proximate interval. This yields solutions that should be zero-dimensional and can be computed using the constraint solution algorithm.[19] Tasks 4 and 5 are performed exactly as in Algorithm 5.3, except that the processing must take place for each face of the proximate interval. That is, each face curve is approximated independently.

The local topology graph for surface approximation differs from curve approximation. For surface approximation, each edge point has a pointer to four neighboring intersections, rather than two. This is because each proximate interval edge is shared by four faces. As shown in Figure 5.27, an edge point is typically included in four face curves, and thus may connect to four neighboring edge points.

[19]Curve approximation intersects the implicit curve with each face of a proximate interval; surface approximation intersects the implicit surface with each edge. The respective approximation algorithms assume that this intersection will result in a finite set of points.

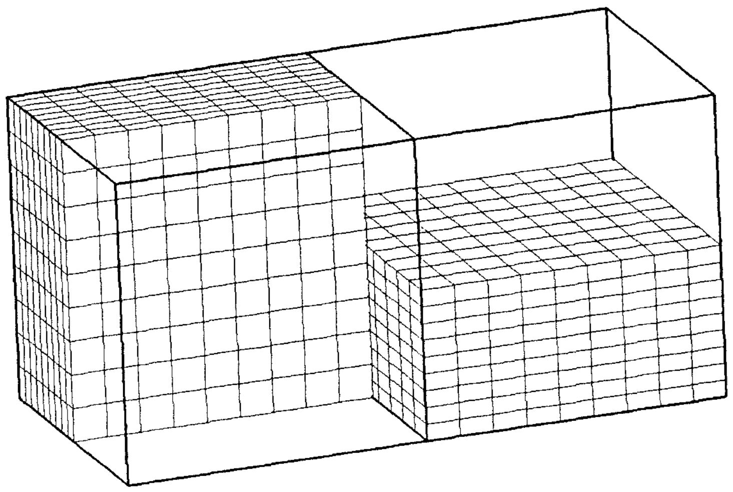

Figure 5.28: Disallowed bordering of proximate intervals – The figure illustrates the the case where a proximate interval contains a face that is not allowed. Two neighboring intervals are shown, one on the left (at the back of an enclosing cube), and one on the right (at the bottom of an enclosing cube). The face to the left of the right interval is not proper, nor is it a superset of the face of its neighbor, the left interval.

5.2.6.1 An Implicit Surface Approximation Algorithm

The five tasks can be simply combined to produce an algorithm for implicit surface approximation.

Algorithm 5.5 (Implicit Surface Approximation Algorithm)

1. **Compute an initial collection of proximate intervals bounding the implicit surface.** An approximation acceptance inclusion function is used to determine whether a region is acceptable or should be subdivided.

2. **Subdivide the initial collection until it satisfies the two global parameterizability criteria.** As discussed previously, the implicit surface and each of its face curves should be globally parameterizable.

3. **Compute the edge points in each proximate interval using Algorithm 5.1.**

4. **For each proper face, compute the connection of edge points.** Because each face curve is globally parameterizable, this can be done with the techniques already

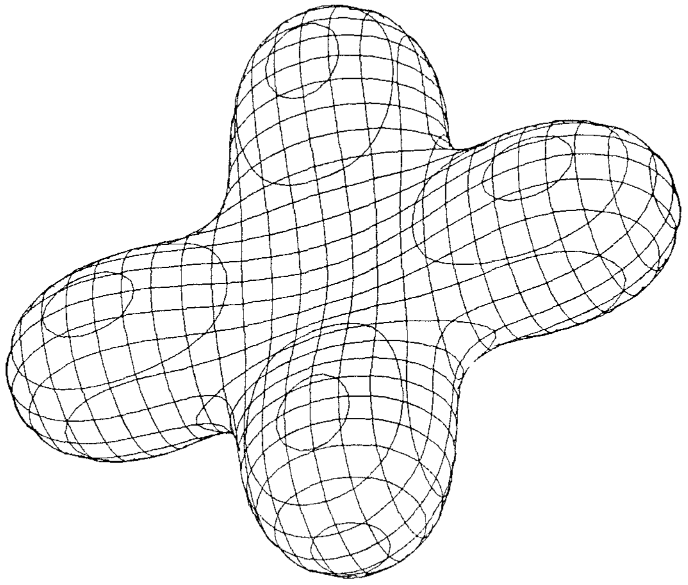

Figure 5.29: Approximation of a blobby implicit surface – The results of the implicit surface approximation algorithm are shown for a blobby surface, described by the implicit equation

$$f(p) = \sum_i \alpha_i \exp^{-\beta_i \|p-q_i\|} = 0$$

In this case, a sum of four such terms was used.

discussed for Algorithm 5.3. After all proper faces have been processed, faces that are not proper are handled by simply aggregating the results for all neighboring proper faces. The algorithm assumes *that each proximate interval face is proper, or is a superset of the set of contiguous faces of all its neighbors.* Situations such as shown in Figure 5.28 are therefore excluded. In practice, eliminating such situations is a simple matter.

5. **Perform computations on the finished surface network.** For example, a polygonal mesh approximating an implicit surface can be generated. In each proximate interval, the face curves are traversed to form a closed curve around the proximate interval's boundary. A set of triangles can then be generated whose vertices are the edge points, and whose edges are the the approximated face curves.

Figure 5.29 illustrates the results of Algorithm 5.5 to generate a polygonal approximation to an implicitly defined "blobby" surface [BLIN82].

Chapter 6

Conclusion

An approach to shape design may be broken down into three parts: representation, interface, and tools. The representation defines what a shape is. The interface allows shapes to be specified. The tools determine what can be done with shapes. This research has focused on a new representation, interface, and set of tools, called generative modeling, that solve some of the problems of geometric modeling systems studied in the past.

Generative modeling represents a shape as the image of a parametric function over a rectilinear subset of $\mathbf{R}^n$. Parametric functions are built using a set of recursive operators, such as the arithmetic operators. Associated with each operator is a set of methods, which perform all the primitive shape computations needed by the tools. All the tools described in this thesis require only the following methods:

- evaluate the parametric function at a point
- evaluate the parametric function on a uniform rectilinear lattice
- evaluate an inclusion function for the parametric function
- take a symbolic partial derivative of the parametric function
- determine whether the parametric function is differentiable over a specified domain

What is the advantage of such a representation? First, the representation is sufficient for shapes of different dimensionality. It can represent both curves and surfaces, shapes parameterized by time or other variables, and shapes embedded in space of any number of dimensions. Second, the representation is high-level. Shapes can be defined using sophisticated operators such as integration, differentiation, and constraint solution. Unlike simple representations such as polyhedra and NURBS, the representation can be matched to a high-level interface without conversions and approximation error. Third, the representation is extensible. Extension is accomplished by adding new primitive operators, with a few attendant methods.

The interface advocated in this thesis is an interpreted language. This language is essentially a textual specification of the operators used in the representation. With a language interface, a modeler can construct meta-shapes – parameterized shapes such as the profile product of Chapter 3. In our research, meta-shapes have proved to be an extremely powerful specification tool. The user can build libraries of meta-shapes, using combinations of the primitive operators. These meta-shapes, in turn, can be used in building higher-level and more convenient meta-shapes. Augmented with such meta-shape libraries, the interface provided the user can be quite complex and powerful, while the basic implementation of the modeling system (i.e., the primitive operators and methods) remains simple.

Certainly, such an interface is not suitable for all users. It requires a fairly sophisticated mathematical background, and a substantial training investment. On the other hand, the specification is well suited for two groups: customizers and researchers. Customizers produce sets of meta-shapes appropriate for their targeted users. For example, a customizer may represent a limited family of parts, so that engineers can edit, assemble, and simulate them. The customizer hides unimportant details and provides an interface with parameters familiar to his users. Researchers can use the power of an interpreted language to test new ideas easily.

The set of tools discussed in this thesis fall into three categories: rendering tools, synthesis tools, and analysis tools. Rendering tools produce images of shapes; synthesis tools allow simple shapes to be combined into more complex, and analysis tools allow computation of physical and geometric properties of shapes.

Most rendering methods appropriate for generative models involve approximating the shape as a collection of simple pieces. This thesis has presented two techniques to do this; one suitable for "quick and dirty" interactive rendering and another allowing robust control of approximation error. Approximated shapes can easily be converted into a form suitable for interactive rendering using z-buffer hardware, or expensive, realistic rendering using ray tracing. Because shapes are represented as the image of parametric functions, approximation can often be accomplished with very little computation.

Tools for rendering, synthesis, and analysis presented in this thesis have been built using the technique of interval analysis. Interval analysis allows computation of global properties of the shape, using inclusion functions. This thesis presents algorithms for solution of two very hard problems: finding solutions to nonlinear constraints, and finding global minima of a nonlinear function subject to nonlinear constraints. By restricting the class of functions that can express constraints and objective functions to those that are formed by recursive composition of primitive operators, these problems are solvable. The two algorithms are useful in themselves, and for a host of other, more advanced geometric computations, such as approximating curves of intersection between shapes. Interval analysis enables the algorithms to control error robustly even when the computation is done using imprecise floating point hardware.

Appendix A

The GENMOD Language for Specifying Parametric Functions

Parametric functions form the backbone of the generative modeling representation. This appendix discusses a language for representing parametric functions that was developed for a prototype modeling system called GENMOD. This language is patterned after the mathematical language of vector calculus and differential geometry.

The GENMOD language was written using a C language substrate. To achieve a more natural syntax, the C language used was extended to allow overloading of the C operators. Several additional operators have also been added. GENMOD contains an interpreter for this extended C language that allows models to be built, edited, analyzed, and displayed interactively. The GENMOD system is extensible. Language primitives can be combined using C functions to produce higher level meta-shapes. Libraries of such meta-shapes can be constructed and extended by the user.

A.1 Language Extensions

This section describes some new features that were added to the C language in developing the GENMOD system.

A.1.1 New Operators

The C language was extended with the addition of several new operators. These operators all begin with the `@` character.

An exponentiation operator `@^` was added that has precedence greater than multiplication and division, but less than a cast. This allows the exponentiation operator to be used in the same way as in the FORTRAN language. Note that overloading another operator, such as `^`, would have allowed exponentiation but with an operator of inappropriate precedence.

Three array creation operators, `@{}`, `@[]`, and `@()`, were also added. These operators take a list of arguments separated by commas, perform appropriate type casting, and create an array of the converted arguments. For example, the C expression `@{1,2,3}` creates an object of type array of size 3 of `int`. If the operator arguments are of mixed type, then each argument is converted to the most "general" type. For example, a mixture of `int` and `double` types will be converted to `double`. Similarly, a mixture of `double` and `MAN` types is converted to type `MAN` (see Section A.2 for a definition of the `MAN` type).

The type of the array element may also be directly specified by placing a type cast after the `@`. For example, `@(double){1,2,3}`, will produce an object of type array of size 3 of type `double`, with elements 1.0, 2.0, and 3.0, respectively.

A.1.2 Overloaded Operators

The following C language operators were overloaded:

- the binary arithmetic operators `+`, `-`, `*`, and `/`
- the unary negation operator `-`
- the comparison operators `>`, `>=`, `<`, `<=`, `==`, and `!=`
- the logical operators `!`, `&&`, `||`
- the index operator `[]`
- the cast operator for type `MAN`
- the new exponentiation operator `@^`
- the new array creation operators `@()`, and `@[]`

The meaning of these overloaded operators will be precisely defined in Section A.3.

A.2 Language Types

Type	Description
MAN	parametric function
MAN_ARRAY	array of parametric functions
MAN_MATRIX	parametric function representing a matrix
INT_ARRAY	array of integers

The GENMOD language uses the standard types defined in the C language. In addition, it defines several new types, shown in the table above. The type MAN is the basic type of a parametric function. Many of the C language operators have been overloaded for the MAN type. For example, the C language's + operator has been overloaded to perform addition of parametric functions.

The MAN type is actually a C structure that keeps track of several characteristics of the parametric function:

- input and output dimension of the function
- specific parametric coordinates used in the function
- methods used by the function for evaluation and analysis

The C language definition of the MAN type is

```
typedef struct mantyp {

  int           outputs;                /* output dimension */
  int           inputs;                 /* input dimension */
  int           input_set[MAXINPUTS];   /* set of coords */
  int           input_list[MAXINPUTS];  /* list of coords */
  void          *prms;                  /* internal parms  */
  void          (*free)();              /* clean up method */
  struct mantyp *(*derivative)();       /* derivative method */
  int           (*point)();             /* evaluation method */
  int           (*inclusion)();         /* inclusion method */

    /* ... */
} *MAN;
```

The C cast operator, (MAN), has been overloaded to convert numeric arguments to type MAN. This conversion results in a constant parametric function.

The MAN_ARRAY type is an array of type MAN, that also keeps track of the size of the array. Its C language definition is:

```
typedef struct {
    MAN *ptr
    int n;
} MAN_ARRAY;
```

The @[] operator has been overloaded to produce the MAN_ARRAY type. For example, if f, g, and h are of type MAN, the C expression @[f,g,h] produces an object of type MAN_ARRAY. The ptr field points to an array containing f, g, and h in succession. The n field has the value 3.

The MAN_MATRIX type contains a parametric function that represents the components of the matrix (of type MAN), but also keeps track of the number of rows and columns in the matrix. Its C language definition is:

```
typedef struct {
    MAN m;
    int r,c;
} MAN_MATRIX;
```

It can be used anywhere the type MAN is used as well as in several special circumstances, such as arguments for the matrix multiply operator.

A.3 Language Primitive Operators

The GENMOD language specifies parametric functions through a set of primitive operators that take lower-level parametric functions (and possibly other parameters) as arguments and create a higher-level parametric function. For example, if two parametric functions f and g exist, then the sum of f and g can be represented using the addition operator on the arguments f and g.

A.3.1 Constants and Parametric Coordinates

Function	Operator	GENMOD example	Explanation
parametric coordinate	`MAN m_x(int)`	`MAN F = m_x(i);`	$F = x_i$
constant	`double`	`MAN F = 3.3;`	$F = 3.3$

Two of the primitive operators in the GENMOD language do not take lower-level MAN arguments. These are the operators that specify a constant or parametric coordinate, shown in the the table above. Parametric coordinates are numbered starting at 0, and are referred to using the variables $x_0, x_1, \ldots$ in the following text.

A.3.2 Arithmetic Operators

Function	Operator	GENMOD example	Explanation
addition	`+`	`MAN F = f + g;`	$F = f + g$
subtraction	`-`	`MAN F = f + g;`	$F = f - g$
multiplication	`*`	`MAN F = f * g;`	$F = f * g$
division	`/`	`MAN F = f / g;`	$F = f/g$
exponentiation	`@^`	`MAN F = f @^ g;`	$F = f^g$
negation	`-`	`MAN F = -f;`	$F = -f$

Arithmetic operators in the GENMOD language include the binary addition, subtraction, multiplication, and division operators, and the unary negation operator. The exponentiation operator, while more fittingly included in the elementary operators of the next section (not the arithmetic operators), is included here because of its similarity with the other binary operators. The binary operators, including exponentiation, can be used in two modes.

In the first mode, if the two parametric function arguments have the same output dimension, then the operator is performed separately for each component on the corresponding components of the two arguments. The result has the same output dimension. For example, if the parametric functions f and g both have output dimension 2, then $f * g$ denotes a parametric function of output dimension 2 whose first coordinate is the product of the first components of f and g, and whose second component is the product of the second components of f and g. Note that the addition operator thus denotes ordinary addition in $\mathbf{R}^n$.

In the second mode, if the output dimension of one argument is 1, and the output dimension of the other argument is greater than 1, then the operator is performed on each component of the multicomponent argument. The result has the output dimension of the multicomponent argument. For example, if f has output dimension 2, $1/f$ takes the reciprocal of each component of f. Similarly, $f * 2$ scales each component of f by 2.

The unary negation operator negates each component of its argument.

A.3.3 Elementary Operators

Function	Operator	GENMOD example	Explanation
sine	`MAN m_sin(MAN)`	`MAN F = m_sin(f);`	$F = \sin f$
cosine	`MAN m_cos(MAN)`	`MAN F = m_cos(f);`	$F = \cos f$
tangent	`MAN m_tan(MAN)`	`MAN F = m_tan(f);`	$F = \tan f$
inverse sine	`MAN m_asin(MAN)`	`MAN F = m_asin(f);`	$F = \sin^{-1} f$
inverse cosine	`MAN m_acos(MAN)`	`MAN F = m_acos(f);`	$F = \cos^{-1} f$
inverse tangent	`MAN m_atan(MAN)`	`MAN F = m_atan(f);`	$F = \tan^{-1} f$
inverse tangent	`MAN m_atan2(MAN,MAN)`	`MAN F = m_atan2(f,g);`	$F = \tan^{-1}(f/g)$
exponential	`MAN m_exp(MAN)`	`MAN F = m_exp(f);`	$F = \exp(f)$
logarithm	`MAN m_log(MAN)`	`MAN F = m_log(f);`	$F = \log(f)$
absolute value	`MAN m_fabs(MAN)`	`MAN F = m_fabs(f);`	$F = \|f\|$
integer floor	`MAN m_floor(MAN)`	`MAN F = m_floor(f);`	$F = \lfloor f \rfloor$
integer ceiling	`MAN m_ceil(MAN)`	`MAN F = m_ceil(f);`	$F = \lceil f \rceil$

The elementary operators work on scalar arguments; that is, the output dimension of the argument or arguments must be 1. The output dimension of the result is also 1.

A.3.4 Vector Operators

Function	Operator	GENMOD example	Explanation
cartesian product	`@()`	`MAN F = @(f,g,h);`	$F(X) = (f, g, h)$
projection	`[]`	`MAN F = f[i];`	$F(X) = f_i$
length	`MAN m_length(MAN)`	`MAN F = m_length(f);`	$F(X) = \|\|f\|\|$
dot product	`MAN m_dot(MAN,MAN)`	`MAN F = m_dot(f,g);`	$F(X) = f \cdot g$
cross product	`MAN m_cross(MAN,MAN)`	`MAN F = m_cross(f,g);`	$F(X) = f \times g$
normalize	`MAN m_normalize(MAN)`	`MAN F = m_normalize(f);`	$F(X) = f/\|\|f\|\|$

The cartesian product operator has two forms. In the first, a list of MAN objects, separated by commas, is combined using cartesian product. There is also a second form, where the MAN objects are specified using an array. Its functional prototype is

```
MAN m_cartesian(MAN_ARRAY funs)
```

The second form is mainly used to specify a cartesian product of an array built programmatically.

The projection operator takes a parametric function argument of arbitrary output dimension and produces a given component of this function. The result is of output dimension 1. The dot product operator works on arguments that have the same output dimension. The cross product operator can only be used on arguments whose output dimension is 3.

A.3.5 Matrix Operators

Matrices can be created using the m_matrix function, which takes a parametric function as its first argument, and number of rows and columns of the matrix as its second and third arguments. Its functional prototype is given by

```
MAN_MATRIX m_matrix(MAN components,int r,int c)
```

The product of rows and columns must equal the output dimension of the first argument. Transpose, inverse, and determinant operators exist, with the following functional prototypes

```
MAN_MATRIX m_transpose(MAN_MATRIX m)
MAN_MATRIX m_inverse(MAN_MATRIX m)
MAN        m_determinant(MAN_MATRIX m)
```

The inverse and determinant functions both expect a square matrix argument.

For example, assuming m is a parametric function of output dimension 9, a 3 by 3 matrix, and its transpose, inverse and determinant can be created using

```
MAN M = m_matrix(m,3,3);
MAN Mt = m_transpose(M);
MAN Minv = m_inverse(M);
MAN det = m_determinant(M);
```

Arithmetic operations on matrices are also available, shown in the next table.

Function	Operator	GENMOD example	Explanation
addition	+	`MAN_MATRIX F = A + B;`	$F = A + B$
subtraction	-	`MAN_MATRIX F = A - B;`	$F = A - B$
negation	-	`MAN_MATRIX F = -M;`	$F = -M$
multiplication	*	`MAN_MATRIX F = A*B;`	$F = AB$
row projection	[]	`MAN F = M[1];`	F is second row of M

The addition and subtraction operators both check that the matrices added or subtracted have the same size. Similarly, the multiplication operator requires its operands to be of suitable size for multiplication (i.e., number of columns of first operand equals number of rows of second). The row projection operator produces a result of type `MAN` representing the specified row of the matrix. The output dimension of the result is the number of columns in the matrix.

A.3.6 Integral and Derivative Operators

The derivative operator takes partial derivatives of its first argument with respect to any parametric coordinate whose index is specified as the second coordinate. Its functional prototype is

```
MAN m_derivative(MAN in,int parameter)
```

For example, the function

```
m_derivative(f,i)
```

returns the parametric function $\frac{\partial f}{\partial x_i}$.

The integral operator integrates functions numerically using Romberg integration (see Numerical Recipes [PRES86]). The function being integrated, as well as the upper and lower bounds of integration, are specified as arguments and may depend on any number of parameters. Its functional prototype is

```
MAN m_integrate(MAN integrand,MAN lower,MAN upper,int parameter)
```

For example, the function

```
m_integrate(f,b,a,i)
```

returns the parametric function $\int_b^a f dx_i$.

A.3.7 Curves and Tables

The curve operator has the functional prototype

```
MAN m_crv(char *curve_file,MAN in)
```

The `m_crv` function takes the name of a file, produced using a curve editor program, and creates a parametric curve that is evaluated over the parametric function `in`. For example, the function

```
m_crv("cross.crv",m_x(0))
```

produces a parametric curve parameterized by x_0, whose shape is specified in the file `cross.crv`.

The table operator produces a function that linearly interpolates a multidimensional data set. Its functional prototype is

```
MAN m_table(double *samples,INT_ARRAY dimen,MAN in)
```

The `samples` argument contains the samples to be interpolated. The `dimen` argument is an array of dimensions, specifying the organization of the samples. Assume `dimen` contains $s+1$ entries $n_0, n_1, \ldots, n_s$. The samples are arranged as a multidimensional rectilinear table of points, each having n_0 coordinates. The table has s dimensions, of size n_1, n_2, ..., n_s, respectively. Samples are stored in a linear fashion, with the dimension whose size has the lowest index varying the most rapidly. The `in` parameter specifies a table input to be interpolated. It should be of output dimension s, with each coordinate varying between 0 and 1. The resulting parametric function is of output dimension n_0.

A.3.8 Relational Operators

Function	Operator	GENMOD example	Explanation
greater	`>`	`MAN F = f > g;`	$F = \begin{cases} 1 & \text{if } f > g \\ 0 & \text{otherwise} \end{cases}$
greater or equal	`>=`	`MAN F = f >= g;`	$F = \begin{cases} 1 & \text{if } f \geq g \\ 0 & \text{otherwise} \end{cases}$
less	`<`	`MAN F = f < g;`	$F = \begin{cases} 1 & \text{if } f < g \\ 0 & \text{otherwise} \end{cases}$
less or equal	`<=`	`MAN F = f <= g;`	$F = \begin{cases} 1 & \text{if } f \leq g \\ 0 & \text{otherwise} \end{cases}$
equal	`==`	`MAN F = f == g;`	$F = \begin{cases} 1 & \text{if } f = g \\ 0 & \text{otherwise} \end{cases}$
not equal	`!=`	`MAN F = f != g;`	$F = \begin{cases} 1 & \text{if } f \neq g \\ 0 & \text{otherwise} \end{cases}$

Relational operators are used in to define conditions for branching and constraint solution. They are analogous to the C language relational operators. Each of the two parametric function arguments must be of the same output dimension. The result is the logical conjunction of the relational operator applied to each coordinate of the two arguments. For example, if g and h are parametric functions of output dimension 2, then

```
g == h
```

is a parametric function that is 1 if the corresponding components of g and h are equal (i.e., if $g_1 = h_1$ and $g_2 = h_2$), and 0 otherwise.

A.3.9 Logical Operators

Function	Operator	GENMOD example	Explanation
and	`&&`	`MAN F = f && g;`	$F = \begin{cases} 1 & \text{if } f \neq 0 \text{ and } g \neq 0 \\ 0 & \text{otherwise} \end{cases}$
or	`||`	`MAN F = f || g;`	$F = \begin{cases} 1 & \text{if } f \neq 0 \text{ or } g \neq 0 \\ 0 & \text{otherwise} \end{cases}$
not	`!`	`MAN F = !f;`	$F = \begin{cases} 1 & \text{if } f = 0 \\ 0 & \text{otherwise} \end{cases}$

The logical operators are analogous to the C language logical operators. Each of the parametric function inputs must be of output dimension 1.

A.3.10 Conditional and Branching Operators

Three operators can be used for branching type functionality. The C language `?:` ternary operator has been overloaded to do an if-then-else branch. For example, the parametric function

```
f < 0 ? -f : f
```

returns a function that is the absolute value of the function f.

A second type of branch returns a parametric function indexed by a number returned by another parametric function. Its functional prototype is

```
MAN m_index(MAN_ARRAY array.MAN index)
```

For example,

```
m_index(@[f0,f1,f2,f3],g);
```

returns the function f_i where i is computed by $i = \lfloor g \rfloor$. g should therefore be a parametric function of output dimension 1, with a value in the range $[0, 4)$.

A third type of branch takes an array of guard clauses and an array of an equal number of functions to evaluate. The result is the the value of the first function whose clause is true. Its functional prototype is

```
MAN m_case(MAN_ARRAY guards.MAN evals)
```

For example,

```
m_case(@[f < 0,1],@[-f,f])
```

returns a function that is the absolute value of the function f.

A.3.11 Evaluate Operator

GENMOD supports two operators that compose already defined parametric functions. That is, the operators evaluate a parametric function on the output of another parametric function. The first operator, `m_eval`, takes a parametric function and substitutes another parametric function for one of its input coordinates. Its functional prototype is given by

```
MAN m_eval(MAN fun,int parameter,MAN at)
```

For example, let $g(x_0, x_1)$ and $h(x_2)$ be two parametric functions. The evaluation operator

```
m_eval(g,1,h)
```

then yields the parametric function $g(x_0, h)$.

A second form, `m_eval_all`, substitutes an output coordinate of a parametric function for each input coordinate of another parametric function. Its functional prototype is given by

```
MAN m_eval_all(MAN fun,INT_ARRAY inputs,MAN at)
```

In this case, the array `inputs` specifies which input coordinate of `fun` is replaced by each output of the parametric function `at`. For example, let $g(x_0, x_1, x_2)$ be a parametric function and $h(x_3, x_4)$ be a parametric function of output dimension 3. The operator

```
m_eval_all(g,@[0,1,2],h)
```

then yields the parametric function $g(h_1, h_2, h_3)$ where h_i denotes the i-th output coordinate of h.

A.3.12 Inverse Operator

The inverse operator computes the parameter where a given function matches another function. Its functional prototype is

```
MAN m_inverse(MAN invert,MAN match,int parameter)
```

Both the `invert` and `match` functions must be of output dimension 1. In addition, `invert` must be a monotonic function of the parametric coordinate indexed by `parameter`. The result of the operator is the value of the coordinate indexed by `parameter` where the value of `invert` equals the value of `match`. For example, if $f(x_0)$ and $g(x_1)$ are two scalar parametric functions,

```
    m_inverse(f,g,0)
```

produces the value of x_0 where $f = g$. This result is therefore a function of x_1.

A.3.13 Constraint Solution and Global Minization Operators

The constraint solution operator has the following functional prototype:

```
    MAN m_solve(MAN constraint,MAN domain,INT_ARRAY parms,MAN acc)
```

The `constraint` argument is a parametric function representing the constraint to be solved, over a region specified by the `domain` argument. The `parms` argument specifies the indices of the parametric coordinates over which the constraint solution is to take place. The output dimension of `domain` should equal twice the number of elements in the `parms` array. Let the parametric function supplied as the `domain` argument by the parametric function D, of output dimension $2n$, and let the `parms` array contain the n indices $i_1, i_2, \ldots, i_n$. Then the constraint is computed over the domain where

$$\begin{aligned} x_{i_1} &\in [D_1, D_2] \\ x_{i_2} &\in [D_3, D_4] \\ &\vdots \\ x_{i_n} &\in [D_{2n-1}, D_{2n}] \end{aligned}$$

Finally, the `acc` argument represents the tolerance in parameter space[1] with which to compute the constraint solution (see Section 5.1.3). The resulting parametric function is of output dimension $2n$, and represents a solution point in the parameter space of the constraint problem.

For example, let $f(x_0)$ and $g(x_1, x_2)$ be two parametric functions of output dimension 2. The function

```
    h = m_solve(f == g,@(MAN)(0,1,-1,1),@[0,1],1e-6)
```

[1]The parameter space of the constraint problem consists of the variables $x_{i_1}, \ldots, x_{i_n}$ over which the constraint solution takes place.

then returns a parametric function of output dimension 2 that is a function of x_2. This function is mathematically described as

$$h(x_2) = \begin{pmatrix} h_1(x_2) \\ h_2(x_2) \end{pmatrix} \ni f(h_1) = g(h_2, x_2)$$

where $h_1 \in [0,1]$ and $h_2 \in [-1,1]$.

The global minimization operator is similar, but has an additional argument representing the objective function to be minimized. Its functional prototype is

```
MAN m_minimize(MAN obj,MAN constraint,MAN domain,
                    INT_ARRAY parms,MAN acc)
```

In the case of both `m_solve` and `m_minimize`, a parametric function representing a single solution to the problem is returned. Alternate forms also exist that return **all** solutions, up to some maximum number. The technique of solution aggregation (described in Section 5.1.3.2) is used to compute a set of disjoint intervals bounding solutions. The midpoint of the interval is then used as the returned solution. Sections 5.1.3 and 5.1.4 discuss how these operators can be evaluated and bounded.

The global minimization operator also has an alternate form that returns the minimum value of the objective function rather than a point in parameter space that minimizes it. Of course, one can always reconstruct the minimum value of the objective function by evaluating it at the returned global minimizer. However, if only the minimum function value is required, this alternate form produces a better bound on the minimum function value than would be obtained by deriving it from a bound on the set of global minimizers. This is apparent, for example, for the case in which the objective function has more than one distinct minimizer.

A.4 Language Extensibility: Building Higher-Level Operators

Given these primitive operators on parametric functions, the modeler can then construct higher-level operators by defining C functions. These C functions take parametric functions as input, and produce a new parametric function using nested composition of the primitive operators. This section presents three examples of how useful, higher-level operators can be constructed.

A.4.1 Interpolation Operator

The `m_interp` function defines a linear interpolation operator on parametric functions:

```
MAN m_interp(MAN t,MAN a,MAN b)
{
    return a + (b - a)*t;
}
```

This function takes three parametric functions as input: a and b are the functions to be interpolated, and t specifies the interpolation variable. For example, the code sequence

```
MAN p1 = @(MAN)(0,0);
MAN p2 = @(MAN)(1,1);
MAN seg = m_interp(m_x(0),p1,p2);
```

produces the parametric function `seg` that is a line segment in two dimensions parameterized by x_0 and continuing from the point $(0, 0)$ to the point $(1, 1)$. Note that the parametric functions a and b can be of any inpu or output dimension, as long as they have the same output dimension. This allows linear interpolation of curves, surfaces, or any other shape.

A.4.2 Concatenation Operator

The `m_concat` function defines uniform concatenation of an array of shapes in a parametric coordinate (see Section 2.2.2.2.6 for an explanation of uniform concatenation).

```
MAN m_concat(int parm, MAN in, MAN_ARRAY array)
{
    MAN a[MAXCONCAT];
    int n = array.n, i;
    MAN_ARRAY tmp;

    for (i = 0; i < n; i++) {
        a[i] = m_eval(array.ptr[i],parm,in*n - i);
    }

    tmp.ptr = a;
    tmp.n = n;

    return m_index(in*n,tmp);
}
```

For example, the function

```
MAN c1 = m_crv("crv1",m_x(0));
MAN c2 = m_crv("crv2",m_x(0));
MAN c3 = m_crv("crv3",m_x(0));
MAN c = m_concat(0,m_x(0),@[c1,c2,c3]);
```

returns a parametric function that concatenates the three curves `c1`, `c2`, and `c3`.

A.4.3 Reparameterization Operator

The **`m_reparameterize_by_arclength`** operator reparameterizes its argument by arclength. It assumes that its single argument is a curve, (i.e. that it has input dimension at least 1), and prints an error message otherwise. The parametric coordinate reparameterized is assumed to be the input coordinate of `curve` with the lowest index (stored in the local variable `parm`). This coordinate is assumed to vary from 0 (at the start of the curve) to 1 (at the end of the curve).

```
MAN m_reparameterize_by_arclength(MAN curve)
{
    if (curve->inputs < 1) {
        printf("m_resample_arclength: manifold is not a curve\n");
        return 0;
    }
    int parm = curve->input_list[0];
    MAN tanlen = m_length(m_derivative(curve,parm));
    MAN curvelen = m_integrate(tanlen,0,m_x(parm),parm);
    MAN curvelen_total = m_eval(curvelen,parm,1);
    MAN curvelen_linear = m_interp(m_x(parm),0,curvelen_total);
    MAN newinput = m_inverse(curvelen,curvelen_linear,parm);

    return m_eval(curve,parm,newinput);
}
```

Note that the **`m_interp`** operator, defined previously, has been used in this new definition. It is used to specify a linearly varying arclength from 0 to the total arclength of the curve. See Section 2.2.2.2.9 for a more complete discussion of reparameterization by arclength.

Appendix B

GENMOD Code Examples

This appendix gives the GENMOD code for the more complicated examples of Chapter 3: the sphere/cylinder fillet example of Section 3.1.2.1.2, the screwdriver tip examples of Section 3.1.3, and the bottle example of Section 3.1.4.

B.1 Sphere/Cylinder Fillet Example

The following GENMOD code defines a surface `fillet`, which is a smooth filletting surface between a cylinder and a sphere. The code is an example of the idea of hermite interpolation for filletting discussed in Section 3.1.2.1.2. Note that similar code to produce a fillet between arbitrary surfaces could be accompished using the global minimization operator, rather than implementing the analytic ray/sphere and ray/cylinder intersection formulae.

```
/* solves || u + v t ||^2 == r^2 */
static MAN m_solve_len(MAN u,MAN v,MAN r)
{
    MAN a = m_dot(v,v);
    MAN b = 2*m_dot(u,v);
    MAN c = m_dot(u,u) - r@^2;
    return (-b - m_sqrt(b@^2 - 4*a*c)) / (2*a);
}

/* returns nearest intersection with sphere */
MAN m_ray_sph(MAN a,MAN b,MAN o,MAN r)
{
    MAN t = m_solve_len(a-o,b,r);
    return a + b*t;
}

/* returns nearest intersection with cylinder */
```

```
MAN m_ray_cyl(MAN a,MAN b,MAN o,MAN d,MAN r)
{
    MAN t = m_solve_len(o-a+d*m_dot(a-o,d),d*m_dot(b,d)-b,r);
    return a + b*t;
}

/* returns normal to sphere centered at o, at point p */
MAN m_sph_nor(MAN o,MAN p)
{
    return m_normalize(p-o);
}

/* returns normal to cylinder of origin o, direction d, at point p */
MAN m_cyl_nor(MAN o,MAN d,MAN p)
{
    MAN q = o + d*m_dot(p-o,d);
    return m_normalize(p-q);
}

MAN u = m_x(0);
MAN v = m_x(1);
MAN w = m_x(2);

/* cylinder origin, direction, and radius */
MAN cyl_o = @(MAN)(0,0,0);
MAN cyl_d = @(MAN)(1,0,0);
MAN cyl_r = 0.6;

/* sphere origin and radius */
MAN sph_o = @(MAN)(0,-0.1,1.5);
MAN sph_r = 0.6;

/* sphere and cylinder surfaces */
MAN cyl = @(m_interp(v,-1,1),m_circle(2*pi*u)*cyl_r);
MAN sph = m_sphere(u*2*pi,v*pi)*sph_r + sph_o;

/* ray origin (a) and direction (b) for a collection
   of rays, arranged in circle in the xy plane */
MAN a = @(m_circle(m_x(0)*2*pi)*0.4,0.5);
MAN b = @(MAN)(0,0,1);

/* intersection of rays with cylinder */
MAN c1 = m_ray_cyl(a,-b,cyl_o,cyl_d,cyl_r);
MAN c1tan = m_normalize(m_derivative(c1,0));
MAN c1nor = m_cyl_nor(cyl_o,cyl_d,c1);
MAN c1d = m_cross(c1nor,c1tan);

/* intersection of rays with sphere */
MAN c2 = m_ray_sph(a,b,sph_o,sph_r);
MAN c2tan = m_normalize(m_derivative(c2,0));
MAN c2nor = m_sph_nor(sph_o,c2);
MAN c2d = m_cross(c2nor,c2tan);
MAN z = m_interp(w,0.01,1.0);
MAN fillet = m_interp_hermite(v,c1,c2,c1d*z,c2d*z);
```

B.2 Screwdriver Tip Examples

The following GENMOD code defines two surfaces representing the tip of a regular and a Phillips screwdriver. The code is an example of the idea of CPG discussed in Section 3.1.3. The code is dependent on a module that builds curves with a PostScript-like interface. The following are descriptions of the relevant functions:

- `newpath(int coord)`

  specifies the start of a new curve which will be based on parametric coordinate `coord`.

- `closepath()`

  closes a curve begun with `newpath`.

- `getpath(MAN input)`

  returns a parametric function (of type `MAN`), representing the last curve built, parameterized by parametric function `input`.

- `moveto(MAN p)`

  moves to the 2D point `p`.

- `lineto(MAN p)`

  adds a line segment to the curve from the last point to the point `p`.

- `lineto_arc(MAN p,MAN o,MAN r,int min,int cc,MAN fillet)`

  adds a linear segment to the curve from the last point in the direction of point `p`. The segment is ended when it hits a the circle centered at `o` of radius `r`. `min` is a flag specifying whether the first or second intersection of the line segment from the last point to `p` is to be used. `cc` is a flag specifying whether the arc is traversed counterclockwise. `fillet` is a parametric function specifying the radius of a fillet placed between the line segment and the arc. Using the special function `m_null` for this argument removes the fillet.

- `arcto_line(MAN o,MAN r,MAN p1,MAN p2,int min,int cc,MAN fillet)` adds an arc to the curve. The arc is a piece of a circle centered at `o` of radius `r`. The first arc endpoint is determined from the projection of the last point onto the circle. The second arc endpoint is the intersection of the line segment from `p1` to `p2` with the circle. The `min`, `cc`, and `fillet` arguments are as in `lineto_arc`.

We first present the GENMOD code for the regular screwdriver tip. The parametric surface `regular` is the appropriate final result.

```
MAN u = m_x(0);
MAN v = m_x(1);

MAN o = @(MAN)(0,0);
MAN r = 0.5;
MAN fillet = m_null; /* 0 radius fillet */
MAN w = m_interp(v,0.015,0.75);
MAN p0 = @(w/2,-1.0);
MAN p1 = @(w/2,1.0);
MAN p2 = @(-w/2,1.0);
MAN p3 = @(-w/2,-1.0);

newpath(0);
moveto(p0);
lineto_arc(p1,o,r,0,1,fillet);
arcto_line(o,r,p2,p3,1,1,fillet);
lineto_arc(p3,o,r,0,1,fillet);
arcto_line(o,r,p0,p1,1,1,fillet);
closepath();

MAN regular = @(getpath(u),m_interp(v,0,1.0));
```

The Phillips screwdriver tip is based on two curves, shown in Figure B.1. The GENMOD code for the Phillips screwdriver follows. The parametric surface `phillips` is the appropriate final result.

```
MAN u = m_x(0);
MAN v = m_x(1);

MAN o = @(MAN)(0,0);
MAN r = m_crv("radius.crv",v)[1];
MAN depth = m_crv("depth.crv",v);
MAN p = @(depth[1],0);
MAN p1 = @(0,p[0]);
MAN p2 = @(0,-p[0]);

MAN fillet = m_null;
```

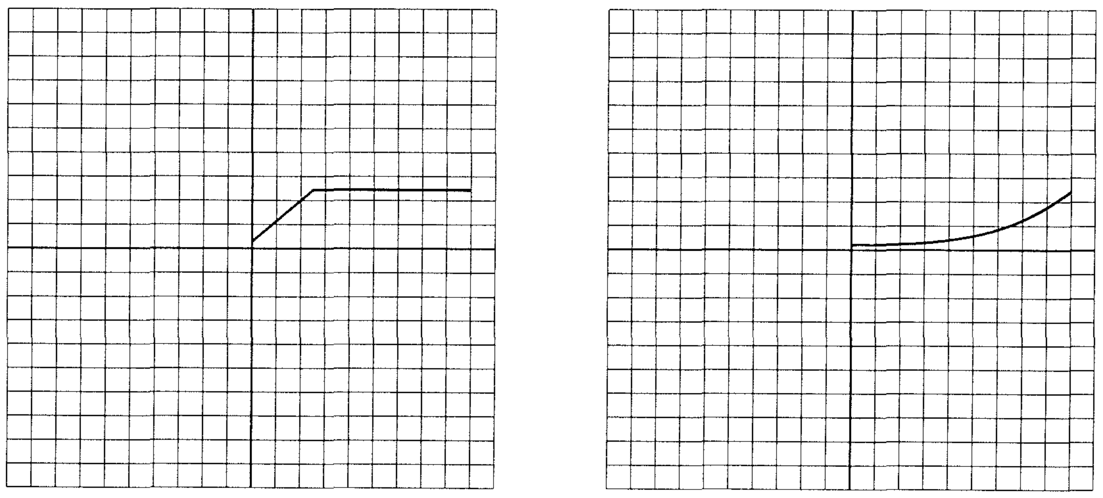

Figure B.1: Curves used in the Phillips screwdriver example

```
MAN theta = pi/2;
MAN d1 = @(m_cos(theta/2),m_sin(theta/2));
MAN d2 = @(d1[0],-d1[1]);
MAN d0 = @(d1[1],d1[0]);
MAN d3 = @(d1[1],-d1[0]);

newpath(0);
moveto(p2);
lineto_arc(p2+d3,o,r,0,1,fillet);
arcto_line(o,r,p+d2,p,1,1,fillet);
lineto(p);
lineto_arc(p+d1,o,r,0,1,fillet);
arcto_line(o,r,p1+d0,p1,1,1,fillet);
lineto(p1);

MAN c = m_mirrorx(getpath(u));
MAN phillips = @(c,depth[0]);
```

B.3 Bottle Example

The following GENMOD code yields the bottle surface of Section 3.1.4. The code is dependent on four curves, shown in Figure B.2. The parametric surface `bottle` is the appropriate final result.

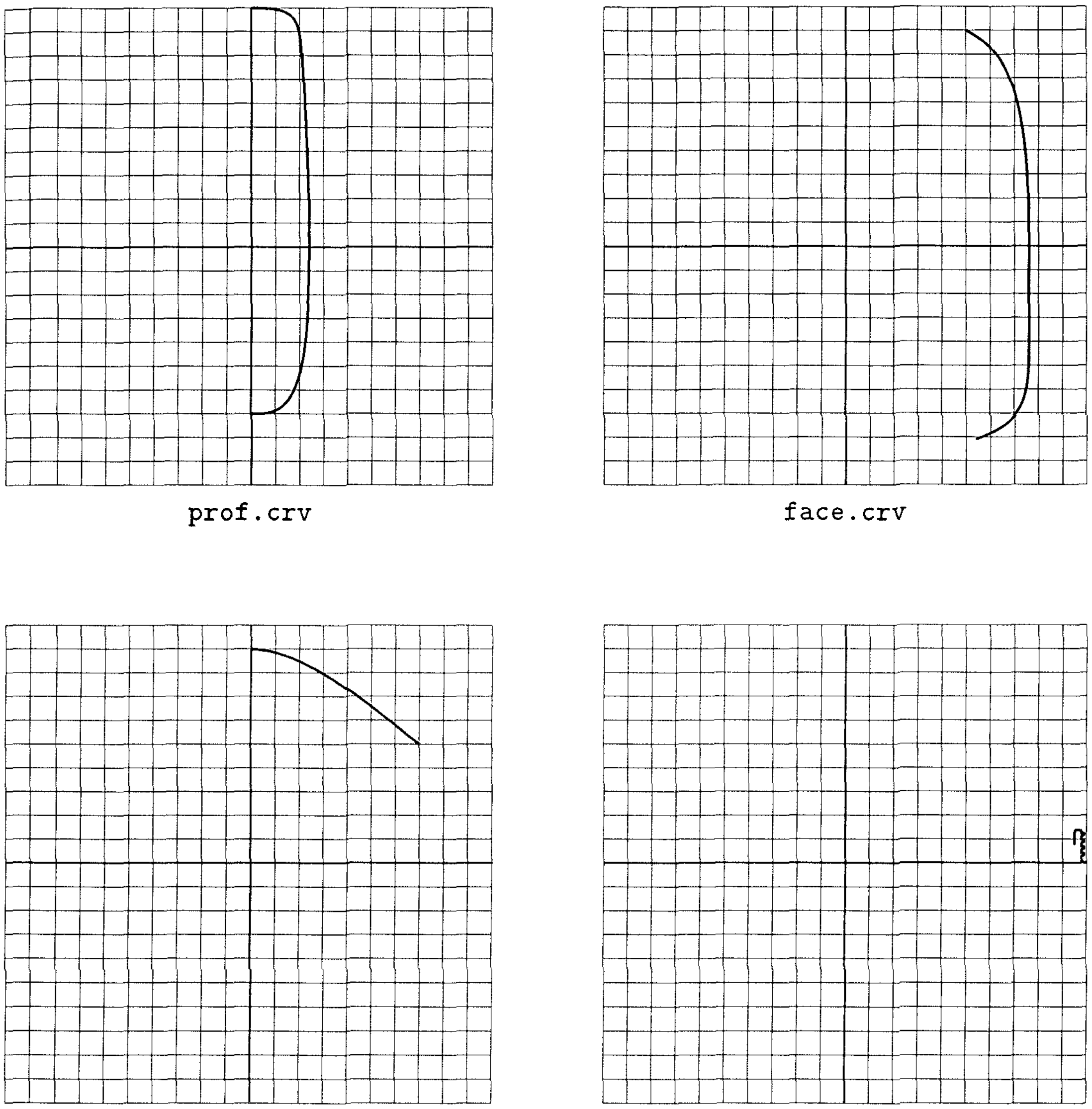

Figure B.2: Curves used in the bottle example — The curve `prof.crv` relates the amount the cross section of the bottle is to be offset (x axis) with the amount of translation in z (y axis). The curve `face.crv` specifies how much the cross section is to be rounded out at the three corner points as it is swept. The curve `top.crv` specifies the shape of the bottle near the top; specifically, how much the cross section is warped upward in z as a function of its distance from the z axis. The curve `prof2.crv` controls the shape of the bottle at the nozzle.

```
/* offset m by radius r */
MAN m_offset(MAN m,MAN r)
{
    MAN n = m_normalize(m_normal2d(m));
    return m + r*n;
}

/* warp m by making its z coordinate
   by a function of its length.  That
   function is given by w             */
MAN m_warp(MAN m,MAN w)
{
    int parm = w->input_list[0];

    MAN d = m_length(m);
    MAN new = m_inverse(w[0],d,parm);
    MAN z = m_eval(w[1],parm,new);

    return @(m,z);
}

/* concatenate a sequence of mermite curves */
MAN m_herm(MAN_ARRAY p,MAN_ARRAY t,int parm,MAN in)
{
    MAN array[20];
    int i;

    for (i = 0; i < p.n-1; i++) {
        MAN p1 = p.ptr[i];
        MAN p2 = p.ptr[i+1];
        MAN t1 = t.ptr[i];
        MAN t2 = t.ptr[i+1];
        array[i] = m_interp_hermite(m_x(parm),p1,p2,t1,t2);
    }
    return m_concat(parm,in,m_array(array,p.n-1));
}

/* reparameterize curve by matching y value
   to that of another curve               */
MAN m_resample_y_by_curve(MAN c1,MAN c2,int parm)
{
    MAN newparm = m_inverse(c1[1],c2[1],parm);
    return m_eval(c1,parm,newparm);
}

/* construct a bottle surface */
MAN m_bottle(MAN prof, MAN _face,MAN top,MAN prof2)
{
    MAN face = m_resample_y_by_curve(_face,prof,1);

    MAN in = m_interp(m_x(0),0.1,0.9);
    MAN q1 = -face[0];
    MAN q2 = face[0];
    MAN q3 = -face[0];
    MAN q4 = face[0];

    MAN p2 = m_interp(0.5*(q1+1),@(MAN)(-1,0),@(MAN)(0,1));
    MAN p3 = m_interp(0.5*(q2+1),@(MAN)(-1,0),@(MAN)(0,1));
    MAN p4 = m_interp(0.5*(q3+1),@(MAN)(0,1),@(MAN)(1,0));
    MAN p5 = m_interp(0.5*(q4+1),@(MAN)(0,1),@(MAN)(1,0));
    MAN p1 = @(p2[0],-p2[1]);
    MAN p6 = @(p5[0],-p5[1]);

    MAN t2 = m_normalize(p3-p2)*0.2;
    MAN t3 = t2;
    MAN t4 = m_normalize(p5-p4)*0.2;
    MAN t5 = t4;
    MAN t1 = @(-t2[0],t2[1]);
    MAN t6 = @(-t5[0],t5[1]);

    MAN c = 0.5*m_herm(@[p1,p2,p3,p4,p5,p6],
                       @[t1,t2,t3,t4,t5,t6],0,in);
    MAN c_ = c*(1+prof[0]);

    /* main body of bottle */
    MAN s = m_warp(c_,top) + @(0,0,prof[1]-1);

    /* "shoulders" of bottle */
    MAN c0 = m_eval(c,1,0.0);
    MAN ctop = m_normalize(c0)*0.1;
    MAN reg = m_interp(m_x(1),ctop,c0);
    MAN s0 = m_warp(reg,top);

    /* nozzle of bottle */
    MAN c2 = m_warp(ctop,top);
    MAN s2 = @( @(c2[0],c2[1])*prof2[0], c2[2] + prof2[1]);

    /* bottom of bottle */
    MAN c1 = (1-m_x(1))*m_eval(c,1,1.0);
    MAN s1 = m_warp(c1,top) + @(0,0,m_eval(prof[1],1,1.0));

    /* concatenate all the pieces */
    return m_concat(1,m_x(1),@[s2,s0,s,s1]);
}

MAN u = m_x(0);
MAN v = m_x(1);
MAN face = m_crv("face.crv",v);
MAN prof = m_crv("prof.crv",v);
MAN top = m_crv("top.crv",v);
MAN prof2 = m_crv("prof2.crv",v);

MAN bottle = m_bottle(prof,face,top,prof2);
```

Bibliography

[BAJA88] Bajaj, C., C. Hoffman, J. Hopcroft, and R. Lynch, "Tracing Surface Intersections," *Computer Aided Geometric Design,* 5, 1988, pp. 285-307.

[BARN85] Barnhill, R.E., "Surfaces in CAGD: A Survey of New Results," Computer Aided Geometric Design, 2, pp. 1-18.

[BARR81] Barr, Alan H., "Superquadrics and Angle Preserving Transformations," *Computer Graphics,* 15(3), August 1981, pp 11-23.

[BARR84] Barr, Alan H., "Global and Local Deformations of Solid Primitives," *Computer Graphics,* 18(3), July 1984, pp. 21-30.

[BARR86] Barr, Alan H., "Ray Tracing Deformed Surfaces," *Computer Graphics,* 20(4), August 1986, pp. 287-296.

[BARS88] Barsky, Brian, *Computer Graphics and Geometric Modeling Using Beta-splines,* Springer-Verlag, New York, 1988.

[BART87] Bartels, R., J. Beatty, and B. Barsky, *An Introduction to Splines for Use in Computer Graphics and Geometric Modeling,* Morgan Kaufmann, Los Altos, CA, 1987.

[BART89] Bartels, R., and R.T. Hardock, "Curve-to-Curve Associations in Spline-Based Inbetweening and Sweeping," *Computer Graphics,* 23(3), July 1989, pp. 167-174.

[BAUM72] Baumgart, B.G., *Winged Edge Polyhedron Representation,* Technical Report STAN-CS-320, Computer Science Department, Stanford University, Palo Alto, CA, 1972.

[BAUM74] Baumgart, B.G., *Geometric Modeling for Computer Vision,* Ph.D. Thesis, Report AIM-249, STAN-CS-74-463, Computer Science Department, Stanford University, Palo Alto, CA, October 1974.

[BAUM87] Baumann, E., "Optimal Centered Forms," *Freiburger IntervallBerichte 87/3,* Institut fur Angewandte Mathematik, Universitat Freiburg, pp. 5-21.

[BEZI74] Bezier, P., "Mathematical and Practical Possibilities of UNISURF," in Barnhill, R.E., and R.F. Riesenfeld, eds. *Computer Aided Geometric Design,* Academic Press, New York, 1974.

[BINF71] Binford, T., in *Visual Perception by Computer, Proceedings of the IEEE Conference on Systems and Control,* Miami, FL, December 1971.

[BLIN78] Blinn, J.F., *Computer Display of Curved Surfaces,* Ph.D. Thesis, Department of Computer Science, University of Utah, Salt Lake City, UT, December 1978.

[BLIN82] Blinn, J.F., "A Generalization of Algebraic Surface Drawing," *ACM Transactions on Graphics*, 1(3), July 1982, pp. 235-256.

[BLOO88] Bloomenthal, J., "Polygonisation of Implicit Surfaces," *Computer Aided Geometric Design,* 5, 1988, pp. 341-355.

[BOHM84] Bohm, W., G. Farin, and J. Kahmann, "A Survey of Curve and Surface Methods in CAGD," *Computer Aided Geometric Design*, 1, pp. 1-60.

[BORN81] Borning, A., "The Programming Language Aspects of Thinglab, a Constraint-Oriented Simulation Laboratory," *ACM Trabsactions on Programming Languages and Systems*, 3(4), October 1981,pp. 353-387.

[BOYS79] Boyse, J.W., "Interference Detection Among Solids and Surfaces," *Communications of the ACM,* 22(1), Jan. 1979, pp. 3-9.

[BOYS82] Boyse, J.W., and J.E. Gilchrist, "GMSolid: Interactive Modeling for Design and Analysis of Solids," *IEEE Computer Graphics and Applications,* 2(2), March 1982, pp. 27-40.

[BRON85] Bronsvoort, W.F., and F. Klok, "Ray Tracing Generalized Cylinders," *ACM Transactions on Graphics,* 1(3), pp. 235-256.

[BROW82] Brown, C.M., "PADL-2: A Technical Summary," *IEEE Computer Graphics and Applications,* 2(2), March 1982, pp. 69-84.

[CARL82a] Carlson, W.E., "An Algorithm and Data Structure for 3D Object Synthesis using Surface Patch Intersections," *Computer Graphics,* 16(3), July 1982, pp. 255-263.

[CARL82b] Carlson, W.E., *Techniques for Generation of Three Dimensional Data for use in Complex Image Synthesis,* Ph.D. Thesis, Ohio State University, Sept. 1982.

[CHIY83] Chiyakura, H., and F. Kimura, "Design of Solids with Free-Form Surfaces," *Computer Graphics,* 17(3), July 1983, pp. 289-298.

[COHE80] Cohen, E., T. Lyche, and R. Riesenfeld, "Discrete B-Splines and Subdivision Techniques in Computer-Aided Geometric Design and Computer Graphics," *Computer Graphics and Image Processing,* 14(2), October 1980, pp. 87-11.

[COHE83] Cohen, E., "Some Mathematical Tools for a Modeler's Workbench," *IEEE Computer Graphics and Applications,* 5(2), pp. 63-66.

[COON67] Coons, S.A., "Surfaces for Computer Aided Design of Space Forms," MIT Project MAC, MAC-TR-41, Massachusetts Institute of Technology, Cambridge, MA, June 1967.

[COQU87] Coquillart, S. "A Control Point Based Sweeping Technique," *IEEE Computer Graphics and Applications,* 7(11), 1987, pp. 36-45.

[COQU90] Coquillart, S., "Extended Free-Form Deformation: A Sculpturing Tool for 3D Geometric Modeling," *Computer Graphics,* 24(4), August 1990, pp. 187-196.

[CROC87] Crocker, G.A., and W.F. Reinke, "Boundary Evaluation of Non-Convex Primitives to Produce Parametric Trimmed Surfaces," *Computer Graphics,* 21(4), July 1897, pp. 129-136.

[DEBO72] deBoor, C., "On Calculating with B-splines," *Journal of Approximation Theory,* 6, 1972, pp. 50-62.

[DEBO78] deBoor, C. *A Practical Guide to Splines,* Applied Mathematical Sciences, Volume 27, Springer-Verlag, New York, 1978.

[DONA85] Donahue, B., *Modeling Complex Objects with Generalized Sweeps,* M.S. Thesis, University of Utah, 1985.

[FARO85] Farouki, R.T., "Exact Offset Procedures for Simple Solids," *Computer Aided Geometric Design,* 2, 1985, pp. 257-280.

[FARO86] Farouki, R.T., "The Approximation of Non-Degenerate Offset Surfaces," *Computer Aided Geometric Design,* 3, 1986, pp. 15-44.

[FAUX79] Faux, I.D., and M.J. Pratt, *Computational Geometry for Design and Manufacture,* Halsted, Chichester, England, 1980.

[FOLE90] Foley, James D., Andries van Dam, Steven K. Feiner, and John F. Hughes, *Computer Graphics Principles and Practice*, Second Edition, Addison-Wesley Publishing Company, Reading, MA, 1990.

[FRAN81] Franklin, W.F. and Alan H. Barr, "Faster Calculation of Superquadrics," *IEEE Computer Graphics and Applications,* 1(3), 1981, pp. 41-47.

[GABR85] Gabriel, S.A., and James T. Kajiya, "Spline Interpolation in Curved Manifolds," *SIGGRAPH85 Course Notes, State of the Art*, 1985.

[GOLD83] Goldman, R.N., "Quadrics of Revolution," *IEEE Computer Graphics and Applications*, 3(2), 1983, pp. 68-76.

[GOLD84] Goldman, R.N., T.W. Sederberg, and D.C. Anderson, "Vector Elimination: A Technique for the Implicitization, Inversion, and Intersection of Planar Parametric Rational Polynomial Curves," *Computer Aided Geometric Design,* 1, 1984, pp. 327-356.

[GORD74] Gordon, W., and R.E. Riesenfeld, "B-spline Curves and Surfaces," in *Computer Aided Geometric Design,* Barnhill, R.E. and R.F. Riesenfeld, ed., Academic Press, New York, 1974.

[HANR83] Hanrahan, P., "Ray Tracing Algebraic Surfaces," *Computer Graphics,* 17(3), July 1983, pp. 83-90.

[HANR89] Hanrahan, P., "A Survey of Ray-Surface Intersection Algorithms," in Glassner, A.S., ed., *An Introduction to Ray Tracing,* Academic Press, London, 1989, pp. 79-119.

[HILD76] Hildebrand, Francis B., *Advanced Calculus for Applications*, Prentice-Hall Inc., Englewood Cliffs, NJ, 1976, pp. 269-341.

[HOFF85] Hoffman, C., and J. Hopcroft, *Automatic Surface Generation in Computer Aided Design,* TR-85-661, Department of Computer Science, Cornell University, Jan. 1985.

[HOFF88] Hoffman, C.M., *A Dimensionality Paradigm for Surface Interrogations,* Technical Report CSD-TR-837, Computer Sciences Department, Purdue University, West Lafayette, IN, Dec. 1988.

[JENS66] Jenson, J.E., ed., *Forging Industry Handbook,* Forging Industry Association, Ann Arbor Press, Cleveland, OH, 1966.

[JOY86] Joy, K.I., and M.N. Bhetanabhotla, "Ray Tracing Parameteric Patches Utilizing Numerical Techniques and Ray Coherence," *Computer Graphics,* 20(4), August 1986, pp. 279-285.

[NELS85] G. Nelson, "Juno, a constraint-based graphics system," SIGGRAPH '85, 19(3), July 1985, pp. 235-243.

[KAJI82] Kajiya, James T., "Ray Tracing Parametric Patches," *Computer Graphics,* 16(3), July 1982, pp. 245-254.

[KAJI83] Kajiya, James T., "Ray Tracing Procedurally Defined Objects," *Computer Graphics,* 17(3), July 1983, pp. 91-102.

[KAJI89] Kajiya, James T., and Timothy L. Kay, "Rendering Fur with Three Dimensional Textures," *Computer Graphics,* 23(3), July 1989, pp. 271-280.

[KALR89] Kalra, Devendra, and Alan H. Barr, "Guaranteed Ray Intersections with Implicit Surfaces," *Computer Graphics,* 23(3), July 1989, pp. 297-304.

[KERN88] Kernigan, Brian W., and Dennis M. Ritchie, *The C Programming Language Second Edition,* Prentice Hall, Englewood Cliffs, New Jersey, 1988.

[KOCH84] Kochanek, D., and R. Bartels, "Interpolating Splines with Local Tension, Continuity, and Bias Control," *Computer Graphics,* 18(3), July 1984, pp. 33-41.

[LAID86] Laidlaw, D.H., W.B. Trumbore, and J.F. Hughes, "Constructive Solid Geometry for Polyhedral Objects," *Computer Graphics,* 20(4), August 1986, pp. 161-170.

[LANE80] Lane, J., L. Carpenter, T. Whitted, and J. Blinn, "Scan Line Methods for Displaying Parametrically Defined Surfaces," *IEEE Transactions on Pattern Analysis and Machine Intelligence,* PAMI-2(1), January 1980, pp. 35-46.

[LEE80] Lee, Y.T., and A.A.G. Requicha, *Algorithms for Computing the Volume and other Integral Properties of Solid Objects,* Technical Memo No. 35, Production Automation Project, University of Rochester, Rochester, NY, 1980.

[LEE82a] Lee, Y.T., and A.A.G. Requicha, "Algorithms for Computing the Volume and Other Integral Properties of Solids. Part 1, Known Methods and Open Issues," *Communications of the ACM,* 25(9), Sept. 1982, pp. 635-641.

[LEE82b] Lee, Y.T., and A.A.G. Requicha, "Algorithms for Computing the Volume and Other Integral Properties of Solids. Part 2, A Family of Algorithms Based on Representation Conversion and Cellular Approximation," *Communications of the ACM,* 25(9), Sept. 1982, pp. 642-650.

[LIEN84] Lien, S. and James T. Kajiya, "A Symbolic Method for Calculating Integral Properties of Arbitary Nonconvex Polyhedra," *IEEE Computer Graphics and Applications,* 4(10), 1984, pp. 35-41.

[LOSS74] Lossing, D.L., and A.L. Eshleman, "Planning a Common Data Base for Engineering and Manufacturing," *SHARE XLIII*, Chicago, IL, Aug. 1974.

[MIDD85] Middleditch, A.E., and K.H. Sears, "Blend Surfaces for Set Theoretic Volume Modelling Systems," *Computer Graphics*, 19(3), July 1985, pp. 161-170.

[MILL87] Miller, J.R., "Geometric Approaches to Nonplanar Quadric Surface Intersection Curves," *ACM Transactions on Graphics*, 6(4), October 1987, pp. 274-307.

[MOOR66] Moore, R.E., *Interval Analysis*, Prentice Hall, Englewood Cliffs, New Jersey, 1966.

[MOOR79] Moore, R.E., *Methods and Applications of Interval Analysis*, SIAM, Philadelphia.

[MORT85] Mortenson, Michael E., *Geometric Modeling*, John Wiley and Sons, New York, 1985.

[MUDU84] Mudur, S.P., and P.A. Koparkar, "Interval Methods for Processing Geometric Objects," *IEEE Computer Graphics and Applications*, 4(2), Feb, 1984, pp. 7-17.

[NAYL90] Naylor, B., J. Amanatides, and W. Thibault, "Merging BSP Trees Yields Polyhedral Set Operations," *Computer Graphics*, 24(4), August 1990, pp. 115-124.

[NEWM73] Newman, William M., and Robert F. Sproull, *Principles of Interactive Comuter Graphics*, McGraw-Hill Book Company, New York, 1973.

[NISH83] Nishita, H., H. Ohno, T. Kawata, I. Shirakawa, and K. Omura, "LINKS-1: A Parallel Pipelined Multicomputer System for Image Creation," *Proceedings of the Tenth International Symposium on Computer Architecture, ACM SIGARCH Newsletter*, 11(3), 1983, pp. 387-394.

[OKIN73] Okino, N., and H. Kubo, "Technical Information System For Computer-Aided Design, Drawing, and Manufacturing," *Proceedings of the Second PROLAMAT 73*, 1973.

[PUTN86] Putnam, L.K., and P.A. Subrahmanyam, "Boolean Operations on N-Dimensional Objects," *IEEE Computer Graphics and Applications,* 6(6), June 1986, pp. 43-51.

[PRES86] Press, William H., Brian P. Flannery, Saul A. Teukolsky, and William T. Vetterling, *Numerical Recipes,* Cambridge University Press, Cambridge, England, 1986.

[RATS84] Ratschek, H. and J. Rokne, *Computer Methods for the Range of Functions,* Ellis Horwood Limited, Chichester, England, 1984.

[RATS88] Ratschek, H. and J. Rokne, *New Computer Methods for Global Optimization,* Ellis Horwood Limited, Chichester, England, 1988.

[REQU74] Requicha, A.A.G., N. Samueal, and H. Voelcker, *Part and Assembly Description Languages — Part 2,* Technical Memo 20b, Production Automation Project, University of Rochester, Rochester, NY, 1974.

[REQU77a] Requicha, A.A.G., *Mathematical Models of Rigid Solids,* Technical Memo NO. 28, Production Automation Project, University of Rochester, Rochester, NY, 1977.

[REQU77b] Requicha, A.A.G., *Part and Assembly Description Languages — Part 1 Dimensioning and Tolerancing,* Technical Memo No. 19, Production Automation Project, University of Rochester, Rochester, NY, 1977.

[REQU77c] Requicha, A.A.G., and H.B. Voelcker, *Constructive Solid Geometry,* Technical Memo No. 25, Production Automation Project, University of Rochester, Rochester, NY, 1977.

[REQU78] Requicha, A.A.G., and R.B. Tilove, *Mathematical Foundations of Constructive Solid Geometry: General Topology of Regular Closed Sets,* Technical Memo No. 27, Production Automation Project, University of Rochester, Rochester, NY, 1978.

[REQU80] Requicha, A.A.G., "Representations for Rigid Solids: Theory, Methods, and Systems," *ACM Computing Surveys,* 12(4), December 1980, pp. 437-464.

[REQU85] Requicha, A.A.G., and H.B. Voelcker, "Boolean Operations in Solid Modeling: Boundary Evaluation and Merging Algorithms," *Proceedings of the IEEE*, 73(1), January 1985, pp. 30-44. b-reps may be combined, using regularized boolean set operators to create new b-reps algorithms for combining polyhedral objects

[RIES73] Riesenfeld, R.F., *Applications of B-spline Approximation to Geometric Problems of Computer Aided Design*, Ph.D. Thesis, Syracuse University, 1973.

[ROCK86] Rockwood, A.P., and J. Owen, "Blending Surfaces in Solid Modeling," in *Geometric Modeling,* Farin, G., ed., SIAM, 1986.

[ROSS84] Rossignac, J.R., and A.A.G. Requicha, "Constant Radius Blending in Solid Modeling," *Comp. Mech. Engr.,* 3, pp. 65-73.

[ROSS86a] Rossignac, J.R., and A.A.G. Requicha, "Offsetting Operations in Solid Modeling," *Computer Aided Geometric Design*, 3, 1986, pp. 129-148.

[ROSS86b] Rossignac, J.R., and A.A.G. Requicha, "Depth-Buffering Display Techniques for Constructive Solid Geometry," *IEEE Computer Graphics and Applications,* 6(9), September 1986, pp. 29-39.

[ROSS88] Rossignac, J.R., P. Borrel, and L.R. Nackman, "Interactive Design with Sequences of Parameterized Transformations," IBM Research Report RC 13740 (#61565), Yorktown Heights, NY, June 1988.

[SARR83] Sarraga, R.F., "Algebraic Methods for Intersections of Quadric Surfaces in GMSOLID," *Computer Graphics and Image Processing,* 22(2), May 1983, pp. 222-238.

[SCHW82] Schweitzer, D., and E. Cobb, "Scanline Rendering of Parametric Surfaces," *Computer Graphics,* 16(3), July 1982, pp. 265-271.

[SEDE83] Sederberg, T.W., *Implicit and Parametric Curves and Surfaces for Computer Aided Geometric Design,* Ph.D. Thesis, Mechanical Engineering, Purdue University, 1983.

[SEDE84] Sederberg, T.W., and D.C. Anderson, "Ray Tracing Steiner Patches," *Computer Graphics,* 18(3), July 1984, pp. 159-164.

[SEDE85] Sederberg, T.W., "Piecewise Algebraic Surface Patches," *Computer Aided Geometric Design,*, 2, 1985, pp. 53-59.

[SEDE86a] Sederberg, T.W., and S.R. Parry, "Free-Form Deformation of Solid Geometric Models," *Computer Graphics,* 20(4), August 1986, pp. 151-160.

[SEDE86b] Sederberg, T.W., and S.R. Parry, "A Comparison of Curve Intersection Algorithms," *Computer Aided Geometric Design,* 18, 1986, pp. 58-63.

[SEDE89] Sederberg, T.W., and A.K. Zundel, "Scan Line Display of Algebraic Surfaces," *Computer Graphics,* 23(3), July 1989, pp. 147-156.

[SEGA90] Segal, Mark, "Using Tolerances to Guarantee Valid Polyhedral Modeling Results," *Computer Graphics,* 24(4), August 1990, pp. 105-114.

[SHAN87] Shantz, M., and S. Lien, "Shading Bicubic Patches," *Computer Graphics,* 21(4), July 1987, pp. 189-196.

[SHAN89] Shantz, M., and S. Chang, "Rendering Trimmed NURBS with Adaptive Forward Differencing," *Computer Graphics,* 23(3), July 1989, pp. 189-198.

[SHIG80] Shigley, J.E., and J.J. Uicker, Jr., *Theory of Machines and Mechanisms,* McGraw-Hill Book Company, New York, 1980.

[SNYD87] Snyder, John M., and Alan H. Barr, "Ray Tracing Complex Models Containing Surface Tessellations", *Computer Graphics,* 21(4), July 1987, pp. 119-128.

[SUTH63] Sutherland, I., "Sketchpad, a Man-Machine Graphical Communication System", PhD Thesis, MIT, January 1963.

[TAMM84] Tamminen, M., and H. Samet, "Efficient Octree Conversion by Connectivity Labeling," *Computer Graphics,* 18(3), July 1984, pp. 43-51.

[THOM84] Thomas, S.W., *Modeling Volumes Bounded by B-Spline Surfaces,* Ph.D. Thesis, Technical Report UUCS-84-009, Department of Computer Science, University of Utah, Salt Lake City, UT, June 1984.

[THOM85] Thompson, Joe F., Z.U.A. Warsi, and C. Wayne Mastin, *Numerical Grid Generation*, North-Holland, New York, 1985.

[TILL83] Tiller, W., "Rational B-Splines for Curve and Surface Representation," *IEEE Computer Graphics ans Applications*, 3(6), September 1983, pp. 61-69.

[TILL84] Tiller, W., and E.G. Hanson, "Offsets of 2-Dimensional Profiles," *IEEE Computer Graphics and Applications,* 4(9), 1984, pp. 36-46.

[TILO77] Tilove, R.B., *A Study of Set-Membership Classification,* Technical Memo No. 30, Production Automation Project, University of Rochester, Rochester, NY, Nov. 1977.

[TILO80b] Tilove, R.B., "Set-Membership Classification: A Unified Approach to Geometric Intersection Problems," *IEEE Transactions on Computers,* C-29(10), 1980, pp. 847-883.

[TIMM77] Timmer, H.G., *Analytic Background for Computation of Surface Intersections,* Douglas Aircraft Company Technical Memorandum CI-250-CAT-77-036, April 1977.

[TIMM80] Timmer, H.G., and J.M. Stern, "Computation of Global Geometric Properties of Solid Objects," *Computer Aided Design,* 12(6), Nov. 1980.

[TOTH85] Toth, Daniel L., "On Ray Tracing Parametric Surfaces," *Computer Graphics,* 19(3), July 1985, pp. 171-179.

[TURN84] Turner, J.A., *A Set-Operation Algorithm for Two and Three-Dimensional Geometric Objects,* Architecture and Planning Research Laboratory, College of Architecture, University of Michigan, Ann Arbor, MI, August 1984.

[VANW84a] van Wijk "Ray Tracing Objects Defined by Sweeping Planar Cubic Splines," *ACM Transactions on Graphics,* 3(3), 1984, pp. 223-237.

[VANW84b] van Wijk "Ray Tracing Objects Defined by Sweeping a Sphere," *Proceedings of Eurographics 1984*, 1984, pp. 73-82.

[VONH85] Von Herzen, Brian P.,“Sampling Deformed, Intersecting Surfaces with Quadtrees,” Caltech CS Technical Report 5179:TR:85, pp. 1-40.

[VONH87] Von Herzen, Brian P. and Alan H. Barr,“Accurate Sampling of Deformed, Intersecting Surfaces with Quadtrees,” *Computer Graphics*, 21(4), July 1987, pp. 103-110.

[VONH89] Von Herzen, Brian P., *Applications of Surface Networks to Sampling Problems in Computer Graphics,* Ph.D. Thesis, California Institute of Technology, 1989.

[VONH90] Von Herzen, B., A.H. Barr, and H.R. Zatz, “Geometric Collisions for Time-Dependent Parametric Surfaces,” *Computer Graphics,* 24(4), August 1990, pp. 39-48.

[WEIL85] Weiler, K., “Edge-Based Data Structures for Solid Modeling in Curved-Surface Environments,” *IEEE Computer Graphics and Applications,* 5(1), January 1985, pp. 21-40.

[WANG86] Wang, W.P. and K.K. Wang “Geometric Modelling for Swept Volume of Moving Solids,” *IEEE Computer Graphics and Applications,* 6(12), 1986, pp. 8-17.

[WEIS66] Weiss, R., “BE VISION, a Package of IBM 7090 Programs to Draw Orthographic Views of Combinations of Planes and Quadric Surfaces,” *Journal of the ACM,* 13(2), 1966, pp. 194-204.

[WOON71] Woon, P.Y., and H. Freeman, “A Computer Procedure for Generating Visible Line Drawings of Solids Bounded by Quadric Surfaces,” in *IFIP 1971, v.2,* North Holland, Amsterdam, 1971, pp. 1120-1125.

[WYVI86] Wyvill, G., C. McPheeters, and B. Wyvill, “Data Structures for Soft Objects,” *The Visual Computer*, 2(4), April 1986, pp. 227-234.